

TALLINN UNIVERSITY OF TECHNOLOGY  
DOCTORAL THESIS  
2/2020

# **Synthesis, Characterisation and Catalytic Activity of Enantiopure Triazole-based Halogen Bond Donors**

MIKK KAASIK



TALLINN UNIVERSITY OF TECHNOLOGY

School of Science

Department of Chemistry and Biotechnology

This dissertation was accepted for the defence of the degree of Doctor of Philosophy in Chemistry 13/01/2020

**Supervisor:**

Professor Tõnis Kanger  
School of Science  
Tallinn University of Technology  
Tallinn, Estonia

**Opponents:**

Professor Stefan M. Huber  
Faculty of Chemistry and Biochemistry  
Chair of Organic Chemistry  
Ruhr University Bochum  
Bochum, Germany

Dr. Uno Mäeorg  
Faculty of Science and Technology  
Institute of Chemistry  
University of Tartu  
Tartu, Estonia

**Defence of the thesis:** 13/02/2020, Tallinn

**Declaration:**

Hereby, I declare that this doctoral thesis, my original investigation and achievement, submitted for the doctoral degree at Tallinn University of Technology has not been submitted for doctoral or equivalent academic degree.

Mikk Kaasik

-----  
Signature



European Union  
European Regional  
Development Fund



Investing  
in your future

Copyright: Mikk Kaasik, 2020

ISSN 2585-6898 (publication)

ISBN 978-9949-83-524-9 (publication)

ISSN 2585-6901 (PDF)

ISBN 978-9949-83-525-6 (PDF)



TALLINNA TEHNIKAÜLIKOO  
DOKTORITÖÖ  
2/2020

**Enantiomeerselt puhaste triasooli-põhiste  
halogeensideme doonorite süntees,  
iseloostamine ja katalüütiline aktiivsus**

MIKK KAASIK

**TAL  
TECH**  
KIRJASTUS



# Contents

List of Publications .....	7
Introduction .....	8
Abbreviations .....	9
1 Literature overview .....	11
1.1 The halogen bond .....	11
1.2 Parameters influencing the strength of halogen bonds.....	12
1.2.1 The halogen bond donor.....	13
1.2.2 1,2,3-triazole-based halogen bond donors .....	14
1.2.3 Effect of the solvent on halogen bonding.....	18
1.2.4 Halogen bond acceptors in solution .....	19
1.3 Asymmetric organocatalysis .....	20
1.4 Halogen-bonding catalysis .....	22
1.4.1 Anion-binding-type activation by halogen bonds .....	23
1.4.2 Activation of neutral substrates.....	24
1.4.3 Halogen bonding and asymmetric catalysis.....	27
1.5 Determination of binding constants in solution .....	29
2 Motivation and aims of the present work .....	31
3 Results and discussion.....	32
3.1 Synthesis of halogen bond donors and reference compounds.....	32
3.1.1 Synthesis of 5-halo-1 <i>H</i> -1,2,3-triazoles and corresponding hydrogen-analogues ..	33
3.1.2 Synthesis of 5-halo-1 <i>H</i> -1,2,3-triazolium salts and corresponding hydrogen-analogues .....	39
3.2 Halogen bond donor ability of the triazoles and triazolium salts in the solid state..	41
3.2.1 Compounds with a halogen bond between two donor molecules .....	41
3.2.2 Compounds forming a halogen bond to the counterion .....	42
3.3 XB donor ability of the triazoles and triazolium salts in solution.....	43
3.3.1 Titration experiments using acceptors with an oxygen or a sulphur atom.....	45
3.3.2 Titration experiments using acceptors with a nitrogen atom.....	46
3.3.3 Studies of the enantiodiscrimination ability of XB donors in solution.....	48
3.4 Catalytic activity of the triazole-based XB donors .....	51
3.4.1 Reduction of imine with Hantzsch ester <b>27</b> (unpublished results) .....	51
3.4.2 The Reissert-type reaction (unpublished results) .....	53
3.4.3 Initial results of the cyclisation reaction between Danishefsky's diene <b>42</b> and imine <b>98</b> (unpublished results and <b>Publication IV</b> ).....	54
3.4.4 Determination of the reaction profiles by <sup>1</sup> H NMR spectroscopy .....	56
3.4.5 Mechanistic aspects of the reaction between diene <b>42</b> and imine <b>98</b> .....	59
4 Conclusions .....	64
5 Experimental section.....	65
5.1 Representative procedure for the synthesis of azides from amines, in the example of <i>N</i> -((1 <i>R</i> ,2 <i>R</i> )-2-azidocyclohexyl)pivalamide .....	65
5.2 Representative procedure for the synthesis of azides from alcohols, in the example of compound <i>N</i> -((1 <i>S</i> ,2 <i>S</i> )-2-azido-2,3-dihydro-1 <i>H</i> -inden-1-yl)-2,2,2-trifluoroacetamide	65
5.3 Representative procedure for the synthesis of iodoalkynes from terminal alkynes, in the example of 1-(iodoethynyl)-3,5-bis(trifluoromethyl)benzene.....	66

5.4 Representative procedure for the synthesis of haloalkynes from aldehydes, in the example of 1-(iodoethynyl)-4-nitrobenzene.....	66
5.5 Representative procedure for the CuAAC of iodoalkynes, in the example of compound <b>81b-I</b> .....	66
5.5.1 1-Benzyl-4-(3,5-bis(trifluoromethyl)phenyl)-5-iodo-1 <i>H</i> -1,2,3-triazole <b>92d-I</b> .....	67
5.6 Representative procedure for the synthesis of 5-chlorotriazoles, in the example of compound <b>81d-Cl</b> .....	67
5.7 Representative procedure for the synthesis of 5-bromotriazoles, in the example of compound <b>81d-Br</b> .....	67
5.8 Representative procedure for the synthesis of 1 <i>H</i> -1,2,3-triazoles, in the example of compound <b>81d-H</b> .....	68
5.8.1 1-Benzyl-4-(3,5-bis(trifluoromethyl)phenyl)-1 <i>H</i> -1,2,3-triazole <b>92d-H</b> .....	68
5.8.2 (2 <i>R</i> ,4 <i>S</i> ,5 <i>R</i> )-2-(( <i>R</i> )-(4-(3,5-Bis(trifluoromethyl)phenyl)-1 <i>H</i> -1,2,3-triazol-1-yl)(6-methoxyquinolin-4-yl)methyl)-5-vinylquinuclidine <b>84d-H</b> .....	68
5.9 Representative procedure for the synthesis of triazolium triflates, in the example of compound <b>81d-I-OTf</b> .....	69
5.9.1 1-Benzyl-4-(3,5-bis(trifluoromethyl)phenyl)-5-iodo-3-methyl-1 <i>H</i> -1,2,3-triazol-3-ium trifluoromethanesulfonate <b>92d-I-OTf</b> .....	69
5.9.2 1-Benzyl-4-(3,5-bis(trifluoromethyl)phenyl)-3-methyl-1 <i>H</i> -1,2,3-triazol-3-ium trifluoromethanesulfonate <b>92d-H-OTf</b> .....	69
5.9.3 (2 <i>R</i> ,4 <i>S</i> ,5 <i>R</i> )-2-(( <i>R</i> )-(4-(3,5-Bis(trifluoromethyl)phenyl)-3-methyliumyl-1 <i>H</i> -1,2,3- $\lambda^4$ -triazol-1-yl)(6-methoxy-1-methylquinolin-1-ium-4-yl)methyl)-1-methyl-5-vinylquinuclidin-1-ium trifluoromethanesulfonate <b>84d-H-OTf</b> .....	69
5.10 Representative procedure for the synthesis of triazolium tetrafluoroborates, in the example of compound <b>81a-I-BF<sub>4</sub></b> .....	70
5.11 Representative procedure for the synthesis of triazolium tetrakis-3,5-bis(trifluoromethyl)phenylborates, in the example of compound <b>81e-I-BARF</b> .....	70
5.12 ( <i>E</i> )- <i>N</i> -(4-Methoxyphenyl)-1-phenylethan-1-imine <b>103</b> .....	70
5.13 General procedure for imine <b>103</b> reduction with Hantzsch ester <b>27</b> .....	70
5.14 1-( <i>tert</i> -butyldimethylsilyloxy)-1-isopropoxyethylene <b>107</b> .....	71
5.15 General procedure for the Reissert-type reaction.....	71
5.16 General procedure for the reactions between <b>42</b> and <b>98</b> .....	71
5.17 General information on the <sup>1</sup> H NMR titration experiments.....	71
References.....	75
Acknowledgements.....	81
Abstract.....	82
Lühikokkuvõte.....	83
Appendix 1.....	85
Appendix 2.....	95
Appendix 3.....	101
Appendix 4.....	111
Author's other publications and conference presentations.....	123
Curriculum vitae.....	124
Elulookirjeldus.....	125

## List of Publications

The list of author's publications, on the basis of which the thesis has been prepared:

- I Kaasik, M.; Kaabel, S.; Kriis, K.; Järving, I.; Aav, R.; Rissanen, K.; Kanger, T. Synthesis and Characterisation of Chiral Triazole-Based Halogen-Bond Donors: Halogen Bonds in the Solid State and in Solution. *Chem. - Eur. J.* **2017**, *23*, 7337–7344.
- II Peterson, A.; Kaasik, M.; Metsala, A.; Järving, I.; Adamson, J.; Kanger, T. Tunable Chiral Triazole-Based Halogen Bond Donors: Assessment of Donor Strength in Solution with Nitrogen-Containing Acceptors. *RSC Adv.* **2019**, *9*, 11718–11721.
- III Kaasik, M.; Kaabel, S.; Kriis, K.; Järving, I.; Kanger, T. Synthesis of Chiral Triazole-Based Halogen Bond Donors. *Synthesis* **2019**, *51*, 2128–2135.
- IV Kaasik, M.; Metsala, A.; Kaabel, S.; Kriis, K.; Järving, I.; Kanger, T. Halo-1,2,3-triazolium Salts as Halogen Bond Donors for the Activation of Imines in Dihydropyridinone Synthesis. *J. Org. Chem.* **2019**, *84*, 4294–4303.

## Author's Contribution to the Publications

Contribution to the papers in this thesis are:

- I The author had a major role in the synthetic preparation and characterisation of compounds used in the study. The author had a significant role in the planning and a major role in carrying out the  $^1\text{H}$  NMR titration experiments. The author wrote the manuscript, with contributions from the co-authors, and compiled the supporting information.
- II The author had a major role in the synthetic preparation and characterisation of compounds used in the study. The author had a minor role in the planning of the  $^1\text{H}$  NMR titration experiments. The author had a significant role in the preparation of the manuscript and compilation of the supporting information.
- III The author had a significant role in the synthetic preparation and characterisation of compounds used in the study. The author wrote the manuscript, with contributions from the co-authors, and compiled the supporting information.
- IV The author had a major role in the synthetic preparation and characterisation of compounds used in the study. The author carried out the catalytic experiments. The author wrote the manuscript, with contributions from the co-authors, and compiled the supporting information.

## Introduction

Noncovalent interactions play a significant role in chemistry and biology. Although noncovalent interactions are individually significantly weaker than covalent interactions, the concurrence of several weak interactions can lead to the formation and stabilisation of intricate systems. The instruction manual of life – the DNA double helix – is held together by hydrogen bonds. Chemists also actively utilise hydrogen bonds, and these have been used as supramolecular tools in a broad range of applications, ranging from porous materials in crystal engineering to catalysts in solution. Since the turn of the century, another noncovalent interaction, the halogen bond (XB), in which a halogen acts atypically as an electrophile, has started to receive significant attention. Compared to hydrogen bonds, XBs are generally more directional, can be stronger and can contain different donor atoms. Consequently, XBs have also found their place in the toolbox of supramolecular chemists. One common motif among XB donors is the halo-triazole core, which can generally be accessed in a few simple steps. Furthermore, due to the click approach these donors can be easily tuned to meet the structural requirements of the system under study.

At the turn of the century, organocatalysis broke through to the forefront of the synthetic community and was quickly recognised to be as important as organometallic and enzymatic catalysis in asymmetric synthesis. As life is chiral, one enantiomer can have a significantly different effect on a biological system compared to the other enantiomer, and therefore selective synthesis is one of the main problems of organic synthesis. As the field has reached a point where in most cases the question is no longer whether the compound can be synthesised, but how efficiently, the right tools should be used for specific tasks and there should be choices of what tools to use. Organocatalysts can be divided into covalent and the more broadly applicable noncovalent catalysts, such as the well-explored hydrogen-bonding catalysts. A decade ago, it was realised that XBs can also be utilised in organocatalysis. XBs have now been used to activate carbonyl compounds, imines, halides *etc.* in a variety of reactions. However, so far asymmetric catalysis solely through XB activation has not been achieved.

This doctoral thesis will first give a brief historical overview of halogen bonding and the variables that have an influence on the interaction. Also, approaches to access triazole-based XB donors and their applications will be discussed. Then, an introduction to organocatalysis will be given, followed by an overview of the use of XBs in organocatalytic applications. The aims of the thesis were to develop an approach for the synthesis of enantiomerically pure triazole-based XB donors, to probe the influence of different structural fragments on the donor ability of these compounds and to explore the catalytic activity of this class of XB donors in asymmetric synthesis.

The results demonstrate the general applicability of this approach for the synthesis of enantiopure triazole-based XB donors (**Publications I – IV**). The XB donor properties of the compounds in the solid state were elucidated by single crystal X-ray diffraction analysis (**Publications I, III and IV**) and in solution by  $^1\text{H}$  NMR spectroscopic titration experiments (**Publications I and II**). In addition, the enantiodiscrimination properties of the compounds were probed by  $^1\text{H}$  NMR spectroscopy (**Publications I and II**). Finally, **Publication IV** describes the use of XB donors as catalysts in dihydropyridinone synthesis. In addition to these publications, the results of this thesis have been presented at international conferences in Estonia, Latvia, Germany, Italy, Portugal and the United States of America.

## Abbreviations

Ala	alanine
An	4-methoxyphenyl
bl/bII	batch I/batch II
BARF	tetrakis[3,5-bis(trifluoromethyl)phenyl]borate
BINOL	1,1'-bi-2-naphthol
Boc	<i>tert</i> -butyloxycarbonyl
CPK	space-filling model
CuAAC	Cu(I)-catalysed azide–alkyne cycloaddition
DCE	1,2-dichloroethane
DCM	dichloromethane
Dip	2,6-diisopropylphenyl
DIPEA	<i>N,N</i> -diisopropylethylamine
DMF	<i>N,N</i> -dimethylformamide
DMSO	dimethyl sulfoxide
eq./equiv	equivalent
El	electrophile
ESP	electrostatic potential
EWG	electron withdrawing group
EtOAc	ethyl acetate
FG	functional group
Hal	halogen
HPLC	high-performance liquid chromatography
HSAB	hard and soft (Lewis) acids and bases
inc	incubation
IPA	isopropyl alcohol
Leu	leucine
MeCN	acetonitrile
Mes	2,4,6-trimethylphenyl
Ms	mesyl
MTBE	methyl <i>tert</i> -butyl ether
MW	microwave
NBS	<i>N</i> -bromosuccinimide
NMR	nuclear magnetic resonance
N.R.	no reaction
Nu	nucleophile
Oct	octyl
OTf	trifluoromethanesulfonate/triflate
Ph	phenyl
pK <sub>a</sub>	negative logarithm of the acid dissociation constant
<i>p</i> -TsOH	<i>para</i> -toluenesulfonic acid

<i>rac</i>	racemic
R <sub>DA</sub>	normalised interaction ratio
Ref.	reference
RT	room temperature
RuAAC	Ru-catalysed azide-alkyne cycloaddition
R <sub>XB</sub>	normalised interaction ratio of a halogen bond
TBA	tetrabutylammonium
TBS	<i>tert</i> -butyldimethylsilyl
TBTA	tris[(1-benzyl-1H-1,2,3-triazol-4-yl)methyl]amine
TTA	tris[(1- <i>tert</i> -butyl-1H-1,2,3-triazol-4-yl)methyl]amine
<i>t</i> Bu	<i>tert</i> -butyl
THF	tetrahydrofuran
TLC	thin-layer chromatography
TMA	tetramethylammonium
TMS	trimethylsilyl
<i>t<sub>R</sub></i>	retention time
TrocCl	2,2,2-trichloroethoxycarbonyl chloride
Trp	tryptophan
vdW	van der Waals
XB	halogen bond
$\Delta G$	change in Gibbs free energy
$\Delta H$	change in enthalpy
$\Delta S$	change in entropy



# 1 Literature overview

## 1.1 The halogen bond

Halogen bonding is an attractive interaction between an electrophilic region associated with a halogen atom and a nucleophilic region (Figure 1).<sup>1</sup> The first evidence of this phenomenon dates back to the early 19<sup>th</sup> century, when J. J. Colin *et al.* reported the formation of a complex between iodine and ammonia.<sup>2</sup> Since then there have been several milestones which have increased our knowledge of halogen bonding. P. Pelletier and J. B. Caventou reported that iodine is able to form complexes with anions<sup>3</sup> and O. Rhossopoulos described that halocarbons can also form adducts with Lewis bases.<sup>4</sup> H. A. Benesi, J. H. Hildebrand and R. S. Mulliken rationalised the colour change of iodine in different solvents by the formation of acid-base or charge-transfer complexes.<sup>5,6</sup> Next, O. Hassel *et al.* used X-ray crystallographic studies to elucidate the structural features of adducts formed by bromine with 1,4-dioxane and benzene.<sup>7,8</sup> In the 1990s P. Politzer *et al.* used computational studies to elucidate why halogens form adducts with Lewis bases and coined the term “ $\sigma$ -hole”.<sup>9</sup> A. Legon demonstrated that the essence of the phenomenon in the gas phase is the same as in the solid state and liquid phase.<sup>10</sup> Over the years numerous observations made it clear that scientists across very different fields were exploring the same phenomenon. This started a unification process to describe the phenomenon as a whole and finally culminated in the definition of halogen bonding in 2013. Even so, much is still to be discovered about the basic nature of XBs, which is exemplified by the fact that the first description of astatine acting as an XB donor was offered only in 2018.<sup>11</sup>

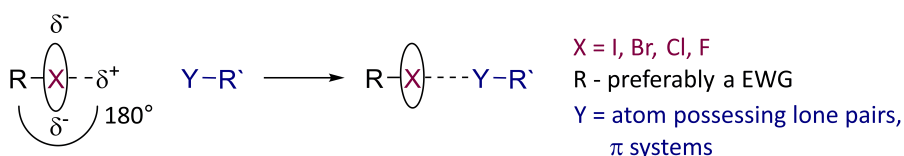


**Figure 1.** The halogen bond.

With the wealth of knowledge gained, research on halogen bonding has shifted more and more to studies of possible applications.<sup>12-16</sup> XBs can be used to complement or substitute other more commonly used and well-studied noncovalent interactions, such as hydrogen bonds and  $\pi$ - $\pi$  stacking, in the design of supramolecular systems. Due to the directionality and tunability of XBs, they can be exploited in the self-assembly processes needed in crystal engineering.<sup>17-19</sup> For example, K. Rissanen *et al.* showed that *N*-iodosuccinimide and hexamethylenetetramine (Figure 2) form a porous structure and the pore size is dependent on the solvent used for the crystallisation of this material.<sup>20</sup> For the above reasons, XBs have also attracted a great deal of attention in the design of new soft materials.<sup>21</sup> Also, research into solution-based applications has increased,<sup>22-24</sup> with the main areas of interest being anion recognition<sup>25</sup> and catalysis.<sup>26-28</sup>

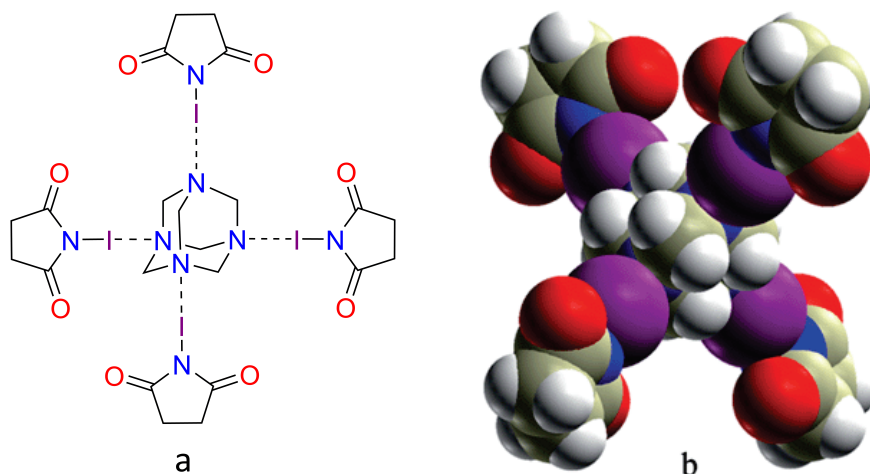


**Figure 2.** *N*-Iodosuccinimide and hexamethylenetetramine complex: a) chemical structure, b) CPK of crystal structure. Adapted from Ref. 20 with permission from The Royal Society of Chemistry.

## 1.2 Parameters influencing the strength of halogen bonds

As a noncovalent interaction, the strength of an XB is affected by both the donor and acceptor participating in the formation of the bond, as well as by the environment, which is the solvent in the case of solution studies. Halogen bonding can be characterised as a strong, specific, and directional interaction. Both the length and the angle of the XB can be directly measured from a crystal structure. An XB is very linear, with RX-Y angles being close to 180° (Figure 1), and is therefore more directional than a hydrogen bond.<sup>29–31</sup> Generally, short and strong XBs are more directional than long and weak ones. In the solid state, the appearance of XBs can be confirmed by the distance between the interacting atoms being less than the sum of their van der Waals (vdW) radii. As the interacting atoms in an XB can vary, the normalised interaction ratio (Equation 1,  $R_{DA}$ ), in which the distance ( $d_{DA}$ ) between the donor (D) atom and the acceptor (A) atom is divided by the sum of the vdW radius ( $r_{vdW}$ ) of the interacting atoms, is used for the comparison of different XBs.<sup>32</sup> In the case of an XB, it is defined as  $R_{XB}$ . Weak XBs have values above 0.9, typical  $R_{XB}$  values range down to 0.75 and very strong XBs have values below 0.7.<sup>12,19,30</sup>

$$\text{Equation 1} \quad R_{DA} = \frac{d_{DA}}{(r_{D,vdW} + r_{A,vdW})}$$

Computations are also commonly used to model XBs and the parameters associated with them, such as the length, the angle and the interaction energy of the XB.<sup>33</sup> As the strength and directionality of the XB are affected by the size of the  $\sigma$ -hole, molecular electrostatic potential (ESP) calculations can be used as guides to donor strength.<sup>34</sup> In solution, titration experiments can be carried out to determine the energetics associated with the interaction, such as  $\Delta H$ ,  $\Delta S$  and, most importantly,  $\Delta G$ , which correlates with the affinity constant  $K_a$  of the formed complex.<sup>24</sup> The strengths of XBs (ranging from 5 to 180 kJ/mol)<sup>29</sup> are comparable to and sometimes exceed the strengths of hydrogen bonds.

### 1.2.1 The halogen bond donor

Compared to hydrogen bonding, with halogen bonding there is more variety when choosing the donor atom from among the group seven elements. Halogens, due to their high electronegativity, are usually considered to be electron-rich, although this is true only to a certain extent, as the electron-rich region is confined to a belt surrounding the halogen atom (Figure 3). It is commonly accepted, that the underlying cause of halogen bonding is the anisotropic distribution of electron density around the halogen atom, when covalently bound to a substituent, brought about by the polarization of electronic charge toward the bond.<sup>35,36</sup> Perpendicular to the belt and opposite to the covalent bond to the halogen atom, an electron-deficient region termed the  $\sigma$ -hole, is formed, which is used to interact with electron-rich entities during the formation of XBs. One can observe the increase in the size of the  $\sigma$ -hole, i.e. the atom becomes more electron-deficient, with the increase in the polarisability of the halogen. Therefore, we can rank the halogens atoms by the increase in XB donor ability: F < Cl < Br < I (Figure 3).<sup>37</sup>

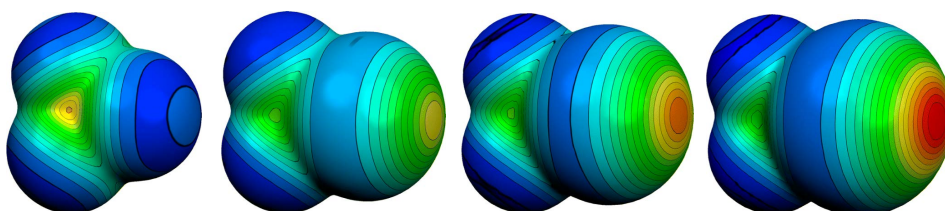


**Figure 3.** From left to right the electrostatic potential in Hartrees, at the 0.001 electrons Bohr<sup>-3</sup> isodensity surfaces of CF<sub>4</sub>, CF<sub>3</sub>Cl, CF<sub>3</sub>Br and CF<sub>3</sub>I (blue – more negative, red more positive). Adapted from Ref. 37 with permission from Springer Nature.

Furthermore, the size of the  $\sigma$ -hole can be tuned by modifying the electron withdrawing ability of the substituent covalently attached to the halogen atom. For example, computations have shown the increase in binding energies in the case of halide anions with the introduction of more electron-withdrawing groups attached to the XB-donating triazole core.<sup>38</sup> In addition, complexes of quinuclidine and *para*-substituted (iodoethynyl)benzenes afford binding energies with a strong linear free energy relationship of the Hammett parameter  $\sigma_{\text{para}}$  and stronger binding affinities were measured for alkynes substituted with electron-withdrawing groups.<sup>39</sup>

Starting with the introduction of dihalogens and interhalogens over 200 years ago, several different XB donor motifs have been employed (Figure 4). Although dihalogens **1**<sup>8</sup> and interhalogens<sup>40</sup> are strong donors, they cannot be modified significantly to meet the varied needs of XB-based applications. In contrast, organic scaffolds offer wider opportunities to tune the XB donor ability of the halogen atom and the overall properties of the donor. Comparing haloalkanes **2**, haloarenes **3** and haloalkynes **4**, the XB donor ability increases with an increase in the *s* character of the orbital hybridisation of the *ipso*-carbon atom.<sup>41</sup> *N*-Haloimides **5** and **6** are strong XB donors, due to the covalent bond between the halogen atom and the electronegative nitrogen atom in addition to the strongly polarising influence of the carbonyl and sulfonyl group.<sup>42</sup> Nitrogen-atom-containing cycles have been widely used as donor motifs (1,2,3-triazoles **7**<sup>43</sup>, pyridines **9**,<sup>44</sup> and imidazoles **11**<sup>45</sup>), and are especially valuable as the quaternisation of the nitrogen atom makes it possible to enhance the electron-withdrawing ability of the heterocycle.<sup>46–48</sup> XB donors with cationic backbones (**8**, **10** and **12**) have shown

greater donor ability than donors with neutral backbones.<sup>38</sup> In the case of anionic acceptors, the charge attraction between the cationic backbone of the donor and an anionic acceptor can additionally contribute to a favourable binding event.

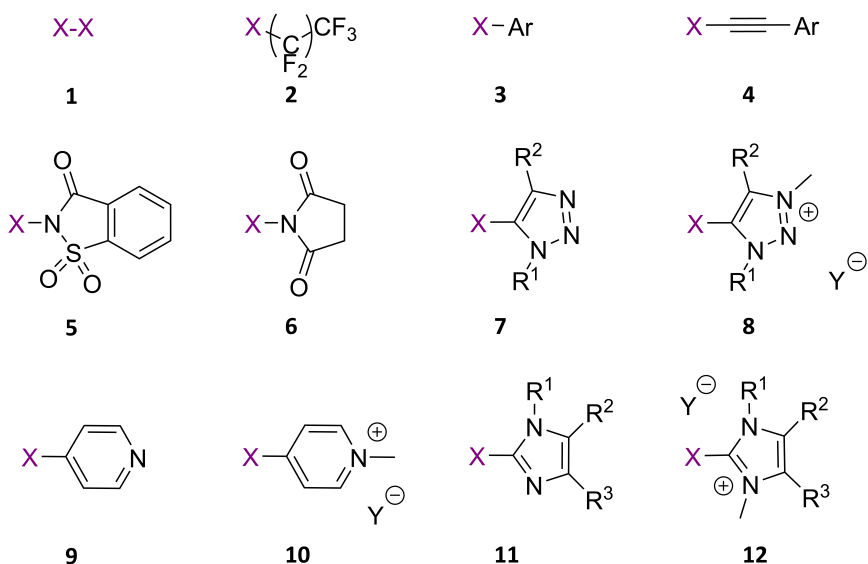
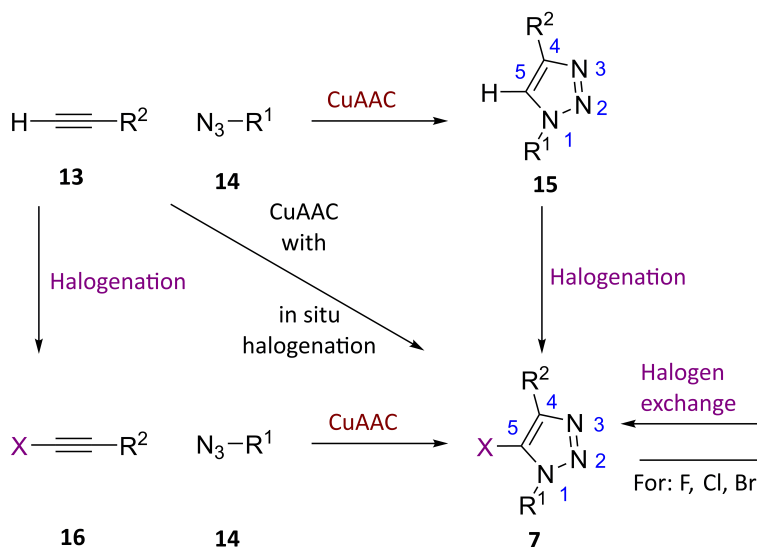


**Figure 4.** Common core scaffolds among XB donors.

### 1.2.2 1,2,3-triazole-based halogen bond donors

The click approach<sup>49</sup> to synthesise triazoles makes it possible to access a broad range of XB donor scaffolds in one or two steps (Scheme 1). The Cu(I)-catalysed azide-alkyne cycloaddition (CuAAC) reaction, utilizing terminal alkynes **13** and giving regioselective access to 1,4-disubstituted 1,2,3-triazoles **15**, has received significant attention over the years.<sup>50,51</sup> Compound **15** can be converted to the corresponding 5-halo-1,2,3-triazoles **7** in a second step.<sup>47,52</sup> Alternatively, the halogenation can be carried out in situ.<sup>53-57</sup> The use of haloalkynes **16** in the click reaction enables one to avoid harsh reaction conditions needed in some of the halogenation reactions of the triazoles. By this approach, it is possible to synthesise 5-chloro-, 5-bromo-, and 5-iodo-1,2,3-triazoles, although with bromo- and chloroalkynes<sup>58,59</sup> elevated temperatures are needed compared to the reaction with iodoalkynes.<sup>57,60-63</sup> One benefit of 5-iodo-1,2,3-triazoles is that they can be used as starting materials in a halogen-exchange reaction to access triazoles containing more electronegative halogens.<sup>64</sup> Finally, 1,2,3-triazolium salts can be converted to 5-halo-1,2,3-triazolium salts **8** via metalation at the C5-position and subsequent metal to halogen exchange.<sup>47</sup>



**Scheme 1.** Click approach to 1H-1,2,3-triazole-based XB donors.

1,2,3-triazoles with a 1,5-disubstituted pattern are obtainable through the ruthenium-catalysed azide alkyne cycloaddition (RuAAC),<sup>65</sup> which can then in principle give access to 4-halo-1H-1,2,3-triazoles. However, CuAAC is far more widely used to access 1,2,3-triazoles with a halogen substituent. Also, when V. V. Fokin *et al.* applied the RuAAC approach with haloalkynes, they obtained the 5-halo-1H-1,2,3-triazole **7** instead of the 4-halo-1H-1,2,3-triazole.<sup>66</sup>

1H-1,2,3-triazoles are characterised by a high degree of aromaticity.<sup>67</sup> However, the subunits are only cross-conjugated,<sup>68</sup> which leads to the ring acting as an electron-donor to substituents at the C4 position and an inductive electron-acceptor to substituents at the N1 position.<sup>67</sup> The three nitrogen atoms in the ring lead to a strongly polarised aromatic  $\pi$  system and  $\sigma$  framework.<sup>69</sup> Due to this, the proton in the C5 position is unusually acidic for an aromatic compound (Figure 5, A). The polarisation can be enhanced via quaternisation, protonation or metal coordination at the N3 position, also leading to an increase in the acidity at C5 (Figure 5, B).<sup>70</sup> However, the influence of quaternisation is not as profound as in the case of imidazoles, comparing the  $pK_a$  values of azoles and azoliums (Figure 5, comparing the acidity order of A to that of B). The imidazolium ring is more acidic than the 1H-1,2,3-triazolium ring, as two electronegative aza-substituents surround the acidic CH position in imidazoles compared to only one aza-substituent in 1H-1,2,3-triazoliums. Because of the additional aza-substituent, the proton in the 1,2,4-triazolium ring is even more acidic than the analogous proton in imidazoliums and 1,2,3-triazoliums. The above reasoning can be used to explain the polarisation of a halogen atom at the C5 position. DFT calculations have shown that the size of the  $\sigma$ -hole increases in the order of halo-1,2,3-triazolium < halo-imidazolium < halo-1,2,4-triazolium.<sup>47</sup> Although, based on the above, 3-halo-1,2,4-triazoliums should be stronger XB donors than 5-halo-1,2,3-triazoliums, nevertheless the latter are more extensively used due to their highly stable structure.<sup>47,67</sup> However, electron-withdrawing *N*-substituents or electron-donating substituents at the C5 position can make the halo-1,2,3-triazoles labile.<sup>67</sup>

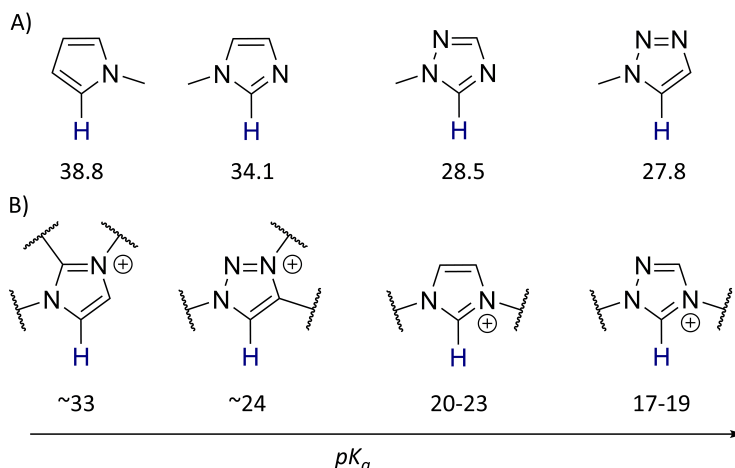


**Figure 5.**  $pK_a$  values of A) selected nitrogen-containing aromatic rings in DMSO from Ref. 71; B) azoliums in  $H_2O$  from Ref. 72–75.

The potential of halo-triazoles as XB donors was first realised by P. D. Beer *et al.*, who designed anion receptors by incorporating iodo-triazolium cores into rotaxanes.<sup>76,77</sup> Since then, both halo-triazoles and halo-triazolium salts have been used as XB donors in a variety of applications. The XB donors are often multidentate to achieve stronger binding with acceptors that can form more than one XB, such as anions. In this instance, the choice of the linker fragments can be used to modify the donor ability.<sup>78</sup> Zn(II) porphyrin was used as a central linker to connect four 5-iodo-1,2,3-triazole cores in an anion receptor resembling a pore.<sup>79</sup> When binaphthalene and phenyl cores were used as sequential linkers, the donors acted as foldamers (Figure 6, **17**).<sup>80</sup> 5-Iodo-1,2,3-triazoles have also been combined with macrocyclic pseudopeptides for the sensing of halide anions.<sup>81</sup> Increasing the donor ability of 5-halo-1,2,3-triazoles without transforming them into triazolium salts can help to avoid solubility issues of the latter in apolar solvents. For this reason, remote quaternisation of pyridyl fragments connected to the triazole core has been used to enhance the XB donor ability of 5-iodo-1,2,3-triazoles.<sup>82–85</sup> The ability to bind halide anions by multidentate XB donors can also be enhanced by pre-organising the triazole rings into a *syn* conformer.<sup>86</sup> There are also examples of the use of monodentate triazole-based XB donors. 5-Iodo-1,2,3-triazoles have been incorporated into a crown ether (Figure 6, **18**) to achieve ion-pair recognition of NaI.<sup>87,88</sup> Examples of the use of neutral XB acceptors with halo-triazoles are extremely rare. In one example by D. Philp *et al.*, complex formation was achieved by combining the donor and acceptor fragments into one molecule (Figure 6, **20**).<sup>43</sup>

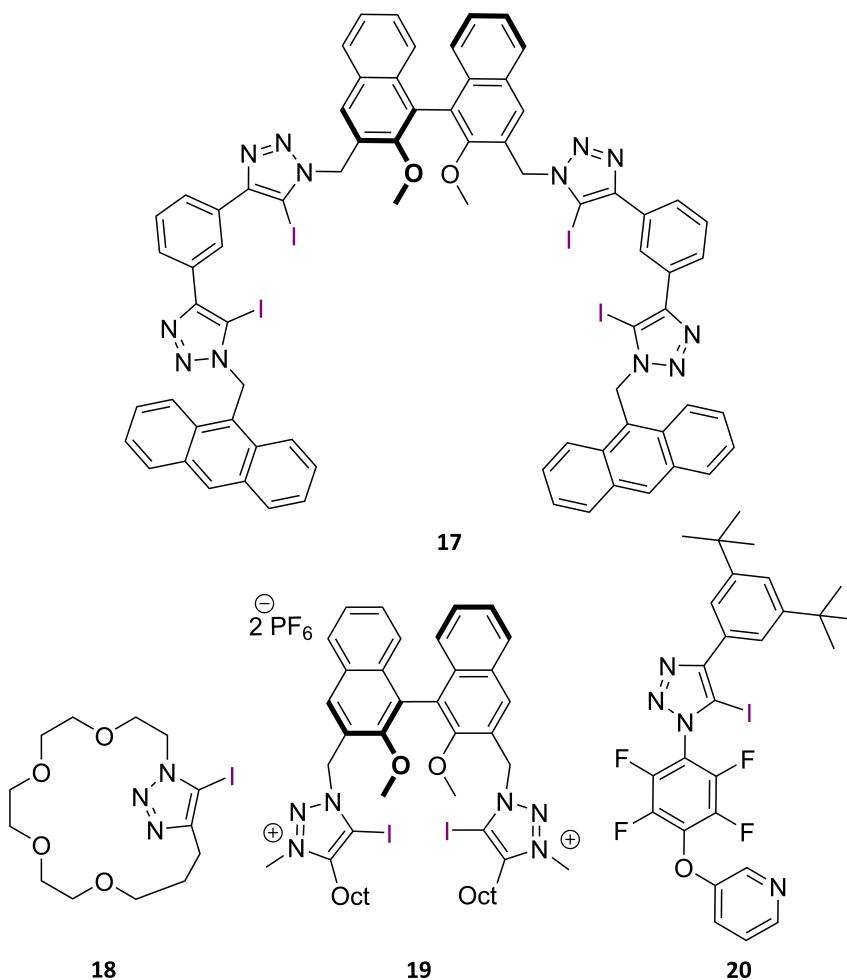


**Figure 6.** Examples of triazole-based XB donors.

The 5-iodo-1,2,3-triazolium core is also a very common motif among anion receptors (Figure 6, **19**).<sup>47,89–92</sup> P. D. Beer *et al.* have utilised the anion-binding ability of iodo-triazolium cores to create molecular shuttles.<sup>93,94</sup> Iodo-triazolium fragments have been used to cross-link polymeric backbones, resulting in a self-healing thin film.<sup>95</sup> S. M. Huber *et al.* have demonstrated the potential of using iodotriazole-based XB donors as activators and catalysts in halogen abstraction reactions.<sup>96–98</sup> Halotriazole-based catalysts have now been applied in Michael and aza-Diels-Alder reactions.<sup>52,99,100</sup>

Another benefit of the click approach is the possibility of using chiral azides to obtain chiral enantiomerically pure XB donors. In several instances, the azides can be accessed in one or two steps using amines and alcohols from the chiral pool. The previously described examples also showcase the use of chiral XB donors, although with achiral acceptors.<sup>81,82</sup> On the other hand, P. D. Beer *et al.* have demonstrated that halotriazole-based donors (Figure 6, **17** and **19**) can be used in the enantiodiscrimination of chiral carboxylate anions (Table 1).<sup>80,90–92</sup>

**Table 1.** Association constant  $K_a$  values<sup>a</sup> [ $M^{-1}$ ] for complexes between **17** and enantiomers of chiral carboxylates.<sup>80</sup>

Entry	Carboxylate <sup>b</sup>	$K_a$ (L)	$K_a$ (D)	$K_a$ (D) / $K_a$ (L)
1	<i>N</i> -Boc-Ala	336	265	0.79
2	<i>N</i> -Boc-Leu	287	436	1.52
3	<i>N</i> -Boc-Trp	200	337	1.69
4	Tartrate	725	932	1.29
5	Glutamate	1483	1363	0.92

<sup>a</sup> Measured by <sup>1</sup>H NMR spectroscopy in CDCl<sub>3</sub>/acetone-d<sub>6</sub> (1/1) (500 MHz, 298 K) and calculated by curve-fitting the data to a 1 : 1 binding isotherm; <sup>b</sup> All anions were introduced as TBA salts.

### 1.2.3 Effect of the solvent on halogen bonding

As a noncovalent interaction, halogen bonding can be compared to hydrogen bonding, and similar to it, strong XBs are generally formed between neutral partners in nonpolar aprotic solvents (Table 2).<sup>101–103</sup> However, in the case of charged systems, stronger XBs are formed in more polar solvents.<sup>78,104</sup> Compared to hydrogen bonds, XBs are very sensitive to Lewis basic solvents, which can even completely outcompete the acceptor for XB formation.<sup>78,101</sup> In the case of protonic solvents, the competition between hydrogen bond and XB formation to acceptors can be a major issue, leading to diminished binding affinities between the XB donor and XB acceptor (Table 2).<sup>76,78,101</sup> However, it has been demonstrated that XBs are not as sensitive to solvent effects as hydrogen bonds are.<sup>105,106</sup> Therefore, XB donors are highly attractive supramolecular synthons to work within aqueous environments, which also shows a benefit of using XB-based anion receptors compared to their hydrogen-containing analogues.<sup>85</sup>

**Table 2.** Influence of the solvent on the association constant  $K_a$ <sup>a</sup> value for the triethylamine and iodoperfluorooctane complex.<sup>101</sup>

Entry	Solvent	$K_a$ ( $M^{-1}$ )
1	cyclohexane	2.8 ± 0.6
2	benzene	2.6 ± 0.5
3	MeCN	1.9 ± 0.4
4	DCM	1.8 ± 0.3
5	acetone	1.3 ± 0.3
6	THF	1.2 ± 0.2
7	dioxane	1.1 ± 0.2
8	<i>t</i> BuOH	0.7 ± 0.3
9	CHCl <sub>3</sub>	0.6 ± 0.4
10	IPA	0.3 ± 0.7

<sup>a</sup> Measured by <sup>19</sup>F NMR spectroscopy in the corresponding solvent (376 MHz, 298 K) and calculated by curve-fitting the data to a 1 : 1 binding isotherm.



### 1.2.4 Halogen bond acceptors in solution

Anions, especially halides, are among the most common XB acceptors and there is an avid interest in using XB-based anion sensors, which has been brought about by the importance of anions in chemical, biological, medical and environmental processes.<sup>107,108</sup> The development of host systems selective for anion recognition is problematic as negative species come in many shapes, have high solvation enthalpies and low charge to radius ratios. Traditionally, noncovalent interactions, predominantly hydrogen bonds, are used with multiple interactions acting in a concerted manner. XBs can complement hydrogen bonds in the design of these hosts. Furthermore, XBs offer several benefits as well: higher levels of tunability, differing steric requirements and greater tolerance towards competitive protic solvents. Generally, it is expected that the affinity of an XB donor to halide anions increases with the increase in the charge density ( $\text{Cl}^- > \text{Br}^- > \text{I}^-$ ),<sup>46,47,109</sup> but there are cases where the selectivity preference is reversed.<sup>48,110</sup> With the design of receptors, it is possible to achieve preferential binding of oxyanions over halide anions<sup>45-47</sup> and preliminary results show the feasibility of using XB-based receptors for the selective recognition of chiral anions.<sup>80,90-92</sup> Receptors based on XB donor units have shown higher anion affinity than the corresponding hydrogen analogues and in the case of chiral anions, only the XB-based receptors have shown a preference for one enantiomer over the other.<sup>90</sup>

Neutral acceptors are generally weaker than the more electron-rich anionic acceptors, although it has been observed that inorganic XB donors can form strong complexes with neutral acceptors.<sup>24</sup> Furthermore, in recent years research of complex formation with anionic acceptors has received more attention than complex formation with neutral acceptors. So far, the studies have focused on obtaining information on the basic nature of halogen bonding, such as the influence of the solvent and the structure of the XB donor/acceptor on the strength of XBs.<sup>39,101-103,105,111-114</sup> Both the polarisability and the electronegativity of the acceptor atom affect the strength of the XB and the most common acceptor atoms in neutral compounds can be ranked as  $\text{O} < \text{S} < \text{N}$  (Figure 7).<sup>113,115</sup> For this reason, amines have been extensively used as XB acceptors. Furthermore, the acceptor ability of an atom is enhanced by the decrease in the s character of the orbital hybridisation of the acceptor atom, which is exemplified by the increase in the binding strength in the series: butanenitrile < pyridine < piperidine (Figure 7).<sup>113,114</sup> Interestingly, cyclic amines give stronger complexes than their acyclic analogues and markedly stronger complexes are formed with quinuclidine.<sup>101,103,113</sup>

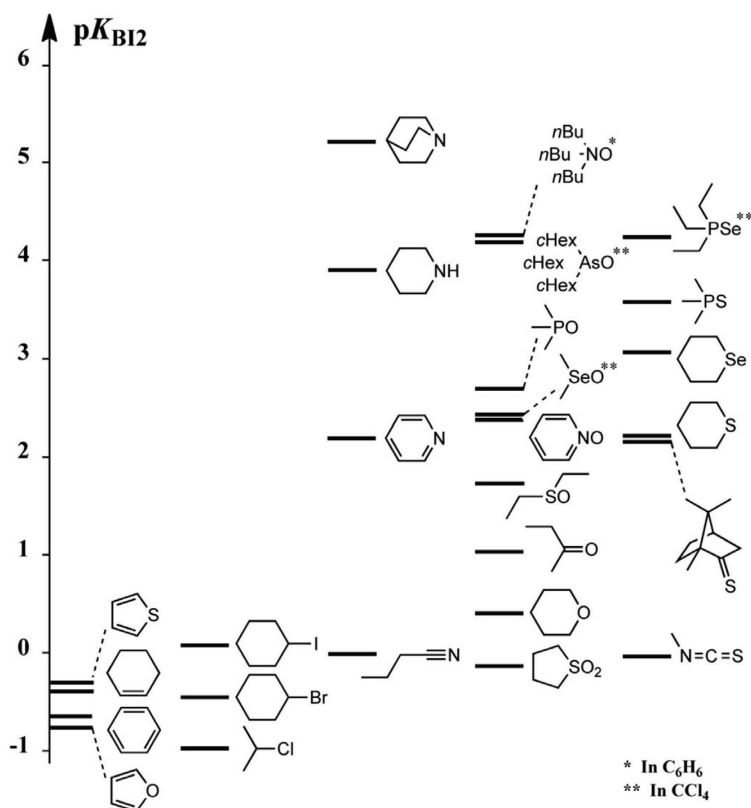
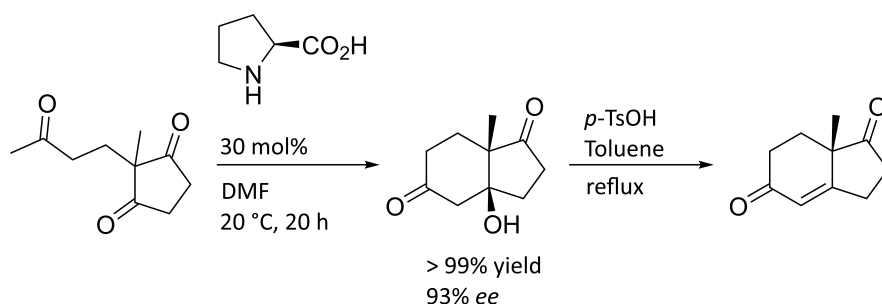


**Figure 7.** Diiodine basicity ( $pK_{BI_2}$ ) chart for Lewis bases. The  $pK_{BI_2}$  corresponds to the logarithm of the affinity constant of the  $[I_2 - \text{Lewis base}]$  complex in alkane at 298 K. Reproduced from Ref. 113 with permission from Wiley-VCH Verlag GmbH & Co. KGaA, Weinheim.

### 1.3 Asymmetric organocatalysis

The use of small organic molecules to accelerate organic transformations can be traced back to the work of E. Knoevenagel more than a century ago.<sup>116</sup> However, the scientific community showed only sporadic interest in the topic and even the success of the Hajos-Parrish-Eder-Sauer-Wiechert reaction (Scheme 2) during the 1970s in the synthesis of steroids could not focus the spotlight of the scientific community on organocatalysis.<sup>117,118</sup> It was only at the end of the 20<sup>th</sup> century that the potential of small organic catalysts was truly realised and the “renaissance” of organocatalysis was brought about through the work of B. List, C. F. Barbas and L. A. Lerner in enamine chemistry<sup>119</sup> and the work of D. W. C. MacMillan *et al.* in iminium chemistry.<sup>120</sup> Organocatalysis has now developed into one of the main branches of asymmetric synthesis.<sup>121–124</sup> Organocatalysts offer several advantages to researchers in academia and industry over the extensively researched organometallic catalysts, such as access to easy and low-cost reactions insensitive to air or moisture. Moreover, as organocatalysts (usually both enantiomers) can be derived from renewable sources with relative ease, they have a lesser impact on the environment than metal-based catalysts, not to mention the hazard and cost issues of toxic metal catalysts in the production waste stream, which has raised industrial interest in organocatalytic processes.



**Scheme 2.** The Hajos–Parrish–Eder–Sauer–Wiechert reaction.

Most importantly, the invented or identified organocatalytic modes of activation, induction and reactivity are generic, i.e. the reactive species can participate in many reaction types and are not confined to a small set of unique transformations.<sup>121</sup> The activation modes are classified from a mechanistic perspective either by the substrate-catalyst interaction character into covalent and noncovalent, or by the chemical nature of the organocatalyst into Lewis base, Lewis acid, Brønsted base and Brønsted acid.<sup>125</sup>

With covalent catalysis, the interaction between the substrate and catalyst is very strong and in principle the catalyst should be able to induce high levels of selectivity. However, the catalyst must be reversibly incorporated into the substrate for some time, which limits the number of usable substrates. For example, in the case of aminocatalysis, primary and secondary amines are used to activate carbonyl compounds (aldehydes and ketones). More precisely, with enamine catalysis (Figure 8, A) enolisable aldehydes and ketones **21** can be  $\alpha$ -functionalised with a variety of electrophiles and with iminium catalysis (Figure 8, B)  $\alpha,\beta$ -unsaturated carbonyls **22** can be  $\beta$ -functionalized with a variety of nucleophiles.<sup>125</sup>

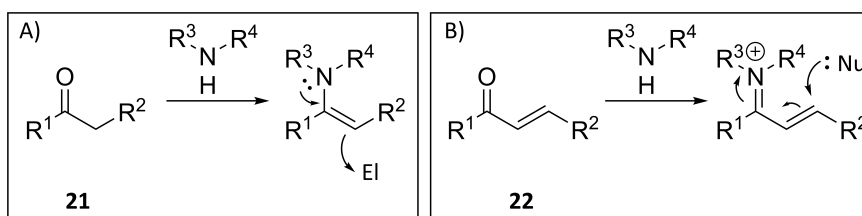


**Figure 8.** Representative covalent modes of activation: A) enamine, B) iminium.

On the other hand, noncovalent interactions are quite weak, which means that several interactions between the substrate and catalyst are needed to achieve high levels of activation and selectivity. This highlights the difficulties associated with noncovalent catalysis and why covalent organocatalysis has been more developed. A benefit of noncovalent catalysis is that a much broader set of substrates can be used, as the presence of free electron pairs or acidic protons in the substrate is enough for the catalyst to activate it. Hydrogen-bonding activation is the most researched activation mode among noncovalent catalysis and one can distinguish between two extremes. At one end, we have hydrogen-bonding catalysis, with the hydrogen still covalently attached to the catalyst during the activation (Figure 9, A). The most common

representatives are ureas and thioureas **23**, amidinium or guanidinium ions, squaramides, and diols. At the other end, we have Brønsted acid catalysis, where the proton has been transferred from the catalyst to the substrate (Figure 9, B). BINOL-derived phosphoric acids **24** are the most important representatives of the latter.<sup>125</sup>

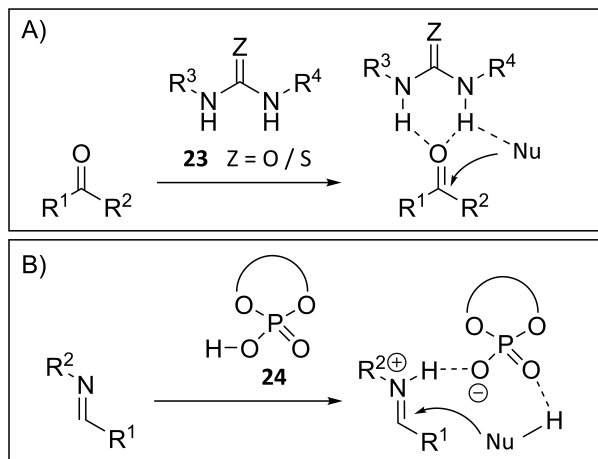
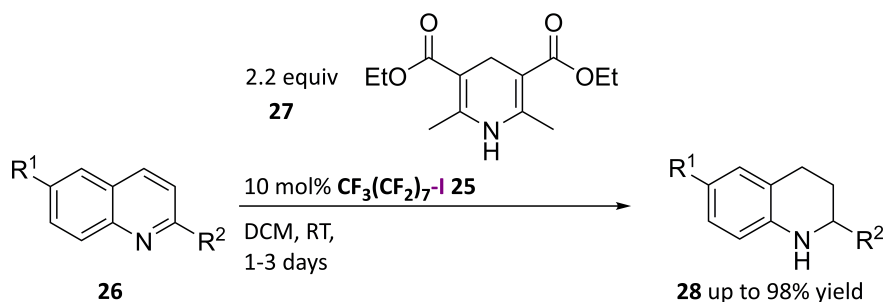


**Figure 9.** Representative modes of noncovalent activation by: A) hydrogen bonds, B) protonation by a Brønsted acid.

In many instances the catalysts act through both covalent and noncovalent interactions or, in the case of bifunctional catalysts, contain an acidic and a basic functionality, which are both needed for catalytic activity.<sup>125</sup>

## 1.4 Halogen-bonding catalysis

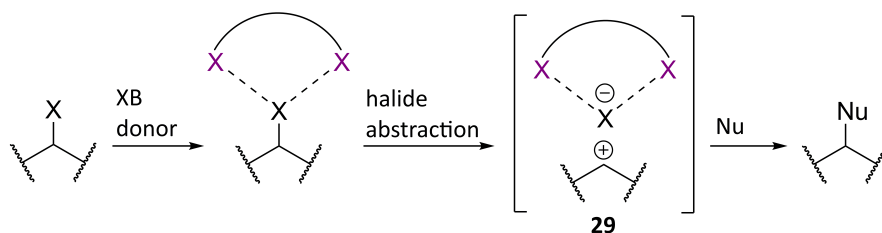
Iodine has been used in organic synthesis for more than a century, but the underlining reason for its catalytic activity has only recently been postulated to come from its ability to act as an XB donor.<sup>84</sup> With iodine and other di-/interhalogens, the possibility of making structural modifications is practically non-existent. Hence in the following sections attention is given to XB donors based on organic scaffolds acting as Lewis acid catalysts. The potential of XB-based catalysts was first realised by C. Bolm *et al.*, who used 1-iodoperfluorooctane **25** to activate quinolines **26** in their reduction with Hantzsch ester **27** (Scheme 3).<sup>126</sup> At the moment, the majority of XB-catalysed reactions can be placed in two groups by the mode of activation: reactions that proceed through anion-binding-type activation and the activation of neutral substances (aldehydes, ketones, imines *etc.*).<sup>26–28</sup> It should also be noted that the majority of catalysts are based on cationic backbones, as in most cases the corresponding neutral XB donors do not demonstrate sufficient catalytic activity.



**Scheme 3.** Hantzsch ester **27** reduction of quinolines **26** catalysed by 1-iodoperfluorooctane **25**.

### 1.4.1 Anion-binding-type activation by halogen bonds

All XB-catalysed reactions under this category have been halide abstraction reactions. This is not surprising, as XBs to halide ions are very strong, enabling the XB donors to remove a halogen from the substrate, turning it into a reactive electrophile **29** (Scheme 4).



**Scheme 4.** General mechanism of XB activation by halide ion abstraction.

Unfortunately, activation by this approach also hinders the use of XB donors as catalysts in this category of reactions, as the formed XBs are so strong that a very persistent complex is formed, and the halide ion ultimately acts as an inhibitor of the catalyst. Therefore, the “goldilocks principle” should be followed: the donor should be sufficiently strong to bind and activate the substrate but not so strong as to stay bound to the acceptor.<sup>127</sup> In the initial experiments, conducted by S. M. Huber *et al.* on the solvolysis of benzhydryl bromide **30**, stoichiometric amounts of the XB donor had to be used and the donors acted merely as activating agents (Figure 10, A and C).<sup>96,128,129</sup> The series of studies also demonstrated the potential of halo-triazoles, such as **37** and its analogues, as activators. An enhancement of activating potential was observed with the increase in donor sites in the activators, with the pyridinium-type donor **38** being the most active. Furthermore, neutral XB donors with enough donor sites can also act as activators in the reaction.<sup>130</sup> When silyl enol ethers **33** are used as nucleophiles, the silylium ion formed in the reaction can trap the halide ion. Therefore, it was later demonstrated that the XB donors can act as true catalysts in the halide abstraction reaction with 1-chloroisochroman **32** as the substrate (Figure 10, B and C).<sup>97</sup> Importantly, the pre-organisation of the bis(imidazolium)-type catalyst **40** into the *syn* configuration led to the enhancement of its catalytic activity. In the case of triazole-based XB donors, the importance of charge enhancement was again demonstrated by P. D. Beer and S. M. Huber *et al.*, although the triazole cores do not need be charged themselves.<sup>98</sup>

Bis(imido-imidazolium)-type donors have also been used for the activation of glycosyl halides.<sup>131</sup>

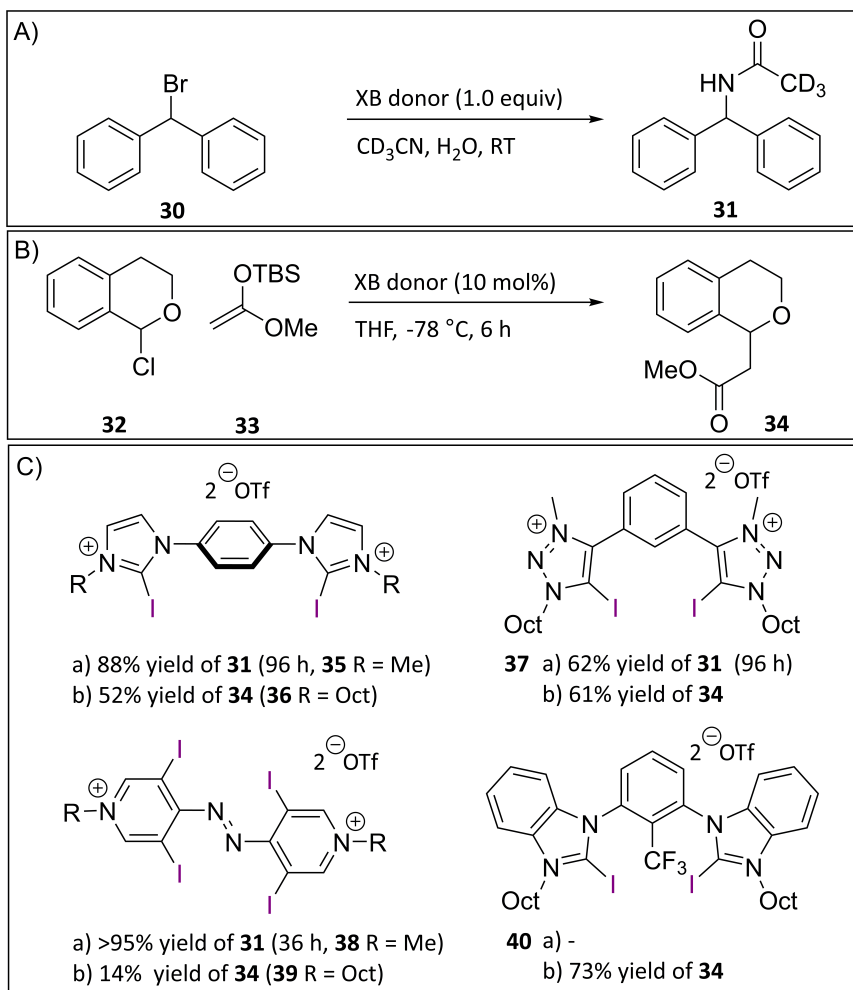


**Figure 10.** A) Solvolysis reaction of bromide **30**, B) activation of isocromane **32**, C) XB donors used as activators in reactions A and as catalysts in reaction B with corresponding yields of **31** or **34**.

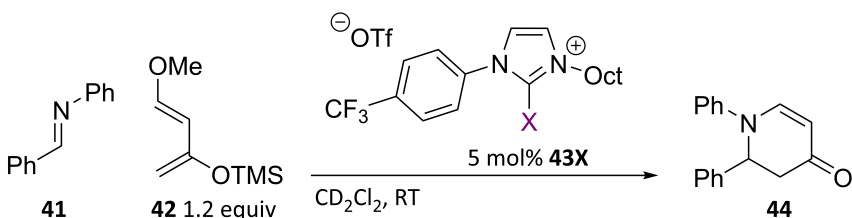
### 1.4.2 Activation of neutral substrates

The reactions that fall under this category are much broader and the model reactions have not been studied as thoroughly as the two reactions in the previous section. In addition, most of the examples still focus on well-known reactions that have been shown to be catalysed by hydrogen bond donors. In 2014 it was shown that Hantzsch ester reduction of quinolines, pyridines and imines can be carried out by using imidazole-based XB donors as catalysts.<sup>127</sup> However, recent computational results suggest that Brønsted acid catalysis might have been the actual mode of activation.<sup>132</sup>

Imines have also been activated by either halo-imidazolium- or halo-triazolium-type XB donors in aza-Diels-Alder reactions.<sup>52,133</sup> Interestingly, in the case of imidazolium-type catalysts **43**, the chloro- and bromo-derivative were more active than the

iodo-derivative, with the activity order matching that of the order of the corresponding affinity constants for the complexes of imine **41** and XB donor **43X** (Table 3). Nevertheless, the highest activity was observed with an iodo-benzimidazolium triflate. Furthermore, the authors presented initial results on the activation of a Mannich reaction with the developed catalyst.

**Table 3.** Aza-Diels-Alder reaction catalysed by **43X** and affinity constants  $K_a$  for the complexes of imine **41** and imidazolium salts **43X**.

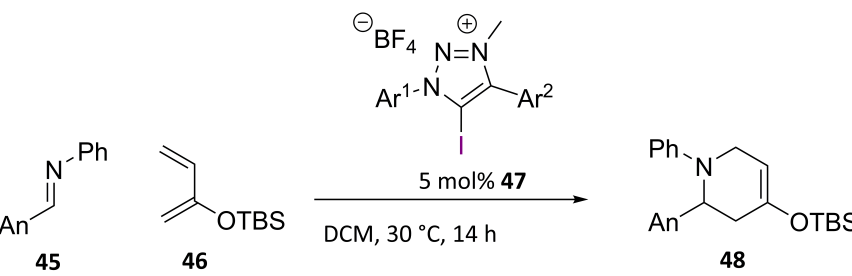


Entry	43X	NMR yield at 20 min (%) <sup>a</sup>	$K_a$ (M <sup>-1</sup> ) with <b>41</b> <sup>b</sup>
1	Cl	66	1,0 ± 0,1
2	Br	75	1,2 ± 0,1
3	I	55	0,9 ± 0,1

<sup>a</sup> Approximate yields from Figure 1 in Ref. 52. <sup>b</sup> Determined by <sup>1</sup>H NMR spectroscopy in CD<sub>2</sub>Cl<sub>2</sub> (400 MHz, 298 K) and calculated by curve-fitting the data to a 1 : 1 binding isotherm.

Surprisingly, with the iodo-triazolium tetrafluoroborates **47**, it was observed that mesityl substituents that hinder the possibility of resonance stabilisation make the XB donors **47** more active (Table 4, entry 3). However, the bulkier diisopropylphenyl substituents deteriorated the catalytic activity (Table 4, entries 2, 4 and 5). These results demonstrate how bulky substituents can be used to affect both the steric environment and the electronic structure of the catalyst.

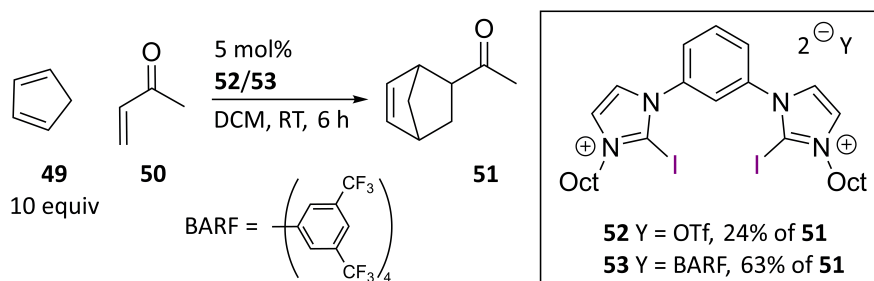
**Table 4.** Aza-Diels-Alder reaction catalysed by iodo-triazolium tetrafluoroborates **47**.<sup>a</sup>



Entry	Ar <sup>1</sup>	Ar <sup>2</sup>	NMR Yield (%)
1	Mes	Ph	47
2	Dip	Ph	26
3	Mes	Mes	93
4	Dip	Mes	64
5	Dip	Dip	49

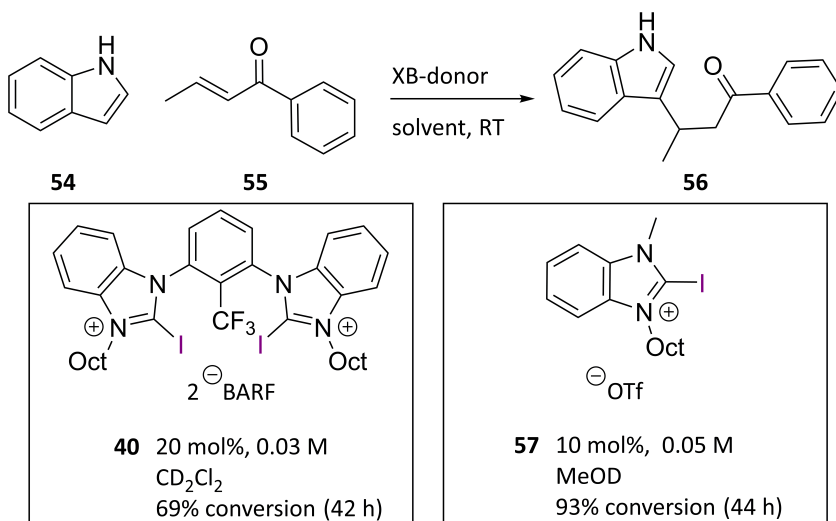
<sup>a</sup> An = 4-methoxyphenyl, Mes = 2,4,6-trimethylphenyl, Dip = 2,6-diisopropylphenyl

Bis(iodo-imidazolium)-type catalysts have been used in the activation of methyl vinyl ketone **50** in the Diels-Alder reaction with cyclopentadiene **49** (Scheme 5).<sup>134,135</sup> The non-coordinating BARF counterion was crucial to achieve high levels of catalytic activity.



**Scheme 5.** Diels-Alder reaction catalysed by bis(iodo-imidazolium) salts.

In 2017 S. M. Huber *et al.* demonstrated the efficiency of bis(iodo-benzimidazolium)-type XB donors (Scheme 6, compound **40**) in acting as catalysts for the activation of crotonophenone **55** in the Friedel-Crafts alkylation of indole **54**.<sup>136</sup> Again, the presence of the BARF counterion was of paramount importance. In contrast, M. Breugst *et al.* showed that a monodentate XB donor with the triflate counterion (Scheme 6, compound **57**) gave better results than the analogous compound containing the BARF counterion.<sup>99</sup> In a similar manner, iodo-imidazolium-type donors have also been used to activate enones and enals for their reaction with thiophenes.<sup>137</sup>

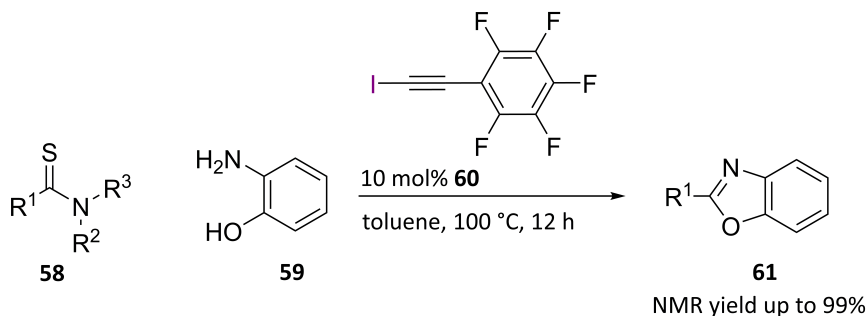


**Scheme 6.** Michael reaction between indole **54** and crotonophenone **55** catalysed by iodo-benzimidazolium salts **40** and **57**.

Tetrabromomethane has been used to activate aldehydes in an aldol-condensation reaction to form chalcones.<sup>138</sup> Recently, bis(iodobenzimidazolium) **40** was used to activate divinyl ketones in the Nazarov cyclization reaction.<sup>139</sup> In 2016, (iodoethyl)perfluorobenzene **60** was used to activate thioamides **58** in the formation

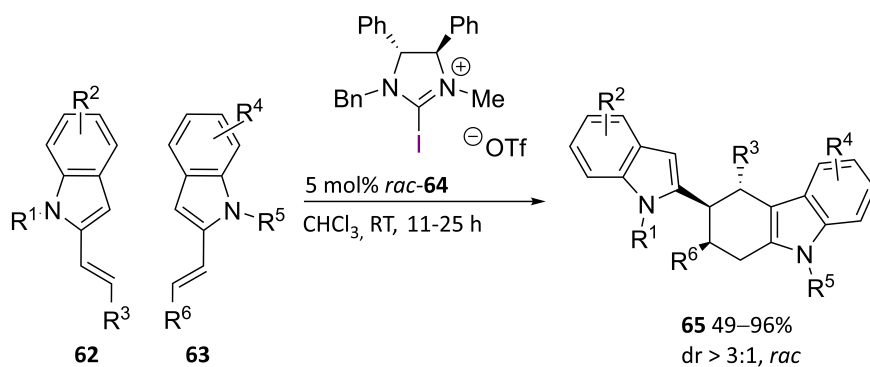


of benzoxazoles **61** (Scheme 7).<sup>140</sup> Surprisingly, iodoalkyne **60** was as active as an iodo-benzimidazolium salt, which has a similar structure to donor **57**.



**Scheme 7.** Iodoalkyne-catalysed synthesis of benzoxazoles.

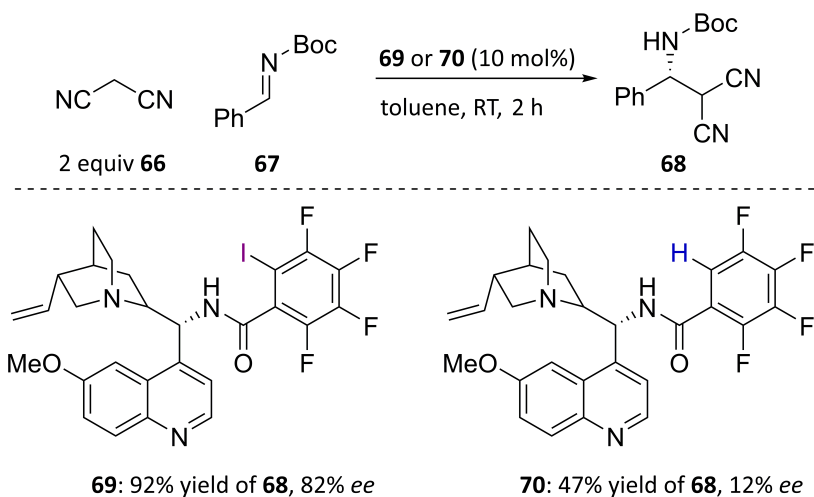
As a final example, in 2018 T. Arai *et al.* published a paper on the [4+2]-cycloaddition of 2-alkenylindoles **62** and **63** (Scheme 8) catalysed by 2-iodoimidazolium salt *rac*-**64**.<sup>141</sup> It was rationalised that the reaction took place by the activation of the indole  $\pi$ -system with an XB. This departure from the more studied activation of heteroatoms highlights the possibilities of XB catalysis and its future directions.



**Scheme 8.** XB activation of the  $\pi$ -systems in a [4 + 2] cycloaddition reaction.

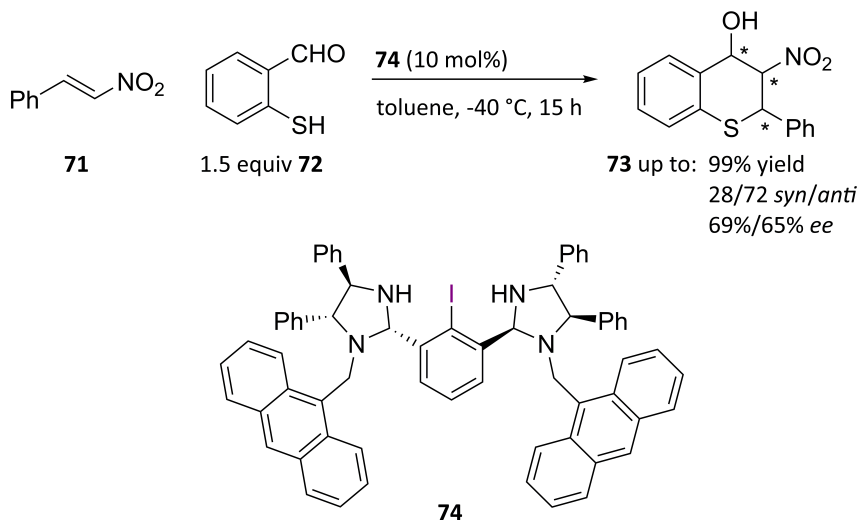
### 1.4.3 Halogen bonding and asymmetric catalysis

Due to similarities between XBs and hydrogen bonds, as well as the fact that hydrogen bonding has been extensively and successfully used in asymmetric catalysis,<sup>142,143</sup> there is interest in applying XB activation in asymmetric catalysis. XBs have been demonstrated to be crucial for the organisation of the Rh(II) catalysts developed by A. B. Charette *et al.* for asymmetric cyclopropanation reactions.<sup>144</sup> If the number of XBs the ligands can form amongst themselves dropped below a threshold value of three, asymmetric induction was almost completely lost. T. Arai *et al.* used XBs for the coordination of imine **67** in an asymmetric Mannich reaction with malononitrile **66** (Scheme 9).<sup>145</sup> Control experiments supported the involvement of XBs in the reaction, as the XB donor fragment of **69** interacted with imine **67** and, if the XB donor capability was removed, the yield of **68** dropped, with almost complete loss of selectivity (Scheme 9, with compound **70**).



**Scheme 9.** Asymmetric Mannich reaction between malononitrile **66** and imine **67**.

Chiral bis(imidazolidine)iodobenzene organocatalyst **74** was used to achieve enantioinduction in the Michael/Henry reaction between nitroalkene **71** and thiosalicyl aldehyde **72** (Scheme 10).<sup>146</sup> However, the exact role of the iodine atom in **74** was not elaborated and therefore it is unclear whether the reaction can be classified under XB catalysis.



**Scheme 10.** Michael/Henry reaction between nitroalkene **71** and thiosalicyl aldehyde **72** catalyzed by chiral bis(imidazolidine)iodobenzene **74**.

With these examples and the work of P. D. Beer *et al.* on using triazole-based XB donors for enantiodiscrimination of chiral anions,<sup>80,90–92</sup> it seems plausible to use XBs in asymmetric catalysis. However, so far there are no examples of asymmetric catalysis solely by XB activation.

## 1.5 Determination of binding constants in solution<sup>147</sup>

Supramolecular chemistry is an interdisciplinary field that investigates the structure and properties of complexes held together by intermolecular interactions.<sup>148</sup> The emergence of this field dates back to the late 1960s, when J. C. Pedersen reported the presence of an unusual interaction between crown-ethers and alkali metal salts.<sup>149</sup> The strength of an intermolecular interaction can be measured by the supramolecular titration method. For example, calorimetric titration was used to determine the strength of the complex of *cis*- and *trans*-dicyclohexyl-18-crown-6 with a potassium ion (Figure 11, A).<sup>150</sup> Although more than two components can make up a supramolecular complex, in the following section only the most typical and simple 1 : 1 equilibria between the components termed host (H) and guest (G) will be discussed (Figure 11, B).

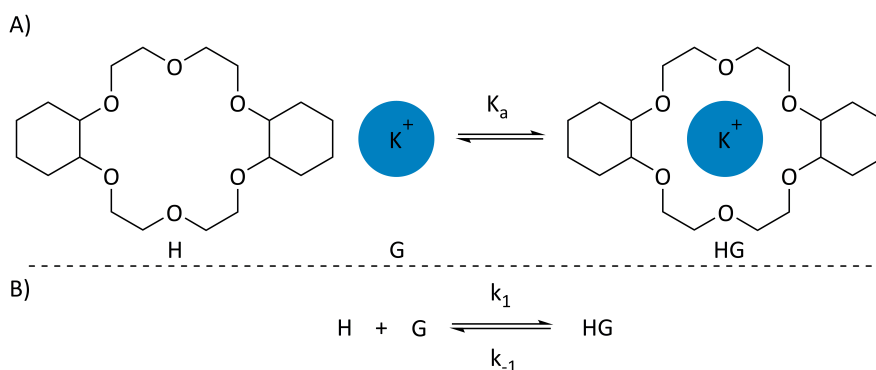


**Figure 11.** Formation of a complex between dicyclohexyl-18-crown-6 with  $K^+$ ; B) Typical equilibria of a 1 : 1 system.

The thermodynamic association constant  $K_a$  (Equation 2) describes how favourable the formation of a complex is compared to the free components and hence is also a measure of the strength of the interactions involved in the formation of the complex. The constant is related to the kinetics of the formation and dissociation of the complex. Therefore, if the measurement of the rate constants is possible, the association constant can also be calculated.

$$\text{Equation 2.} \quad K_a = \frac{[HG]}{[H][G]} = \frac{k_1}{k_{-1}}$$

Alternatively, if the concentration of one of the components can be measured, the initial concentrations and the mass balance of the components can be used to calculate the association constant. This is possible only in exceptional cases. Usually, methods that rely on the indirect determination of the concentration of the complex must be used. In the dilution method, the concentration of one compound (the host) is kept constant, while the concentration of the second compound (the guest) is varied. Both interacting partners can in principle act as either the host or the guest, and therefore the distinction is usually made based on practical factors (the cost, solubility *etc.* of one compound).

The formation of the complex should result in a measurable physical change ( $\gamma$ ), which is monitored throughout the experiment. In the case of NMR spectroscopy, the binding event will lead to a change in the chemical environment and therefore can result in a

change in chemical shift values  $\Delta\delta$ . The observed physical change  $\Delta Y$  is correlated to the concentration of the complex [HG] as  $\Delta Y \sim [HG]$ . It is assumed that during NMR titrations the chemical shift ( $\delta$ ) of interest is the weighted average of the chemical shifts of the free host (H) and the bound host in the complex (HG) due to fast exchange on the NMR timescale. Then, the change in the observed chemical shift ( $\Delta\delta$ ) caused by the addition of the guest correlates with the mole fraction of the complex ( $[HG]/[H_0]$ ) and the difference between the chemical shifts of the complex and free host ( $\delta_{\Delta HG}$ ) (Equation 3).

$$\text{Equation 3} \quad \Delta\delta = \delta_{\Delta HG} \left( \frac{[HG]}{[H_0]} \right)$$

The expected changes from a supramolecular titration experiment can be described by two known ( $[H_0]$  and  $[G_0]$ ) and two unknown ( $K_a$  and  $Y_{\Delta HG}$ , in the case of NMR  $\delta_{\Delta HG}$ ) parameters. The unknown parameters are obtained by non-linear regression of the measured data with the aid of various computer programs that use an algorithm to calculate  $\Delta Y$  and compare it to the measured  $\Delta Y$ . This is done by plotting  $\Delta Y$  as a function of guest added to host, resulting in a titration curve (binding isotherm), which can be fitted to a mathematical model corresponding to the assumed equilibria. During the fitting process, different values for the  $K_a$  and  $Y_{\Delta HG}$  are sampled through the process until a good fit is obtained between Equation 3 and the real experimental data. Moreover, the titration experiment can yield a family of data sets. For example, the change of multiple chemical shifts can be registered with NMR spectroscopy. By carrying out global fitting, the data sets are fitted simultaneously to double the number of data points used in the process and tighten the “error surface” of the model, resulting in a better fit. There are several commercial and custom-written software packages to use for the fitting process, although the chosen program should be compatible with the technique used to gather the data and must handle the binding model of choice.

In the case of NMR spectroscopy, it is possible to obtain good quality spectra with concentrations as low as  $10^{-4}$  M; hence, association constants with values up to  $10^6$  M<sup>-1</sup>, preferably up to  $10^5$  M<sup>-1</sup>, can be directly determined by NMR titration experiments.

## 2 Motivation and aims of the present work

Noncovalent interactions have been successfully used to achieve asymmetric catalysis. Although, XBs offer advantages compared to more studied hydrogen bonds in catalysis, the use of XBs in asymmetric catalysis has so far been limited to only supporting roles. Therefore, achieving asymmetric XB catalysis is highly sought after. The design of a catalyst should ideally be based on an easily modifiable core, as variations in the structure could be needed to reach high levels of activity and selectivity. It was believed that triazole-based XB donors could be outstanding core structures for building a library of catalysts to be applied in asymmetric synthesis. As can be seen from the literature overview, the XB donor ability of halo-triazoles has been described in numerous publications (section 1.2.2) and the possibility of activating substrates with halo-triazoles by XB formation has also been demonstrated (section 1.4). Unfortunately, the interactions between triazole-based XB donors and neutral acceptors have not been well explored.

### The specific aims of the study were:

- to elaborate an efficient synthetic scheme for obtaining enantiomerically pure monodentate or multifunctional XB donors and to characterise their properties in the solid state and in solution;
- to evaluate the XB donor ability of halo-triazoles and halo-triazolium salts with neutral acceptor molecules;
- to examine the influence of the charge, counterions, aromatic substituents and halogen atoms on the donor strength of the triazoles/triazolium salts;
- to explore the viability of using enantiopure triazole-based XB donors as asymmetric catalysts.

### 3 Results and discussion

The results described in this dissertation are based on four publications. The following discussion is organised by predominant themes found in the publications. First, the synthesis of the triazoles and triazolium salts is described (**Publications I – IV**). Then, the donor ability of the synthesised compounds in the solid state is evaluated based on X-ray diffraction analysis of crystal structures (**Publications I, III and IV**) and in solution by  $^1\text{H}$  NMR studies (**Publications I and II**). Finally, the catalytic potential of the XB donors in various reactions is discussed (**Publication IV** and unpublished results).

#### 3.1 Synthesis of halogen bond donors and reference compounds

With the click approach, triazole-based XB donors can be synthesised in a few steps with relative ease (Figure 12, middle). Furthermore, the possibility of choosing from a wide variety of (chiral) azides and alkynes means that a broad range of XB donors with different structural features can be accessed. The influence of these features on the XB donor ability, as well as the catalytic activity, of the triazole-based XB donors can then be explored. With the choice of the alkyne, both the halide substituent (Figure 12, A) and the aromatic substituent can be (Figure 12, B) varied, both of which have a direct influence on the XB donor ability. Also, the substituent pattern of the aromatic ring can be used to introduce stereoisomerism into the XB donors, as atropoisomers might form with sterically crowded aromatic substituents. Quaternisation of the triazole nitrogen atom can make the core even more electron-deficient and increase the XB donor ability of the compounds (Figure 12, D). This can be combined with a change of the counterion, which can influence the solubility and donor ability of the salts (Figure 12, E). Quaternisation can be mimicked by intramolecular hydrogen bonding, without the formation of salts (Figure 12, C). The primary role of the chiral azide is to modify the sterics of the XB donors and through this have access to asymmetric catalysis (Figure 12, F). Furthermore, suitable functional groups can be used to introduce secondary interaction sites into the XB donors, which could be used to enhance the interaction strength between donor and acceptor, or the selectivity of the XB donor towards a certain acceptor (Figure 12, G).

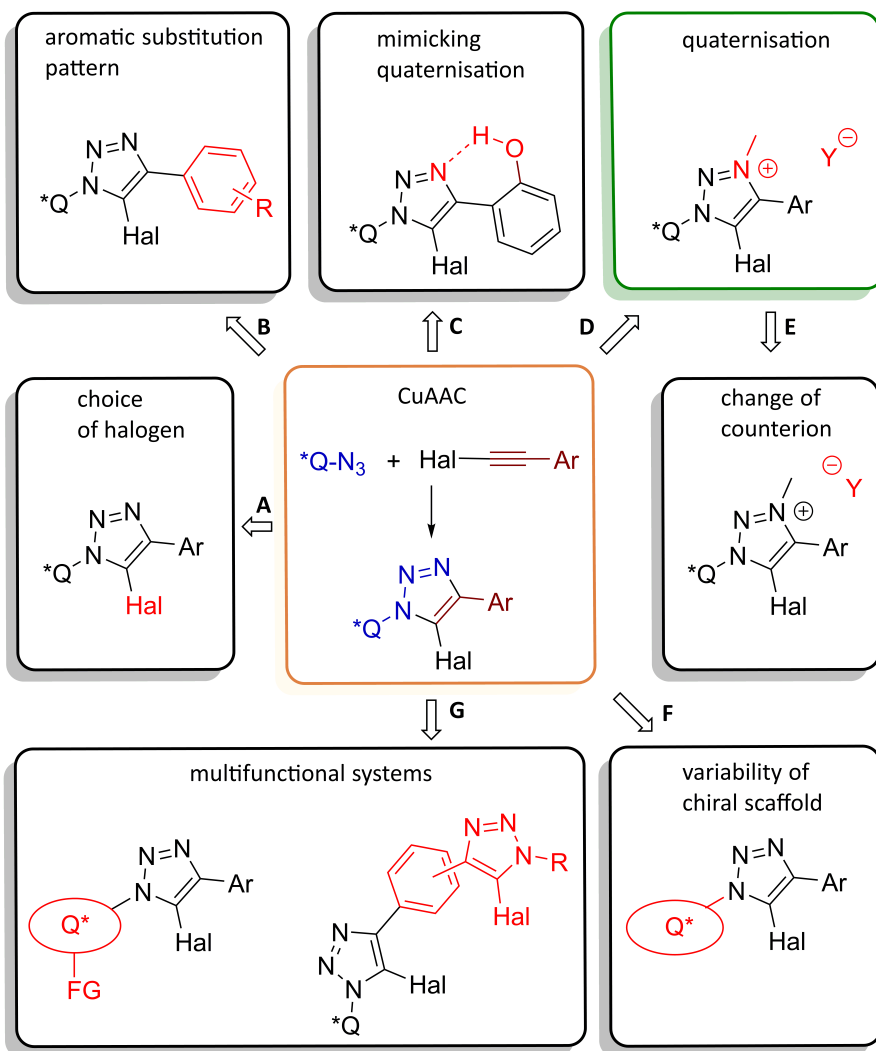
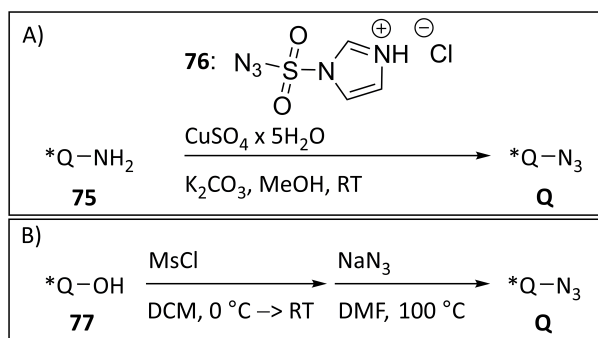


**Figure 12.** Functional group modifications accessible via click approach.

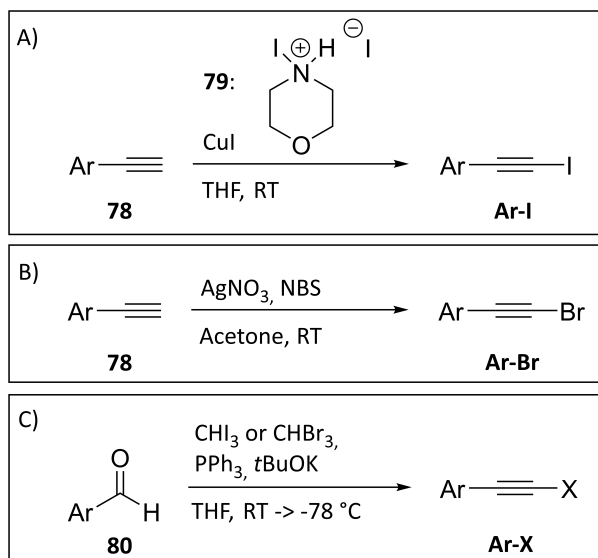
### 3.1.1 Synthesis of 5-halo-1H-1,2,3-triazoles and corresponding hydrogen-analogues

The azides **Q** needed for the click reaction were obtained in one step from amines **75** by azidation with salt **76**<sup>151</sup> (Scheme 11, A), or in two steps from alcohols **77** by mesylation and azidation with NaN<sub>3</sub> (Scheme 11, B). Several of the precursors are accessible directly from the chiral pool.



**Scheme 11.** Synthesis of azides from A) amines **75** or B) alcohols **77**.

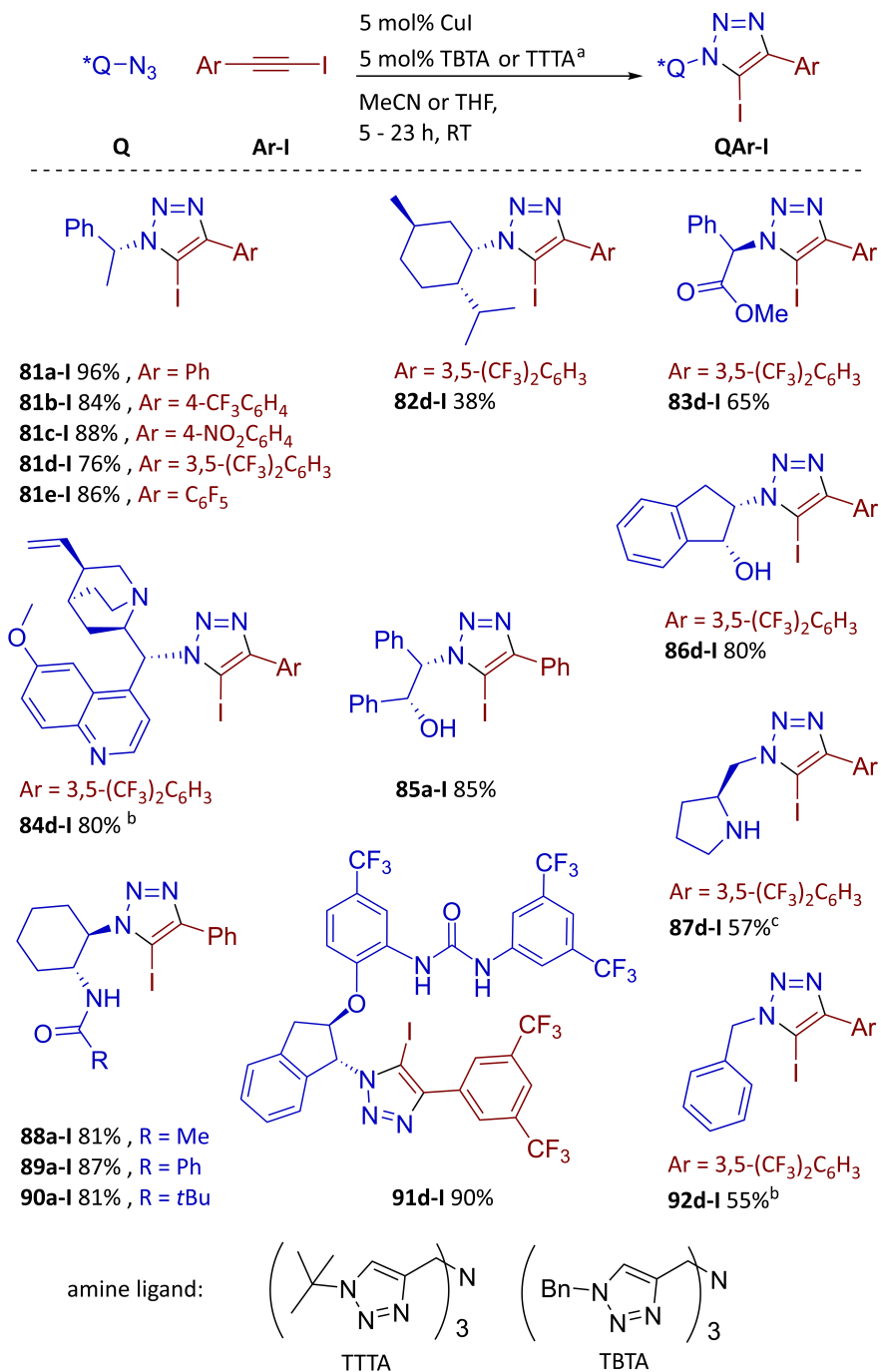
The haloalkynes **Ar-X** were obtained either by iodination of terminal alkynes **78** with *N*-iodomorpholine hydroiodide **79** in the presence of CuI<sup>60</sup> (Scheme 12, A), or by bromination with NBS in the presence of AgNO<sub>3</sub> (Scheme 12, B). The corresponding terminal alkynes **78** were commercially available or were synthesised via a Sonogashira coupling of aryl bromides and trimethylsilylacetylene, followed by TMS deprotection. Alternatively, a Corey-Fuchs-type reaction was also used to synthesise the haloalkynes **Ar-X** directly from aldehydes **80** (Scheme 12, C).<sup>152</sup>



**Scheme 12.** Synthesis of A) iodoalkynes **Ar-I** and B) bromoalkynes **Ar-Br** from terminal alkynes **78** or C) haloalkynes **Ar-X** by the Corey-Fuchs approach from aldehydes **80**.

In the following discussion, the XB donors are referred to by the general code **QAr-X-Y**, in which **Q** refers to a number corresponding to an azide used in the click reaction, **Ar** stands for a letter that corresponds to an aryl substituent. **X** denotes the halogen/hydrogen atom in the triazole and, in the case of triazolium salts, **Y** stands for the counterion, also indicating the number of counterions if multiple counterions are present.





<sup>a</sup> The reactions were run with 0.2 or 0.3 M concentration of the substrate, with MeCN as a solvent with TBTA or THF when TTTA was used; <sup>b</sup> 2 equiv of Et<sub>3</sub>N was used as the amine ligand instead of TTTA or TBTA; <sup>c</sup> combined yield after Boc deprotection of the amino group, yield for the click step: 88%.

**Scheme 13.** Synthesis of 5-iodo-1*H*-1,2,3-triazoles **QAr-I**.

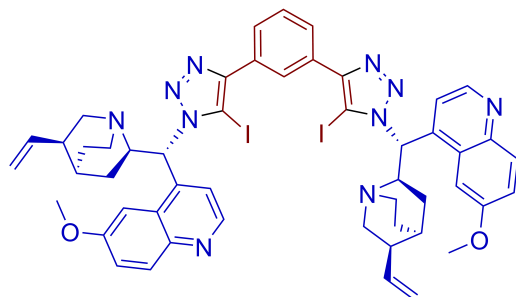
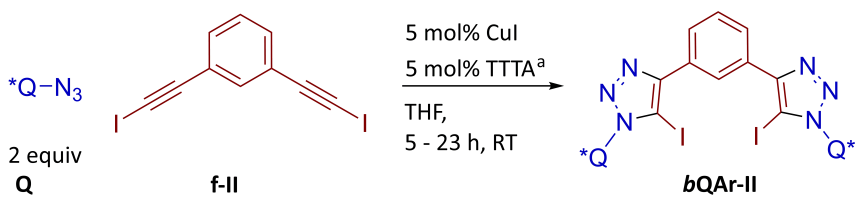
In principle, all of the combinations of triazoles could have been synthesised from the pool of azides and alkynes. However, compounds used to probe the donor strength were mainly synthesised with  $\alpha$ -methylbenzylazide (Scheme 13-17, compounds **81Ar-X** or **81Ar-X-Y**). The lack of other functional groups would have meant that interactions with these triazoles should mainly be XB-based. Initially, a relatively rigid menthol substituent was envisioned to have a role similar to an  $\alpha$ -methylbenzyl substituent, but the click reaction with 3-*epi*-azido menthol was sluggish and gave poor yields for **82d-I** (Scheme 13).

Traditionally, destabilising steric interactions, along with restricted conformational flexibility of the catalyst, have been used to achieve high levels of selectivity.<sup>153</sup> However, flexible catalysts/donors that can form several noncovalent interactions with a partner can lead to a more stable transition state or complex. In the case of **83d-I**, a methyl ester was incorporated into the donor structure, which can lead to stronger binding affinities to XB acceptors containing hydrogen bond donor functionalities. 9-*epi*-Azido quinidine was chosen both for its bulkiness and for the presence of a tertiary amino group that can act as a Brønsted base (Scheme 13, **84d-I**). Compound **87d-I** contains a secondary amino group that can also act as a Brønsted base or as an aminocatalyst with carbonyl compounds, and in this case the iodo-triazole core of **87d-I** can be envisioned as a directing group.

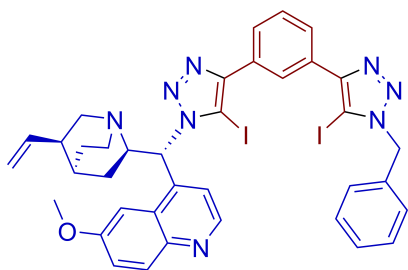
In compounds **85a-I**, **86d-I**, **88a-I**, **89a-I**, **90a-I** and **91d-I**, a hydrogen bond-donating hydroxyl, amido or carbamide group, has been incorporated into the XB donor. As these hydrogen bond donor functionalities contain protons of different acidities, the influence of the secondary hydrogen bond can be probed and used to tune the rigidity of the complexes. Also, the conformational flexibility of the XB donors is affected by the rigidity of the substituent containing the stereocenter, in the case of donor **86d-I** the cyclopentane ring allows little flexibility. With derivatives (**88a-I**, **89a-I** and **90a-I**) from diamino cyclohexane, the substituent of the amido group was varied between a methyl, phenyl or *tert*-butyl substituent, which affect both the acidity of the amido group and its steric environment.

The strength of the XB donor-acceptor complex can also be increased by the introduction of additional XB donor groups into the donor molecule (bi- or multidentate XB donors) if the acceptor molecule (carbonyl compounds, halide anions *etc.*) can form multiple XBs simultaneously. For this reason, diiododiyne **f-II** was used for the synthesis of the bidentate C<sub>2</sub>-symmetric XB donors **b81f-II**, **b84f-II**, **b86f-II** and **b94f-II**, and the unsymmetrical variant **93f-II** (Scheme 14, the letter **b** at the start of the code shows that two molecules of the same azide were incorporated into the triazole). Similarly to monodentate donors, these compounds contain hydrogen bond donors or Brønsted basic sites. It was believed that with bidentate XB donors the substrate would be activated inside the chiral pocket formed by the donor. Greater levels of selectivity might be obtainable with these XB donors as catalysts than with to the use of monodentate donors.

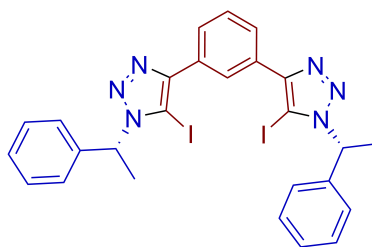
All in all, the click reactions carried out for the synthesis of iodotriazole-based XB donors afforded products in good to excellent yields. The low yield of **82d-I** might have been caused by steric effects (Scheme 13). In the case of **93f-II**, the first click reaction between 1 equiv of diiododiyne **f-II** and 1 equiv of *epi*-azidoquinidine **84** afforded the monocyclised intermediate and the C<sub>2</sub>-symmetric by-product **b84f-II**. Therefore, after the addition of benzyl azide **92**, a mixture of all possible click products from alkyne **f-II**, azides **84** and **92** was obtained, which meant a lower yield of product **93f-II**. The lower yield of **b86f-II** is hard to explain as the click reaction with the same azide afforded **86d-I** with a good yield.



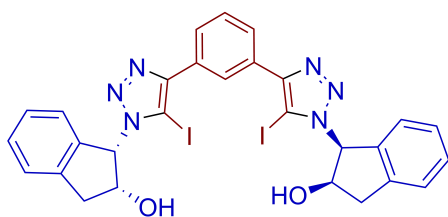
**b84f-II** 60%<sup>b</sup>



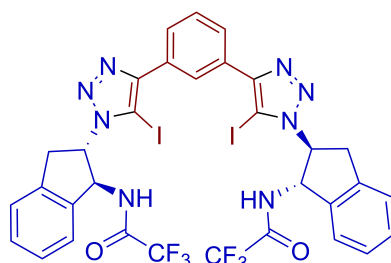
**93f-II** 33%<sup>b,c</sup>



**b81f-II** 74%



**b86f-II** 52%

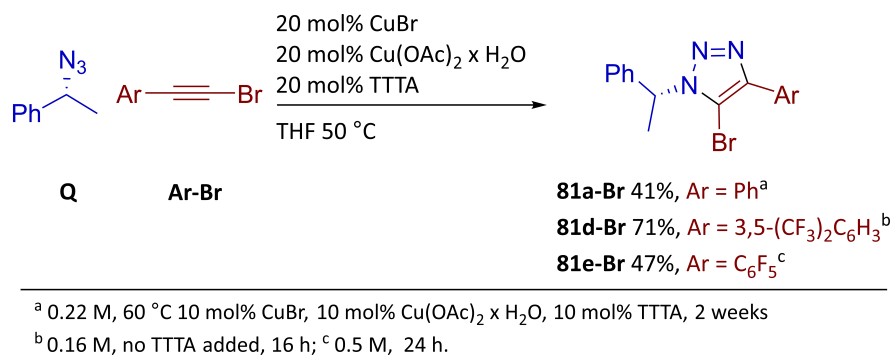


**b94f-II** 94%

<sup>a</sup> The reactions were run with 0.2 or 0.3 M concentration of the substrate; <sup>b</sup> 4 equiv of Et<sub>3</sub>N was used as the amine ligand instead of TTTA; <sup>c</sup> the reaction was started with 1 equiv of 9-*epi*-azido quinidine and 1 equiv of benzyl azide was added subsequently to the reaction mixture.

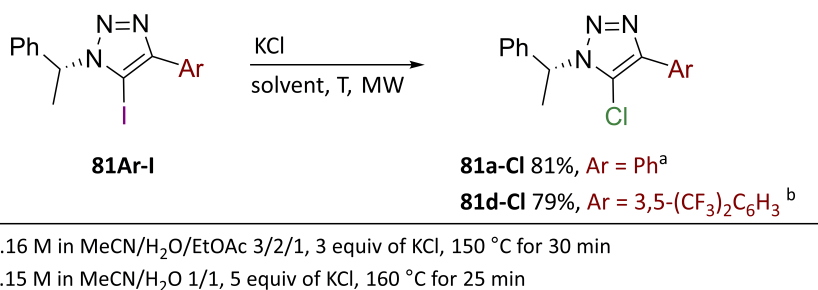
**Scheme 14.** Synthesis of bidentate halotriazole-based XB donors **bQAr-II** and **93f-II**.

For the synthesis of bromo-triazoles, a combination of CuBr and Cu(OAc)<sub>2</sub> was used. First, **81d-Br** was obtained from 1-(bromoethynyl)-3,5-bis(trifluoromethyl)benzene in 71% yield (Scheme 15). In contrast, the reaction with (bromoethynyl)benzene was very sluggish and afforded product **81a-Br** only in 41% yield after two weeks. These conditions proved to be the best, as other minor modifications to the procedure of F. P. J. T. Rutjes *et al.* did not give better results.<sup>58</sup> **81e-Br** was obtained in a higher yield and shorter reaction time, although the addition of TTTA was needed for the reaction to take place at all.



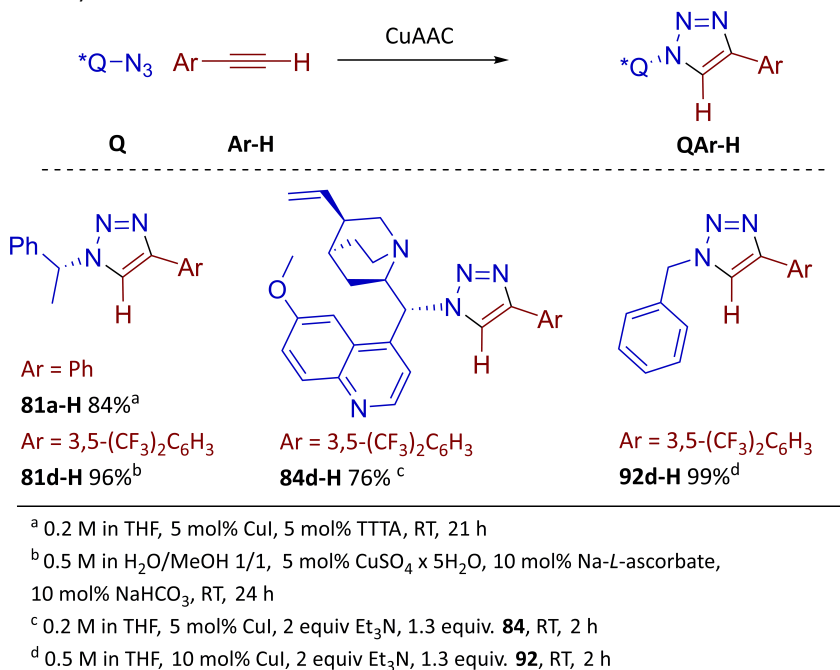
**Scheme 15.** Synthesis of 5-bromo-1H-1,2,3-triazoles **81Ar-Br**.

As XB catalysis is a relatively new catalytic approach, the inclusion of control experiments is highly recommended. These experiments should be used to confirm catalysis by XB activation and to rule out other activation modes. For this reason, the Cl- and H-triazoles were synthesised. Chloro-derivatives are capable of XB formation, but the XB from a chlorine atom should be relatively weak and therefore the donors should generally be less active or even inactive compared to the bromo- and iodo-triazoles. On the other hand, S. Minakata *et al.* have observed higher reactivity of the chloro-derivative compared to the iodo-derivative<sup>133</sup> and a comparison to this result was also of interest at the start of the project. For the synthesis of chloro-triazoles **81a-Cl** and **81d-Cl**, a halogen exchange reaction<sup>64</sup> was carried out starting from iodo-triazoles **81a-I** and **81d-I** in the presence of KCl under microwave conditions, affording the products in very good yields (Scheme 16).



**Scheme 16.** Synthesis of 5-chloro-1H-1,2,3-triazoles **81Ar-Cl**.

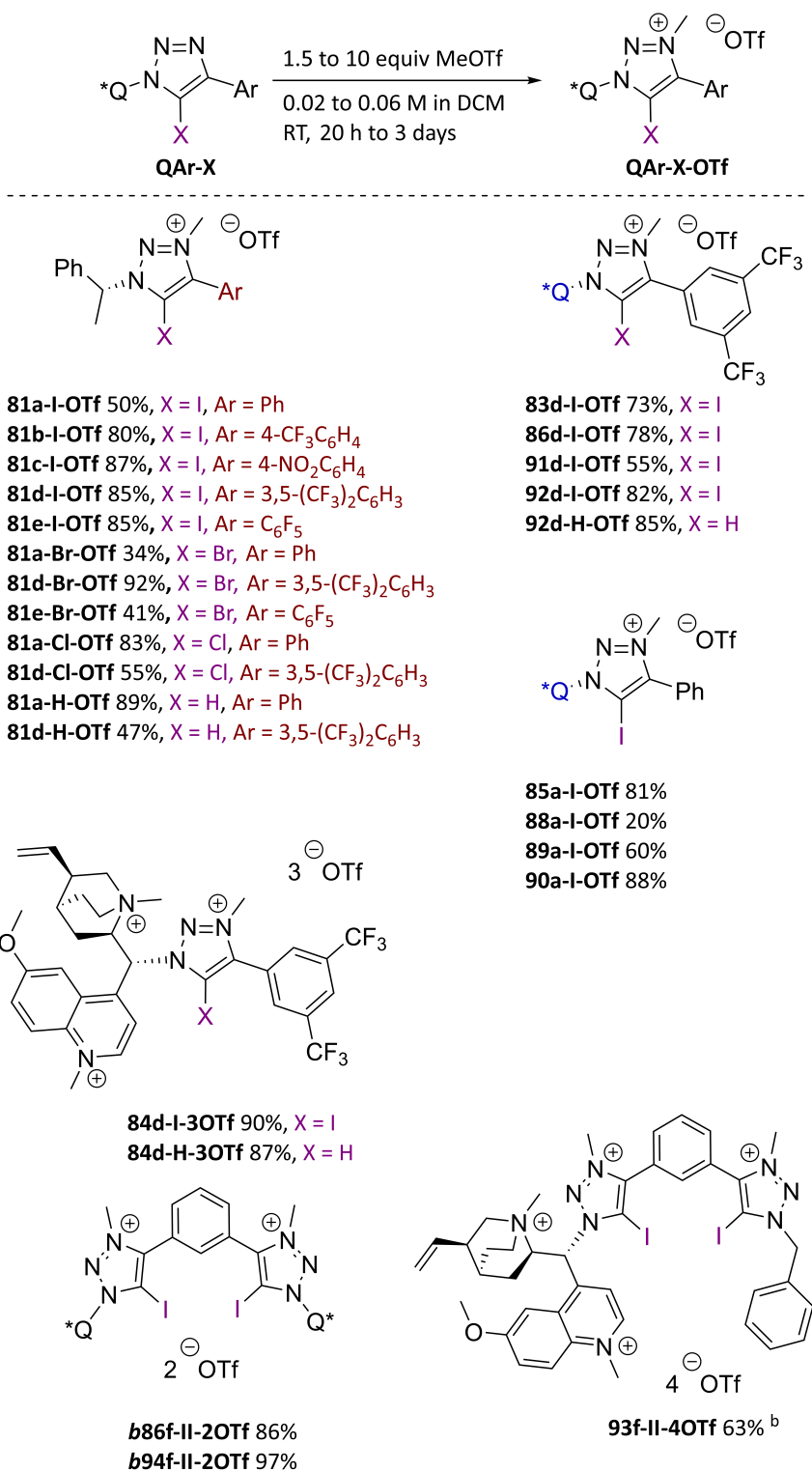
The H-triazoles **81a-H**, **81d-H**, **84d-H** and **92d-H** were also synthesised in very good yields using either CuSO<sub>4</sub> and Na-*L*-ascorbate or CuI in the presence of amine ligands (Scheme 17).



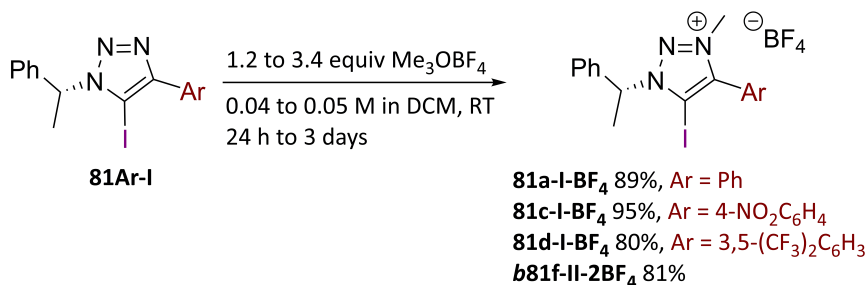
**Scheme 17.** Synthesis of 1H-1,2,3-triazoles QAr-H.

### 3.1.2 Synthesis of 5-halo-1H-1,2,3-triazolium salts and corresponding hydrogen-analogues

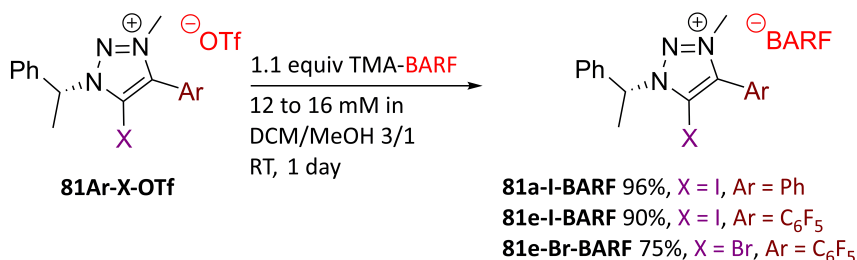
The primary approach to obtain the triazolium salts was quaternisation with methyl triflate (Scheme 18) or trimethyloxonium tetrafluoroborate (Scheme 19). With these reagents almost complete conversions of the starting triazoles into the desired salts were observed. The preferred method of purification was crystallisation, which, depending on the solubility of the salts, resulted in yields varying from 20% to 97% for the triflates and yields from 80% to 95% for the tetrafluoroborates. It is also possible to purify the salts by column chromatography without affecting the yields to a great extent. In the case of **84d-I-3OTf** and **93f-II-4OTf**, other nitrogen atoms were also methylated by methyl triflate. In principle, the protection of the quinoline and quinuclidine nitrogen atoms as *N*-oxides could help avoid this problem.<sup>154,155</sup> However, the oxidation step of the triazole **84d-I** yielded a complex mixture and the desired product could not be isolated. Unfortunately, 9-*epi*-Azido quinidine with protected nitrogen atoms was inactive in the click reaction. Finally, the salts containing the BARF counterion were obtained through the ion exchange of triflate for BARF<sup>134</sup> with yields between 75% and 96% (Scheme 20).



**Scheme 18.** Synthesis of 1H-1,2,3-triazolium trifluoromethanesulfonates.



**Scheme 19.** Synthesis of 5-iodo-1H-1,2,3-triazolium tetrafluoroborates.



**Scheme 20.** Synthesis of 1H-1,2,3-triazolium tetrakis[3,5-bis(trifluoromethyl)phenyl]borates.

## 3.2 Halogen bond donor ability of the triazoles and triazolium salts in the solid state

Throughout the project several crystal structures were obtained from the synthesised compounds. These structures confirmed that the synthesised compounds acted as XB donors in the solid state. In general, the compounds can be categorised in two groups: donors that formed an XB with a second donor molecule and donors that formed an XB with the counterion.

### 3.2.1 Compounds with a halogen bond between two donor molecules

This group is mostly made up of neutral compounds, in which a nitrogen atom of the triazole core (Figure 13, A) or the quinoline core (Figure 13, B) acted as an XB acceptor. Also, in the case of **89a-I-OTf**, an XB was formed to a carbonyl group (see **Publication III**), although crystal structures of triazolium salts contained mostly XBs to the counterion. As all the formed XBs were near linear and had  $R_{\text{XB}}$  values below 0.9, the formed interactions can be considered relatively strong (Table 5). The XB formed by compound **81d-I** was weaker than the XB formed by **81a-I**. This can be explained by the fact that although the stronger electron-withdrawing aromatic substituent increased the donor ability of **81d-I**, it also decreased the acceptor ability of the triazole core (Table 5, entry 2). As expected, the bromo-derivative **81a-Br** formed a weaker XB compared to the other donors (Table 5, entry 6). The potential of compound **b84f-II** to act as a bidentate XB donor can be seen from its crystal structure (see **Publication I**). As the donor sites were facing the same side of the donor in the crystal structure, in the presence of a suitable acceptor bidentate binding can in principle be achieved.

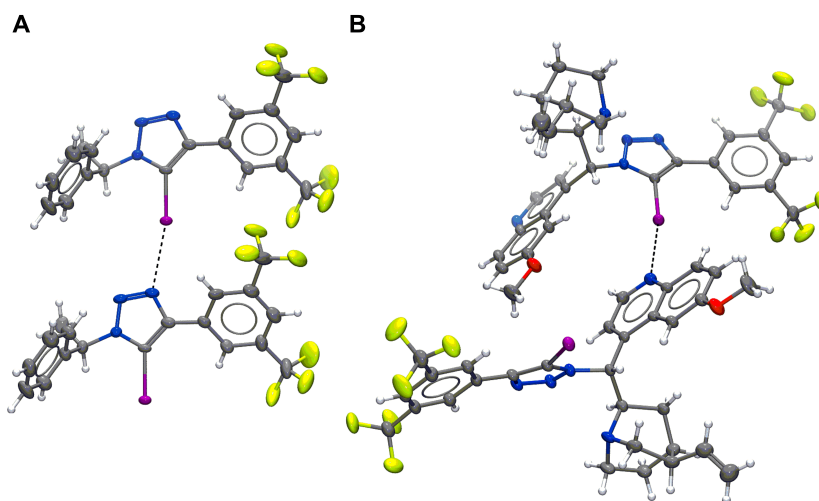


**Figure 13.** X-ray crystal structures of **81d-I** (A) and **84d-I** (B). The atomic displacement ellipsoids are drawn at a 50% probability level.

**Table 5.** Solid-state parameters for compounds forming an XB to a second donor molecule.

Entry	XB donor	XB system	Angle	Distance	$R_{XB}^a$
			C – I ... A (°)	X ... A (Å)	
1	<b>81a-I</b>	C – I ... N <sub>triazole</sub>	167.1	2.854	0.81
2	<b>81d-I</b>	C – I ... N <sub>triazole</sub>	167.4	2.940	0.83
3	<b>82d-I</b>	C – I ... N <sub>triazole</sub>	168.2	2.947	0.84
4	<b>84d-I</b>	C – I ... N <sub>quinoline</sub>	168.8	2.749	0.78
5	<b>b84f-II</b>	C – I ... N <sub>quinoline</sub>	171.4	2.785	0.79
6	<b>81a-Br</b>	C – Br ... N <sub>triazole</sub>	166.0	2.928	0.86
7	<b>89a-I-OTf</b>	C – I ... O <sub>carbonyl</sub>	170.6	2.724	0.78

<sup>a</sup> Sum of van der Waals radii calculated based on the values defined by Bondi.<sup>156</sup> A = Acceptor

### 3.2.2 Compounds forming a halogen bond to the counterion

As the basic nitrogen atom of the triazole core was blocked during the quaternisation process, with limited options available the halogen atom of a triazolium salt formed an XB with the counterion (Figure 14). As with the previous XB donors, relatively strong and linear XBs were formed to the counterion with  $R_{XB}$  values between 0.78 and 0.88 and angles between 158.7° and 172.7° (Table 6). Comparing donors containing different halogen atoms (Table 6, entries 3 - 5), the formed XBs corresponded to the polarisability order of halogens. **81d-I-OTf** formed a stronger XB than donor **81d-Br-OTf** and in the case of **81d-Cl-OTf** no XB was formed, with the counterion placing itself above the triazolium core. Surprisingly, compounds containing the electron-withdrawing *para*-nitrophenyl substituent (Table 6, entries 2 and 9) gave weaker XBs in the solid state than compounds **81b-I-OTf** and **81a-I-BF<sub>4</sub>** (Table 6, entries 1 and 8). In the case of tetrafluoroborate triazolium salts, it is very difficult to explain the observed trends of XB strength. Compounds **81c-I-BF<sub>4</sub>** and **81d-I-BF<sub>4</sub>** formed weaker XBs than the triflate containing salts



**81c-I-OTf** and **81d-I-OTf** (Table 6, comparing entries 9 and 10 to entries 2 and 3), which is in line with the lesser coordinating ability of the tetrafluoroborate counterion. On the other hand, with **81a-I-BF<sub>4</sub>**, one of the strongest XBs in the series was observed (Table 6, entry 8).

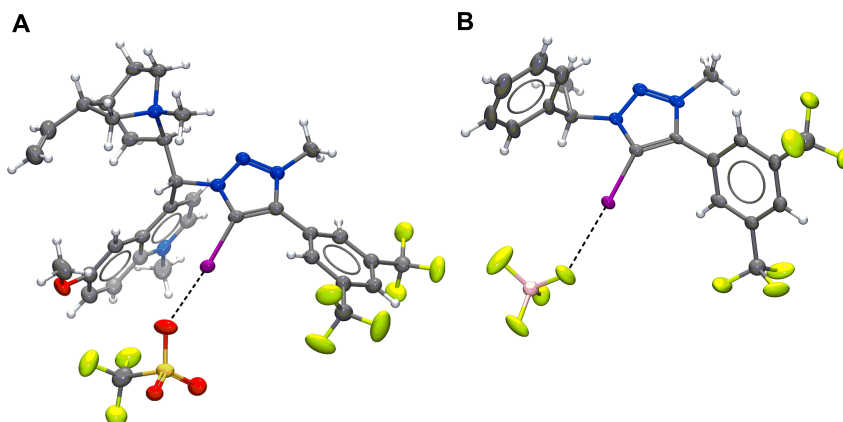


**Figure 14.** X-ray crystal structures of **84d-I-OTf** (A) and **81d-I-BF<sub>4</sub>** (B). Only one OTf<sup>-</sup> counterion, the one involved in the XB is included in the figure of **84d-I-OTf**; the rest are omitted for clarity. The atomic displacement ellipsoids are drawn at a 50% probability level.

**Table 6.** Solid-state parameters for compounds forming an XB to the counterion.

Entry	XB donor	XB system	Angle C – I ... A (°)	Distance X ... A (Å)	R <sub>XB</sub> <sup>a</sup>
1	<b>81b-I-OTf</b>	C – I ... OSO <sub>2</sub> CF <sub>3</sub>	166.5	2.847	0.81
2	<b>81c-I-OTf</b>	C – I ... OSO <sub>2</sub> CF <sub>3</sub>	172.2	2.929	0.84
3	<b>81d-I-OTf</b>	C – I ... OSO <sub>2</sub> CF <sub>3</sub>	168.9	2.82	0.81
4	<b>81d-Br-OTf</b>	C – Br ... OSO <sub>2</sub> CF <sub>3</sub>	163.6	2.870	0.85
5	<b>81d-Cl-OTf</b>	C – Cl ... –	–	–	–
6	<b>83d-I-OTf</b>	C – I ... OSO <sub>2</sub> CF <sub>3</sub>	166.1	2.83	0.81
7	<b>84d-I-OTf</b>	C – I ... OSO <sub>2</sub> CF <sub>3</sub>	172.7	2.715	0.78
8	<b>81a-I-BF<sub>4</sub></b>	C – I ... FBF <sub>3</sub>	171.4	2.736	0.79
9	<b>81c-I-BF<sub>4</sub></b>	C – I ... FBF <sub>3</sub>	167.4	3.025	0.88
10	<b>81d-I-BF<sub>4</sub></b>	C – I ... FBF <sub>3</sub>	158.7	2.890	0.84

<sup>a</sup> Sum of van der Waals radii calculated based on the values defined by Bondi.<sup>156</sup> A = Acceptor

### 3.3 XB donor ability of the triazoles and triazolium salts in solution

To determine the donor ability of the synthesised compounds in solution, titration experiments by <sup>1</sup>H NMR spectroscopy on a 400 MHz or an 800 MHz instrument were carried out, which provided binding affinities for XB donor–acceptor pairs. During the titration experiments the concentration of the XB donor was kept constant while increasing amounts of acceptor (Figure 15; A) were added to the solution. CDCl<sub>3</sub> was used

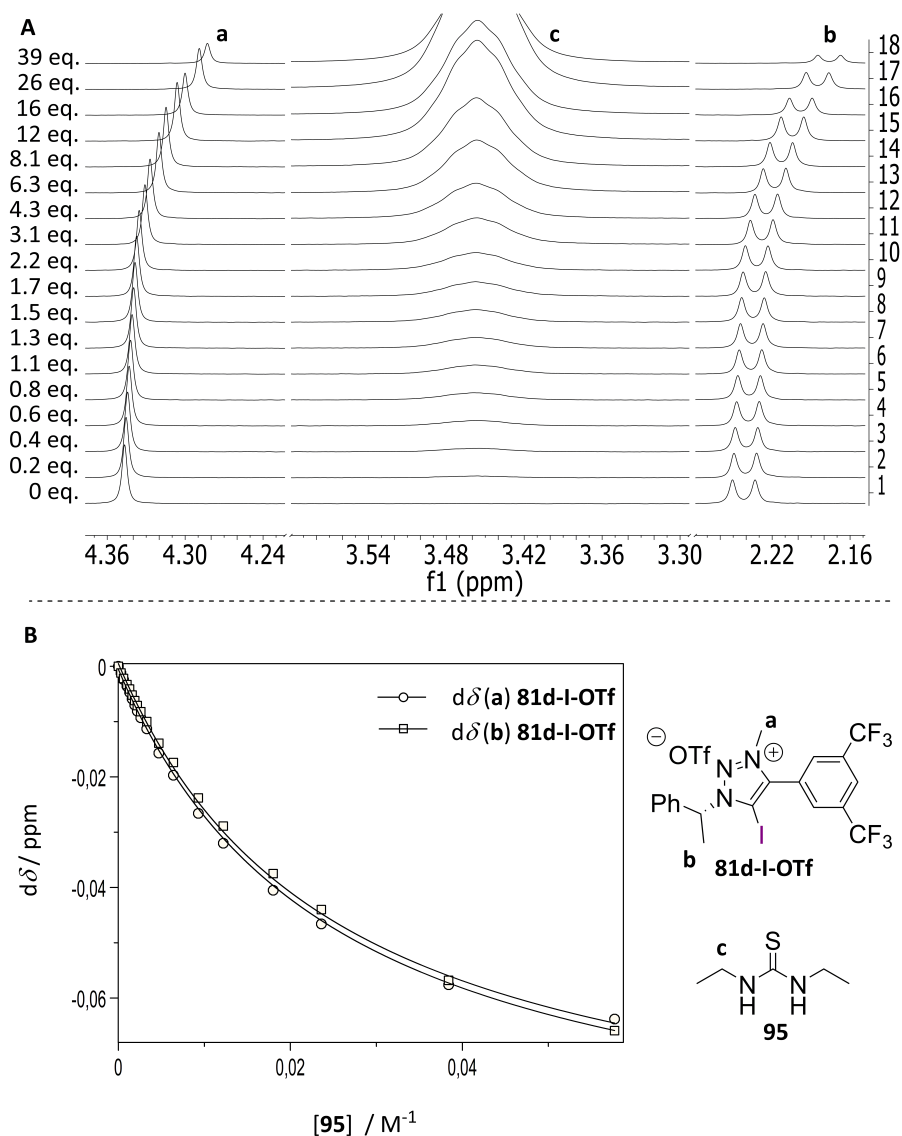


**Figure 15.** A) Outtake of  $^1\text{H}$  NMR spectra ( $\text{CDCl}_3$ , 297 K, 400 MHz) from the titration experiment of **81d-I-OTf** (1.5 mM) with thiourea **95** showing the methyl protons **a** and **b** of **81d-I-OTf** and the methylene protons **c** of **95**. From outtake 1 to 18 increasing equivalents of **95**. B) The corresponding binding isotherm with global fitting of methyl protons **a** and **b**;  $K_a = 42 \pm 2 \text{ M}^{-1}$ .

as the solvent in the experiments as the triazolium salts and acceptors were sufficiently soluble in it and the binding caused observable chemical shift changes of the relevant proton signals. The upfield shifts of the methyl protons **a** and **b** of the XB donor were used as input data for the calculation of binding constants for a 1:1 binding model by non-linear least-squares global fitting using the HypNMR2008<sup>157,158</sup> (Figure 15, B) or BindFit program.<sup>159,160</sup> The results of the titration experiments can be categorised into two groups based on the acceptor atom participating in the bonding event: oxygen or sulphur in (thio)ureas and nitrogen in imines or amines.

### 3.3.1 Titration experiments using acceptors with an oxygen or a sulphur atom

For the first series of titration experiments thioureas were chosen as acceptors (Figure 16). Based on HSAB theory,<sup>161</sup> a soft sulphur atom might be compatible with the soft iodine or bromine atom of the donor and therefore give a strongly bound complex. Despite this, sulphur-based acceptors have not been used as widely in XB chemistry as oxygen- or nitrogen-based acceptors,<sup>13</sup> although there have been examples of sulphur acting as a stronger XB acceptor than oxygen.<sup>105,106</sup> Thiocarbonyl compounds have been used in synthesis, both as reagents and catalysts.<sup>162,163</sup> Furthermore, XBs have been used to activate thioamides in the synthesis of benzoxazoles<sup>140</sup> and to enhance the catalytic activity of thioureas in the *N*-glycofunctionalisation of amides.<sup>164</sup> Therefore, the properties of XBs in terms of thiocarbonyl compounds in solution are of interest in different catalytic applications.

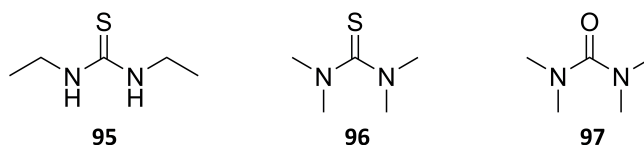


**Figure 16.** Sulphur- and oxygen-based XB acceptors.

The binding constants between diethylthiourea and XB donors were relatively small, but the formation of a complex in solution was favoured over the free acceptor or donor (Table 7). Surprisingly, complex **[95 – 81d-Cl-OTf]** (Table 7, entry 3) was stronger than complex **[95 – 81d-Br-OTf]** (Table 7, entry 2), which does not align with the polarisability order of the halogens. In addition, compound **83d-I-OTf** (Table 7, entry 7), with an ester functionality instead of a methyl group, also bound strongly to diethylthiourea **95** compared to **81d-I-OTf** (Table 7, entry 1). These observations can be explained when a comparison is made to the binding constants obtained with tetramethylthiourea **96**, which gave much lower values (Table 7, entries 9–12). As tetramethylthiourea **96** lacked the acidic NH protons present in diethylthiourea **95**, it is reasonable to assume that the acidic protons of **95** contributed to the observed binding affinities. As chlorine is a stronger hydrogen bond acceptor than bromine, the affinity constant of the **[95 – 81d-Cl-OTf]** complex was higher than that of the **[95 – 81d-Br-OTf]** complex (Table 7, comparing entries 3 and 2). Compound **83d-I-OTf** contained an ester functionality that could have acted as an additional hydrogen bond acceptor site resulting in a higher affinity constant for the **[95 – 83d-I-OTf]** complex (Table 7, comparing entry 7 to 1). Nevertheless, the iodine containing compounds **81d-I-OTf** and **83d-I-OTf** still favoured the formation of a complex in solution with tetramethylthiourea **96**, in contrast to compounds **81d-Br-OTf** and **81d-Cl-OTf**, which did not favour complex formation with **96** (Table 7, entries 10 and 11). **81d-H-OTf** did not interact with thiourea **95** (Table 7, entry 4). Therefore, complexes of iodo-triazolium salts and thioureas were formed through XBs.

**Table 7.** Association constant  $K_a$  values<sup>a</sup> for XB donor pairs with sulphur- and oxygen-based acceptors.

Entry	Donor	Acceptor	$K_a$ ( $M^{-1}$ )
1	81d-I-OTf	95	42 ± 2
2	81d-Br-OTf	95	11 ± 1
3	81d-Cl-OTf	95	29 ± 6 <sup>b</sup>
4	81d-H-OTf	95	–
5	81b-I-OTf	95	35 ± 2
6	81a-I-OTf	95	33 ± 1
7	84d-I-OTf	95	129 ± 12 <sup>c</sup>
8	81d-I-BF <sub>4</sub>	95	58 ± 1
9	81d-I-OTf	96	12 ± 1
10	81d-Br-OTf	96	0.10 ± 0.02 <sup>d</sup>
11	81d-Cl-OTf	96	0.05 ± 0.02 <sup>d</sup>
12	84d-I-OTf	96	20 ± 4 <sup>c</sup>
13	81d-I-OTf	97	6 ± 1

<sup>a</sup> Measured by <sup>1</sup>H NMR spectroscopy in CDCl<sub>3</sub> (400 MHz, 297 K, 1.5 mM donor) and calculated by global fitting of the change in the chemical shifts of methyl protons **a** and **b** to a 1 : 1 binding isotherm using HypNMR2008;<sup>157,158</sup> with the corresponding fitting errors. <sup>b</sup> Fitting based on the change in the chemical shift of methyl protons **b**. <sup>c</sup> Fitting based on the change in the chemical shift of methyl protons **a**. <sup>d</sup> Titration experiment carried out with a 15 mM solution of the donor, calculated by global fitting to a 1 : 1 binding isotherm using SigmaPlot Version 13.0.

With the introduction of the tetrafluoroborate counterion, the value of the affinity constant was increased by 38%, compared to the affinity constants of complexes [95 – 81d-I-OTf] and [95 – 81d-I-BF<sub>4</sub>] (Table 7, entries 1 and 8). This can be explained by the less coordinating nature of tetrafluoroborate counterion compared to the triflate counterion.<sup>165</sup> The use of more electron-rich aromatic substituents caused a decrease of 17% and 21% in the corresponding binding affinities for the complexes of [95 – 81b-I-OTf] and [95 – 81a-I-OTf] compared to that of the binding affinity for the [95 – 81d-I-OTf] complex (Table 7, comparing entries 5 and 6 to entry 1). Thus, in these examples the aromatic substituent has a smaller influence on the donor ability of the triazolium salts compared to the role of the halogen atom or the counterion. The affinity constant for the complex of tetramethylurea **97** and **81d-I-OTf** was half the size of the affinity constant for the complex of tetramethylthiourea **96** and **81d-I-OTf** (Table 7, comparing entries 9 and 13). This demonstrates the higher affinity of the iodine atom to a sulphur atom than an oxygen atom.

### 3.3.2 Titration experiments using acceptors with a nitrogen atom

The formation of a complex between an imine and an XB donor can be used to activate the imine towards a reaction. As described earlier, this strategy has been used to activate imines by XBs in aza-Diels-Alder reactions (Table 3, Table 4). Therefore, the ability of the synthesised triazole-based XB donors to form complexes with imines would show that the XB donors might also be used as activators. Although the addition of imine **41** (Figure 17) to the donor **81d-I-OTf** brought about an upfield shift of the methyl protons **a** and **b**, the obtained data could not be fitted to a 1 to 1 binding model (Table 8, entry 1).

With a more electron-rich imine **98**, fitting to a 1 to 1 binding model was possible and the complex could be characterised with an affinity constant value of  $8 \pm 1 \text{ M}^{-1}$  (Table 8, entry 2). Although small, it is about an order of magnitude larger than the previously described examples between an imine and haloimidazolium triflates **43X** (Table 3), which was successfully used to activate that imine in an aza-Diels-Alder reaction.<sup>133</sup>

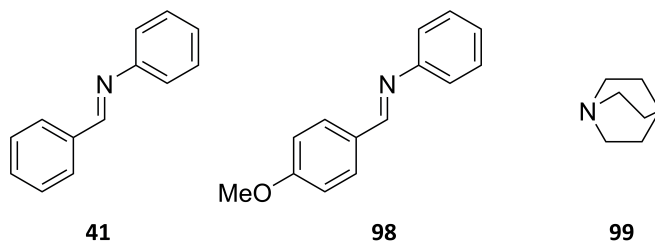


**Figure 17.** Nitrogen-based XB acceptors.

**Table 8.** Association constant  $K_a$  values<sup>a</sup> for XB donor pairs with nitrogen-based acceptors.

Entry	Donor	Acceptor	$K_a$ ( $\text{M}^{-1}$ )
1	<b>81d-I-OTf</b>	<b>41</b>	– <sup>b,c,d</sup>
2	<b>81d-I-OTf</b>	<b>98</b>	$8 \pm 1$ <sup>b,c</sup>
3	<b>81a-I-OTf</b>	<b>99</b>	$57 \pm 5$
4	<b>81a-I-BARF</b>	<b>99</b>	$(1.23 \pm 0.01) \times 10^3$
5	<b>81c-I-OTf</b>	<b>99</b>	$257 \pm 12$ <sup>e</sup>
6	<b>81c-I- BF<sub>4</sub></b>	<b>99</b>	$284 \pm 12$
7	<b>81e-I-OTf</b>	<b>99</b>	$703 \pm 6$
8	<b>81e-I-BARF</b>	<b>99</b>	$(1.1 \pm 0.3) \times 10^4$
9	<b>81a-Br-OTf</b>	<b>99</b>	$(2.98 \pm 0.02) \times 10^{-3}$ <sup>e</sup>
10	<b>81e-Br-BARF</b>	<b>99</b>	– <sup>f</sup>
11	<b>81a-H-OTf</b>	<b>99</b>	$(3.17 \pm 0.01) \times 10^{-5}$
12	<b>81e-I</b>	<b>99</b>	$2.0 \pm 0.3$ <sup>c</sup>

<sup>a</sup> Measured by <sup>1</sup>H NMR spectroscopy in CDCl<sub>3</sub> (800 MHz, 298 K, 1.0 mM donor).  $K_a$  is the average value, based on global fitting of the change in the chemical shifts of methyl protons **a** and **b** to a 1 : 1 binding isotherm of BindFit;<sup>159,160</sup> with corresponding standard errors that are the calculated mean values of two parallel experiments. <sup>b</sup> Measured by <sup>1</sup>H NMR spectroscopy in CDCl<sub>3</sub> (400 MHz, 297 K, 1.5 mM donor) and calculated by global fitting of the change in the chemical shifts to a 1 : 1 binding isotherm using HypNMR2008;<sup>157,158</sup> with the corresponding fitting errors. <sup>c</sup> Fitting based on the change in the chemical shift of methyl protons **b**. <sup>d</sup> The data could not be fitted. <sup>e</sup> 1.5 mM solution of donor. <sup>f</sup>  $K_a$  could not be determined due to the instability of XB donor during the experiment.

The previously described affinity constants were relatively low and therefore the effect of structural modifications on the XB donors' binding ability was difficult to fully assess. Because of this, quinuclidine **99** was chosen as an acceptor in a new series of titration experiments. As quinuclidine is a strong Lewis base, it was able to form a complex even with the neutral donor **81e-I** with a binding constant value of  $2.0 \pm 0.3 \text{ M}^{-1}$  (Table 8, entry 12). Therefore, substituents with enough electron-withdrawing power can

be used to make iodo-triazoles strong enough donors to form complexes in solution with neutral acceptors, examples of which are not that common.<sup>43</sup> Complex formation in the case of the neutral triazole also made it possible to give an estimate of the importance of the introduction of charge. The difference between affinity constant values for the complexes of **[99 – 81e-I]** and **[99 – 81e-I-OTf]** was more than two orders of magnitude (Table 8, comparing entries 12 and 7). Triazolium salt **81e-I-BARF** should provide a better representation for a “naked” cationic backbone, as the BARF counterion is much less coordinating than the triflate counterion, which can compete with quinuclidine more strongly for XB formation. In this case, the difference in binding affinity of the neutral donor compared to the cationic donor amounts to four orders of magnitude (Table 8, comparing entries 12 and 8).

The influence of the aromatic substituents can be estimated by a comparison of affinity constants for the complexes of **[99 – 81a-I-OTf]**, **[99 – 81c-I-OTf]** and **[99 – 81e-I-OTf]** (Table 8, comparing entries 3, 5 and 7). As the electron-withdrawing ability of the substituents was increased, the corresponding affinity constants were increased from 57 M<sup>-1</sup> to 257 M<sup>-1</sup> and 703 M<sup>-1</sup>. The tetrafluoroborate and triflate counterions had a similar influence on the donor ability, as the affinity constant for the **[99 – 81c-I-BF<sub>4</sub>]** complex was only 11% higher than the affinity constant for the **[99 – 81c-I-OTf]** complex (Table 8, comparing entries 5 and 6). On the other hand, a 22-fold and a 16-fold increase was caused by the introduction of the non-coordinating BARF counterion, comparing donor **81a-I-OTf** to **81a-I-BARF** (Table 8, entries 3 and 4) and **81e-I-OTf** to **81e-I-BARF** (Table 8, entries 7 and 8). Therefore, the BARF counterion had a significant influence on the XB donor ability of the triazolium salts. The introduction of the perfluorophenyl substituent had a similar, yet slightly smaller, influence on the XB donor ability.

In the case of compound **81a-H-OTf**, the formation of a complex to quinuclidine was not favoured in solution (Table 8, entry 11). This demonstrated that the complexes previously described were formed through XBs. Also, bromo-derivative **81a-Br-OTf** did not form a favourable complex in solution with quinuclidine (Table 8, entry 9). This is similar to the lack of interaction between **81d-Br-OTf** and tetramethylthiourea **96** (Table 7, entry 10). Compound **81e-Br-BARF**, containing the electron-deficient perfluorophenyl substituent and the non-coordinating BARF counterion, was also used in a titration experiment with quinuclidine. Changes to the shifts of methyl protons were observed by the addition of quinuclidine, but compound **81e-Br-BARF** decomposed during the experiment and no affinity constant was determined (Table 8, entry 10).

### 3.3.3 Studies of the enantiodiscrimination ability of XB donors in solution

First, a <sup>1</sup>H NMR spectrum of a 1 to 1 mixture of XB donor **81d-I-OTf** and chiral thiourea **(S,S)-100** was measured (Figure 18). A comparison of the spectrum of this mixture (Figure 18, B) to the spectrum of free donor (Figure 18, D) and the spectrum of free thiourea (Figure 18, A) at the same concentrations revealed the presence of an interaction between **81d-I-OTf** and **(S,S)-100**. Significant upfield shifts of the signals belonging to the methyl protons **a** and **b** of the donor were observed, which corresponds to the increase in electron density on the donor through XB formation. At the same time, downfield shifts of the signals belonging to the thiourea were also observed, which correlates with the decrease in electron density on the acceptor upon XB formation. The <sup>1</sup>H NMR spectrum was also measured for the **81d-I-OTf** and **(R,R)-100** pair (Figure 18, C), with similar trends in the shifts of the signals belonging to the donor and thiourea. However,

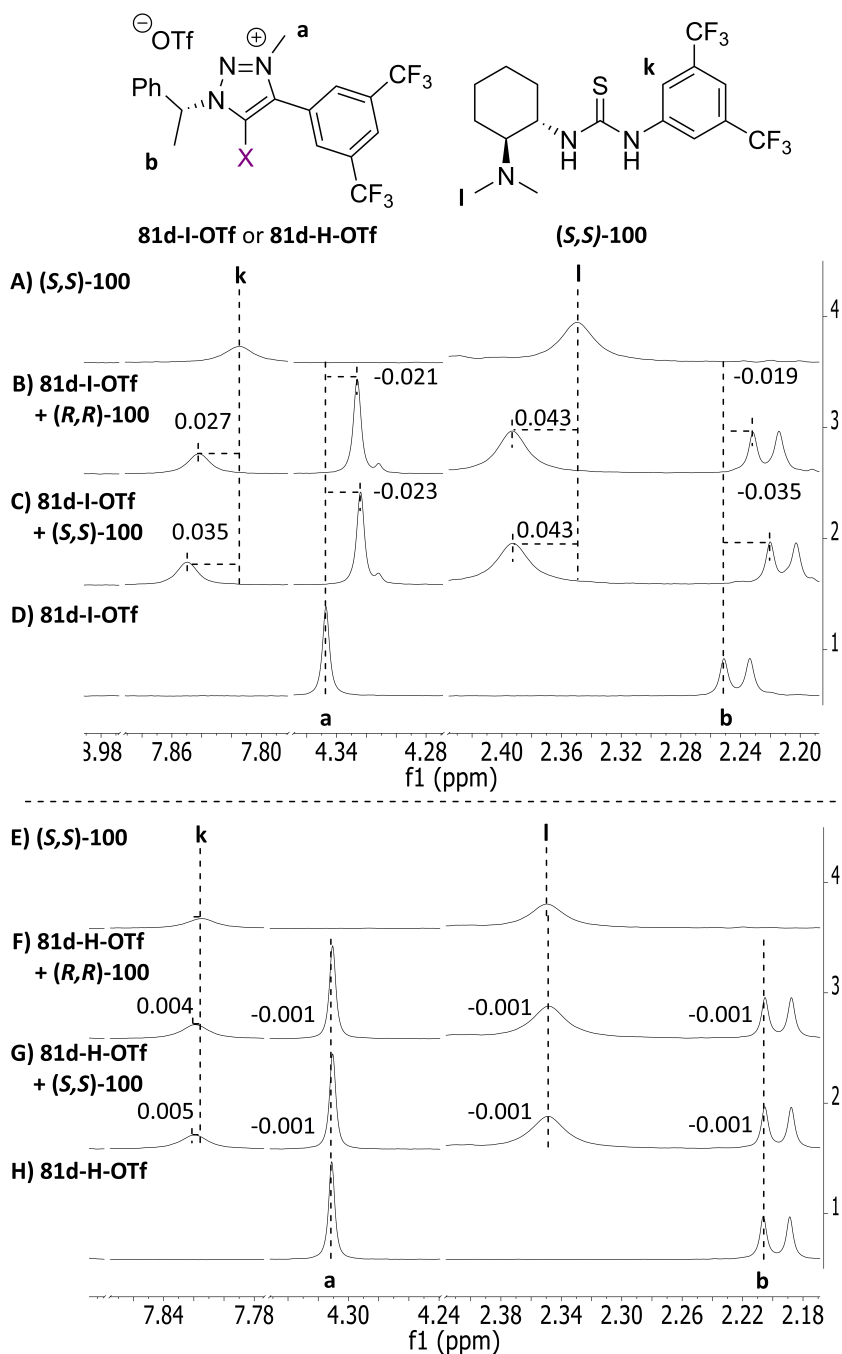


**Figure 18.** <sup>1</sup>H NMR spectra in CDCl<sub>3</sub> (1.5 mM, 297 K, 400 MHz) of A) (S,S)-100, B) a 1:1 mixture of 81d-I-OTf and (S,S)-100, C) a 1:1 mixture of 81d-I-OTf and (R,R)-100, D) 81d-I-OTf; E) (S,S)-100, F) a 1:1 mixture of 81d-H-OTf and (S,S)-100, G) a 1:1 mixture of 81d-H-OTf and (R,R)-100; H) 81d-H-OTf. Positive values indicate a downfield shift and negative values an upfield shift (in ppm) compared with the corresponding resonance signals in either the spectrum of free 81d-I-OTf or (S,S)-100.

there was a difference between the signals belonging to the methyl protons **b** of the donor and aromatic protons **k** belonging to the thiourea in the spectra of the diastereomeric complexes (Figure 18, comparing B and C). Therefore, the complexes were structurally significantly different enough to cause distinctive  $^1\text{H}$  NMR shifts and so **81d-I-OTf** was able to discriminate between the enantiomers of **100**. The formation of the complexes was also supported by the fact that the hydrogen analogue **81d-H-OTf** did not interact with either enantiomer of **100** (Figure 18, E–C). This indicates that the iodine atom was crucial in the process and most likely the complex was held together by the formed XB. As the thiourea contained acidic NH protons, it is reasonable to assume that these contributed to the binding event, as in the case of diethylthiourea **95** (Table 7).

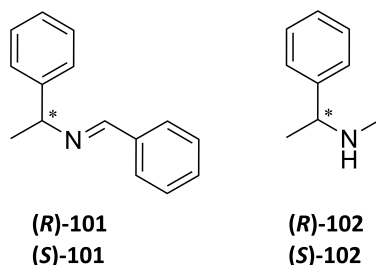


**Figure 19.** Chiral acceptors used in the titration experiments.

Next, titration experiments were carried out using the strongest XB donor **81d-I-BARF** with acceptors **(R)-101** and **(S)-101** (Figure 19). As there was no significant difference between the values of the association constants (Table 9, comparing entries 1 and 2), the donor was not able to discriminate between the enantiomers of imine **101**. Then, amines **(R)-102** and **(S)-102** were used as acceptor molecules to get a stronger interaction, in which case the significance of the differences could hopefully be more adequately determined. Again, the association constants were within the margin of error and no enantiodiscrimination took place (Table 9, comparing entries 3 and 4). Therefore, the  $\alpha$ -methylbenzyl substituent was not sufficiently bulky to differentiate between the enantiomers of the XB acceptors through steric repulsion or other noncovalent interactions. This seemed to be the cause of the large iodine atom, which kept the donor and acceptor at a distance. It is also likely that the contribution from hydrogen bonds, in the case of donor **81d-I-OTf** and enantiomers of thiourea **100**, led to the formation of complexes with different  $^1\text{H}$  NMR properties (Figure 18).

**Table 9.** Association constant  $K_a$  values<sup>a</sup> for the chiral acceptor and donor **81e-I-BARF** pairs.

Entry	Donor	Acceptor	$K_a$ ( $\text{M}^{-1}$ )
1	<b>81e-I-BARF</b>	<b>(R)-101</b>	$6.1 \pm 0.7$
2	<b>81e-I-BARF</b>	<b>(S)-101</b>	$6.0 \pm 0.8$
3	<b>81e-I-BARF</b>	<b>(R)-102</b>	$94 \pm 7$
4	<b>81e-I-BARF</b>	<b>(S)-102</b>	$91 \pm 5$

<sup>a</sup> Measured by  $^1\text{H}$  NMR spectroscopy in  $\text{CDCl}_3$  (800 MHz, 298 K, 1.0 mM donor).  $K_a$  is the average value, based on global fitting of the change in the chemical shifts of methyl protons **a** and **b** to 1 : 1 binding isotherm of BindFit;<sup>159,160</sup> with corresponding standard errors that are the calculated mean values of two parallel experiments.

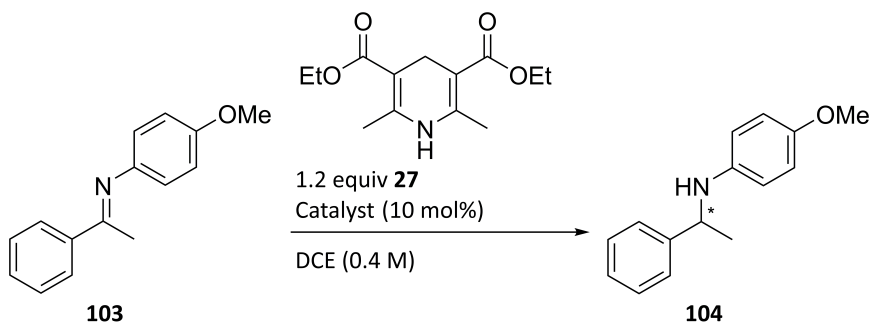


### 3.4 Catalytic activity of the triazole-based XB donors

To evaluate the catalytic activity of the synthesised triazole-based XB donors, several model reactions were screened. Reactions in which an imine acts as an electrophile, were chosen. Secondly, the Reissert-type reaction was chosen due to its similarity to halide abstraction reactions. In the catalytic experiments, the choice of XB donors was mostly limited to monofunctionalised XB donors containing the benzyl or  $\alpha$ -methylbenzyl substituent (compounds **92d-I-OTf**, **81Ar-X** or **81Ar-X-Y**) to simplify the determination of activation by XBs.

#### 3.4.1 Reduction of imine with Hantzsch ester **27** (unpublished results)

Previously C. H. Tan *et al.* had demonstrated the Hantzsch ester **27** reduction of imines activated by iodo-imidazolium salts.<sup>127</sup> Because of this, the triazolium salts were tested in the reduction of **103** with **27** (Scheme 21).



**Scheme 21.** Imine **103** reduction with Hantzsch ester **27**.

Although the reaction proceeded faster with compound **84d-I-3OTf** than with compound **84d-H-3OTf**, both of the triazolium salts demonstrated remarkable catalytic activity (Table 10, comparing entries 1 and 2). Therefore, structural features other than the halogen atom had a significant catalytic activity and XB activation could not be confirmed. In the case of compound **92d-I-OTf**, no reaction took place at room temperature (Table 10, entry 3). When the reaction was heated to 50 °C, almost full conversion was observed within five hours (Table 10, entry 4).

**Table 10.** Catalytic effect of triazolium salts on imine **103** reduction with Hantzsch ester **27**.

Entry	Catalyst	Time	Temperature	Conversion
1	<b>84d-I-3OTf</b>	1 day	RT	97%
2	<b>84d-H-3OTf</b>	1 day	RT	80%
3 <sup>a</sup>	<b>92d-I-OTf</b>	1 day	RT	N.R.
4 <sup>a</sup>	<b>92d-I-OTf</b>	5 h	50 °C	95%

<sup>a</sup> Solvent MeNO<sub>2</sub>:DCE (1:1)

To shed light on the process, samples were taken at regular intervals from the reaction mixture and analysed by <sup>1</sup>H NMR spectroscopy. This revealed the decomposition of the catalyst **92d-I-OTf** (Figure 20) and the formation of its protonated analogue **92d-H-OTf**.

The decomposition of the catalyst also coincided with the formation of product **104**. Compound **92d-H-OTf** was also catalytically active, although significantly less so and the kinetics of the reaction resembled that of a normal reaction without an induction period (Figure 21). When  $K_2CO_3$  was added to the reaction mixture with **92d-I-OTf**, the decomposition of the catalyst was accelerated, but no product **104** formation was observed (Figure 22). These observations suggest that catalyst decomposition at elevated temperatures led to the formation of an acidic species, which acted as the true catalyst. A recent publication also raised questions about the activation of quinolines by XBs and found support for the Brønsted acid-catalysed pathway.<sup>132</sup>

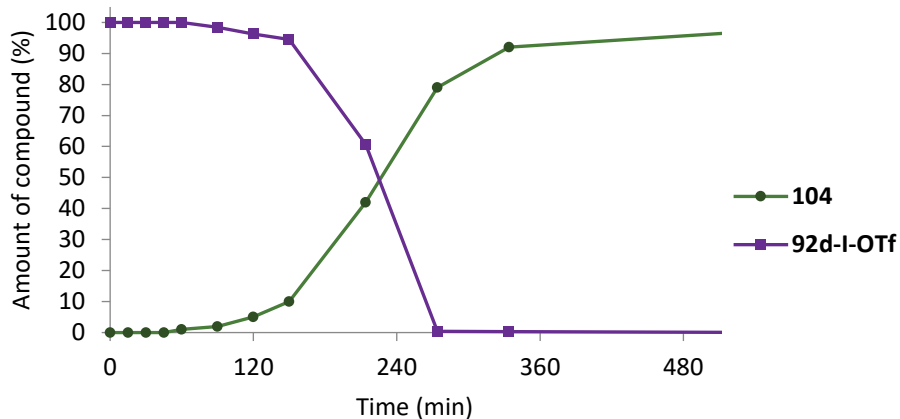


**Figure 20.** Reduction of **103** with Hantzsch ester **27** catalysed by **92d-I-OTf**.

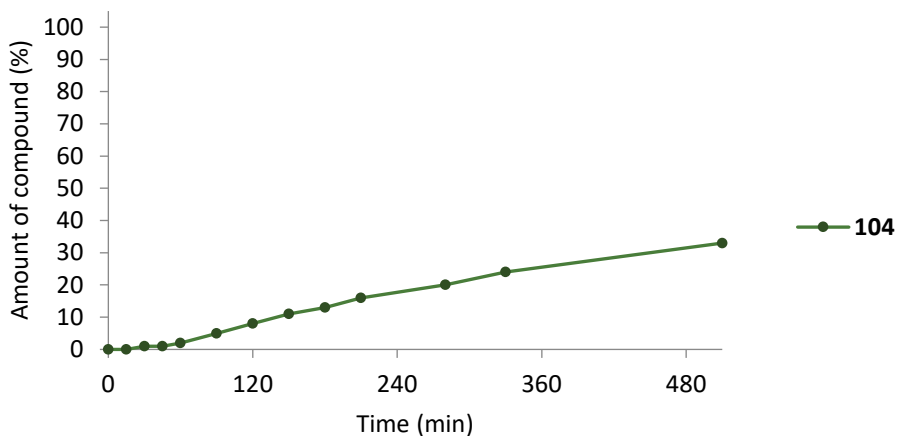


**Figure 21.** Reduction of **103** with Hantzsch ester **27** catalysed by **92d-H-OTf**.

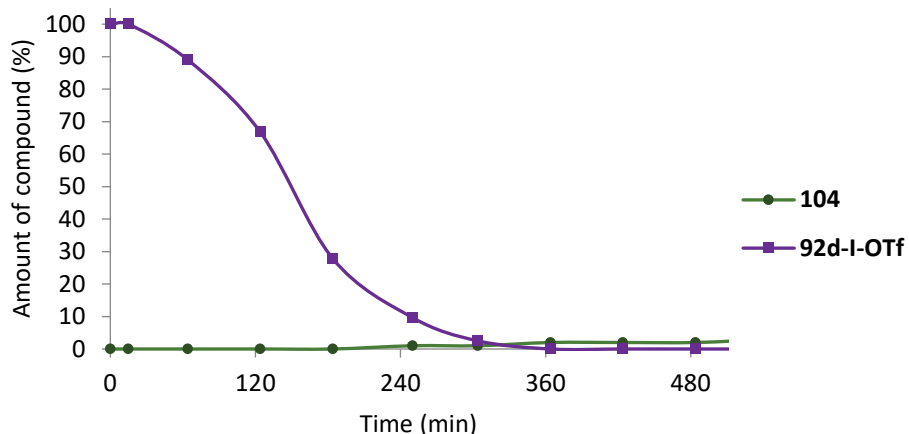
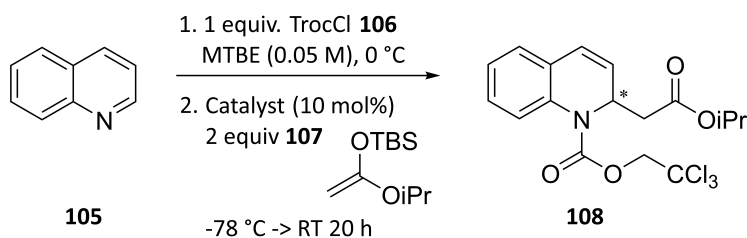


**Figure 22.** Reduction of **103** with Hantzsch ester **27** catalysed by **92d-I-OTf** with added  $K_2CO_3$ .

### 3.4.2 The Reissert-type reaction (unpublished results)

Quinoline **105** can be activated by acylation of the nitrogen atom in the aromatic ring, typically by an acyl chloride, such as **106** (Scheme 22).<sup>166</sup> This leads to the formation of an ion pair adduct, which can react with a nucleophile, for example a silyl enol ether **107**. The ion pair intermediate can be activated further by the binding of the anionic counterion. By this approach, enantiopure hydrogen bond donors have been used to make the ion pair chiral and obtain the product enantioselectively.<sup>167</sup> As the reaction proceeds through an intermediate ion pair, it is similar to halogen abstraction reactions, which have been carried out by XB catalysis. However, there are no examples of the use of XBs to accelerate the Reissert-type reaction of quinoline.



**Scheme 22.** Alkylation of quinoline **105** in a Reissert-type reaction.

Neutral bidentate XB donors were tested as catalysts, but the reactions provided the product **108** only in very low yields (Table 11, entries 1-3). Moreover, the product was obtained as a racemate or in selectivities near the margin of error. In principle, bidentate halo-triazolium salts should bind more strongly to the counterion and increase the reactivity of the intermediate more than monodentate donors. Unfortunately, the use of bidentate salts was not possible due to the very poor solubility of the salts in MTBE.

**Table 11.** Catalytic activity of bidentate triazoles in the alkylation reaction of quinoline **105**.

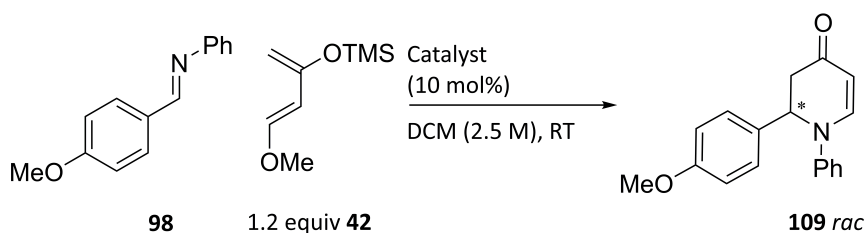
Entry	Catalyst	Yield	ee <sup>a</sup>
<b>1</b>	<b>b81f-II</b>	15%	6%
<b>2</b>	<b>b84f-II</b>	10%	rac
<b>3</b>	<b>93f-II</b>	15%	rac

<sup>a</sup> Determined by HPLC analysis on a chiral stationary phase.

### 3.4.3 Initial results of the cyclisation reaction between Danishefsky's diene **42** and imine **98** (unpublished results and Publication IV)

S. Minakata *et al.* had demonstrated the catalytic activity of halo-benzimidazolium salts in the aza-Diels-Alder reaction between imine **41** and Danishefsky's diene **42** (Table 3).<sup>133</sup> Therefore, it was decided to test the triazolium salts in this reaction. Imine **98** was used as the dienophile, as it had demonstrated higher affinity to the donor **81d-I-OTf** compared to imine **41** (Table 8, comparing entry 1 to entry 2).

No reaction took place between diene **42** and imine **98** (Scheme 23) without the addition of a catalyst (Table 12, entry 1). Also, no reaction took place in the presence of neutral donors **81a-I** and **81d-I** (Table 12, entries 2 and 3). With 10 mol% of XB donor **81a-I-OTf**, a very fast reaction took place, resulting in 96% conversion of imine **98** in one hour (Table 12, entry 4). Although enantiopure donors were used in the model reaction, product **109** was obtained as a racemate in these and later examples. Compound **81d-H-OTf** was markedly less active than **81a-I-OTf**, as only 66% conversion was observed after one day (Table 12, entry 6). With equivalent amounts of TBA-Cl and **81a-I-OTf**, a precipitate formed, and no reaction took place in one day (Table 12, entry 7). When the reaction was carried out at diluter conditions of 0.15 M, no precipitate formed, and no product formation was observed in four days (Table 12, entry 8). In the absence of TBA-Cl at a 0.15 M concentration, the conversion of the imine **98** was 92% after 7.5 hours (Table 12, entry 5).



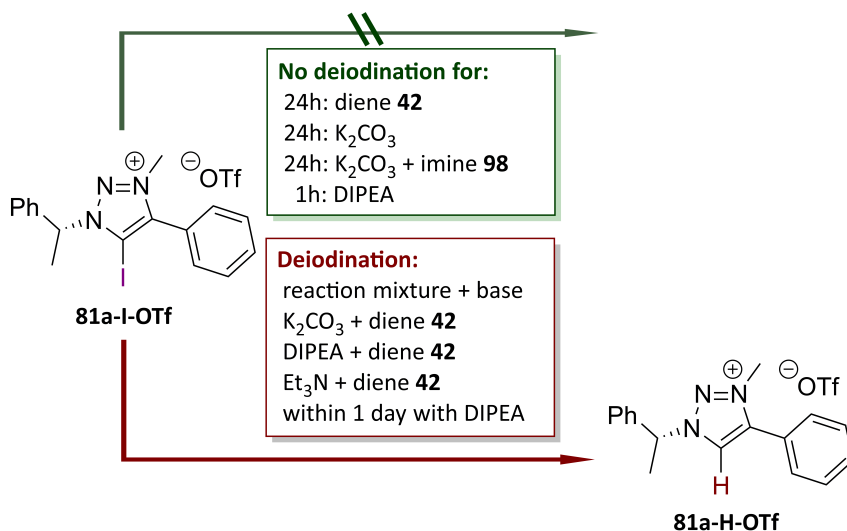
**Scheme 23.** Aza-Diels-Alder reaction between diene **42** and imine **98**.

**Table 12.** Initial results on the catalytic activity of the XB donors in the aza-Diels-Alder reaction.

Entry <sup>a</sup>	Catalyst	Additive (equiv)	Time	Conversion <sup>e</sup>
<b>1</b>	–	-	4 days	N.R.
<b>2<sup>a</sup></b>	<b>81a-I</b>	-	4 days	N.R.
<b>3<sup>a</sup></b>	<b>81d-I</b>	-	4 days	N.R.
<b>4</b>	<b>81a-I-OTf</b>	-	1h	96%
<b>5<sup>b</sup></b>	<b>81a-I-OTf</b>	-	7.5h	92%
<b>6</b>	<b>81a-H-OTf</b>	-	1 day	66%
<b>7<sup>c</sup></b>	<b>81a-I-OTf</b>	TBA-Cl	1 day	N.R.
<b>8<sup>b</sup></b>	<b>81a-I-OTf</b>	TBA-Cl	1 day	N.R.
<b>9<sup>d</sup></b>	<b>81a-I-OTf</b>	K <sub>2</sub> CO <sub>3</sub>	1 day	N.R.
<b>10<sup>d</sup></b>	<b>81a-I-OTf</b>	DIPEA	1 day	N.R.

<sup>a</sup> 20 mol% catalyst; <sup>b</sup> 0.15 M in DCM; <sup>c</sup> formation of precipitate; <sup>d</sup> decomposition of catalyst and formation of **81a-H-OTf**; <sup>e</sup> conversion determined by the ratio of product to imine using <sup>1</sup>H NMR spectroscopy.

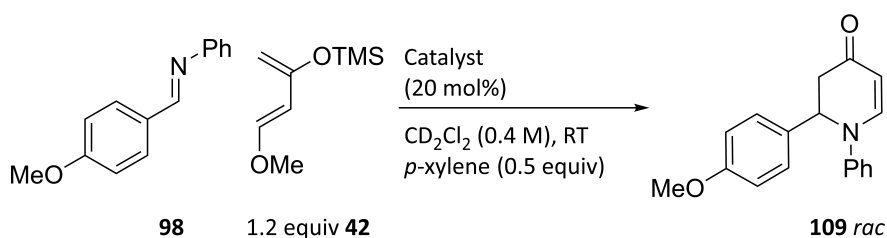
Next, reactions containing bases as additives were conducted to rule out the possibility of Brønsted acid catalysis. No reaction took place in one day in the presence of either K<sub>2</sub>CO<sub>3</sub> or DIPEA (Table 12, entries 9 and 10). Therefore, Brønsted acids present in the catalyst or formed during the reaction could have acted as the true catalyst. On the other hand, catalyst **81a-I-OTf** decomposition through deiodination was observed under these conditions, which could also explain the absence of a reaction. <sup>1</sup>H NMR analysis of mixtures of XB donor **81a-I-OTf** in the presence of bases and/or substrates were then carried out. Donor **81a-I-OTf** was stable for one day in the presence of only Danishefsky's diene **42** or K<sub>2</sub>CO<sub>3</sub> or a mixture of imine **98** and K<sub>2</sub>CO<sub>3</sub> (Scheme 24). With DIPEA, **81a-I-OTf** was stable for at least one hour but showed signs of deiodination after the first day. Also, donors used in the titration experiments with quinuclidine **99**, except **81e-Br-BARF** (Table 8, entry 10), showed no signs of deiodination throughout the titration experiments. When K<sub>2</sub>CO<sub>3</sub>, DIPEA or Et<sub>3</sub>N was added to a mixture of Danishefsky's diene and donor **81a-I-OTf**, which decomposed more rapidly and the formation of **81a-H-OTf** was observed. Therefore, the combination of diene **42** and the bases facilitated the rapid deiodination of donor **81a-I-OTf**.



**Scheme 24.** Deiodination of **81a-I-OTf** in the presence of various compounds.

### 3.4.4 Determination of the reaction profiles by $^1H$ NMR spectroscopy

To get a better understanding of the reaction between diene **42** and imine **98**, the reaction was monitored by  $^1H$  NMR spectroscopy. To use the method, the reaction had to proceed at a lower rate and therefore the experiments were carried out at a 0.4 M concentration in  $CD_2Cl_2$  using a 20 mol% loading of the donor (Scheme 25). *p*-Xylene was used as an internal standard and the decrease in the signal corresponding to the methoxy group of imine **98** was used to calculate the conversion.



**Scheme 25.** The model reaction used to study the catalytic activity of the triazolium salts.

The monitoring of the reaction by  $^1H$  NMR revealed two things that might have gone unnoticed. Firstly, there was a lag period present that preceded a rapid period of conversion of imine **98** to product **109** (Figure 23, red line). Secondly, the rate of the reaction was dependent on the batch of diene **42** in use and on how long that batch had been in use. If the diene **42** was used a few days after its first use, then the reaction proceeded at a slower pace and the delay at the start of the reaction was prolonged (Figure 23, comparing the brown, blue and orange lines). Due to this, only those results are compared in which the experiments were carried out with the same batch of diene **42**. Also, the experiments were carried out in as short a time as possible.

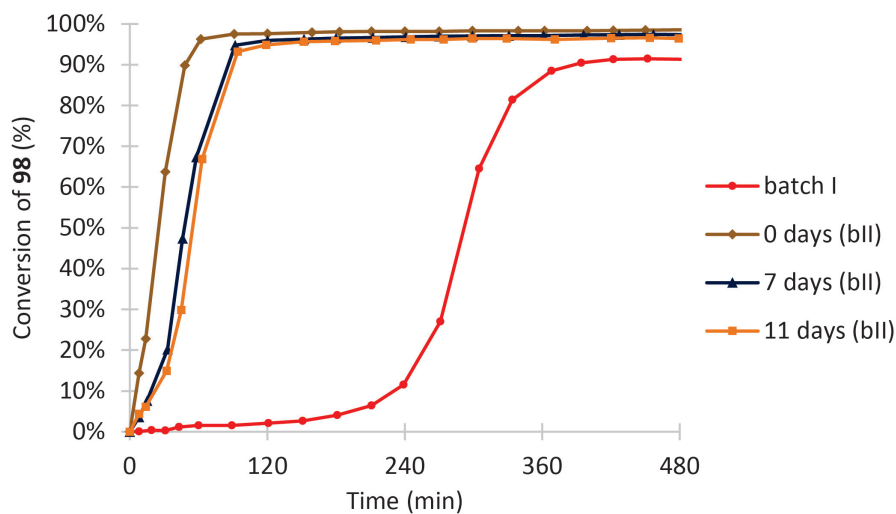


**Figure 23.** Influence of different batches of Danishefsky's diene **42** and time after opening on the model reaction with catalyst **81a-I-OTf**.

Reactions containing different halogens as the donor atoms in the triazolium salts proceeded at different rates, which followed the polarisability order of the halogens: **81a-I-OTf** (Figure 24, red line) was the most active, with **81a-Br-OTf** the reaction proceeded more slowly, nevertheless reaching completion within eight hours (Figure 24, black line), and **81a-Cl-OTf** (Figure 24, blue line) was the least active. The replacement of the halogen atom with a hydrogen atom made the triazolium salt almost inactive, as with **81a-H-OTf** only a marginal reaction was observed (Figure 24, yellow line).

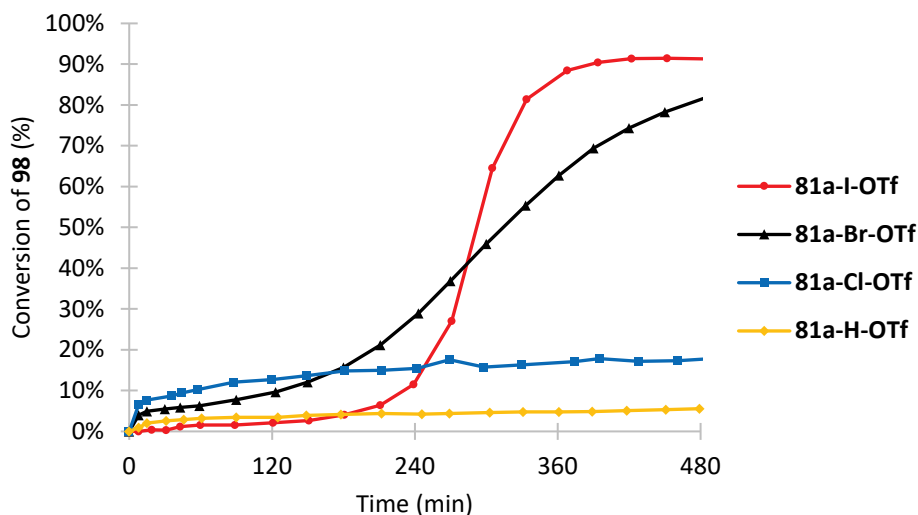


**Figure 24.** Dependence of the conversion of the model reaction on the halogen/hydrogen atom of the triazole ring in the catalyst.

The choice of counterion was also significant, as no reaction took place with compound **81c-I-BF<sub>4</sub>** containing the tetrafluoroborate counterion (Figure 25, pink line). This was surprising, as S. Fukuzawa *et al.* had used only triazolium salts containing this counterion to catalyse the aza-Diels-Alder reaction.<sup>52</sup> However, the inactivity might have been caused by the significant decomposition of **81c-I-BF<sub>4</sub>** in the reaction mixture in contrast to compounds **81a-I-OTf** and **81a-I-BARF**, which only showed marginal levels of decomposition (See page S12 of the SI of **Publication IV**). When using **81a-I-BARF**, the reaction profile was more like that of a typical reaction without a lag period (Figure 25, green line). However, the reaction did not proceed to completion within eight hours as did the reaction with **81a-I-OTf** (Figure 25, red line).

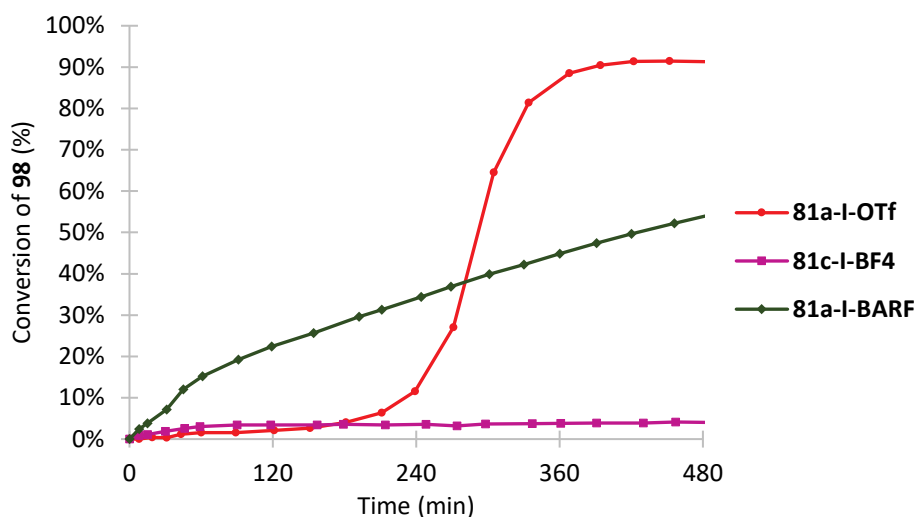


**Figure 25.** Dependence of the conversion of the model reaction on the counterion of the catalyst.

Experiments to determine the influence of the aromatic substituent were conducted with another batch of diene **42**. As the lag period was shorter and the reaction proceeded much faster, there seemed to be no difference between the phenyl and *para*-nitrophenyl substituent (Figure 26, comparing the red and green lines). In the case of compound **81e-I-OTf** containing the perfluorophenyl substituent, the rate of the reaction was the fastest and **81e-I-OTf** was also used successfully at a two mol% loading as the reaction was over in three hours (Figure 26, the two orange lines). The lowering of the catalyst loading also revealed the presence of a lag period, which means that **81e-I-OTf** acted in a similar manner to the other donors **81Ar-I-OTf**, and in the case of a very active donor the lag period could go unnoticed.



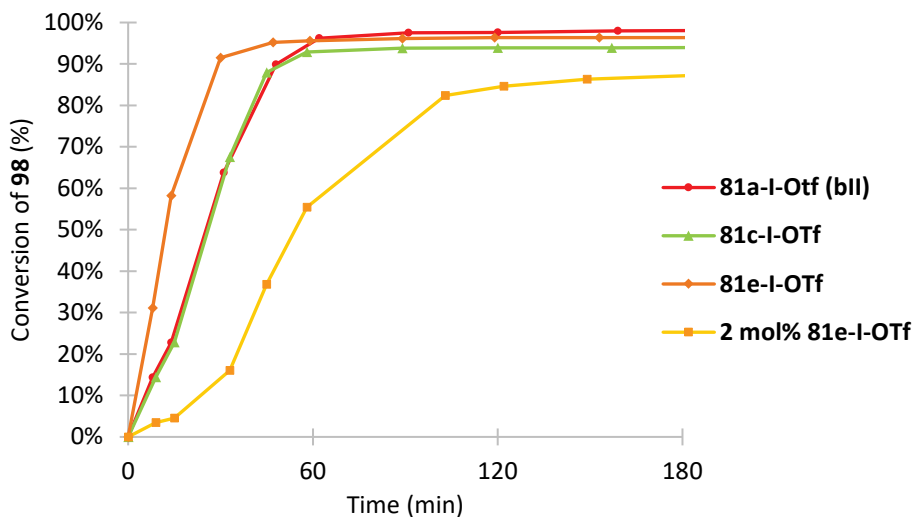


**Figure 26.** Influence of the aromatic substituent of the catalyst on the conversion of the model reaction.

### 3.4.5 Mechanistic aspects of the reaction between diene **42** and imine **98**

The different observations described herein made it difficult to fully explain the obtained results. The catalytic activity of the triazolium salts was very dependent on the halogen atom present in the donor and somewhat dependent on the aromatic substituent. In addition, **81a-H-OTf** was almost inactive. Therefore, the catalytic activity manifests itself through the halogen atom and the rest of the donor structure does not have catalytic activity. The fact that imines were able to form a complex with the XB donors (Table 8, entry 2; Table 9, entries 1 and 2) and the inhibition of the reaction by TBACl, which is a better XB acceptor, also supports the hypothesis that the reaction proceeded through the XB activation of imine **98**. In the case of **81a-Br-OTf**, the possibility that Br<sub>2</sub> acted as the true catalyst was ruled out, as the reaction was not affected by the presence of cyclohexene, which would have reacted rapidly with Br<sub>2</sub> and effectively quenched it (Figure 27).<sup>98,136</sup> The decomposition of **81c-I-BF<sub>4</sub>** was deduced from the reduction of the signals belonging to the donor and the appearance of signals similar to its analogue substituted with a hydrogen atom. This meant that **81c-I-BF<sub>4</sub>** decomposed in a similar manner to the triflate salts and, as no reaction took place, the decomposition products were inactive.

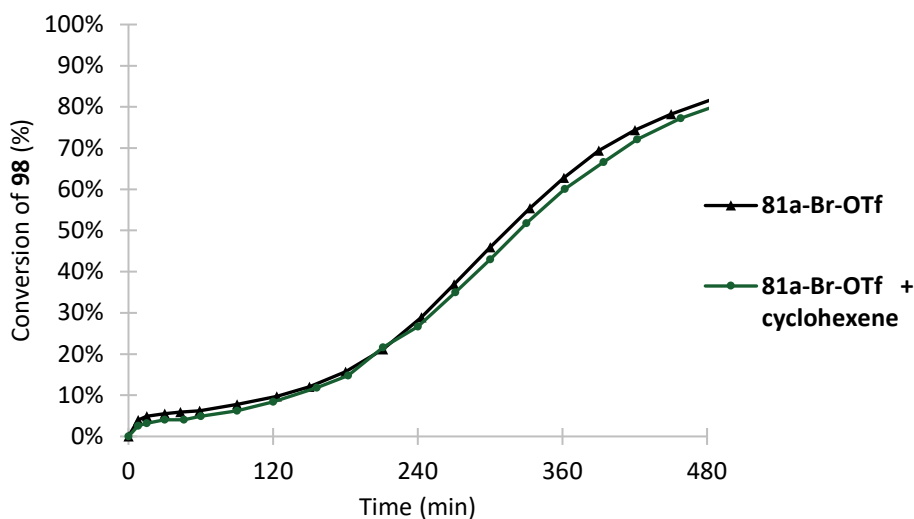


**Figure 27.** Control experiment with catalyst **81a-Br-OTf** in the presence of an equivalent amount of cyclohexene.

The sigmoidal curve corresponding to the conversion of imine **98** hints at the formation of a true catalyst during the reaction. TMS-OTf has been demonstrated to act as a catalyst in the Mannich reaction<sup>168</sup> and aza-Diels-Alder reaction.<sup>169</sup> In addition, the possibility of hidden Brønsted acid catalysis could not be ruled out. Both could have been valid alternative catalytic routes. However, it is difficult to explain why Brønsted acids or TMS-OTf would have been inhibited by the presence of TBA-Cl. Furthermore, if these species were acting as true catalysts, then the rate of the reaction should not have been affected by the choice of the halogen atom or the aromatic substituent. Also, when HRMS was used to monitor the reaction, the presence of TMS-OTf in the reaction mixture was not observed. The strange influence of the counterion on the rate of the reaction and the fact that triflate salts were the most active could also support catalysis by TMS-OTf. However, the influence of the counterion on the catalytic activity of XB donors is not well understood and inconsistent trends have been observed in previous publications as well.<sup>97,170</sup>

One possible reason for the sigmoidal curve was that the catalyst formed aggregates in solution that impeded the donor from entering the catalytic cycle. The formation of aggregates by the donors was deduced from the <sup>1</sup>H NMR spectra of the donors measured at different concentrations. For example, the signals corresponding to the alkyl protons of **81a-I-OTf** were shifted downfield in diluter samples (Figure 28).

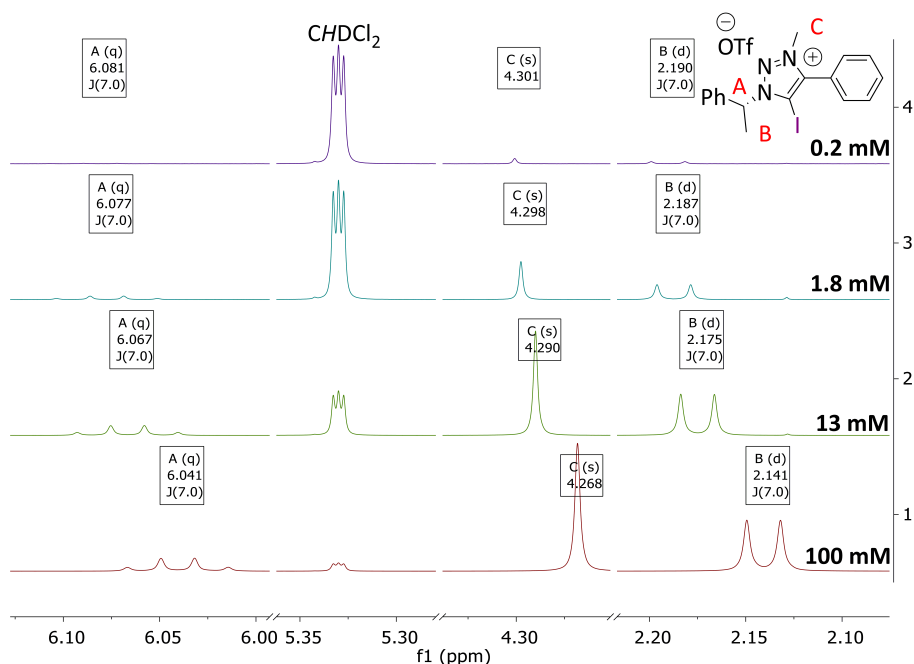


**Figure 28.** Outtakes of  $^1\text{H}$  NMR spectra ( $\text{CD}_2\text{Cl}_2$ , 297 K, 400 MHz) of the donor **81a-I-OTf** at concentrations: 0.2 mM, 1.8 mM, 13 mM and 100 mM. The change in the shifts of the peaks corresponding to **81a-I-OTf** methyl (B, C) and methine (A) protons upon dilution indicate that **81a-I-OTf** self-aggregates.

The lag period at the start of the reaction could have been caused by the kinetics of de-aggregation, during which the donor was released and then entered the catalytic cycle. To test this, incubation experiments were carried out in which the catalyst was added to a solution of either diene **42**, imine **98** or product **109** for 30 minutes prior to the addition of the missing starting compounds. It was presumed that one of these compounds would accelerate de-aggregation and therefore incubation would result in a faster reaction. In the case of imine **98** and product **109**, no difference from the regular reaction was observed (Figure 29, comparing the red and blue lines to the orange line). Also, the possibility of autocatalysis by product **109** can be ruled out as the reaction was not accelerated by the product. On the other hand, the incubation with diene **42** slowed down the reaction (Figure 29, grey line). This together with the observations that the rate of the reaction was dependent on the quality of diene **42** and that significant decomposition of the catalyst was observed in the presence of both a base and diene **42** hint that the catalyst interacts with the diene or its decomposition product.

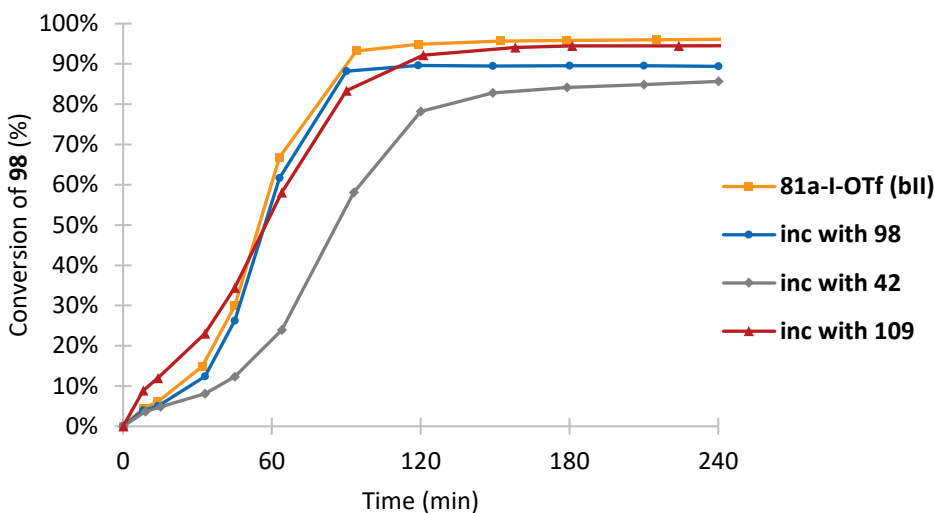
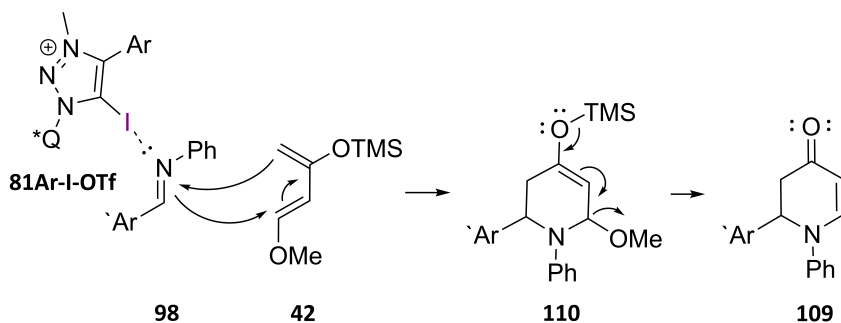


**Figure 29.** Incubation experiments carried out with catalyst **81a-I-OTf** using compounds **42**, **98** and **109**. During these experiments the catalyst **81a-I-OTf** was solubilised in  $\text{CD}_2\text{Cl}_2$  and *p*-xylene solution for 20 minutes before adding compound **42**, **98** or **109** to the mixture. After 30 minutes the missing starting compound(s) was added, and the reaction was monitored using the standard procedure.

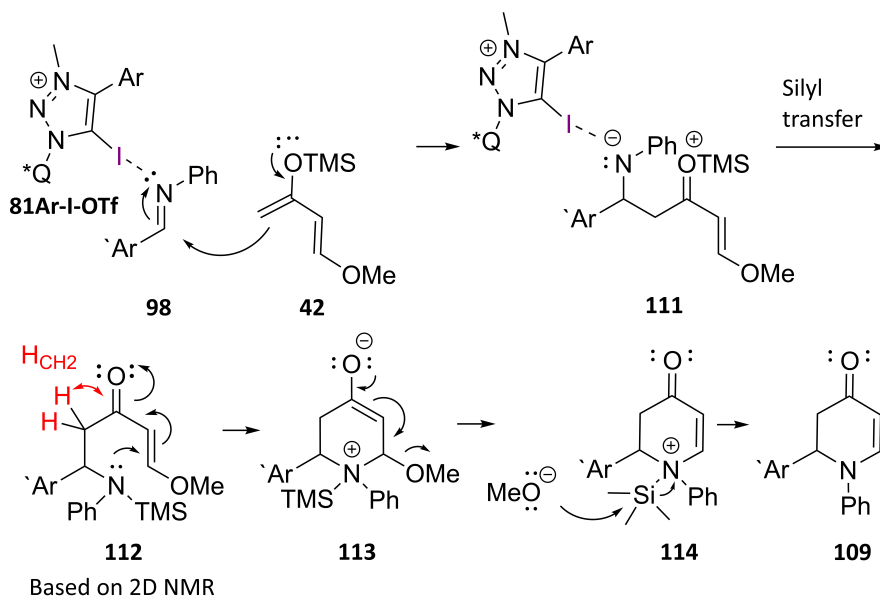
It was initially proposed, similarly to the work done by S. Minakata *et al.*, that the reaction between diene **42** and imine **98** would yield the dihydropyridinone **109** through an aza-Diels-Alder pathway (Scheme 26).<sup>133</sup>



**Scheme 26.** Aza-Diels-Alder pathway for product **109** formation.

However, it was observed that at the onset of the reaction an intermediate started to form, which usually disappeared by the end of the reaction (see Figure 7 **Publication IV**). This implies that a stepwise path to product formation could have taken place, which is not uncommon for these reactions.<sup>171</sup> Additional evidence came from the analysis of 2D NMR spectra of the reaction mixture (see page S13 and S14 in the SI of **Publication IV**). From these spectra it was inferred that the intermediate contained a methylene group between a polar methine group and a carbonyl group that was conjugated to a *trans*-double bond and the intermediate most likely contained two methoxy groups (see page S15 in the SI of **Publication IV**). HRMS measured for samples taken from the reaction mixture confirmed the presence of species formed from diene **42** addition to imine **98**, in which both of the methoxy groups were still present. Based on previous

results and the observations, the reaction could proceed through an initial Mannich reaction between the activated imine **98** and diene **42**, which would lead to the observed intermediate **111** (Scheme 27). Following the possible transfer of the silyl group, compound **112** could then give an intramolecular Michael reaction to form the six-membered ring, which would ultimately lead to product **109** after desilylation and demethoxylation. However, the possibility that in parallel the reaction proceeded by the aza-Diels-Alder pathway cannot be ruled out.



**Scheme 27.** Stepwise pathway through consecutive Mannich and intramolecular Michael reactions to product **109** formation.

## 4 Conclusions

- An efficient route for the synthesis of enantiopure mono- and bidentate as well as bifunctional halo-triazoles and halo-triazolium salts based on the click reaction was developed.
- The halo-triazoles and halo-triazolium salts acted as XB donors in the solid state and formed relatively strong XBs with another donor molecule or with the counterion.
- XB donors formed complexes in  $\text{CDCl}_3$  with amines, imines, ureas and thioureas. The corresponding association constants differed up to four orders of magnitude, with the strongest binding measured to quinuclidine. Furthermore, the complexes with imines, ureas and thioureas had not been previously described.
- An iodine atom in the triazole/triazolium salt was needed to form favourable complexes in  $\text{CDCl}_3$  with the acceptor molecules. The introduction of a charge was also of critical importance to obtain sufficiently strong XB donors and caused the increase of the affinity constant value for the complex with quinuclidine by four orders of magnitude.
- An iodine or a bromine atom in the triazolium salt core was necessary for its catalytic activity in the model reaction; the desired dihydropyridinone may have formed through the Mannich/Michael or the Diels-Alder pathway.
- The counterion had a major effect on the XB donor ability of iodo-triazolium salts and hence also on their catalytic activity.
- Electron-deficient aromatic rings increased the XB donor ability to a lesser extent than the choice of counterion and halogen atom among the studied XB donors. The perfluorophenyl substituent had the highest impact on donor strength.
- Enantiopure  $\alpha$ -methylbenzyl-substituted iodo-triazole was capable of enantiodiscrimination of chiral thiourea via noncovalent interactions, including halogen bonding. However, the triazole-based XB donors were inefficient at discriminating between enantiomers of screened imine and amine, and as catalysts for enantioselective reactions with prochiral substrates.

## 5 Experimental section

All commercially available reagents were used without further purification. DCM was dried by distillation over P<sub>2</sub>O<sub>5</sub>, and MeOH and THF were dried by distillation over sodium metal. All air or moisture sensitive reactions were carried out under an argon atmosphere using oven-dried glassware. The reactions were monitored by thin layer chromatography (TLC) with silica gel-coated aluminium plates (Merck 60 F254) and visualised with KMnO<sub>4</sub>, anisaldehyde, vanillin or ninhydrine stain, or by <sup>1</sup>H NMR spectroscopy. NMR spectra were measured on a Bruker Avance III 400 MHz or a Bruker Avance III 800 MHz instrument. The spectra are reported in parts per million ( $\delta$ ) referenced to the residual solvent signal [CDCl<sub>3</sub>  $\delta$  = 7.26 ppm, CD<sub>3</sub>OD  $\delta$  = 3.31 ppm, [D<sub>6</sub>]DMSO  $\delta$  = 2.50 ppm, [D<sub>6</sub>]Acetone  $\delta$  = 2.05 ppm (for <sup>1</sup>H NMR), CDCl<sub>3</sub>  $\delta$  = 77.16 ppm, CD<sub>3</sub>OD  $\delta$  = 49.00 ppm, [D<sub>6</sub>]DMSO  $\delta$  = 39.52 ppm, [D<sub>6</sub>]Acetone  $\delta$  = 29.84 ppm (for <sup>13</sup>C NMR)]. Information on crystallographic details is included in the supporting information of **Publications I, III and IV**. Yields refer to chromatographically purified or crystallised products. A CEM Discover microwave reactor was used for the microwave-assisted synthesis of 5-chloro-1*H*-1,2,3-triazoles. The reaction vessel was sealed with a Teflon cap and the reaction temperature was monitored by a non-contact infrared sensor. The exact synthetic procedures of the non-commercial reagents and end products, along with their characterisation, are described in **Publications I–IV** and the corresponding supporting information (Please use Table 13 as a guide). The following section contains procedures for the unpublished results and representative/general procedures for the catalytic experiments or synthesis of XB donors.

### 5.1 Representative procedure for the synthesis of azides from amines, in the example of *N*-((1*R*,2*R*)-2-azidocyclohexyl)pivalamide

*N*-((1*R*,2*R*)-2-Aminocyclohexyl)pivalamide (0.174 g, 0.877 mmol) was dissolved in a suspension of K<sub>2</sub>CO<sub>3</sub> (0.15 g, 1.10 mmol) and CuSO<sub>4</sub> × 5H<sub>2</sub>O (0.007 mg, 0.028 mmol) in MeOH (4 mL). Imidazole-1-sulfonyl azide hydrochloride **76** (0.22 g, 1.05 mmol) was added and the mixture was stirred at RT overnight. The solvent was removed under reduced pressure, and then the solid was dissolved in H<sub>2</sub>O (10 mL), acidified with HCl (20 mL, 1 M) and extracted with DCM (4 × 10 mL). The combined organic layers were dried over MgSO<sub>4</sub>, filtered and concentrated. The crude product was purified by column chromatography on silica gel (starting from 0% MeOH/NH<sub>3</sub> in DCM) to provide the desired azide as a colourless solid (0.189 g, 96% yield).

### 5.2 Representative procedure for the synthesis of azides from alcohols, in the example of compound *N*-((1*S*,2*S*)-2-azido-2,3-dihydro-1*H*-inden-1-yl)-2,2,2-trifluoroacetamide

2,2,2-Trifluoro-*N*-((1*S*,2*R*)-2-hydroxy-2,3-dihydro-1*H*-inden-1-yl)acetamide (0.266 g, 1.09 mmol) and triethylamine (0.453 mL, 3.26 mmol) were dissolved in DCM (8 mL) under an argon atmosphere, and then the reaction mixture was cooled to 0 °C. Methanesulfonyl chloride (0.127 mL, 1.63 mmol) was added drop-wise and the reaction mixture was allowed to warm to RT and was stirred for two hours. The reaction mixture was diluted with DCM (10 mL), after which water (10 mL) was added and the phases were separated. The aqueous phase was additionally extracted with DCM (3 × 10 mL), and the combined

organic phases were dried over Na<sub>2</sub>SO<sub>4</sub>. Filtration and removal of the solvent under reduced pressure provided the crude product, which was purified by column chromatography on silica gel (starting from 2% of EtOAc in DCM) to provide the mesylate as a white solid (0.343 g, 1.06 mmol, 98% yield). Mesylate (0.340 g, 1.05 mmol) was dissolved in DMF (3 mL) and sodium azide (0.104 g, 1.59 mmol) was added. The reaction mixture was stirred at 100 °C overnight. After cooling to RT, water (6 mL) was added; the aqueous layer was extracted with EtOAc (4 x 10 mL) and dried over Na<sub>2</sub>SO<sub>4</sub>. The crude product was filtered, concentrated and purified by column chromatography on silica gel (starting from 10% of EtOAc in petroleum ether) to provide the desired azide as colourless crystals (0.245 g, 86% yield).

### **5.3 Representative procedure for the synthesis of iodoalkynes from terminal alkynes, in the example of 1-(iodoethynyl)-3,5-bis(trifluoromethyl)benzene**

1-Ethynyl-3,5-bis(trifluoromethyl)benzene (0.641 g, 2.69 mmol), dissolved in THF (20 mL), was treated with CuI (0.051 g, 0.268 mmol) and 4-iodomorpholine hydroiodide **79** (1.01 g, 2.95 mmol) and the reaction mixture was stirred for 3 h at RT. The suspension was poured onto a pad of neutral alumina and the filtrate was collected under reduced pressure. The solid phase was washed with DCM (2 x 20 mL) and the combined organic fractions were washed with a solution of Na<sub>2</sub>S<sub>2</sub>O<sub>3</sub> (20 mL, 5% w/w). The organic phase was dried over Na<sub>2</sub>SO<sub>4</sub> and concentrated under reduced pressure to give 1-(iodoethynyl)-3,5-bis(trifluoromethyl)benzene as an orange oil (0.85 g, 88% yield).

### **5.4 Representative procedure for the synthesis of haloalkynes from aldehydes, in the example of 1-(iodoethynyl)-4-nitrobenzene**

Iodoform (4.10 g, 10.42 mmol), triphenylphosphine (2.87 g, 10.94 mmol) and *t*BuOK (1.11 g, 9.93 mmol) were added to THF (20 mL) under an argon atmosphere. The suspension was stirred at RT for five minutes and turned brown. 4-nitrobenzaldehyde (0.75 g, 4.96 mmol) was added. After 30 minutes, the brown suspension was cooled to -78 °C and *t*BuOK (2.80 g, 24.95 mmol) was added. After an additional 30 minutes the reaction was quenched with brine (90 mL) at -78 °C. After warming to RT the two layers were separated and the aqueous phase was extracted with diethyl ether (3 x 90 mL). The combined organic phase was passed through a phase separator, concentrated and purified by column chromatography on silica gel (starting from 0% of EtOAc in petroleum ether) to provide 1-(iodoethynyl)-4-nitrobenzene as a yellow solid (1.17 g, 86% yield).

### **5.5 Representative procedure for the CuAAC of iodoalkynes, in the example of compound **81b-I****

CuI (0.005 g, 0.027 mmol) and TTTA (0.012 mg, 0.027 mmol) were dissolved in freshly distilled THF (1.5 mL) under an argon atmosphere and stirred at RT for 30 min. 1-(Iodoethynyl)-4-(trifluoromethyl)benzene (0.163 g, 0.551 mmol) and (*R*)-(1-azidoethyl)benzene (0.083 g, 0.564 mmol), dissolved in THF (1.2 mL), were added and the reaction mixture was stirred at RT for 18 h. The reaction mixture was concentrated, NH<sub>4</sub>OH (10 mL, 10 % w/w) was added and the aqueous phase was extracted with DCM (3 x 10 mL). The combined organic phase was washed with brine (10 mL), passed through



a phase separator, concentrated and purified by column chromatography on silica gel (starting from 5% of EtOAc in petroleum ether) to provide triazole **81b-I** as pale yellow crystals (0.205 g, 84% yield).

#### 5.5.1 1-Benzyl-4-(3,5-bis(trifluoromethyl)phenyl)-5-iodo-1*H*-1,2,3-triazole **92d-I**

CuI (0.015 g, 0.082 mmol) and Et<sub>3</sub>N (0.23 mL, 1.64 mmol) were dissolved in THF (2.0 mL) under an argon atmosphere and stirred for 10 min at RT. 1-(Iodoethynyl)-3,5-bis(trifluoromethyl)benzene (0.335 g, 0.9 mmol) and benzylazide (0.109 g, 0.82 mmol), dissolved in THF (2.0 mL), were added and the reaction mixture was stirred for 4 h at RT. The reaction mixture was concentrated, NH<sub>4</sub>OH (5 mL, 10 % w/w) was added and the aqueous phase was extracted with DCM (6 x 10 mL). The combined organic phase was dried over anhydrous Na<sub>2</sub>SO<sub>4</sub>, concentrated and purified by column chromatography on silica gel (from 2% of EtOAc in petroleum ether) to provide **92d-I** after the removal of the solvent under reduced pressure as pale yellow crystals (0.226 g, 55% yield). <sup>1</sup>H NMR (400 MHz, CDCl<sub>3</sub>) δ 8.48 (s, 2H), 7.89 (s, 1H), 7.42 – 7.29 (m, 5H), 5.71 (s, 2H). <sup>13</sup>C NMR (101 MHz, CDCl<sub>3</sub>) δ 147.6, 133.9, 132.6, 132.1 (q, *J* = 33.6 Hz), 129.2, 128.9, 128.0, 127.5 – 127.2 (m), 123.3 (q, *J* = 272.9 Hz), 122.4 – 122.1 (m, *J* = 7.6, 3.8 Hz), 54.8. The iodine bonded C-atom was not detected because of low intensity of the signal.

#### 5.6 Representative procedure for the synthesis of 5-chlorotriazoles, in the example of compound **81d-Cl**

Triazole **81d-I** (0.150 g, 0.293 mmol) was dissolved in MeCN (1.0 mL) in a microwave vial, water (1.0 mL) and KCl (0.110 g, 1.47 mmol) were added to the mixture and the vial was sealed with a Teflon cap. The vial was placed in a microwave reactor and heated at 160 °C for 25 min. The reaction mixture was cooled, diluted with water and the aqueous phase was extracted with EtOAc (5 x 10 mL). The combined organic phase was dried over anhydrous Na<sub>2</sub>SO<sub>4</sub>, concentrated and purified by column chromatography on silica gel (starting from 1% of EtOAc in petroleum ether) to provide triazole **81d-Cl** as a pale-yellow oil (0.097 g, 79% yield).

#### 5.7 Representative procedure for the synthesis of 5-bromotriazoles, in the example of compound **81d-Br**

1-(Bromoethynyl)-3,5-bis(trifluoromethyl)benzene (0.150 g, 0.473 mmol) and (*R*)-(1-azidoethyl)benzene (0.071 g, 0.482 mmol) were dissolved in THF (3.0 mL). CuBr (0.014 g, 0.095 mmol) and Cu(OAc)<sub>2</sub> x H<sub>2</sub>O (0.020 mg, 0.100 mmol) were added and the reaction mixture was stirred at 50 °C overnight. The reaction mixture was cooled and concentrated, and the residue diluted with water. The aqueous phase was extracted with DCM (4 x 10 mL). The combined organic phase was dried over anhydrous MgSO<sub>4</sub>, concentrated and purified by column chromatography on silica gel (starting from 1% of EtOAc in petroleum ether) to provide triazole **81d-Br** as a yellow oil (0.157 g, 71% yield).

## 5.8 Representative procedure for the synthesis of 1*H*-1,2,3-triazoles, in the example of compound 81d-H

CuSO<sub>4</sub> x 5H<sub>2</sub>O (0.009 g, 0.036 mmol), Na-*L*-ascorbate (0.016 g, 0.081 mmol) and NaHCO<sub>3</sub> (0.006 g, 0.071 mmol) were dissolved in H<sub>2</sub>O (0.8 mL). 1-ethynyl-3,5-bis(trifluoromethyl)benzene (0.201 g, 0.845 mmol) and (*R*)-(1-azidoethyl)benzene (0.113 g, 0.768 mmol), dissolved in MeOH (0.8 mL), were added and the reaction mixture was stirred at RT for 24 h. The reaction mixture was concentrated, NH<sub>4</sub>OH (8 mL, 10 % w/w) was added and the aqueous phase was extracted with DCM (4 x 8 mL). The combined organic phase was washed with brine (5 mL), passed through a phase separator, concentrated and purified by column chromatography on silica gel (from 5% of EtOAc in petroleum ether) to provide triazole **81d-H** as a colourless oil that solidified upon standing in the refrigerator (0.259 g, 96% yield).

### 5.8.1 1-Benzyl-4-(3,5-bis(trifluoromethyl)phenyl)-1*H*-1,2,3-triazole 92d-H

CuI (0.008 g, 0.075 mmol) and Et<sub>3</sub>N (0.21 mL, 1.5 mmol) were dissolved in THF (1.0 mL) under an argon atmosphere and stirred for 10 min at RT. 1-(Ethynyl)-3,5-bis(trifluoromethyl)benzene (1.0 mmol in Et<sub>2</sub>O) and benzylazide (0.10 g, 0.75 mmol), dissolved in THF (0.5 mL), were added and the reaction mixture was stirred for 2 h at RT. The reaction mixture was concentrated, NH<sub>4</sub>OH (5 mL, 10 % w/w) was added and the aqueous phase was extracted with DCM (6 x 10 mL). The combined organic phase was dried over anhydrous Na<sub>2</sub>SO<sub>4</sub>, concentrated and purified by column chromatography on silica gel (from 5% of EtOAc in petroleum ether) to provide triazole **92d-H** as pale yellow crystals (0.277 g, 99% yield). <sup>1</sup>H NMR (400 MHz, CDCl<sub>3</sub>) δ 8.25 (s, 2H), 7.82 (s, 1H), 7.81 (s, 1H), 7.46 – 7.38 (m, 3H), 7.37 – 7.30 (m, 2H), 5.61 (s, 2H). <sup>13</sup>C NMR (101 MHz, CDCl<sub>3</sub>) δ 145.7, 134.3, 132.8, 132.4 (q, *J* = 33.5 Hz), 129.5, 129.3, 128.3, 125.9 – 125.5 (m, *J* = 2.8 Hz), 123.3 (q, *J* = 272.8 Hz), 121.9 – 121.4 (m), 120.6, 54.7.

### 5.8.2 (2*R*,4*S*,5*R*)-2-((*R*)-(4-(3,5-Bis(trifluoromethyl)phenyl)-1*H*-1,2,3-triazol-1-yl)(6-methoxyquinolin-4-yl)methyl)-5-vinylquinuclidine 84d-H

CuI (0.004 g, 0.02 mmol) and Et<sub>3</sub>N (0.11 mL, 0.8 mmol) were dissolved in THF (1.0 mL) under an argon atmosphere and stirred for 10 min at RT. 1-(Ethynyl)-3,5-bis(trifluoromethyl)benzene (0.5 mmol in Et<sub>2</sub>O) and *e*-azido-quinidine (0.14 g, 0.4 mmol), dissolved in THF (1.0 mL), were added and the reaction mixture was stirred for 2 h at RT. The reaction mixture was concentrated, NH<sub>4</sub>OH (5 mL, 10 % w/w) was added and the aqueous phase was extracted with DCM (3 x 10 mL). The combined organic phase was dried over anhydrous Na<sub>2</sub>SO<sub>4</sub>, concentrated and purified by column chromatography on silica gel (from 1% of MeOH in DCM) to provide triazole **84d-H** after the removal of the solvent under reduced pressure as pale yellow crystals (0.179 g, 76% yield). <sup>1</sup>H NMR (400 MHz, CDCl<sub>3</sub>) δ 8.82 (t, *J* = 6.2 Hz, 1H), 8.20 (s, 2H), 8.05 (t, *J* = 7.2 Hz, 1H), 7.86 (s, 1H), 7.75 (s, 1H), 7.60 (d, *J* = 4.6 Hz, 1H), 7.52 (d, *J* = 2.6 Hz, 1H), 7.40 (dd, *J* = 9.2, 2.6 Hz, 1H), 6.53 (d, *J* = 10.9 Hz, 1H), 5.89 (ddd, *J* = 17.0, 10.5, 6.2 Hz, 1H), 5.18 – 5.07 (m, 2H), 3.98 (s, 3H), 4.02 – 3.90 (m, 1H), 3.18 – 3.09 (m, 1H), 3.08 – 2.82 (m, 3H), 2.33 (dd, *J* = 15.7, 7.6 Hz, 1H), 1.80 (s, 1H), 1.75 – 1.60 (m, 2H), 1.58 – 1.46 (m, 1H), 1.37 – 1.24 (m, 1H). <sup>13</sup>C NMR (101 MHz, CDCl<sub>3</sub>) δ 159.0, 147.5, 145.2, 145.1, 140.4, 139.2, 132.9, 132.3, 132.2 (q, *J* = 33.5 Hz), 128.2, 125.9 – 125.5 (m), 123.3 (q, *J* = 272.8 Hz), 122.7, 121.6 – 121.3 (m), 119.7, 119.4, 115.1, 100.6, 60.3, 58.3, 55.9, 53.6, 49.6, 47.5, 39.1, 27.7, 26.7, 26.6.

## 5.9 Representative procedure for the synthesis of triazolium triflates, in the example of compound **81d-I-OTf**

Triazole **81d-I** (0.090 g, 0.176 mmol) was dissolved in DCM (3.5 mL) under an argon atmosphere. Methyl triflate (0.030 mL, 0.264 mmol) was added drop-wise and the reaction mixture was stirred at RT for three days. Et<sub>2</sub>O (5.0 mL) was added to the reaction mixture and fine precipitate formed, which was filtered to provide trifluoromethanesulfonate salt **81d-I-OTf** as colourless crystals (0.101 g, 85% yield).

### 5.9.1 1-Benzyl-4-(3,5-bis(trifluoromethyl)phenyl)-5-iodo-3-methyl-1*H*-1,2,3-triazol-3-ium trifluoromethanesulfonate **92d-I-OTf**

Triazole **92d-I** (0.212 g, 0.426 mmol) was dissolved in DCM (9.0 mL) under an argon atmosphere. Methyl triflate (0.145 mL, 1.28 mmol) was added drop-wise and the reaction mixture was stirred overnight at RT. The reaction mixture was concentrated, DCM (3.0 mL) and Et<sub>2</sub>O (2.0 mL) were added and fine precipitate formed, which was filtered to provide trifluoromethanesulfonate salt **92d-I-OTf** as off-white crystals (0.230 g, 82% yield). <sup>1</sup>H NMR (400 MHz, MeOD) δ 8.38 (s, 1H), 8.35 (s, 2H), 7.58 – 7.51 (m, 2H), 7.51 – 7.40 (m, 3H), 5.98 (s, 2H), 4.29 (s, 3H). <sup>13</sup>C NMR (101 MHz, MeOD) δ 146.2, 134.2 (q, *J* = 34.3 Hz), 133.0, 132.6, (q, *J* = 5.8 Hz), 130.7, 130.4, 130.1, 127.1, 127.0 – 126.9 (m), 124.2 (d, *J* = 272.7 Hz) 93.1, 59.3, 39.9.

### 5.9.2 1-Benzyl-4-(3,5-bis(trifluoromethyl)phenyl)-3-methyl-1*H*-1,2,3-triazol-3-ium trifluoromethanesulfonate **92d-H-OTf**

Triazole **92d-H** (0.214 g, 0.577 mmol) was dissolved in DCM (10 mL) under an argon atmosphere. Methyl triflate (0.20 mL, 1.73 mmol) was added drop-wise and the reaction mixture was stirred for two days at RT. The reaction mixture was concentrated, DCM (3.0 mL) and Et<sub>2</sub>O (2.0 mL) were added and fine precipitate formed, which was filtered to provide trifluorosulfonic salt **92d-H-OTf** as off-white crystals (0.264 g, 85% yield). <sup>1</sup>H NMR (400 MHz, CDCl<sub>3</sub>) δ 8.70 (s, 1H), 8.16 (s, 2H), 8.09 (s, 1H), 7.60 – 7.52 (m, *J* = 14.0, 7.5 Hz, 2H), 7.49 – 7.38 (m, 3H), 5.82 (s, 2H), 4.26 (s, 3H).

### 5.9.3 (2*R*,4*S*,5*R*)-2-((*R*)-(4-(3,5-Bis(trifluoromethyl)phenyl)-3-methyliumyl-1*H*-1,2,3λ<sup>4</sup>-triazol-1-yl))(6-methoxy-1-methylquinolin-1-ium-4-yl)methyl)-1-methyl-5-vinylquinuclidin-1-ium trifluoromethanesulfonate **84d-H-OTf**

Triazole **84d-H** (0.136 g, 0.23 mmol) was dissolved in DCM (5.0 mL) under an argon atmosphere. Methyl triflate (0.27 mL, 2.3 mmol) was added drop-wise and the reaction mixture was stirred overnight at RT. The reaction mixture was concentrated, DCM (3.0 mL) and Et<sub>2</sub>O (2.0 mL) were added and fine precipitate formed, which was filtered to provide trifluorosulfonic salt **84d-H-OTf** as off-white crystals (0.215 g, 87% yield). <sup>1</sup>H NMR (400 MHz, MeOD) δ 9.39 (s, 1H), 9.23 (d, *J* = 6.2 Hz, 1H), 8.55 (d, *J* = 9.7 Hz, 1H), 8.44 (d, *J* = 6.2 Hz, 1H), 8.32 (s, 2H), 8.29 (s, 1H), 8.17 (d, *J* = 2.6 Hz, 1H), 8.01 (dd, *J* = 9.7, 2.4 Hz, 1H), 7.83 (d, *J* = 9.7 Hz, 1H), 5.87 – 5.70 (m, 2H), 5.38 (d, *J* = 17.4 Hz, 1H), 5.26 (d, *J* = 10.6 Hz, 1H), 4.66 (s, 3H), 4.48 (s, 3H), 4.34 – 4.19 (m, 1H), 4.26 (s, 3H), 3.99 (t, *J* = 11.7 Hz, 1H), 3.91 – 3.77 (m, 2H), 3.05 (s, 3H), 3.03 – 2.94 (m, 1H), 2.34 – 2.24 (m, 1H), 2.23 – 2.14 (m, 1H), 2.11 (bs, 1H), 2.00 – 1.90 (m, 1H), 1.41 – 1.30 (m, 1H). <sup>13</sup>C NMR (101 MHz, MeOD) δ 163.5, 148.2, 146.32, 144.0, 137.1, 137.1, 134.0 (d, *J* = 34.4 Hz), 132.5, 132.16 – 131.70 (m), 131.3, 130.4, 127.1 – 126.6 (m), 125.6, 124.3, 124.1 (q, *J* = 272.3 Hz), 123.3,

121.6 (q,  $J = 318.6$  Hz), 118.1, 103.5, 66.8, 62.6, 60.9, 58.8, 58.2, 51.1, 47.1, 40.7, 3.0, 27.8, 27.2, 24.3.

### 5.10 Representative procedure for the synthesis of triazolium tetrafluoroborates, in the example of compound **81a-I-BF<sub>4</sub>**

Triazole **81a-I** (0.124 g, 0.330 mmol) was dissolved in DCM (6.5 mL) under an argon atmosphere. Trimethyloxonium tetrafluoroborate (0.061 mg, 0.412 mmol) was added and the reaction mixture was stirred at RT for 24 h. The reaction was quenched by adding MeOH (10.0 mL) and stirred for 1 h. After the removal of the solvents under reduced pressure, the crude product was dissolved in MeOH (10.0 mL), Et<sub>2</sub>O (5.0 mL) was added to the solution and a fine precipitate formed, which was filtered. The crystallisation was repeated a second time using MeOH (5.0 mL) and Et<sub>2</sub>O (25.0 mL) to provide **81a-I-BF<sub>4</sub>** as colourless crystals (in total: 0.140 g, 89% yield).

### 5.11 Representative procedure for the synthesis of triazolium tetrakis-3,5-bis(trifluoromethyl)phenylborates, in the example of compound **81e-I-BARF**

Triazolium **81e-I-OTf** (0.096 g, 0.152 mmol) was dissolved in a mixture of DCM (9.5 mL) and MeOH (3.2 mL), tetramethylammonium BARF (0.156 g, 0.166 mmol) was added and the reaction mixture was stirred at RT for 24 h. After the removal of the solvents under reduced pressure, the precipitate was suspended in Et<sub>2</sub>O (6.5 mL), stirred at RT for 10 minutes and 45 minutes at -20 °C. The precipitate was removed by filtration and discarded. The filtrate was concentrated under reduced pressure and purified by column chromatography on silica gel (starting from 5% of MeOH in DCM/petroleum ether 1/1) to provide **81e-I-BARF** as an off white solid (0.184 g, 90% yield).

### 5.12 (*E*)-*N*-(4-Methoxyphenyl)-1-phenylethan-1-imine **103**

Acetophenone (1.09 g, 9.07 mmol) and *p*-anisidine (1.1 mL, 9.56 mmol) were dissolved in toluene (30 mL), the flask was equipped with a Dean-Stark trap with 3 Å molecular sieves was placed. The reaction mixture was refluxed for one day, then cooled to RT and concentrated under reduced pressure. Purification by crystallisation from a mixture of EtOAc (10 mL) and hexane (30 mL) at 0 °C provided the imine **103** as yellow needles (0.88 g, 43%). <sup>1</sup>H NMR (400 MHz, CDCl<sub>3</sub>) δ 8.03 – 7.91 (m, 3H), 7.51 – 7.40 (m, 2H), 6.92 (d,  $J = 8.7$  Hz, 2H), 6.76 (d,  $J = 8.7$  Hz, 2H), 3.82 (s, 3H), 2.26 (s, 3H).

### 5.13 General procedure for imine **103** reduction with Hantzsch ester **27**

XB donor (8.0 mmol, 0.05 equiv), imine **103** (0.160 mmol, 1 equiv) and Hantzsch ester **27** (0.192 mmol, 1.2 equiv) were dissolved in DCE (0.400 mL) and the reaction mixture was placed in an oil bath at 50 °C. Samples were taken from the reaction mixture at approximately 15-, 30- and 60-minute intervals and analysed by <sup>1</sup>H NMR spectroscopy. The ratio of imine **103** to product **104** was used to calculate the conversion. Product **104**: <sup>1</sup>H NMR (400 MHz, CDCl<sub>3</sub>) δ 7.41 – 7.30 (m,  $J = 15.1, 10.8, 4.7$  Hz, 4H), 7.28 – 7.21 (m, 1H), 6.75 – 6.66 (m, 2H), 6.53 – 6.45 (m, 2H), 4.43 (q,  $J = 6.7$  Hz, 1H), 3.71 (s, 3H), 1.51 (d,  $J = 6.7$  Hz, 3H). <sup>13</sup>C NMR (101 MHz, CDCl<sub>3</sub>) δ 152.0, 145.6, 141.7, 128.7, 126.9, 126.0, 114.9, 114.7, 55.9, 54.4, 25.3.

### 5.14 1-(*tert*-butyldimethylsilyloxy)-1-isopropoxyethylene **107**

The silyl enol ether **107** was obtained according to ref.<sup>172</sup> (1.44 g, 43%). <sup>1</sup>H NMR (400 MHz, CDCl<sub>3</sub>) δ 4.20 (hept, *J* = 6.1 Hz, 1H), 3.27 (d, *J* = 2.3 Hz, 1H), 3.09 (d, *J* = 2.2 Hz, 1H), 1.25 (d, *J* = 6.1 Hz, 6H), 0.93 (s, 9H), 0.17 (s, 6H). <sup>13</sup>C NMR (101 MHz, CDCl<sub>3</sub>) δ 159.9, 70.0, 61.7, 25.8, 21.8, 18.3, -4.4.

### 5.15 General procedure for the Reisert-type reaction

Quinoline **105** (0.102 mmol, 1 equiv) was dissolved in MTBE (2 mL) under an argon atmosphere and was cooled to 0 °C. Then, 2,2,2-trichloroethyl chloroformate **106** (0.102 mmol, 1 equiv) was added and the reaction mixture was stirred for 40 min, before cooling to -78 °C. The XB donor (0.010 mmol, 0.1 equiv) and the silyl enol ether **107** (0.203 mmol, 2 equiv) were added sequentially and the reaction mixture was allowed to warm to RT over a 20 h period. Direct purification of the reaction mixture by column chromatography on silica gel (starting from 5% of EtOAc in petroleum ether) provided the product **108** as a colourless oil. <sup>1</sup>H NMR (400 MHz, CDCl<sub>3</sub>) δ 7.66 (bs, 1H), 7.28 – 7.19 (m, 1H), 7.17 – 7.09 (m, 2H), 6.54 (d, *J* = 9.5 Hz, 1H), 6.15 (dd, *J* = 9.5, 5.9 Hz, 1H), 5.52 (q, *J* = 7.3 Hz, 1H), 5.04 (bs, 1H), 4.98 (p, *J* = 6.3 Hz, 1H), 4.71 (bs, 1H), 2.46 (d, *J* = 7.4 Hz, 2H), 1.21 (t, *J* = 5.9 Hz, 6H). HPLC (Chiralcel OD-H; hexane/*i*PrOH; 99/1; 1 mL/min; 25°C; 300 nm) *t*<sub>R</sub> = 11.27, *t*<sub>R</sub> = 13.86 min.

### 5.16 General procedure for the reactions between **42** and **98**

All of the crystallised XB donors were additionally purified by column chromatography (starting from 5% of MeOH in DCM) before their use in the catalytic experiments. Danishefsky's diene **42** (purity 96%) was purchased from Alfa Aesar and used as received. The XB donor (0.052 mmol, 0.2 equiv) was dissolved in a stock solution of CD<sub>2</sub>Cl<sub>2</sub> (0.650 mL) containing **98** (0.4 M, 1.0 equiv) and *p*-xylene (0.2 M, 0.5 equiv). Then 0.600 mL of the solution was transferred to a NMR tube and the <sup>1</sup>H spectrum was measured. Danishefsky's diene **42** (0.063 mL, 1.3 equiv) was added and the <sup>1</sup>H spectra were measured at approximately 8-, 15- and 30-minute intervals for at least the first 8 h of the reaction. In certain cases, product **109** was isolated by purification with column chromatography on silica gel (starting from 20% of EtOAc in petroleum ether) to provide **109** as a yellow oil with yields usually 10% lower than the corresponding conversion.

Parameters specific to the experiment: T = 297 K, Relaxation delay = 36 s, Number of Scans = 8. The data processing was performed using MestreNova. The spectra were phased, baseline-corrected and zero-filled (to spectrum size 128K). Then a line-fitting function (deconvolution) was used to more accurately integrate the peaks corresponding to the protons of the methoxy group of imine **98** and the methyl group of *p*-xylene.

### 5.17 General information on the <sup>1</sup>H NMR titration experiments

A stock solution of XB donor was prepared in CDCl<sub>3</sub>. The XB acceptor solution was prepared by dissolving the acceptor in a fixed amount of the donor solution to ensure the concentration of XB donor would not change during the experiment. All of the solutions were prepared using Hamilton® Gastight syringes, and samples were weighed on a microbalance with an accuracy of 6 µg. CDCl<sub>3</sub> was dried over 3Å molecular sieves to keep the water content to a minimum. Small aliquots from the XB acceptor stock solution

were added increasingly (from 0 to 150-300  $\mu\text{l}$ ) to the NMR tube containing 600  $\mu\text{l}$  of the XB donor stock solution. The concentration of each XB acceptor stock solution was based on the predicted XB binding strength. For the quantitative measurement, depending on the concentration of the XB donor; 4, 8 or 32 scans were collected with up to 20 s relaxation delays depending on the donor. The upfield shifts of methyl protons of the XB donor were monitored during the experiment. The chemical shifts were referenced based on a  $\text{CHCl}_3$  residual peak at 7.26 ppm.  $K_a$  values were determined using non-linear regression analysis.

For the experiments with thioureas **95**, **96**, urea **97**, imines **41** and **98**: a 1.5 mM stock solution of XB donor was used, except in the case of the experiments between acceptor **96** and XB donors **81d-Br-OTf** and **81d-Cl-OTf**, in which 15 mM stock solutions were used.  $^1\text{H}$  NMR titration experiments were performed on a Bruker Avance 400 MHz spectrometer at 297 K.  $K_a$  values were determined using non-linear regression analysis. For the fitting of the binding data, a global 1:1 binding isotherm of the HypNMR2008<sup>157,158</sup> program was used (except in the case of [**96-81d-Br-OTf**] and [**96-81d-Cl-OTf**], in which the program SigmaPlot Version 13.0 was used). The given standard error depicts error from curve fit calculations

For the experiments with quinuclidine **99**: a 1.0 mM stock solution of XB donor was used, except in the case of the experiments with the XB donors **81c-I-OTf** and **81a-Br-OTf**, in which 1.5 mM stock solutions were used.  $^1\text{H}$  NMR titration experiments were performed on a Bruker Avance III 800 MHz spectrometer at 298 K. For the fitting of the binding data, a 1:1 binding isotherm of BindFit<sup>159,160</sup> was used (freely available at <http://supramolecular.org>). The standard errors given are the calculated mean values of the two parallel experiments.

**Table 13.** Supporting information concerning compounds discussed in the thesis but not presented in the Experimental section can be found in the corresponding publications.<sup>a</sup>

Entry	Compound number in thesis	Compound number in Publication			
		I	II	III	IV
1	<b>a-Br</b>		+		+
2	<b>a-H</b>	+			
3	<b>a-I</b>	+	+	+	
4	<b>b-I</b>	+			
5	<b>c-I</b>		+		+
6	<b>d-Br</b>	+			
7	<b>d-H</b>	+			
8	<b>d-I</b>	+		+	
9	<b>e-Br</b>		+		
10	<b>e-I</b>		+		+
11	<b>f-II</b>	<b>6</b>		+	
12	<b>TBTA</b>	<b>TBTA</b>	+	<b>TBTA</b>	
13	<b>TMA-BARF</b>		+		+
14	<b>TTTA</b>	<b>TTTA</b>	+	<b>TTTA</b>	<b>TTTA</b>
15	<b>41</b>	<b>10</b>			
16	<b>76</b>		+	+	

17	<b>79</b>	+	+		
18	<b>81</b>	+	+	+	<b>4</b>
19	<b>81a-Br</b>		+		+
20	<b>81a-Br-OTf</b>		<b>4-OTf</b>		<b>10</b>
21	<b>81a-Cl</b>				+
22	<b>81a-Cl-OTf</b>				<b>11</b>
23	<b>81a-H</b>		+		+
24	<b>81a-H-OTf</b>		<b>6-OTf</b>		<b>12</b>
25	<b>81a-I</b>	<b>3e</b>	+		<b>6a</b>
26	<b>81a-I-BARF</b>		<b>1-BARF</b>		<b>9a</b>
27	<b>81a-I-BF<sub>4</sub></b>		<b>1-BF<sub>4</sub></b>		<b>8a</b>
28	<b>81a-I-OTf</b>	<b>4e</b>	<b>1-OTf</b>		<b>7a</b>
29	<b>81b-I</b>	<b>3d</b>			
30	<b>81b-I-OTf</b>	<b>4d</b>			
31	<b>81c-I</b>		+		<b>6c</b>
32	<b>81c-I-BF<sub>4</sub></b>		<b>2-BF<sub>4</sub></b>		<b>8c</b>
33	<b>81c-I-OTf</b>		<b>2-OTf</b>		<b>7c</b>
34	<b>81d-Br</b>	<b>3b</b>			
35	<b>81d-Br-OTf</b>	<b>4b</b>			
36	<b>81d-Cl</b>	<b>3c</b>			
37	<b>81d-Cl-OTf</b>	<b>4c</b>			
38	<b>81d-H</b>	+			
39	<b>81d-H-OTf</b>	<b>4k</b>			
40	<b>81d-I</b>	<b>3a</b>			<b>6d</b>
41	<b>81d-I-BF<sub>4</sub></b>	<b>5a</b>			
42	<b>81d-I-OTf</b>	<b>4a</b>			<b>7d</b>
43	<b>81e-Br</b>		+		
44	<b>81e-Br-BARF</b>		<b>5-BARF</b>		
45	<b>81e-Br-OTf</b>		+		
46	<b>81e-I</b>		<b>7</b>		<b>6b</b>
47	<b>81e-I-BARF</b>		<b>3-BARF</b>		
48	<b>81e-I-OTf</b>		<b>3-OTf</b>		<b>7b</b>
49	<b>b81f-II</b>	<b>3h</b>			
50	<b>b81f-II-2BF<sub>4</sub></b>	<b>5h</b>			
51	<b>82</b>			+	
52	<b>82d-I</b>			<b>8</b>	
53	<b>83</b>	+			
54	<b>83d-I</b>	<b>3f</b>			
55	<b>83d-I-OTf</b>	<b>4f</b>			
56	<b>84</b>	+			
57	<b>84d-I</b>	<b>3g</b>			
58	<b>84d-I-3OTf</b>	<b>4g</b>			
59	<b>b84f-II</b>	<b>3i</b>			

60	85			+	
61	85a-I			5	
62	85a-I-OTf			5-OTf	
63	86			+	
64	86d-I			6	
65	86d-I-OTf			6-OTf	
66	b86f-II			9	
67	b86f-II-2OTf			9-OTf	
68	87			+	
69	87d-I			7	
70	88			+	
71	88a-I			4a	
72	88a-I-OTf			4a-OTf	
73	89			+	
74	89a-I			4b	
75	89a-I-OTf			4b-OTf	
76	90			+	
77	90a-I			4c	
78	90a-I-OTf			4c-OTf	
79	91			+	
80	91d-I			14	
81	91d-I-OTf			14-OTf	
82	92	+	+		
83	93f-II	3j			
84	93f-II-4OTf	4j			
85	94			+	
86	b94f-II			10	
87	b94f-II-2OTf			10-OTf	
88	98	11			1
89	(R)-101		(R)-8		
90	(S)-101		(S)-8		
91	(R)-102		(R)-9		
92	(S)-102		(S)-9		
93	109				3

<sup>a</sup> In certain instances the publication may only contain a reference to the synthetic procedure used to obtain the compound or its commercial availability. + – the compound does not have a number in the publication; however, the publication contains the synthetic procedure or how the compound was obtained.



## References

1. Desiraju, G. R., Shing Ho, P., Kloo, L., Legon, A. C., Marquardt, R., Metrangolo, P., Politzer, P., Resnati, G., Rissanen, K. *Pure Appl. Chem.*, **2013**, *85*, 1711–1713.
2. Colin, J. J., de Claubry, H. *Ann. Chim*, **1814**, *90*, 87–100.
3. Pelletier, P., Caventou, J. J. *Ann Chim*, **1819**, *10*, 142–177.
4. Rhoussopoulos, O. *Ber. Dtsch. Chem. Ges.*, **1883**, *16*, 202–203.
5. Benesi, H. A., Hildebrand, J. H. *J. Am. Chem. Soc.*, **1949**, *71*, 2703–2707.
6. Mulliken, R. S. *J. Am. Chem. Soc.*, **1950**, *72*, 600–608.
7. Hassel, O., Hvoslef, J. *Acta Chem. Scand.*, **1954**, *8*, 873.
8. Hassel, O., Stromme, K. O. *Acta Chem. Scand.*, **1958**, *12*, 1146–1147.
9. Brinck, T., Murray, J. S., Politzer, P. *Int. J. Quantum Chem.*, **1992**, *44*, 57–64.
10. Legon, A. C. *Angew. Chem., Int. Ed.*, **1999**, *38*, 2686–2714.
11. Guo, N., Maurice, R., Teze, D., Graton, J., Champion, J., Montavon, G., Galland, N. *Nat. Chem.*, **2018**, *10*, 428–434.
12. Montaña, Á. M. *ChemistrySelect*, **2017**, *2*, 9094–9112.
13. Cavallo, G., Metrangolo, P., Milani, R., Pilati, T., Priimagi, A., Resnati, G., Terraneo, G. *Chem. Rev.*, **2016**, *116*, 2478–2601.
14. Wang, H., Wang, W., Jin, W. J. *Chem. Rev.*, **2016**, *116*, 5072–5104.
15. Metrangolo, P., Meyer, F., Pilati, T., Resnati, G., Terraneo, G. *Angew. Chem., Int. Ed.*, **2008**, *47*, 6114–6127.
16. Gilday, L. C., Robinson, S. W., Barendt, T. A., Langton, M. J., Mullaney, B. R., Beer, P. D. *Chem. Rev.*, **2015**, *115*, 7118–7195.
17. Christopherson, J. C., Topić, F., Barrett, C. J., Friščić, T. *Cryst. Growth Des.*, **2018**, *18*, 1245–1259.
18. Li, B., Zang, S.-Q., Wang, L.-Y., Mak, T. C. W. *Coord. Chem. Rev.*, **2016**, *308*, 1–21.
19. Troff, R. W., Mäkelä, T., Topić, F., Valkonen, A., Raatikainen, K., Rissanen, K. *Eur. J. Org. Chem.*, **2013**, 1617–1637.
20. Raatikainen, K., Rissanen, K. *CrystEngComm*, **2011**, *13*, 6972–6977.
21. Berger, G., Soubhye, J., Meyer, F. *Polym. Chem.*, **2015**, *6*, 3559–3580.
22. Tepper, R., Schubert, U. S. *Angew. Chem., Int. Ed.*, **2018**, *57*, 6004–6016.
23. Jentzsch, A. V. *Pure Appl. Chem.*, **2015**, *87*, 15–41.
24. Beale, T. M., Chudzinski, M. G., Sarwar, M. G., Taylor, M. S. *Chem. Soc. Rev.*, **2013**, *42*, 1667–1680.
25. Brown, A., Beer, P. D. *Chem. Commun.*, **2016**, *52*, 8645–8658.
26. Bulfield, D., Huber, S. M. *Chem. - Eur. J.*, **2016**, *22*, 14434–14450.
27. Sutar, R., Huber, S. M. *ACS Catal.*, **2019**, 9622–9639.
28. Bamberger, J., Ostler, F., Mancheño, O. G. *ChemCatChem*, **2019**, *11*, 5198–5211.
29. Metrangolo, P., Neukirch, H., Pilati, T., Resnati, G. *Acc. Chem. Res.*, **2005**, *38*, 386–395.
30. Rissanen, K. *CrystEngComm*, **2008**, *10*, 1107–1113.
31. Huber, S. M., Scanlon, J. D., Jimenez-Izal, E., Ugalde, J. M., Infante, I. *Phys. Chem. Chem. Phys.*, **2013**, *15*, 10350–10357.
32. Lommerse, J. P. M., Stone, A. J., Taylor, R., Allen, F. H. *J. Am. Chem. Soc.*, **1996**, *118*, 3108–3116.
33. Kolář, M. H., Hobza, P. *Chem. Rev.*, **2016**, *116*, 5155–5187.
34. Kolář, M., Hostaš, J., Hobza, P. *Phys. Chem. Chem. Phys.*, **2014**, *16*, 9987–9996.
35. Politzer, P., Murray, J. S., Clark, T. *Phys. Chem. Chem. Phys.*, **2013**, *15*, 11178–11189.

36. Politzer, P., Murray, J. S. *ChemPhysChem*, **2013**, *14*, 278–294.
37. Clark, T., Hennemann, M., Murray, J. S., Politzer, P. *J. Mol. Model.*, **2007**, *13*, 291–296.
38. Nepal, B., Scheiner, S. *J. Phys. Chem. A*, **2015**, *119*, 13064–13073.
39. Dumele, O., Wu, D., Trapp, N., Goroff, N., Diederich, F. *Org. Lett.*, **2014**, *16*, 4722–4725.
40. Zingaro, R. A., Hedges, R. M. *J. Phys. Chem.*, **1961**, *65*, 1132–1138.
41. Awwadi, F. F., Willett, R. D., Peterson, K. A., Twamley, B. *J. Phys. Chem. A*, **2007**, *111*, 2319–2328.
42. Puttreddy, R., Jurček, O., Bhowmik, S., Mäkelä, T., Rissanen, K. *Chem. Commun.*, **2016**, *52*, 2338–2341.
43. Maugeri, L., Asencio-Hernández, J., Lébl, T., Cordes, D. B., Slawin, A. M. Z., Delsuc, M. A., Philp, D. *Chem. Sci.*, **2016**, *7*, 6422–6428.
44. Xu, K., Ho, D. M., Pascal, R. A. *J. Org. Chem.*, **1995**, *60*, 7186–7191.
45. Sabater, P., Zapata, F., López, B., Fernández, I., Caballero, A., Molina, P. *Dalt. Trans.*, **2018**, *47*, 15941–15947.
46. Cametti, M., Raatikainen, K., Metrangolo, P., Pilati, T., Terraneo, G., Resnati, G. *Org. Biomol. Chem.*, **2012**, *10*, 1329–1333.
47. Tepper, R., Schulze, B., Jäger, M., Friebe, C., Scharf, D. H., Görls, H., Schubert, U. S. *J. Org. Chem.*, **2015**, *80*, 3139–3150.
48. Riel, A. M. S., Decato, D. A., Sun, J., Massena, C. J., Jessop, M. J., Berryman, O. B. *Chem. Sci.*, **2018**, *9*, 5828–5836.
49. Kolb, H. C., Finn, M. G., Sharpless, K. B. *Angew. Chem., Int. Ed.*, **2001**, *40*, 2004–2021.
50. Meldal, M., Tomøe, C. W. *Chem. Rev.*, **2008**, *108*, 2952–3015.
51. Haldón, E., Nicasio, M. C., Pérez, P. J. *Org. Biomol. Chem.*, **2015**, *13*, 9528–9550.
52. Haraguchi, R., Hoshino, S., Sakai, M., Tanazawa, S., Morita, Y., Komatsu, T., Fukuzawa, S. *Chem. Commun.*, **2018**, *54*, 10320–10323.
53. Barsoum, D., Brassard, C., Deeb, J., Okashah, N., Sreenath, K., Simmons, J., Zhu, L. *Synthesis*, **2013**, *45*, 2372–2386.
54. Li, L., Hao, G., Zhu, A., Liu, S., Zhang, G. *Tetrahedron Lett.*, **2013**, *54*, 6057–6060.
55. Barsoum, D. N., Okashah, N., Zhang, X., Zhu, L. *J. Org. Chem.*, **2015**, *80*, 9542–9551.
56. Li, L., Xing, X., Zhang, C., Zhu, A., Fan, X., Chen, C., Zhang, G. *Tetrahedron Lett.*, **2018**, *59*, 3563–3566.
57. Brotherton, W. S., Clark, R. J., Zhu, L. *J. Org. Chem.*, **2012**, *77*, 6443–6455.
58. Kuijpers, B. H. M., Dijkmans, G. C. T., Groothuys, S., Quaedflieg, P. J. L. M., Blaauw, R. H., Van Delft, F. L., Rutjes, F. P. J. T. *Synlett*, **2005**, 3059–3062.
59. McIntosh, M. L., Johnston, R. C., Pattawong, O., Ashburn, B. O., Naffziger, M. R., Cheong, P. H. Y., Carter, R. G. *J. Org. Chem.*, **2012**, *77*, 1101–1112.
60. Hein, J. E., Tripp, J. C., Krasnova, L. B., Sharpless, K. B., Fokin, V. V. *Angew. Chem., Int. Ed.*, **2009**, *48*, 8018–8021.
61. García-Álvarez, J., Díez, J., Gimeno, J. *Green Chem.*, **2010**, *12*, 2127–2130.
62. Pérez, J. M., Crosbie, P., Lal, S., Díez-González, S. *ChemCatChem*, **2016**, *8*, 2222–2226.
63. Chung, R., Vo, A., Fokin, V. V., Hein, J. E. *ACS Catal.*, **2018**, *8*, 7889–7897.
64. Worrell, B. T., Hein, J. E., Fokin, V. V. *Angew. Chem., Int. Ed.*, **2012**, *51*, 11791–11794.

65. Johansson, J. R., Beke-Somfai, T., Said Stålsmeden, A., Kann, N. *Chem. Rev.*, **2016**, *116*, 14726–14768.
66. Oakdale, J. S., Sit, R. K., Fokin, V. V. *Chem. - Eur. J.*, **2014**, *20*, 11101–11110.
67. Schulze, B., Schubert, U. S. *Chem. Soc. Rev.*, **2014**, *43*, 2522–2571.
68. Waterloo, A. R., Kunakom, S., Hampel, F., Tykwinski, R. R. *Macromol. Chem. Phys.*, **2012**, *213*, 1020–1032.
69. Adam, W., Grimison, A. *Theor. Chim. Acta*, **1967**, *7*, 342–351.
70. Bakbak, S., Leech, P. J., Carson, B. E., Saxena, S., King, W. P., Bunz, U. H. F. *Macromolecules*, **2006**, *39*, 6793–6795.
71. Matulis, V. E., Halauko, Y. S., Ivashkevich, O. A., Gaponik, P. N. *J. Mol. Struct.: THEOCHEM*, **2009**, *909*, 19–24.
72. Magill, A. M., Yates, B. F. *Aust. J. Chem.*, **2004**, *57*, 1205.
73. Higgins, E. M., Sherwood, J. A., Lindsay, A. G., Armstrong, J., Massey, R. S., Alder, R. W., O'Donoghue, A. C. *Chem. Commun.*, **2011**, *47*, 1559–1561.
74. Massey, R. S., Collett, C. J., Lindsay, A. G., Smith, A. D., O'Donoghue, A. C. *J. Am. Chem. Soc.*, **2012**, *134*, 20421–20432.
75. Donnelly, K. F., Petronilho, A., Albrecht, M. *Chem. Commun.*, **2013**, *49*, 1145–1159.
76. Kilah, N. L., Wise, M. D., Serpell, C. J., Thompson, A. L., White, N. G., Christensen, K. E., Beer, P. D. *J. Am. Chem. Soc.*, **2010**, *132*, 11893–11895.
77. Kilah, N. L., Wise, M. D., Beer, P. D. *Cryst. Growth Des.*, **2011**, *11*, 4565–4571.
78. Walter, S. M., Kniep, F., Rout, L., Schmidtchen, F. P., Herdtweck, E., Huber, S. M. *J. Am. Chem. Soc.*, **2012**, *134*, 8507–8512.
79. Gilday, L. C., White, N. G., Beer, P. D. *Dalt. Trans.*, **2013**, *42*, 15766–15773.
80. Borissov, A., Lim, J. Y. C., Brown, A., Christensen, K. E., Thompson, A. L., Smith, M. D., Beer, P. D. *Chem. Commun.*, **2017**, *53*, 2483–2486.
81. Mungalpara, D., Stegmüller, S., Kubik, S. *Chem. Commun.*, **2017**, *53*, 5095–5098.
82. Lim, J. Y. C., Marques, I., Félix, V., Beer, P. D. *J. Am. Chem. Soc.*, **2017**, *139*, 12228–12239.
83. Langton, M. J., Marques, I., Robinson, S. W., Félix, V., Beer, P. D. *Chem. - Eur. J.*, **2016**, *22*, 185–192.
84. Breugst, M., von der Heiden, D. *Chem. - Eur. J.*, **2018**, *24*, 9187–9199.
85. Langton, M. J., Robinson, S. W., Marques, I., Félix, V., Beer, P. D. *Nat. Chem.*, **2014**, *6*, 1039–1043.
86. Tepper, R., Schulze, B., Görls, H., Bellstedt, P., Jäger, M., Schubert, U. S. *Org. Lett.*, **2015**, *17*, 5740–5743.
87. Tepper, R., Schulze, B., Bellstedt, P., Heidler, J., Görls, H., Jäger, M., Schubert, U. S. *Chem. Commun.*, **2017**, *53*, 2260–2263.
88. Zhou, L., Lu, Y., Xu, Z., Peng, C., Liu, H. *Struct. Chem.*, **2018**, *29*, 533–540.
89. Mercurio, J. M., Knighton, R. C., Cookson, J., Beer, P. D. *Chem. - Eur. J.*, **2014**, *20*, 11740–11749.
90. Lim, J. Y. C., Marques, I., Ferreira, L., Félix, V., Beer, P. D. *Chem. Commun.*, **2016**, *52*, 5527–5530.
91. González, L., Zapata, F., Caballero, A., Molina, P., Ramírez De Arellano, C., Alkorta, I., Elguero, J. *Chem. - Eur. J.*, **2016**, *22*, 7533–7544.
92. Lim, J. Y. C., Marques, I., Félix, V., Beer, P. D. *Chem. Commun.*, **2018**, *54*, 10851–10854.
93. Barendt, T. A., Robinson, S. W., Beer, P. D. *Chem. Sci.*, **2016**, *7*, 5171–5180.

94. Barendt, T. A., Docker, A., Marques, I., Félix, V., Beer, P. D. *Angew. Chem., Int. Ed.*, **2016**, *55*, 11069–11076.
95. Tepper, R., Bode, S., Geitner, R., Jäger, M., Görls, H., Vitz, J., Dietzek, B., Schmitt, M., Popp, J., Hager, M. D., Schubert, U. S. *Angew. Chem., Int. Ed.*, **2017**, *56*, 4047–4051.
96. Kniep, F., Rout, L., Walter, S. M., Bensch, H. K. V., Jungbauer, S. H., Herdtweck, E., Huber, S. M. *Chem. Commun.*, **2012**, *48*, 9299–9301.
97. Jungbauer, S. H., Huber, S. M. *J. Am. Chem. Soc.*, **2015**, *137*, 12110–12120.
98. Dreger, A., Engelage, E., Mallick, B., Beer, P. D., Huber, S. M. *Chem. Commun.*, **2018**, *54*, 4013–4016.
99. Von Der Heiden, D., Detmar, E., Kuchta, R., Breugst, M. *Synlett*, **2018**, *29*, 1307–1313.
100. Squitieri, R. A., Fitzpatrick, K. P., Jaworski, A. A., Scheidt, K. A. *Chem. - Eur. J.*, **2019**, *60208*, 10069–10073.
101. Sarwar, M. G., Dragisic, B., Salsberg, L. J., Gouliaras, C., Taylor, M. S. *J. Am. Chem. Soc.*, **2010**, *132*, 1646–1653.
102. Hawthorne, B., Fan-Hagenstein, H., Wood, E., Smith, J., Hanks, T. *Int. J. Spectrosc.*, **2013**, *2013*, 1–10.
103. Cabot, R., Hunter, C. A. *Chem. Commun.*, **2009**, 2005–2007.
104. Sarwar, M. G., Dragisič, B., Dimitrijevič, E., Taylor, M. S. *Chem. - Eur. J.*, **2013**, *19*, 2050–2058.
105. Robertson, C. C., Perutz, R. N., Brammer, L., Hunter, C. A. *Chem. Sci.*, **2014**, *5*, 4179–4183.
106. Robertson, C. C., Wright, J. S., Carrington, E. J., Perutz, R. N., Hunter, C. A., Brammer, L. *Chem. Sci.*, **2017**, *8*, 5392–5398.
107. Evans, N. H., Beer, P. D. *Angew. Chem., Int. Ed.*, **2014**, *53*, 11716–11754.
108. Molina, P., Zapata, F., Caballero, A. *Chem. Rev.*, **2017**, *117*, 9907–9972.
109. Sarwar, M. G., Dragisic, B., Sagoo, S., Taylor, M. S. *Angew. Chem., Int. Ed.*, **2010**, *49*, 1674–1677.
110. Zapata, F., Caballero, A., White, N. G., Claridge, T. D. W., Costa, P. J., Félix, V., Beer, P. D. *J. Am. Chem. Soc.*, **2012**, *134*, 11533–11541.
111. Ciancaleoni, G., MacChioni, A., Rocchigiani, L., Zuccaccia, C. *RSC Adv.*, **2016**, *6*, 80604–80612.
112. Puttreddy, R., Jurček, O., Bhowmik, S., Mäkelä, T., Rissanen, K. *Chem. Commun.*, **2016**, *52*, 2338–2341.
113. Laurence, C., Graton, J., Berthelot, M., El Ghomari, M. J. *Chem. - Eur. J.*, **2011**, *17*, 10431–10444.
114. Metrangolo, P., Panzeri, W., Recupero, F., Resnati, G. *J. Fluor. Chem.*, **2002**, *114*, 27–33.
115. Pinter, B., Nagels, N., Herrebout, W. A., De Proft, F. *Chem. - Eur. J.*, **2013**, *19*, 519–530.
116. List, B. *Angew. Chem., Int. Ed.*, **2010**, *49*, 1730–1734.
117. Eder, U., Sauer, G., Wiechert, R. *Angew. Chem., Int. Ed.*, **1971**, *10*, 496–497.
118. Hajos, Z. G., Parrish, D. R. *J. Org. Chem.*, **1974**, *39*, 1612–1615.
119. List, B., Lerner, R. A., Barbas, C. F. *J. Am. Chem. Soc.*, **2000**, *122*, 2395–2396.
120. Ahrendt, K. A., Borths, C. J., MacMillan, D. W. C. *J. Am. Chem. Soc.*, **2000**, *122*, 4243–4244.
121. MacMillan, D. *Nature*, **2008**, *455*, 304–308.

122. Berkessel, A., Gröger, H. *Asymmetric Organocatalysis: From Biomimetic Concepts to Applications in Asymmetric Synthesis*, Wiley-VCH Verlag GmbH & Co. KGaA, Weinheim, **2005**.
123. Torres, R. R., Ed. *Stereoselective Organocatalysis*, John Wiley & Sons, Inc., Hoboken, New Jersey, **2013**.
124. Dalko, P. I., Ed. *Comprehensive Enantioselective Organocatalysis*, Wiley-VCH Verlag GmbH & Co. KGaA, Weinheim, **2013**.
125. Moyano, A. In *Stereoselective Organocatalysis*, R. R. Torres, Ed.; John Wiley & Sons, Inc., Hoboken, New Jersey **2013**; pp. 11–80.
126. Bruckmann, A., Pena, M. A., Bolm, C. *Synlett*, **2008**, 900–902.
127. He, W., Ge, Y. C., Tan, C. H. *Org. Lett.*, **2014**, *16*, 3244–3247.
128. Walter, S. M., Kniep, F., Herdtweck, E., Huber, S. M. *Angew. Chem., Int. Ed.*, **2011**, *50*, 7187–7191.
129. Kniep, F., Walter, S. M., Herdtweck, E., Huber, S. M. *Chem. - Eur. J.*, **2012**, *18*, 1306–1310.
130. Kniep, F., Jungbauer, S. H., Zhang, Q., Walter, S. M., Schindler, S., Schnapperelle, I., Herdtweck, E., Huber, S. M. *Angew. Chem., Int. Ed.*, **2013**, *52*, 7028–7032.
131. Castelli, R., Schindler, S., Walter, S. M., Kniep, F., Overkleeft, H. S., Van der Marel, G. A., Huber, S. M., Codée, J. D. C. *Chem. - Asian J.*, **2014**, *9*, 2095–2098.
132. Ser, C. T., Yang, H., Wong, M. W. *J. Org. Chem.*, **2019**, *84*, 10338–10348.
133. Takeda, Y., Hisakuni, D., Lin, C. H., Minakata, S. *Org. Lett.*, **2015**, *17*, 318–321.
134. Jungbauer, S. H., Walter, S. M., Schindler, S., Rout, L., Kniep, F., Huber, S. M. *Chem. Commun.*, **2014**, *50*, 6281–6284.
135. Heinen, F., Engelage, E., Dreger, A., Weiss, R., Huber, S. M. *Angew. Chem., Int. Ed.*, **2018**, *57*, 3830–3833.
136. Gliese, J. P., Jungbauer, S. H., Huber, S. M. *Chem. Commun.*, **2017**, *53*, 12052–12055.
137. Ge, Y., Yang, H., Heusler, A., Chua, Z., Wong, M. W., Tan, C. *Chem. – An Asian J.*, **2019**, *14*, 2656–2661.
138. Kazi, I., Guha, S., Sekar, G. *Org. Lett.*, **2017**, *19*, 1244–1247.
139. Dreger, A., Wonner, P., Engelage, E., Walter, S. M., Stoll, R., Huber, S. M. *Chem. Commun.*, **2019**, *55*, 8262–8265.
140. Matsuzawa, A., Takeuchi, S., Sugita, K. *Chem. - Asian J.*, **2016**, *11*, 2863–2866.
141. Kuwano, S., Suzuki, T., Yamanaka, M., Tsutsumi, R., Arai, T. *Angew. Chem., Int. Ed.*, **2019**, *131*, 10326–10330.
142. Nishikawa, Y. *Tetrahedron Lett.*, **2018**, *59*, 216–223.
143. Zhao, B. L., Li, J. H., Du, D. M. *Chem. Rec.*, **2017**, *17*, 994–1018.
144. Lindsay, V. N. G., Charette, A. B. *ACS Catal.*, **2012**, *2*, 1221–1225.
145. Kuwano, S., Suzuki, T., Hosaka, Y., Arai, T. *Chem. Commun.*, **2018**, *54*, 3847–3850.
146. Arai, T., Suzuki, T., Inoue, T., Kuwano, S. *Synlett*, **2017**, *28*, 122–127.
147. Thordarson, P. *Chem. Soc. Rev.*, **2011**, *40*, 1305–1323.
148. Lehn, J. M. *Science*, **1993**, *260*, 1762–1763.
149. Pedersen, C. J. *J. Am. Chem. Soc.*, **1967**, *89*, 2495–2496.
150. Izatt, R. M., Rytting, J. H., Nelson, D. P., Haymore, B. L., Christensen, J. J. *Science*, **1969**, *164*, 443–444.
151. Goddard-Borger, E. D., Stick, R. V. *Org. Lett.*, **2007**, *9*, 3797–3800.
152. Michel, P., Rassat, A. *Tetrahedron Lett.*, **1999**, *40*, 8579–8581.
153. Crawford, J. M., Sigman, M. S. *Synthesis*, **2019**, *51*, 1021–1036.

154. Bolje, A., Košmrlj, J. *Org. Lett.*, **2013**, *15*, 5084–5087.
155. Limnios, D., Kokotos, C. G. *Chem. - Eur. J.*, **2014**, *20*, 559–563.
156. Bondi, A. *J. Phys. Chem.*, **1964**, *68*, 441–451.
157. Frassinetti, C., Ghelli, S., Gans, P., Sabatini, A., Moruzzi, M. S., Vacca, A. *Anal. Biochem.*, **1995**, *231*, 374–382.
158. Frassinetti, C., Alderighi, L., Gans, P., Sabatini, A., Vacca, A., Ghelli, S. *Anal. Bioanal. Chem.*, **2003**, *376*, 1041–1052.
159. Hibbert, D. B., Thordarson, P. *Chem. Commun.*, **2016**, *52*, 12792–12805.
160. <http://supramolecular.org/> (accessed November 26, 2019).
161. Pearson, R. G. *J. Am. Chem. Soc.*, **1963**, *85*, 3533–3539.
162. Metzner, P. In *Organosulfur Chemistry I. Topics in Current Chemistry*, vol 204., P. C. B. Page, Ed.; Springer, Berlin, Heidelberg, Heidelberg, Germany **1999**; pp. 127–181.
163. Connon, S. J. *Chem. - Eur. J.*, **2006**, *12*, 5418–5427.
164. Kobayashi, Y., Nakatsuji, Y., Li, S., Tsuzuki, S., Takemoto, Y. *Angew. Chem., Int. Ed.*, **2018**, *57*, 3646–3650.
165. Strauss, S. H. *Chem. Rev.*, **1993**, *93*, 927–942.
166. Kielland, N., Lavilla, R. In *Synthesis of Heterocycles via Multicomponent Reactions II. Topics in Heterocyclic Chemistry*, vol 25., R. Orru, and E. Ruijter, Eds.; Springer, Berlin, Heidelberg, Heidelberg, Germany **2010**; pp. 127–168.
167. Zurro, M., Asmus, S., Bamberger, J., Beckendorf, S., García Mancheño, O. *Chem. - Eur. J.*, **2016**, *22*, 3785–3793.
168. Pilli, R. A., Russowsky, D. *J. Chem. Soc. Chem. Commun.*, **1987**, 1053–1054.
169. Kawecky, R. *Tetrahedron Asymmetry*, **2006**, *17*, 1420–1423.
170. Saito, M., Tsuji, N., Kobayashi, Y., Takemoto, Y. *Org. Lett.*, **2015**, *17*, 3000–3003.
171. Girling, P. R., Kiyoi, T., Whiting, A. *Org. Biomol. Chem.*, **2011**, *9*, 3105–3121.
172. Wenzel, A. G., Jacobsen, E. N. *J. Am. Chem. Soc.*, **2002**, *124*, 12964–12965.

## Acknowledgements

This work was conducted in the Department of Chemistry and Biotechnology of the School of Science at Tallinn University of Technology. This work has been supported by the Estonian Ministry of Education and Research (Grant Nos. IUT19-32, IUT 19-9, PUT692 and PUT1468), the Centre of Excellence in Molecular Cell Engineering (2014-2020.4.01.15-0013) and the Academy of Finland (K.R.: grant no. 263256, 265328 and 292746). This work has been partially supported by ASTRA "TUT Institutional Development Programme for 2016-2022" Graduate School of Functional Materials and Technologies" (2014-2020.4.01.16-0032).

I am grateful to my supervisor, Prof. Tõnis Kanger, for introducing me to the world of organocatalysis in my first year of bachelor studies and for his support from that point on. Thank you for offering me the challenging, yet very interesting topic of asymmetric XB catalysis for my PhD studies and allowing me to tinker around with my ideas. I thank Kärt and Artur for helping me to get started in the world of science when I was much greener. I also thank all of my other colleagues who have contributed in one way or another to my research and publications: Aleksander-Mati, Benjamin, Egle, Jasper, Jevgenija, Kari, Maria, Marina, Raminton, Riina, Rudolf, Tiina and Trine, and especially to Anna for her dedication to the titration experiments in **Publication II**, Sandra for her commitment to the X-ray analysis of the crystal structures and for her help in the initial titration experiments, Kadri for her help on the synthesis of the XB donors, especially the more complicated ones.

I thank all of my past and present colleagues from the fourth floor. A special shout-out goes to the members of lab 428 for their help throughout the years, merry moments and introducing me to a different side of rock: Aleksandra, Dmitri, Estelle, Kristin, Maksim and Mariliis. I am grateful to Kristin, for her help and patience on a wide variety of problems, ranging from chemical to administrative issues. I am thankful to Estelle, Kadri and Lukáš for having a look at my thesis and helping me improve it. I thank all the past and present members of the boardgame crew for the fun nights spent in the common room.

I thank Dr. Martin Breugst for hosting me at the University of Cologne and the European Regional Development Fund for making this research visit possible. Also, thank you Jonas for a warm welcome and your help during my stay in Cologne.

I am very grateful to my mum, dad and sister for their support throughout my studies. Tiirik, thank you for exploring the downsides of hiking with me and you still owe me that bonfire.

## Abstract

### Synthesis, Characterisation and Catalytic Activity of Enantiopure Triazole-based Halogen Bond Donors

Halogen bonding is a noncovalent interaction that has been used in crystalline solids engineering, in the design of soft materials, receptors and catalysts. Halogen bonding is often compared to hydrogen bonding. However, halogen bonds (XBs) are more directional, more tunable and can be stronger than hydrogen bonds. The use of hydrogen bonds in organocatalysis is a common mode of activation. Due to the similarities to hydrogen bonding and the possible advantages gained from their differences, halogen bonding has also been used in organocatalytic applications. Similarly, to hydrogen bonds, XBs have been used to activate halides in halogen abstraction reactions or carbonyl compounds and imines in a wide variety of other reactions. Although, enantiodiscrimination by XBs is possible and XBs have been demonstrated to play crucial roles in enantioselective reactions, so far there are no examples of asymmetric catalysis solely by XB activation. It was envisioned that triazole-based XB donors could be used to achieve asymmetric XB catalysis.

The results and discussion part of this doctoral thesis is divided into four subchapters. The first subchapter describes the synthesis of enantiomerically pure triazole-based XB donors. The second subchapter describes the donor ability of these compounds in the solid state determined by single crystal X-ray diffraction analysis. In the third subchapter, the results of the titration experiments carried out by  $^1\text{H}$  NMR spectroscopy are used to evaluate the donor ability of these compounds in solution, along with the influence of structural modifications on the donor ability. Also, the enantiodiscrimination properties of the donors in solution are discussed. The fourth subchapter describes the use of the XB donors as catalysts in the Hantzsch ester reduction of an imine, in the Reissert-type reaction of quinoline and in dihydropyridinone synthesis.

The results demonstrate that a broad range of enantiopure triazole-based XB donors can be accessed via the click approach. Also, due to the robustness of the click approach, several functional groups are tolerated in the synthesis and therefore multifunctional XB donors can be accessed with ease. Iodotriazole-based XB donors can form complexes in solution with imines, amines, ureas and thioureas through XBs. Of importance are the first examples of measured affinity constants for complexes of thioureas, imines and an urea with iodotriazolium salts, in addition to a relatively rare example of complex formation between an iodotriazole and the neutral acceptor quinuclidine. Furthermore, from these experiments it was concluded that the introduction of charge has the greatest influence on the donor ability of the iodotriazole-based XB donors. It was also observed that, in the case of triazolium salts, the introduced aromatic substituents had a smaller influence on the donor ability of these compounds than did the counterion. Also, both the choice of the halogen atom and the counterion had a significant influence on the catalytic activity of the donors in dihydropyridinone synthesis, which can proceed through a Mannich/Michael or an aza-Diels-Alder pathway. The Hantzsch ester reduction of an imine and the Reissert-type reaction were not catalysed through XBs. Although enantiopure catalysts were used, no enantioselectivity was observed and  $^1\text{H}$  NMR spectroscopic experiments revealed that  $\alpha$ -methylbenzyl-substituted iodo-triazoles are inefficient at discriminating enantiomers of screened imine and amine. However, if multiple interactions between a donor and an acceptor can take place, as in the case of the complex with chiral thiourea, enantiodiscrimination was achieved.



## Lühikokkuvõte

# Enantiomeerselt puhaste triasooli-põhiste halogeensideme doonorite süntees, iseloomustamine ja katalüütiline aktiivsus

Halogeenside (XB) on mittekovalentne interaktsioon, mis on leidnud kasutust kristallsete tahkiste, pehmete materjalide, retseptorite ja katalüsaatorite disainis. Võrreldes enamasti kasutatavate vesiniksidemetega on halogeensidemed rohkem suunatud ja nende omadused suuremal määral muudetavad, ning need võivad olla tugevamad. Aktivatsioon vesiniksidemete kaudu on väga levinud lähenemine organokatalüüsis. Sarnasuste tõttu vesinik- ja halogeensidemete vahel on viimased samuti leidnud rakendust organokatalüüsis, samas tulenevalt nende erinevustest on halogeensidemetel mitmeid eriliseid. Sarnaselt vesiniksidemetele on halogeensidemeid kasutatud haloalkaanide aktiveerimiseks haliidi asenduse reaktsioonides, ning ka karbonüülühendite ja imiinide aktiveerimiseks erinevates reaktsioonides. Kuigi halogeensidemeid on rakendatud enantiomeeride eristamiseks ja on näidatud nende võtmerolli teatud asümmeetrilistes reaktsioonides, siis siiani puudub pretsedent, kus reaktsioon oleks läbi viidud enantioselektiivselt ainuüksi halogeensideme aktivatsiooni kaudu. Triasooli-põhised halogeensideme doonorid on kergesti sünteesitavad ja nende struktuur ning omadused varieeritavad, mistõttu on need head mudelühendid asümmeetrilise XB katalüüsi uurimiseks.

Doktoritöö tulemuste ja arutelu osa on valminud nelja publikatsiooni põhjal, ning on jaotatud neljaks alapeatükiks vastavalt publikatsioonide läbivatele teemadele. Esmalt käsitletakse enantiomeerselt puhaste triasooli-põhiste halogeensideme doonorite sünteesi. Järgnevalt kirjeldatakse nende ühendite poolt moodustatavaid halogeensidemeid tahkes faasis kristallstruktuuri analüüsi kaudu. Kolmandas alapeatükis kasutatakse tuumamagnetresonantspektroskoopia vahendusel teostatud tiitrimiskatsete tulemusi sünteesitud ühendite XB doonorvõime ja seda mõjutavate faktorite hindamiseks lahuses. Ühtlasi käsitletakse ka antud ühendite võimet eristada imiinide, amiinide ja tiokarbamiidide enantiomeere. Neljandas alapeatükis kirjeldatakse sünteesitud doonorite kasutamist katalüsaatoritena imiini taandamise, kinoliini alküleerimise ja dihüdropüridinooni sünteesi näitel.

XB doonorite sünteesiks on välja töötatud lähenemine, mille kaudu on varieeritavad kõik XB doonorvõimet mõjutavad asendajad. Kuna klikk-keemia on väga robustne, siis antud meetodi abil on võimalik sünteesida erinevaid funktsionaalrühmi sisaldavaid, samuti ka multifunktsionaalseid, XB doonoreid. Iodotriasooli-põhised XB doonorid moodustavad lahuses komplekse imiinide, amiinide, karbamiidide ja tiokarbamiididega. Esmakordselt näidati kompleksi teket lahuses tiokarbamiidide, karbamiidide ja imiinide ning iodotriasooliumsoolade vahel ja ühtlasi määrati nende komplekside tugevused. Mõõdeti ka iodotriasooli ja kinuklidiini vahelise kompleksi tugevus, mis on üks vähestest näidetest, kus halotriasool moodustab lahuses kompleksi neutraalse ühendiga. Näidati, et iodotriasooli-tüüpi doonorite puhul suurendab XB doonorvõimet kõige enam triasooli tuuma elektrontiheduse vähendamine lämmastikuaatomi kvaterniseerimise kaudu. Iodotriasooliumsoolade korral mõjutasid aromaatsed asendajad XB doonorvõimet vähem kui vastasiooni valik. Nii doonoraatomi kui ka vastasiooni valik omasid märkimisäärset mõju antud ühendite katalüütilisele aktiivsusele dihüdropüridinooni sünteesi reaktsioonis, mis võis kulgeda kas Mannichi/Michaeli või asa-Diels-Alder

mehhanismi kaudu. Ei leidnud kinnitust fakt, et antud ühendid katalüüsivad imiini taandamise ja kinoliini alküleerimise reaktsioone XB vahendusel. Kuigi antud doonorid on enantiomeerselt puhtad, siis reaktsioonides ei tuvastatud asümmeetrilist induktsiooni. Tuumamagnetresonantsspektroskoopia katsete põhjal võib öelda, et  $\alpha$ -metüülbensüül-asendatud iodotriasoolid ei ole võimelised eristama imiini ega amiini enantiomeere. Samas tiokarbamiidi enantiomeere on antud triasoolidega võimalik teineteisest eristada, mistõttu tuleks edaspidi kasutada multifunktsionaalseid XB doonoreid asümmeetrilise induktsiooni saavutamiseks.

## Appendix 1

### Publication I

Kaasik, M.; Kaabel, S.; Kriis, K.; Järving, I.; Aav, R.; Rissanen, K.; Kanger, T. Synthesis and Characterisation of Chiral Triazole-Based Halogen-Bond Donors: Halogen Bonds in the Solid State and in Solution. *Chem. - Eur. J.* **2017**, *23*, 7337–7344.

Reproduced by permission of Wiley-VCH Verlag GmbH & Co. KGaA, Weinheim.



## Halogen Bonds

## Synthesis and Characterisation of Chiral Triazole-Based Halogen-Bond Donors: Halogen Bonds in the Solid State and in Solution

Mikk Kaasik,<sup>[a]</sup> Sandra Kaabel,<sup>[a]</sup> Kadri Kriis,<sup>[a]</sup> Ivar Järving,<sup>[a]</sup> Riina Aav,<sup>[a]</sup> Kari Rissanen,<sup>[b]</sup> and Tõnis Kanger<sup>\*[a]</sup>

**Abstract:** A general platform for the synthesis of various chiral halogen-bond (XB) donors based on the triazole core and the characterisation of factors that influence the strength of the halogen bond in the solid state and in solution are reported. The characterisation of XB donors in the solid state by X-ray crystallography and in solution by

<sup>1</sup>H NMR titration can be used to aid the design of new XB donors. We describe the first example of a XB between iodotriazoles and thioureas in solution. In addition, the enantio-discrimination of acceptors in solution through halogen-bond participation is described.

## Introduction

A halogen bond (XB) is a noncovalent interaction between an electrophilic halogen atom and some nucleophilic counterpart of the same or another molecule.<sup>[1]</sup> The feature governing the XB is its directionality, primarily a result of the anisotropic distribution of electron density on the polarised halogen atom that leads to the formation of an electron-deficient region called the  $\sigma$  hole.<sup>[2]</sup> As the  $\sigma$  hole of the halogen atom is located exactly on the elongation of the covalent bond in which the halogen atom is involved, the XB is almost linear.<sup>[3]</sup> Another feature of the XB is the tunability of its strength, which is dependent on the nature of the interacting counterparts. In general, the XB donor ability of a halogen can be tuned by subtle structural modifications that affect the electron-withdrawing ability of moieties covalently bound to the halogen atom or the steric environment surrounding the halogen atom. In addition, the XB donor strength increases in the order of increasing polarisability, that is,  $F < Cl < Br < I$ ,<sup>[4]</sup> with the most commonly used acceptor atoms ranked in the order  $O < S < N$ .<sup>[5]</sup>

These phenomena have been widely exploited in crystal engineering to construct supramolecular complexes and networks.<sup>[6]</sup> The application of the XB in solutions is more challenging.<sup>[7]</sup> The most exciting application is the use of XBs in organocatalysis. Similarities between the XB and the hydrogen

bond make XB donors potential organocatalysts. Although hydrogen-bonding catalysis is well documented,<sup>[8]</sup> the number of papers concerning XB catalysis is still quite limited. Bolm and co-workers were the first to use XB catalysis in the reduction of quinoline with the Hantzsch ester.<sup>[9]</sup> Since then several other articles have been published,<sup>[10–12]</sup> mainly by Huber and co-workers. However, to the best of our knowledge, there are no examples of asymmetric XB catalysis. To move towards that, information on how different XB donor and acceptor entities and their substituents influence the strength of halogen bonds is needed. For example, a too weak XB donor might not be sufficiently Lewis acidic to form an XB with the acceptor, whereas a too strong XB donor may bind irreversibly to the acceptor. Therefore it is essential that the strength of the XB follows the “Goldilocks” principle.<sup>[11f]</sup>

The halogen-substituted 1,2,3-triazole core is a common motif among XB donors.<sup>[13]</sup> Despite this, only one example of halotriazole-based XB catalysis has been published.<sup>[11g]</sup> These compounds can be synthesised in one step through a click reaction from readily available substrates.<sup>[14,15]</sup> Various chiral azides, different halides or differently substituted aromatics can be used, which means that the structural variations of the obtained XB donors is very broad. This opens up ample opportunities for further studies of the application of halotriazoles as XB catalysts. Because of this, a family of halotriazoles was synthesised and their XB donor abilities assessed by X-ray crystallography and solution NMR studies. Acceptors containing a sulfur or a nitrogen atom were chosen for solution studies as the propensity of  $sp^2$ -hybridised sulfur<sup>[16]</sup> and imines<sup>[11c,f]</sup> to form XBs is known. These acceptors could also be considered as model compounds of possible substrates in organocatalytic applications. It is also noteworthy that although a sulfur atom is a common acceptor in the solid state, only a few examples have been reported regarding its use as an XB acceptor in solution, and those mainly deal with molecular iodine as the do-

[a] M. Kaasik, S. Kaabel, Dr. K. Kriis, Dr. I. Järving, Dr. R. Aav, Prof. Dr. T. Kanger  
Department of Chemistry and Biotechnology  
Tallinn University of Technology  
Akadeemia tee 15, 12618 Tallinn (Estonia)  
E-mail: tonis.kanger@ttu.ee

[b] Prof. Dr. K. Rissanen  
Department of Chemistry, University of Jyväskylä  
Nanoscience Center, P.O. Box 35, 40014 Jyväskylä (Finland)

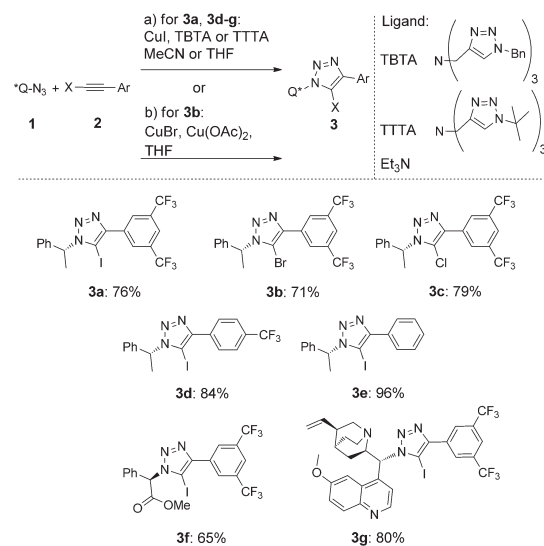
Supporting information and the ORCID identification number(s) for the author(s) of this article can be found under:  
<https://doi.org/10.1002/chem.201700618>.

nor.<sup>[15d-f]</sup> Finally, the enantiodiscrimination capability of iodo-triazolium salts towards chiral thiourea was addressed.

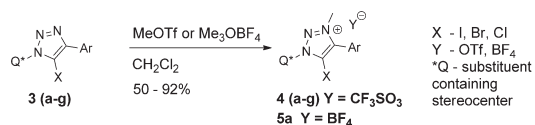
## Results and Discussion

A library of triazole and triazolium XB donors with different substitution patterns was synthesised by a cycloaddition reaction as the key transformation. The obtained triazoles differ from each other in terms of the main entities that determine the XB donor ability of a compound. The triazoles **3a-c** (Scheme 1) and the corresponding triazolium salts **4a-c** (Scheme 2) contain different halogen atoms (iodine, bromine and chlorine, respectively). Two, one or no trifluoromethyl substituents in the aromatic ring (**3a, d, e** and the corresponding salts) have clearly different electronegativities influencing the XB donor abilities.<sup>[5b,17]</sup> The influence of trifluoromethanesulfonate (triflate) and tetrafluoroborate counter ions (**4a** and **5a**, respectively) on XB strength can also be compared. All the synthesised XB donors were chiral, thereby enabling the enantioselective recognition of acceptors to be investigated.<sup>[13a]</sup> Donors with two halogen atoms (**3h-j, 4j** and **5h**) could act by bidentate coordination with acceptors (Scheme 3).<sup>[13d,18]</sup>

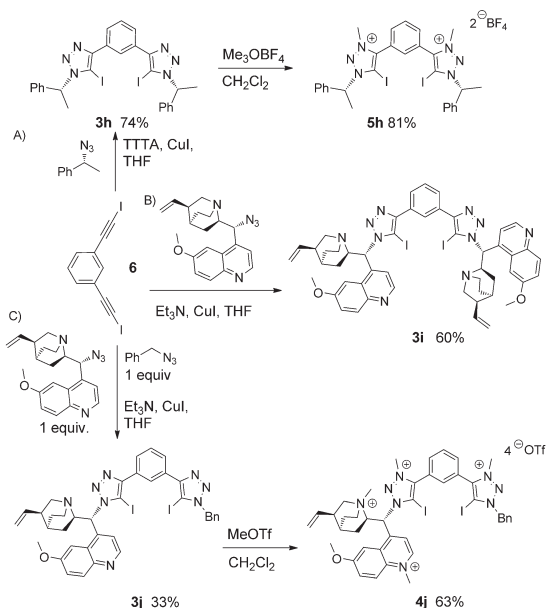
The XB donors were synthesised by a click reaction between enantiomerically pure azide **1** and iodo-<sup>[15a]</sup> or bromoalkyne <sup>[15b]</sup>



Scheme 1. Synthesis of monodentate XB donors **3a-g**.



Scheme 2. Quaternisation of triazoles **3a-g**.



Scheme 3. Synthesis of bidentate XB donors **3h-j, 4j** and **5h**.

**2** to afford halo-substituted triazoles **3** in good-to-excellent yields (Scheme 1). The chiral azides were derived from (*R*)- $\alpha$ -methylbenzylamine (for **3a-e**), (*R*)-phenylglycine (for **3f**) or quinine (for **3g**). In addition, the aromatic substituents 3,5-bis(trifluoromethyl)phenyl, 4-trifluoromethylphenyl and phenyl were varied in the alkyne starting compounds **2**. In most cases, tris[(1-benzyl-1*H*-1,2,3-triazol-4-yl)methyl]amine (TBTA) or tris[(1-*tert*-butyl-1*H*-1,2,3-triazol-4-yl)methyl]amine (TTTA) was used as a ligand in the click reaction (**3a,d-f**), although Et<sub>3</sub>N was used in the case of **3g** (Scheme 1a). Bromine derivative **3b** was obtained by a CuBr/Cu(OAc)<sub>2</sub>-catalysed click reaction in THF (Scheme 1b). The XB donor containing a chlorine atom in the triazole ring (**3c**) was synthesised from the iodotriazole **3a** through a halogen-exchange reaction.<sup>[19]</sup>

Quaternisation of a nitrogen atom can lead to a triazole core that is even more electron deficient, polarising the C–X bond and enlarging the  $\sigma$  hole (Scheme 2).<sup>[13d,17]</sup> Quaternisation of the triazole ring was carried out by using methyl triflate or trimethyloxonium tetrafluoroborate to afford the triflate salts **4a-g** and the tetrafluoroborate salt **5a** in reasonable-to-good yields (Scheme 2, experimental details are described in the Supporting Information). In the case of compound **3g**, the reaction was not selective; the tris-triflate salt **4g** was produced that was insoluble in chloroform. Methylation of the nitrogen atoms of the quinuclidine and quinoline ring can be avoided by protecting them as *N*-oxides.<sup>[20]</sup> Regrettably, this strategy did not yield the desired product.

C<sub>2</sub>-symmetric bidentate XB donors **3h**<sup>[19g]</sup> and **3i** were derived from aromatic diiodoalkyne **6** (Scheme 3). For the synthesis of the non-symmetrically substituted bidentate donor **3j**, diyne **6** was treated with equimolar amounts of benzyl azide

and an alkaloid-based azide. In addition, **3h** was converted into bis-tetrafluoroborate salt **5h** and **3j** was converted into the corresponding tetrakis-triflate salt **4j**.

The first evidence of the XB donor properties of the synthesised compounds was obtained by single-crystal X-ray crystallography in the solid state. The presence of halogen bonds can be ascertained by the distance between the interacting atoms being less than the sum of the van der Waals radii. The strength of an XB between different atoms can be found by using the normalised interaction ratio  $R_{DA} = d_{DA}/(r_{D,vdW} + r_{A,vdW})$  with  $r$  defined as vdW radius, in which  $d_{DA}$  (in Å), the distance between the donor (D) atom and the acceptor (A) atom, is divided by the sum of the van der Waals radii (in Å) of D and A. In the case of an XB, it is defined as  $R_{XB}$  and the XB can be considered to be strong if  $R_{XB} < 0.9$ .<sup>[3,21]</sup> Quantitative data obtained from single-crystal X-ray diffraction analyses are presented in Table 1 and the structures are illustrated in Figures 1–3 (CCDC href = "https://summary.ccdc.cam.ac.uk/structure-summary?doi=10.1002/chem.201700618" > 1522079–1522089 contain the supplementary crystallographic data for this paper. These data are provided free of charge by "http://www.ccdc.cam.ac.uk/"The Cambridge Crystallographic Data Centre).

The synthesised compounds can be divided into two groups: neutral triazoles and triazolium salts. They are clearly differentiated from each other by the type of atoms halogen-bonded in the crystalline state. The XB is, in the case of neutral donors, formed between the iodine atom and a nitrogen atom of another donor (Table 1, entries 1–4). Compound **3a** forms the XB with the nitrogen atom of the triazole core (Figure 1A), whereas **3g** forms the XB with the nitrogen atom of the quinoline fragment (Figure 1B). To exclusively evaluate the influence of the substituents of the triazole ring on the strength of the XB (expressed as  $R_{XB}$ ), we can only directly compare X-ray structures in which the XB is formed with the same acceptor entity, as the strength of the bond depends both on the donor and the acceptor. Accordingly, it was determined that the XB between **3g** and **3g** is stronger than that between **3a** and **3a**, as the nitrogen of the quinoline fragment is a better acceptor than the nitrogen of the electron-deficient triazole fragment (Table 1, entries 1 and 3). Furthermore, it is assumed that the

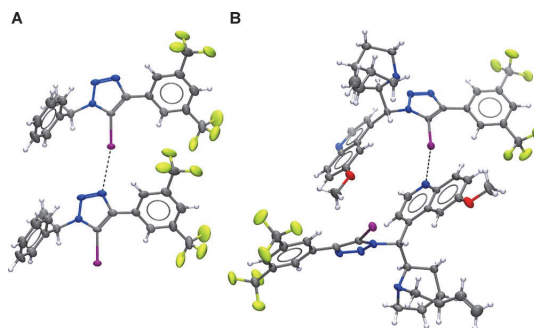


**Figure 1.** X-ray structures of **3a** (A) and **3g** (B). The atomic displacement ellipsoids are drawn at the 50% probability level.

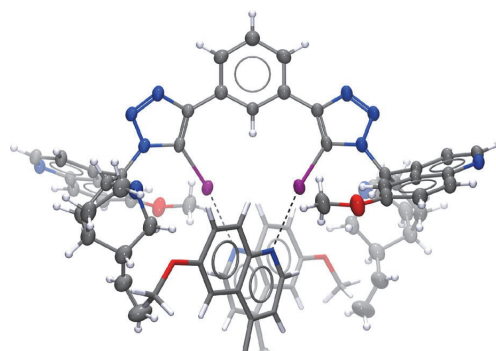


**Figure 2.** X-ray structure of **3i**. Atomic displacement ellipsoids are drawn at the 30% probability level. Solvent molecules have been omitted and only the quinoline fragments of the two **3i** acceptor units are displayed for clarity. The acceptor fragments are drawn as sticks.

electronegative trifluoromethyl groups on the phenyl ring of compound **3a** decrease the acceptor ability of the triazole nitrogen to a greater extent than increasing the donor ability of the iodine. This assumption is supported by the fact that the XB between **3e** and **3e** is stronger than that between **3a** and **3a** (Table 1, entries 1 and 2). Steric effects seem to have little

Table 1. Solid-state bonding parameters for XB donors.					
Entry	XB donor	XB system	Angle C–X…A [°] <sup>[a]</sup>	Distance X…A [Å] <sup>[a]</sup>	$R_{XB}$ <sup>[b]</sup>
1	<b>3a</b>	C–I…N <sub>triazole</sub>	167.4(2)	2.940(5)	0.833
2	<b>3e</b>	C–I…N <sub>triazole</sub>	167.1(2)	2.854(6)	0.808
3	<b>3g</b>	C–I…N <sub>quinoline</sub>	168.8(1)	2.749(3)	0.779
4	<b>3i</b>	C–I…N <sub>quinoline</sub>	171.4(3)	2.785(8)	0.789
5	<b>4a</b>	C–I…OSO <sub>2</sub> CF <sub>3</sub>	168.9(4)	2.82(1)	0.807
6	<b>4b</b>	C–Br…OSO <sub>2</sub> CF <sub>3</sub>	163.6(2)	2.870(6)	0.852
7	<b>4c</b>	C–Cl	–	–	–
8	<b>4d</b>	C–I…OSO <sub>2</sub> CF <sub>3</sub>	166.5(1)	2.847(3)	0.813
9	<b>4f</b>	C–I…OSO <sub>2</sub> CF <sub>3</sub>	166.1(5)	2.83(1)	0.809
10	<b>4g</b>	C–I…OSO <sub>2</sub> CF <sub>3</sub>	172.7(2)	2.715(3)	0.776
11	<b>5a</b>	C–I…FBF <sub>3</sub>	158.7(2)	2.890(3)	0.838

[a] Standard deviations are given in parentheses. [b] Sum of the van der Waals radii calculated based on the values defined by Bondi (see ref. [22]).

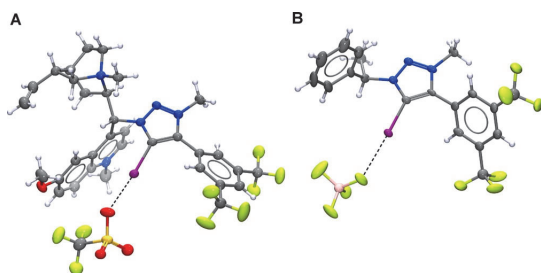


**Figure 3.** X-ray structures of **4g** (A) and **5a** (B). Only one OTf<sup>-</sup> counter ion, the one involved in XB bonding, is included in the structure of **4g**; the rest have been omitted for clarity. Atomic displacement ellipsoids are drawn at the 50% probability level.

influence on the strength of the XB (Figure 2), as **3i** with two bulky quinoline fragments forms two comparably strong C–I...N<sub>quinoline</sub> halogen bonds to **3g**, which has only one quinoline unit (Table 1, entries 3 and 4).

Cationic XB donors (Table 1, entries 5–11) form halogen bonds with their counter ions (Figure 3). Changing the halogen atom in the triazole core from iodine to bromine or chlorine has a profound effect on the strength of the XB (Table 1, entries 5–7), to the extent that **4c** does not form an XB with the triflate anion. This is in agreement with previous studies showing the importance of the polarisability and electronegativity of the halogen atom on the strength of the XB.<sup>[2,4]</sup> Electron-withdrawing trifluoromethyl groups on the phenyl ring of **4a** and **d** (Table 1, entries 5 and 8) have little effect on the XB strength. The electron-withdrawing methyl ester group as the N-substituent of the triazole core in compound **4f** has no effect on the strength of the XB (Table 1, entries 5 and 9). Similarly to the neutral XB donor, the salt **4g** containing the bulky quinidine substituent forms the strongest XB in the series of cationic XB donors. Finally, based on the X-ray data, the oxygen of the triflate counter ion is a better XB acceptor than the fluorine of the tetrafluoroborate counter ion (Table 1, entries 5 and 11).

Overall, the observed XBs of the cationic XB donors are not noticeably stronger than those of the neutral donors. The increase in XB donor strength by quaternisation is penalised by the presence of a weaker XB acceptor, as an oxygen atom (moreover in a weakly coordinating triflate anion) is a weaker acceptor than a nitrogen atom. As the strength of the XB relies on the interplay of multiple simultaneous effects, pin-pointing the effect of a single substituent needs to be addressed cautiously. Nonetheless, the observed XBs are relatively strong, as all of them have  $R_{\text{XB}}$  values less than 0.86. In all cases the XB adopts a near-linear geometry, with the greatest distortion of the XB from linearity in the crystals of compounds **4b** and **5a**, which also form the weakest halogen bonds (Table 1, entries 6 and 11).

The strength of the XB in the solid state cannot be directly extrapolated to solution. The compounds involved are fixed in the crystal structure in one preferable conformation by packing forces, whereas in solution XB formation can be influenced

by steric effects created by the conformational freedom of the molecule. In addition, solvent effects in solution must be accounted for, as interactions between a solvent molecule and the donor/acceptor will also interfere with XB formation.

To confirm the XB donor strength of the synthesised compounds in solution a series of <sup>1</sup>H NMR titration experiments were carried out in CDCl<sub>3</sub>.<sup>[5b,d,13,18c–f,21a]</sup> During the titration experiments the concentration of the XB donor was kept constant while increasing amounts of acceptor (Figure 4) were added to the solution. The upfield shifts of the methyl protons **a** and **b** of the XB donor were monitored during the titration experiment (Figure 5A) and used to calculate the binding constants for a 1:1 binding model by non-linear least-squares

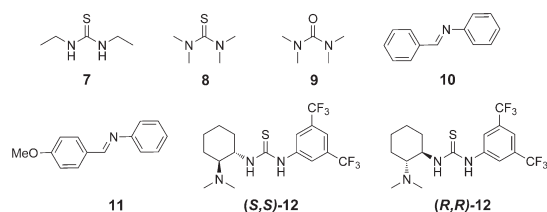


**Figure 4.** XB acceptors used in this study.

global fitting using the HypNMR2008 program (Figure 5B).<sup>[23]</sup> Owing to solubility issues in CDCl<sub>3</sub>, compounds **4g**, **4j** and **5h** were not used, even though multidentate XB donors have shown higher binding affinities.<sup>[18a,f]</sup>

First, the influence of the halogen atom on the formation of an XB with thiourea **7** in solution was studied. As expected, the binding constant for the iodine-containing complex [**4a–7**] is the largest of the three (Table 2, entries 1–3). Surprisingly, the chlorine-containing triazole **4c** has a higher binding constant with **7** than the bromine-containing donor **4b** (Table 2, entries 2 and 3). It is assumed that hydrogen bonding between the acidic N–H protons of the thiourea **7** and the electron-rich equatorial belt of the halogen atom are able to assist in XB formation.<sup>[2,24]</sup> To eliminate the influence of hydrogen bonding through acidic N–H protons on the titration results *N,N,N',N'*-tetramethylthiourea **8** was used in the experiment with donors **4a–4c** (Table 2, entries 9–11). The binding constant for the complex [**4a–8**] is lower than that for the complex [**4a–7**]; complex formation between the triazolium salt **4b** or **4c** and thiourea **8** is also not favoured. This confirms the participation of the hydrogen bond in the formation of a complex with **7**. A chlorine atom is more electronegative and less polarisable than a bromine or iodine atom. Because of this, the  $\sigma$  hole of the chlorine atom is generally weaker than the  $\sigma$  hole of the iodine or bromine atom, and therefore hydrogen bonding is the major contributor to the relatively large binding constant of the [**4c–7**] complex. On the other hand, the bromine atom is a weaker XB donor than iodine and also a weaker hydrogen-bond acceptor than chlorine; therefore the binding constant for the [**4b–7**] complex is the smallest of the three (Table 2, entries 1–3). To gain additional evidence for the XB in solution, compound **4k** (Figure 5) containing a hydrogen atom instead



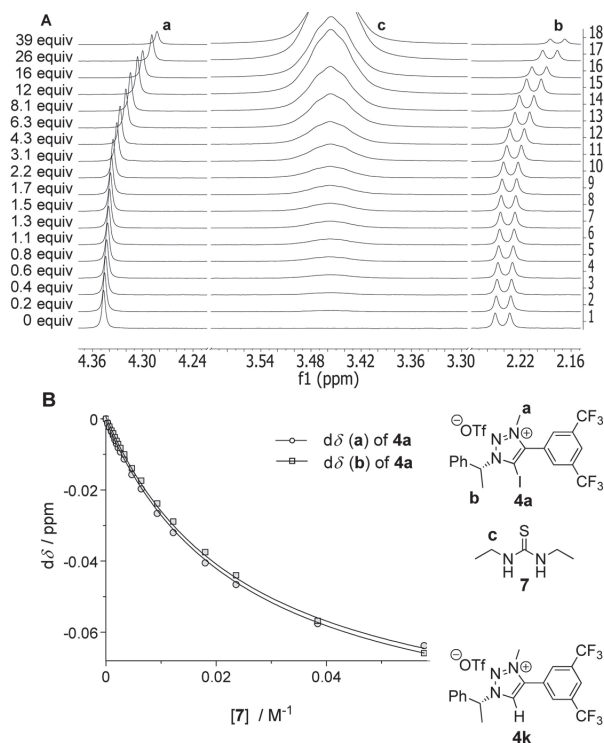


**Figure 5.** A)  $^1\text{H}$  NMR spectra ( $\text{CDCl}_3$ , 297 K, 400 MHz) from the titration experiment of **4a** (1.5 mM) with thiourea **7** showing the methyl protons **a** and **b** of **4a** and the methylene protons **c** of **7**. Spectra 1 to 18 show the variation in the chemical shifts with increasing equivalents of **7**. B) The corresponding binding isotherm with global fitting for methyl protons **a** and **b** ( $K_{\text{a}} = 42 \pm 2 \text{ M}^{-1}$ ).

Table 2. Binding constants $K_{\text{a}}$ of XB complexes in $\text{CDCl}_3$ at 297 K.			
Entry	XB donor	XB acceptor	$K_{\text{a}}^{[\text{a}]}$ [ $\text{M}^{-1}$ ]
1	<b>4a</b>	<b>7</b>	$42 \pm 2$
2	<b>4b</b>	<b>7</b>	$11 \pm 1$
3	<b>4c</b>	<b>7</b>	$29 \pm 6^{[\text{b}]}$
4	<b>4d</b>	<b>7</b>	$35 \pm 2$
5	<b>4e</b>	<b>7</b>	$33 \pm 1$
6	<b>4f</b>	<b>7</b>	$129 \pm 12^{[\text{c}]}$
7	<b>4k</b>	<b>7</b>	–
8	<b>5a</b>	<b>7</b>	$58 \pm 1$
9	<b>4a</b>	<b>8</b>	$12 \pm 1$
10	<b>4b</b>	<b>8</b>	$0.10 \pm 0.02^{[\text{d}]}$
11	<b>4c</b>	<b>8</b>	$0.05 \pm 0.02^{[\text{d}]}$
12	<b>4f</b>	<b>8</b>	$20 \pm 4^{[\text{c}]}$
13	<b>4a</b>	<b>9</b>	$6 \pm 1$
14	<b>4a</b>	<b>10</b>	–
15	<b>4a</b>	<b>11</b>	$8 \pm 1^{[\text{c}]}$

[a] Global fitting based on the change in the chemical shifts of methyl protons **a** and **b** with the corresponding fitting errors. [b] Fitting based on the change in the chemical shift of methyl protons **b**. [c] Fitting based on the change in the chemical shift of methyl protons **a**. [d] Titration experiment carried out with 15 mM concentration of donor **4**.

of a halogen atom was synthesised by the click reaction followed by subsequent quaternisation with methyl triflate. During the titration of **4k** with thiourea **7**, the resonance frequencies of the methyl protons **a** and **b** did not change, which indicates the absence of an interaction (Table 2, entry 7). This shows the structural importance of the iodine atom in **4a** and that **4a** acts as an XB donor in solution.

Lowering the electron-withdrawing power of the aromatic substituent has little effect on the binding constant as the constants for the [**4d–7**] and [**4e–7**] complexes are identical and only slightly smaller than the binding constant for the [**4a–7**] complex (Table 2, entries 1, 4 and 5). The position of the trifluoromethyl group in the aromatic ring must also be considered, because it affects the triazolium core only through induction. The NMR results taken together with X-ray results indicate that trifluoromethyl groups and their substitution pattern should be suitable to fine-tune the halotriazolium XB donor. The largest binding constant was measured between compounds **4f** and **7** (Table 2, entry 6). In the solid state, the  $R_{\text{XB}}$  values for **4a** and **4f** are practically identical (Table 1, entries 5 and 9). Therefore, it is assumed that additionally to the XB, hydrogen bonding between the hydrogen atoms of thiourea **7** and the ester functionality of **4f** also contribute to the observable binding constant. To eliminate the possibility of hydrogen-bond formation, **4f** was titrated with tetramethylthiourea **8** (Table 2, entry 12). A significantly smaller binding constant for the [**4f–8**] complex compared with the binding constant for the [**4f–7**] complex confirms the presence of additional hydrogen bonding in the case of the latter. Nevertheless, the ester functionality has some effect on the XB strength as the binding constant for the

[**4f–8**] complex is slightly larger than that for the [**4a–8**] complex (Table 2, entries 9 and 12). Counter ion effects in halogen bonding are as yet not fully understood and it might not be as simple as using a less coordinating counter ion to enhance the XB strength.<sup>[10a, 11d]</sup> The binding constant for the [**4a–7**] complex is lower than that for the [**5a–7**] complex (Table 2, entries 1 and 8), presumably because the triflate counter ion interacts more strongly with the iodine of the triazolium than the tetrafluoroborate counter ion (based on X-ray data, Table 1, entries 5 and 11).

Donor **4a** was additionally used in titration experiments with urea **9**. The exchange of a sulfur atom for an oxygen atom brought about a two-fold decrease in the binding constant (Table 2, entries 9 and 13). This again indicates that thio-carbonyl compounds could be better suited as substrates in organocatalytic applications of halogen bonding than carbonyl compounds. Finally, **4a** was used in titration experiments with imines **10** and **11** (Table 2, entries 14 and 15). Unfortunately, no significant interaction was detected between **4a** and **10**. Introducing an electron-donating methoxy group into the aromatic ring of imine **10** made it possible to measure the binding con-

stant for the [4a–11] complex (Table 2, entry 15). Although the binding constant is quite small, it is still larger than previously reported binding constants for halogen bonds to imines.<sup>[11c]</sup>

So far only a handful of studies have addressed the issue of enantiodiscrimination through XBs. Beer and co-workers described the enantioselective recognition of chiral anions of BINOL-based XB donors.<sup>[13a]</sup> A separation based on the XBs of polyhalogenated 4,4'-bipyridines by HPLC was investigated by Peluso and co-workers.<sup>[25]</sup> To evaluate the enantiodiscrimination properties of the synthesised donors, the NMR spectra of the chiral acceptors (*R,R*)-12 and (*S,S*)-12 in 1:1 mixtures with chiral donor 4a were studied (Figure 6). A complex is formed

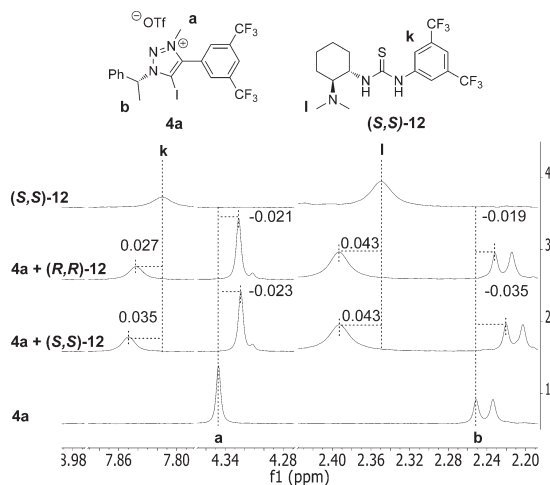


**Figure 6.** <sup>1</sup>H NMR spectra in CDCl<sub>3</sub> (1.5 mm, 297 K, 400 MHz) of 1) 4a, 2) a 1:1 mixture of 4a and (*S,S*)-12, 3) a 1:1 mixture of 4a and (*R,R*)-12 and 4) (*S,S*)-12. Positive values indicate a downfield shift and negative values an upfield shift (in ppm) compared with the corresponding resonance signals in either the spectrum of free 4a or (*S,S*)-12.

upon the addition of (*R,R*)-12 or (*S,S*)-12 to 4a, as is evident by the noticeable upfield shifts of the methyl protons a (−0.021 or −0.023 ppm, respectively) and b (−0.019 or −0.035 ppm) of 4a and the downfield shifts of methine protons k (0.027 or 0.035 ppm) and *N*-methyl protons l (0.043 ppm) of (*R,R*)-12 and (*S,S*)-12. Different changes in the chemical shifts were expected as the complexes formed are diastereomeric.

To confirm that the observed changes in the chemical shifts of 4a and the enantiomers of 12 were caused by XBs, the interaction with compound 4k, for which the possibility of the formation of a complex through a XB is excluded, was examined (Figure 7). When 4k was used in 1:1 mixtures with (*R,R*)-12 or (*S,S*)-12 there was little change in the chemical shifts of interest. More importantly, the spectra corresponding to the 1:1 mixtures are practically identical, which indicates that two diastereoisomeric complexes were not formed. Thus, it can be concluded that the complexation of donor 4a and thiourea 12 takes place by XB participation and that the donor 4a can differentiate between enantiomeric thioureas 12 by chiral recog-

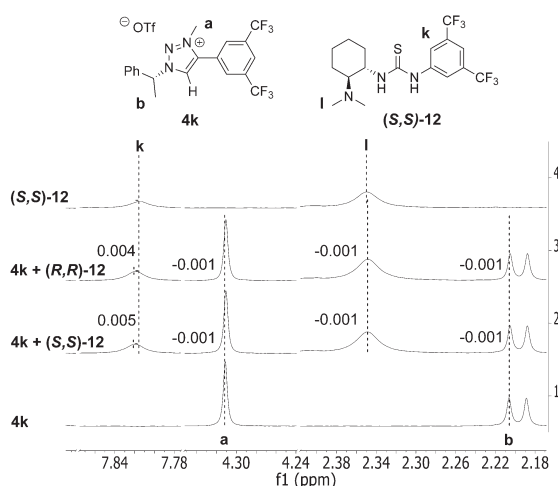


**Figure 7.** <sup>1</sup>H NMR spectra in CDCl<sub>3</sub> (1.5 mm, 297 K, 400 MHz) of 1) 4k, 2) a 1:1 mixture of 4k and (*S,S*)-12, 3) a 1:1 mixture of 4k and (*R,R*)-12 and 4) (*S,S*)-12. Positive values indicate a downfield shift and negative values an upfield shift (in ppm) compared with the corresponding resonance signals in either the spectrum of free 4k or (*S,S*)-12.

niton. To the best of our knowledge, this is the first example of the enantiodiscrimination of neutral acceptors by XB participation.

## Conclusion

Various chiral halotriazole and -triazolium XB donors that differ from each other in terms of the main entities that define XB donor properties have been synthesised. We have shown that the general approach for the characterisation of XB donors in the solid state by X-ray crystallography and in solution by <sup>1</sup>H NMR titration can be used to aid the design of new XB donors. Structural modifications influence the strength of the XB to a varying degree and can thus be grouped into two. The choice of halogen used in the donor is crucial for XB formation. Also, the strength of the XB is affected considerably by the choice of counter ion. On the other hand, trifluoromethyl groups on the phenyl substituent have little impact on XB strength. Substituents that have a weak influence on the XB donor ability are also important for the fine-tuning of an XB catalyst and thus trifluoromethyl groups should be suitable for this purpose. We have described the first examples of XBs between iodotriazoles and neutral acceptors in solution (thioureas 7, 8 and 12, urea 9 and imine 11). Among the acceptors, thioureas show a higher affinity towards XB formation, especially if there is the possibility of additional hydrogen-bond formation. Finally, evidence that the synthesised compounds are capable of enantiodiscrimination in solution was obtained. Thus, we have provided a platform for the synthesis and characterisation of chiral XB donors. Our ongoing investigations are focused on the applications of the synthesised donors in the field of asymmetric organocatalysis.

## Experimental Section

**General:** All commercially available reagents were used without further purification.  $\text{CH}_2\text{Cl}_2$  was dried by distillation over  $\text{P}_2\text{O}_5$ , MeOH over sodium metal. All air- or moisture-sensitive reactions were carried out under argon atmosphere using oven-dried glassware. The reactions were monitored by TLC with silica gel coated aluminium plates (Merck 60 F254) and visualised with  $\text{KMnO}_4$ , anisaldehyde or ninhydrin stain. Yields refer to chromatographically purified or crystallised products.  $^1\text{H}$  NMR spectra were recorded on a Bruker Avance III 400 MHz instrument at 400 MHz and chemical shifts ( $\delta$ ) are reported referenced to the residual solvent signal ( $\text{CDCl}_3$ :  $\delta = 7.26$  ppm; MeOD:  $\delta = 3.31$  ppm).  $^1\text{H}$  NMR data are reported as follows: chemical shift  $\delta$  [ppm], multiplicity (s=singlet, brs=broad singlet, d=doublet, t=triplet, q=quartet, dd=doublet of doublets, m=multiplet), coupling constant  $J$  [Hz], relative integration.  $^{13}\text{C}$  NMR spectra were recorded at 101 MHz and chemical shifts ( $\delta$ ) are reported referenced to the residual solvent signal ( $\text{CDCl}_3$ :  $\delta = 77.16$  ppm; MeOD:  $\delta = 49.00$  ppm). HRMS spectra were recorded with an Agilent Technologies 6540 UHD Accurate-Mass Q-TOF LC/MS spectrometer by using Agilent Jet Stream-ESI ionisation. MS spectra were recorded on a Shimadzu GSMS-QP2010 spectrometer using EI at 70 eV. Optical rotations were measured with an Anton Paar GWB Polarimeter MCP500. IR spectra were recorded on a Bruker Tensor 27 FT infrared spectrophotometer. Single crystal X-ray diffraction data was collected at 123 K on Rigaku Compact HomeLab diffractometer, equipped with a Saturn 944 HG CCD detector and Oxford Cryostream cooling system using monochromatic  $\text{Cu-K}\alpha$  radiation (1.54178 Å) from a MicroMaxTM-003 sealed tube microfocus X-ray source (details are available in the Supporting Information).

### Synthesis of triazoles

#### (*R*)-4-[3,5-Bis(trifluoromethyl)phenyl]-5-iodo-1-(1-phenylethyl)-1*H*-1,2,3-triazole (**3a**)

CuI (0.013 g, 0.068 mmol) and TBTA (0.038 mg, 0.072 mmol) were dissolved in degassed MeCN (4.0 mL) under argon atmosphere and stirred at room temperature for 30 min. 1-(Iodoethyl)-3,5-bis(trifluoromethyl)benzene (0.495 g, 1.36 mmol) and (*R*)-1-azidoethylbenzene (0.201 g, 1.37 mmol) dissolved in MeCN (2.8 mL) were added and the reaction mixture was stirred at room temperature for 8 h, during which a brown suspension formed. The reaction mixture was concentrated,  $\text{NH}_4\text{OH}$  (10 mL, 10% w/w) was added and the aqueous phase was extracted with  $\text{CH}_2\text{Cl}_2$  ( $4 \times 10$  mL). The combined organic phases were dried over anhydrous  $\text{Na}_2\text{SO}_4$ , concentrated and purified by column chromatography on silica gel (from 5% of EtOAc in petroleum ether) to provide triazole **3a** as colourless crystals (0.530 g, 76% yield). M.p.  $> 125^\circ\text{C}$  (decomp.);  $[\alpha]_{\text{D}}^{25} = 13.5$  ( $c = 0.30$  in chloroform);  $^1\text{H}$  NMR (400 MHz,  $[\text{D}]_x$ chloroform):  $\delta = 8.46$  (brs, 2H), 7.89 (brs, 1H), 7.44–7.24 (m, 5H), 5.82 (q,  $J = 7.1$  Hz, 1H), 2.14 ppm (d,  $J = 7.1$  Hz, 3H);  $^{13}\text{C}$  NMR (101 MHz,  $[\text{D}]_x$ chloroform):  $\delta = 147.2$ , 139.8, 132.6, 132.1 (q,  $J = 33.6$  Hz), 129.2, 128.6, 127.7–127.5 (m), 123.4 (q,  $J = 272.8$  Hz), 122.2–122.1 (m), 122.3–122.0 (m), 77.9, 62.1, 22.4 ppm; IR (KBr):  $\tilde{\nu} = 3097$  (w), 1618 (w), 1520 (w), 1458 (w), 1137 (s), 899 (m), 700  $\text{cm}^{-1}$  (m); HRMS (ESI):  $m/z$  calcd for  $\text{C}_{18}\text{H}_{13}\text{F}_6\text{N}_3$ : 512.0053  $[M+H]^+$ ; found: 512.0048.

The synthesis of the other triazoles is described in the Supporting Information.

### Synthesis of triazolium salts

#### (*R*)-4-[3,5-Bis(trifluoromethyl)phenyl]-5-iodo-3-methyl-1-(1-phenylethyl)-1*H*-1,2,3-triazol-3-ium trifluoromethanesulfonate (**4a**)

Triazole **3a** (0.090 g, 0.176 mmol) was dissolved in  $\text{CH}_2\text{Cl}_2$  (3.5 mL) under argon atmosphere. Methyl triflate (0.030 mL, 0.264 mmol) was added dropwise and the reaction mixture was stirred at room temperature for 3 days.  $\text{Et}_2\text{O}$  (5.0 mL) was added to the reaction mixture and the fine precipitate that formed was filtered to provide trifluoromethanesulfonate salt **4a** as colourless crystals (0.101 g, 85% yield). M.p. 185–189  $^\circ\text{C}$ ;  $[\alpha]_{\text{D}}^{25} = 33.9$  ( $c = 0.21$  in methanol);  $^1\text{H}$  NMR (400 MHz,  $[\text{D}]_x$ methanol):  $\delta = 8.38$  (brs, 1H), 8.33 (brs, 2H), 7.54–7.40 (m, 5H), 6.27 (q,  $J = 6.9$  Hz, 1H), 4.33 (s, 3H), 2.14 ppm (d,  $J = 6.9$  Hz, 3H);  $^{13}\text{C}$  NMR (101 MHz,  $[\text{D}]_x$ methanol):  $\delta = 146.1$ , 138.5, 134.2 (q,  $J = 34.2$  Hz), 132.7–132.4 (m), 130.5, 130.4, 128.2, 127.0, 124.2 (q,  $J = 272.1$  Hz), 123.4, 93.1, 67.7, 40.0, 22.0 ppm; IR (KBr):  $\tilde{\nu} = 3067$  (w), 1624 (w), 1498 (w), 1455 (w), 1142 (s), 1029 (s), 850 (w), 704 (m), 639  $\text{cm}^{-1}$  (s); HRMS (ESI):  $m/z$  calcd for  $\text{C}_{19}\text{H}_{15}\text{F}_6\text{N}_3$   $[M-\text{CF}_3\text{O}_3\text{S}]^+$ : 526.0209; found: 526.0207.

The synthesis of the other triazolium salts is described in the Supporting Information.

### Acknowledgements

The authors thank the Estonian Ministry of Education and Research (Grant Nos. IUT 19-32, IUT 19-9, PUT1468 and PUT692), the Centre of Excellence in Molecular Cell Engineering (2014-2020.4.01.15-0013) and the Academy of Finland (K.R.: grant no. 263256, 265328 and 292746) for financial support. We thank Ms. Tiina Aid and Dr. Mati Müürisepp for IR and MS measurements.

### Conflict of interest

The authors declare no conflict of interest.

**Keywords:** donor–acceptor systems · halogen bonds · heterocycles · NMR titrations · X-ray diffraction

- [1] G. R. Désiraju, P. S. Ho, L. Kloo, A. C. Legon, R. Marquardt, P. Metrangolo, P. Politzer, G. Resnati, K. Rissanen, *Pure Appl. Chem.* **2013**, *85*, 1711–1713.
- [2] For recent reviews, see: a) H. Wang, W. Wang, W. J. Jin, *Chem. Rev.* **2016**, *116*, 5072–5104; b) M. H. Kolař, P. Hobza, *Chem. Rev.* **2016**, *116*, 5155–5187; c) P. Politzer, J. S. Murray, G. V. Janjic, S. D. Zarić, *Crystals* **2014**, *4*, 12–31; d) P. Politzer, J. S. Murray, T. Clark, *Phys. Chem. Chem. Phys.* **2013**, *15*, 11178–11189; e) T. Clark, *Wiley Interdiscip. Rev.: Comput. Mol. Sci.* **2013**, *3*, 13–20; f) P. Politzer, K. E. Riley, F. A. Bulat, J. S. Murray, *Comput. Theor. Chem.* **2012**, *998*, 2–8.
- [3] a) K. Rissanen, *CrystEngComm* **2008**, *10*, 1107–1113; b) J. P. M. Lommerse, A. J. Stone, R. Taylor, F. H. Allen, *J. Am. Chem. Soc.* **1996**, *118*, 3108–3116.
- [4] a) P. Metrangolo, J. S. Murray, T. Pilati, P. Politzer, G. Resnati, G. Terraneo, *Cryst. Growth Des.* **2011**, *11*, 4238–4246; b) P. Politzer, J. S. Murray, T. Clark, *Phys. Chem. Chem. Phys.* **2010**, *12*, 7748–7757; c) P. Metrangolo, H. Neukirch, T. Pilati, G. Resnati, *Acc. Chem. Res.* **2005**, *38*, 386–395.
- [5] a) Q. Shi, H. Su, Y. Liu, W. Wub, Y. Lu, *Comput. Theor. Chem.* **2014**, *1027*, 79–83; b) O. Dumele, D. Wu, N. Trapp, N. Goroff, F. Diederich, *Org. Lett.* **2014**, *16*, 4722–4725; c) B. Pinter, N. Nagels, W. A. Herrebout, F. De Proft, *Chem. Eur. J.* **2013**, *19*, 519–530; d) R. Cabot, C. A. Hunter, *Chem.*

- Commun.* **2009**, 2005–2007; e) P. Metrangolo, W. Panzeri, F. Recupero, G. Resnati, *J. Fluorine Chem.* **2002**, 114, 27–33.
- [6] For recent reviews, see: a) B. Li, S.-Q. Zang, L.-Y. Wang, T. C. W. Mak, *Coord. Chem. Rev.* **2016**, 308, 1–21; b) G. Cavallo, P. Metrangolo, R. Milani, T. Pilati, A. Priimagi, G. Resnati, G. Terraneo, *Chem. Rev.* **2016**, 116, 2478–2601; c) L. C. Gilday, S. W. Robinson, T. A. Barendt, M. J. Langton, B. R. Mullaney, P. D. Beer, *Chem. Rev.* **2015**, 115, 7118–7195; d) G. Berger, J. Soubhaya, F. Meyer, *Polym. Chem.* **2015**, 6, 3559–3580; e) A. Mukherjee, S. Tothadi, G. R. Desiraju, *Acc. Chem. Res.* **2014**, 47, 2514–2524; f) L. P. Wolters, P. Schyman, M. J. Pavan, W. L. Jorgensen, M. Bickelhaupt, S. Kozuch, *Wiley Interdiscip. Rev.: Comput. Mol. Sci.* **2014**, 4, 523–540.
- [7] For reviews focusing on XB in solution, see: a) A. Brown, P. D. Beer, *Chem. Commun.* **2016**, 52, 8645–8658; b) A. V. Jentzsch, *Pure Appl. Chem.* **2015**, 87, 15–41; c) A.-C. Carlsson, A. X. Vega, M. Erdélyi, *Top. Curr. Chem.* **2014**, 359, 49–76; d) T. M. Beale, M. G. Chudzinski, M. G. Sarwar, M. S. Taylor, *Chem. Soc. Rev.* **2013**, 42, 1667–1680; e) M. Erdélyi, *Chem. Soc. Rev.* **2012**, 41, 3547–3557.
- [8] For recent reviews, see: a) X. Fang, C.-J. Wang, *Chem. Commun.* **2015**, 51, 1185–1197; b) L. Albrecht, H. Jiang, K. A. Jørgensen, *Chem. Eur. J.* **2014**, 20, 358–368; c) P. Chauhan, S. Mahajan, U. Kaya, D. Hack, D. Enders, *Adv. Synth. Catal.* **2015**, 357, 253–281; d) S. Narayanaperumal, D. G. Rivera, R. C. Silva, M. W. Paixão, *ChemCatChem* **2013**, 5, 2756–2773.
- [9] H. A. Bruckmann, M. A. Pena, C. Bolm, *Synlett* **2008**, 900–902.
- [10] For recent reviews, see: a) D. Bulfield, S. M. Huber, *Chem. Eur. J.* **2016**, 22, 14434–14450; b) S. Schindler, S. M. Huber, *Top. Curr. Chem.* **2014**, 359, 167–204.
- [11] a) A. Matsuzawa, S. Takeuchi, K. Sugita, *Chem. Asian J.* **2016**, 11, 2863–2866; b) M. Saito, N. Tsuji, Y. Kobayashi, Y. Takemoto, *Org. Lett.* **2015**, 17, 3000–3003; c) Y. Takeda, D. Hisakuni, C.-H. Lin, S. Minakata, *Org. Lett.* **2015**, 17, 318–321; d) S. H. Jungbauer, S. M. Huber, *J. Am. Chem. Soc.* **2015**, 137, 12110–12120; e) S. H. Jungbauer, S. M. Huber, S. Schindler, L. Rout, F. Kniep, S. M. Huber, *Chem. Commun.* **2014**, 50, 6281–6284; f) W. He, Y.-C. Ge, C.-H. Tan, *Org. Lett.* **2014**, 16, 3244–3247; g) F. Kniep, L. Rout, S. M. Huber, H. K. V. Bensch, S. H. Jungbauer, E. Herdtweck, S. M. Huber, *Chem. Commun.* **2012**, 48, 9299–9301; h) F. Kniep, S. H. Jungbauer, Q. Zhang, S. M. Huber, S. Schindler, I. Schnapperelle, E. Herdtweck, S. M. Huber, *Angew. Chem. Int. Ed.* **2013**, 52, 7028–7032; *Angew. Chem.* **2013**, 125, 7166–7170.
- [12] For computational studies on the application of XB in catalysis, see: a) M. Breugst, E. Detmar, D. von der Heiden, *ACS Catal.* **2016**, 6, 3203–3212; b) V. de P. N. Nziko, S. Scheiner, *J. Org. Chem.* **2016**, 81, 2589–2597; c) C. W. Kee, M. W. Wong, *J. Org. Chem.* **2016**, 81, 7459–7470; d) N. Heinz, M. Dolg, A. Berkessel, *J. Comput. Chem.* **2015**, 36, 1812–1817.
- [13] a) J. Y. C. Lim, I. Marques, L. Ferreira, V. Félix, P. D. Beer, *Chem. Commun.* **2016**, 52, 5527–5530; b) T. A. Barendt, A. Docker, I. Marques, V. Félix, P. D. Beer, *Angew. Chem. Int. Ed.* **2016**, 55, 11069–11076; c) L. González, F. Zapata, A. Caballero, P. Molina, C. R. de Arellano, I. Alkorta, J. Elguero, *Chem. Eur. J.* **2016**, 22, 7533–7544; d) R. Tepper, B. Schulze, M. Jäger, C. Friebe, D. H. Scharf, H. Görls, U. S. Schubert, *J. Org. Chem.* **2015**, 80, 3139–3150; e) B. R. Mullaney, B. E. Partridge, P. D. Beer, *Chem. Eur. J.* **2015**, 21, 1660–1665.
- [14] For reviews on copper(I)-catalysed alkyne–azide cycloaddition reactions, see: a) E. Haldón, M. C. Nicasio, P. J. Pérez, *Org. Biomol. Chem.* **2015**, 13, 9528–9550; b) L. Liang, D. Astruc, *Coord. Chem. Rev.* **2011**, 255, 2933–2945; c) J. E. Hein, V. V. Fokin, *Chem. Soc. Rev.* **2010**, 39, 1302–1315; d) M. Meldal, C. W. Tørnøe, *Chem. Rev.* **2008**, 108, 2952–3015.
- [15] a) J. E. Hein, J. C. Tripp, L. B. Krasnova, K. B. Sharpless, V. V. Fokin, *Angew. Chem. Int. Ed.* **2009**, 48, 8018–8021; *Angew. Chem.* **2009**, 121, 8162–8165; b) B. H. M. Kuipers, G. C. T. Dijkmans, S. Groothuys, P. J. L. M. Quaedflieg, R. H. Blaauw, F. L. van Delft, F. P. J. T. Rutjes, *Synlett* **2005**, 3059–3062.
- [16] a) Y. Le Gal, D. Lorcay, O. Jeannin, F. Barrière, V. Dorcet, J. Liefbrig, M. Fourmigué, *CrystEngComm* **2016**, 18, 5474–5481; b) F. Topić, K. Rissanen, *J. Am. Chem. Soc.* **2016**, 138, 6610–6616; c) L. Koskinen, S. Jääskeläinen, P. Hirva, M. Haukka, *Cryst. Growth Des.* **2015**, 15, 1160–1167; d) C. C. Robertson, R. N. Perutz, L. Brammer, C. A. Hunter, *Chem. Sci.* **2014**, 5, 4179–4183; e) C. Laurence, J. Graton, M. Berthelot, M. J. El Ghomari, *Chem. Eur. J.* **2011**, 17, 10431–10444; f) M. C. Aragoni, M. Arca, F. A. Devillanova, A. Garau, F. Isaia, V. Lippolis, G. Verani, *Coord. Chem. Rev.* **1999**, 184, 271–290.
- [17] a) B. Nepal, S. Scheiner, *Chem. Eur. J.* **2015**, 21, 13330–13335; b) B. Nepal, S. Scheiner, *J. Phys. Chem. A* **2015**, 119, 13064–13073.
- [18] a) S. M. Walter, F. Kniep, L. Rout, F. P. Schmidtchen, E. Herdtweck, S. M. Huber, *J. Am. Chem. Soc.* **2012**, 134, 8507–8512; b) S. M. Walter, F. Kniep, E. Herdtweck, S. M. Huber, *Angew. Chem. Int. Ed.* **2011**, 50, 7187–7191; *Angew. Chem.* **2011**, 123, 7325–7329; c) A. Caballero, N. G. White, P. D. Beer, *Angew. Chem. Int. Ed.* **2011**, 50, 1845–1848; *Angew. Chem.* **2011**, 123, 1885–1888; d) E. Dimitrijević, O. Kvak, M. S. Taylor, *Chem. Commun.* **2010**, 46, 9025–9027; e) K. Raatikainen, G. Cavallo, P. Metrangolo, K. Rissanen, G. Resnati, G. Terraneo, *Cryst. Growth Des.* **2013**, 13, 871–877; f) M. G. Sarwar, B. Dragisic, S. Sagoo, M. S. Taylor, *Angew. Chem. Int. Ed.* **2010**, 49, 1674–1677; *Angew. Chem.* **2010**, 122, 1718–1721.
- [19] B. T. Worrell, J. E. Hein, V. V. Fokin, *Angew. Chem. Int. Ed.* **2012**, 51, 11791–11794; *Angew. Chem.* **2012**, 124, 11961–11964.
- [20] a) A. Bolje, J. Košmrlj, *Org. Lett.* **2013**, 15, 5084–5087; b) D. Limnios, C. G. Kokotos, *Chem. Eur. J.* **2014**, 20, 559–563.
- [21] a) R. Puttreddy, O. Jurčák, S. Bhowmik, T. Mäkelä, K. Rissanen, *Chem. Commun.* **2016**, 52, 2338–2341; b) R. W. Troff, T. Mäkelä, F. Topić, A. Valkonen, K. Raatikainen, K. Rissanen, *Eur. J. Org. Chem.* **2013**, 1617–1637.
- [22] A. Bondi, *J. Phys. Chem.* **1964**, 68, 441–451.
- [23] a) C. Frassinetti, S. Ghelli, P. Gans, A. Sabatini, M. S. Moruzzi, A. Vacca, *Anal. Biochem.* **1995**, 231, 374–382; b) C. Frassinetti, L. Alderighi, P. Gans, A. Sabatini, A. Vacca, S. Ghelli, *Anal. Bioanal. Chem.* **2003**, 376, 1041–1052.
- [24] a) P. Politzer, J. S. Murray, M. C. Concha, *J. Mol. Model.* **2008**, 14, 659–665; b) F.-F. Wang, J.-H. Hou, Z.-R. Li, D. Wu, Y. Li, Z.-Y. Lu, W.-L. Cao, *J. Chem. Phys.* **2007**, 126, 144301–144305.
- [25] a) P. Peluso, V. Mamaneb, E. Aubert, A. D. R. Dallocchio, A. Dore, P. Pale, S. Cossu, *J. Chromatogr. A* **2016**, 1467, 228–238; b) P. Peluso, V. Mamaneb, E. Aubert, S. Cossu, *J. Chromatogr. A* **2014**, 1345, 182–192.

Manuscript received: February 10, 2017

Accepted manuscript online: March 7, 2017

Version of record online: May 10, 2017

## Appendix 2

### Publication II

Peterson, A.; Kaasik, M.; Metsala, A.; Järving, I.; Adamson, J.; Kanger, T. Tunable Chiral Triazole-Based Halogen Bond Donors: Assessment of Donor Strength in Solution with Nitrogen-Containing Acceptors. *RSC Adv.* **2019**, *9*, 11718–11721.

Reproduced by permission of The Royal Society of Chemistry.






 Cite this: *RSC Adv.*, 2019, 9, 11718

## Tunable chiral triazole-based halogen bond donors: assessment of donor strength in solution with nitrogen-containing acceptors†

 Anna Peterson,<sup>‡ab</sup> Mikk Kaasik,<sup>‡b</sup> Andrus Metsala,<sup>b</sup> Ivar Järving,<sup>b</sup> Jasper Adamson<sup>\*a</sup> and Tõnis Kanger<sup>‡b</sup>

 Received 6th March 2019  
Accepted 4th April 2019

DOI: 10.1039/c9ra01692a

rsc.li/rsc-advances

Strong halogen bond (XB) donors are needed for the activation of neutral substrates. We demonstrate that XB donor properties of iodo-triazoles can be significantly enhanced by quaternization in combination with varying the counterion and aromatic substituent, exemplified by association constants with quinuclidine as high as  $1.1 \times 10^4 \text{ M}^{-1}$ .

Halogen bond (XB) based applications utilize the attractive interaction between a Lewis acidic halogen atom and a Lewis base.<sup>1</sup> From the turn of the century numerous publications have focused on the use of XBs in the solid state<sup>2</sup> and more recently, in solution as well.<sup>3</sup> Among these applications the potential of XBs in catalysis<sup>4</sup> and anion recognition should be highlighted.<sup>5</sup> As shown by Huber *et al.* these fields can be closely associated, exemplified by halide abstraction reactions.<sup>6</sup>

Compared to anion recognition, the recognition of neutral species in solution has received less attention. Studies with neutral acceptors have a primary focus on the fundamental nature of halogen bonding, such as the influence of the solvent and the structure of the XB donor/acceptor on the strength of XBs.<sup>7</sup> Amines have usually been used as neutral acceptors in these studies for their high affinity towards XB donors. This property can potentially be utilized in the detection of biologically relevant amines by XBs.<sup>8</sup> From the synthetic point of view, the activation of neutral species through XBs is also a topic of high interest.<sup>9</sup> In general, compared to anions, neutral acceptors form weaker complexes with organic XB donors.<sup>1d,3c</sup> Therefore, XB donors with stronger halogen bonding ability should be used for the activation of neutral compounds. From a catalyst design perspective, information on the extent different structural fragments affect XB donor ability is of great value.

Recently, we became interested in applying XBs in asymmetric catalysis. Chiral 5-halo-1,2,3-triazoles are among the best

candidates of catalysts to achieve this goal.<sup>6b,9b,d</sup> The triazoles are readily available through a Cu-catalysed click reaction<sup>10</sup> and access to a broad range of alkynes with the possibility to quaternize the triazole core makes it feasible to enhance the donor ability of the triazole. In addition, the availability of many chiral azides offers wide opportunities for the design of new chiral XB donor systems.<sup>11</sup> We have shown the potential of these compounds to interact with various possible substrates and in enantiodiscrimination.<sup>12</sup> Due to relatively low affinity constants with thiourea acceptors, it was difficult to fully assess how structural modifications affect XB donors' binding ability. Therefore, a stronger XB acceptor has to be selected for this kind of analysis. Anionic species are known to give large affinity constants with halo-triazolium salts,<sup>13</sup> however, in these complexes charge attraction plays a key role in XB formation. We therefore chose quinuclidine,<sup>7d,h-k</sup> a neutral monodentate XB acceptor with a readily accessible lone pair, for screening of the effect of XB donor analogues (Fig. 1) on XB strength. Herein we describe the formation of complexes between triazole-based XB donors and quinuclidine in solution with emphasis on the influence of aromatic substituents and counterions on XB donor strength and investigate the XB donors' ability to discriminate between enantiomers of chiral imines and amines.

A collection of monodentate XB donors shown in Fig. 1 were synthesized (see ESI† for details). To determine the effect of structural changes, the triazolium salts were modified by introducing a perfluorophenyl or a *p*-nitrophenyl substituent instead of a phenyl substituent, changing the counterions and varying the halogen atoms. The XB donor ability of the synthesized compounds was determined through their respective association constants with quinuclidine in CDCl<sub>3</sub> based on <sup>1</sup>H NMR titration experiments. To evaluate the XB strength more accurately, the titration experiments were carried out in duplicate. The results are summarized in Table 1.

<sup>a</sup>Chemical Physics Laboratory, National Institute of Chemical Physics and Biophysics, Akadeemia tee 23, 12618, Tallinn, Estonia. E-mail: jasper.adamson@kbfi.ee

<sup>b</sup>Department of Chemistry and Biotechnology, School of Science, Tallinn University of Technology, Akadeemia tee 15, 12618 Tallinn, Estonia. E-mail: tonis.kanger@taltech.ee

† Electronic supplementary information (ESI) available: Experimental procedures, titration experiments, computational information and copies of <sup>1</sup>H and <sup>13</sup>C NMR spectra. See DOI: 10.1039/c9ra01692a

‡ These authors contribute equally to this work.



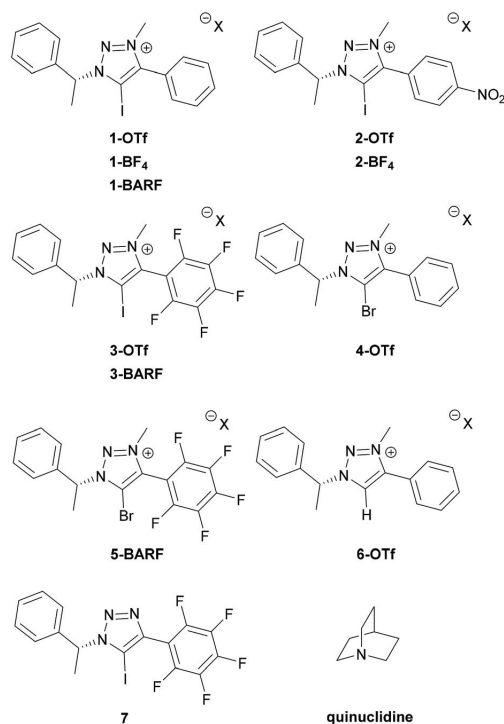


Fig. 1 XB donors and reference compound under study.

Table 1 Association constant  $K_a$  values<sup>a</sup> of the XB donor–quinuclidine pairs

Entry	XB donor	$K_a$ , M <sup>-1</sup>
1	1-OTf	57 ± 5
2	1-BARF	(1.23 ± 0.01) × 10 <sup>3</sup>
3	2-OTf	257 ± 12
4	2-BF <sub>4</sub>	284 ± 12
5	3-OTf	703 ± 6
6	3-BARF	(1.1 ± 0.3) × 10 <sup>4</sup>
7	4-OTf	<1
8	5-BARF	n.d. <sup>b</sup>
9	6-OTf	<1
10	7	2.0 ± 0.3

<sup>a</sup> Association constant  $K_a$  measured in CDCl<sub>3</sub> at 298 K and determined by fitting the <sup>1</sup>H NMR titration data to 1 : 1 binding isotherm of BindFit.<sup>15</sup> The given  $K_a$  and standard error are the calculated mean values of two parallel experiments. Full details given in the ESI. <sup>b</sup>  $K_a$  could not be determined due to the instability of XB donor during the experiment.

To evaluate the influence of substituents of the aromatic ring that connects directly to the triazolium core on XB formation ability of the triazolium salts, a perfluorinated and a nitro-substituted derivative (3-OTf and 2-OTf, respectively) were compared with the unsubstituted phenyl derivative 1-OTf (Table 1, entries 1, 3 and 5). The affinity towards quinuclidine

decreases in the order of 3-OTf > 2-OTf > 1-OTf which corresponds to the decrease of the size of the  $\sigma$ -hole on the iodine atom.<sup>14</sup> The perfluorinated XB donor had more than twice as high affinity towards quinuclidine as the NO<sub>2</sub>-containing XB donor and over an order of magnitude higher affinity when compared to 1-OTf. The strong XB donating ability of perfluorinated XB donors is explained by its highly electronegative fluorine substituents that significantly increase the polarization of the C–X bond, therefore increasing the  $\sigma$ -hole.<sup>7d,7i</sup> The electron-withdrawing nitro group in compound 2-OTf is similarly essential to enhance its XB donor ability, albeit less strongly compared to the more electron deficient perfluorophenyl group in 3-OTf. To determine that the changes in chemical shifts were indeed induced by halogen bonding, the nonhalogenated analogue 6-OTf was synthesized which expectedly did not interact favourably with quinuclidine (Table 1, entry 9).

The effects of anionic counterions were characterised based on triflate (1-OTf, 2-OTf, 3-OTf), tetrafluoroborate (2-BF<sub>4</sub>) and tetrakis[3,5-bis(trifluoromethyl)phenyl]borate (1-BARF, 3-BARF) containing triazolium salts. Due to poor solubility, the comparison to 1-BF<sub>4</sub> could not be made. In general, the change of the counterion affected XB strength substantially in accordance with their coordination ability.<sup>16</sup> The less coordinating tetrafluoroborate containing triazolium salt 2-BF<sub>4</sub> showed higher affinity towards quinuclidine compared to the triflate containing salt 2-OTf (Table 1, entries 3 and 4). The introduction of the BARF counterion increased XB strength by more than one order of magnitude (Table 1, comparing entries 1 and 5 to entries 2 and 6). To the best of our knowledge, the obtained affinity constant between quinuclidine and 3-BARF is among the highest affinities reported so far for a neutral acceptor.<sup>3e,7</sup> Usually XBs are stronger in apolar solvents than in more polar solvents<sup>7e,f,i</sup> and as a comparison, the association constant is only a magnitude smaller than that for the complex between quinuclidine and I<sub>2</sub> measured in heptane.<sup>7h</sup>

The strength of the XB is known to decrease based on the polarization of the halogen atom and the increase of electronegativity in the order of I > Br > Cl > F.<sup>1</sup> In our <sup>1</sup>H NMR titration study, the iodo-triazolium analogue (1-OTf) displayed moderate affinity towards quinuclidine whereas the corresponding bromine analogue (4-OTf) did not show any affinity towards quinuclidine altogether (Table 1, entry 7, also see ESI† for details). The absence of complex formation with the bromine derivative agrees with a similar outcome in our previous investigation.<sup>12</sup> In an attempt to obtain a complex containing a bromine atom as the donor, a bromo-triazolium salt 5-BARF with the strongly electronegative pentafluorophenyl substituent was synthesized. Nevertheless, the changes undertaken made the donor too labile and upon the titration experiment dehalogenation prevented the determination of the affinity constant (Table 1, entry 8, also see ESI† for details).

Quaternization of the triazole core has been critical to obtain compounds with sufficient XB donor ability.<sup>13b,17</sup> To ascertain the impact of charge in the triazole core, neutral perfluorinated triazole 7 was also titrated with quinuclidine. The obtained affinity constant is indeed very low. However, this result is of importance in its own right as there are only a few examples





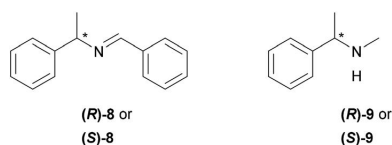


Fig. 2 Chiral XB acceptors under study.

describing complex formation in solution between a neutral halo-triazole and a neutral acceptor.<sup>18</sup> The difference between the neutral XB donor (7) and its charged derivative (3-OTf) is more than two orders of magnitude (Table 1, entries 5 and 10). However, if the counterion acts as an acceptor and competes with quinuclidine for XB formation, triazole 7 should be compared to 3-BARF, which has the less coordinating BARF counterion and therefore provides a better representation for a “naked” cationic backbone. In this case, the difference in binding ability of four orders of magnitude was observed (Table 1, entries 6 and 10).

Furthermore, <sup>1</sup>H NMR titrations measurements were performed using both enantiomers of chiral imine 8 and amine 9 (Fig. 2) to determine whether the XB donors are able to selectively interact with chiral substances. For these experiments, 3-BARF was chosen as the donor due to the highest binding affinity towards quinuclidine. The XB donor showed no preference towards either enantiomer of the selected acceptors since no differences between the two enantiomers  $K_a$  values were observed in either case (Table 2, entries 1 and 2; entries 3 and 4). Nevertheless, the affinity constant between amine 9 and 3-BARF is considerably higher compared to the only reported example, where the XB strength between an organic XB donor and secondary amine was measured.<sup>7</sup> The affinity constant between perfluorohexyl iodide and piperidine was <1 in all three solvents used in that study. The difference compared to the binding strength of quinuclidine can partly be explained by the fact that cyclic amines are better acceptors than acyclic amines.<sup>7</sup>

Calculations were performed on the CAM/B3LYP<sup>19</sup> level of theory using DEF2TZVP basis set<sup>20</sup> to model the interaction between both enantiomers of amine 9 and 3-OTf. The calculated complexes in the vacuum and in CHCl<sub>3</sub> had similar energy values (see ESI† for details). The substituents on the triazole core are most likely not sufficiently bulky to differentiate between the two enantiomers through steric repulsion or by

Table 2 Association constant  $K_a$  values<sup>a</sup> of the chiral acceptor and 3-BARF pairs

Entry	XB acceptor	$K_a$ , M <sup>-1</sup>
1	(R)-8	6.1 ± 0.7
2	(S)-8	6.0 ± 0.8
3	(R)-9	94 ± 7
4	(S)-9	91 ± 5

<sup>a</sup> Association constant  $K_a$  measured in CDCl<sub>3</sub> at 298 K and determined by fitting the <sup>1</sup>H NMR titration data to 1 : 1 binding isotherm of BindFit.<sup>15</sup> The given  $K_a$  and standard error are the calculated mean values of two parallel experiments. Full details given in the ESI.

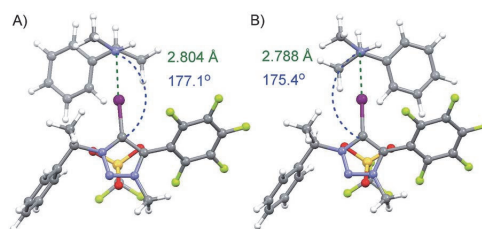


Fig. 3 Calculated minimum energy complexes formed through a XB between donor 3-OTf and (S)- or (R)-enantiomer of amine 9 (A and B respectively).

other noncovalent interactions (Fig. 3). This could also explain our previously obtained results of enantiodiscrimination experiments, where Takemoto's catalyst<sup>21</sup> was used as an acceptor and that suggest that both hydrogen and halogen bonding interactions influenced the binding of enantiomers.<sup>12</sup> Therefore, a more beneficial approach would be to use multidentate or bifunctional XB donors that form more rigid complexes. For example, Beer *et al.* has shown that chiral bidentate XB donors that contain at least two halo-triazole cores are suitable for differentiating between enantiomers.<sup>13a,22</sup>

In conclusion, we have once again shown the pivotal role of charge on XB donor strength. In addition, by changing the aromatic substituent and the counterion, the XB donor properties of triazole-based donors can be enhanced even further. This is exemplified by the fact that the donors form complexes with quinuclidine with association constants covering almost four orders of magnitude. To the best of our knowledge, the reported association constants are comparable to the largest described between an amine and an organic XB donor in solution. Enantiodiscrimination of acceptors 8 and 9 by the most powerful donor 3-BARF was not observed. However, information obtained during this study can aid to move towards more selective donors.

## Conflicts of interest

There are no conflicts to declare.

## Acknowledgements

The present study was supported by Estonian Ministry of Education and Research (Grant No. IUT 19-32, IUT 19-9, IUT 23-7, PUT1468 and PRG399) and the Centre of Excellence in Molecular Cell Engineering 2014-2020.4.01.15-0013 as well as the Centre of Excellence TK134. We thank Dr Aleksander-Mati Müürisepp for the IR spectra, Dr Kadri Kriis and Mrs Egle Rinaldo for their help on the synthesis.

## Notes and references

- (a) Á. M. Montaña, *ChemistrySelect*, 2017, 2, 9094; (b) G. Cavallo, P. Metrangolo, R. Milani, T. Pilati, A. Priimagi, G. Resnati and G. Terraneo, *Chem. Rev.*, 2016, 116, 2478; (c) H. Wang, W. Wang and W. J. Jin, *Chem. Rev.*, 2016, 116,



- 5072; (d) L. C. Gilday, S. W. Robinson, T. A. Barendt, M. J. Langton, B. R. Mullaney and P. D. Beer, *Chem. Rev.*, 2015, **115**, 7118.
- 2 (a) J.-C. Christopherson, F. Topić, C. J. Barrett and T. Friščić, *Cryst. Growth Des.*, 2018, **18**, 1245; (b) B. Li, S.-Q. Zang, L.-Y. Wang and T. C. W. Mak, *Coord. Chem. Rev.*, 2016, **308**, 1; (c) G. Berger, J. Soubhy and F. Meyer, *Polym. Chem.*, 2015, **6**, 3559; (d) A. Mukherjee, S. Tothadi and G. R. Desiraju, *Acc. Chem. Res.*, 2014, **47**, 2514; (e) R. W. Troff, T. Mäkelä, F. Topić, A. Valkonen, K. Raatikainen and K. Rissanen, *Eur. J. Org. Chem.*, 2013, **2013**, 1617; (f) K. Rissanen, *CrystEngComm*, 2008, **10**, 1107.
- 3 (a) A. V. Jentzsch, *Pure Appl. Chem.*, 2015, **87**, 15; (b) A.-C. C. Carlsson, A. X. Veiga and M. Erdélyi, *Top. Curr. Chem.*, 2014, **359**, 49; (c) T. M. Beale, M. G. Chudzinski, M. G. Sarwar and M. S. Taylor, *Chem. Soc. Rev.*, 2013, **42**, 1667.
- 4 (a) M. Breugst and D. von der Heiden, *Chem.–Eur. J.*, 2018, **24**, 9187; (b) D. Bulfield and S. M. Huber, *Chem.–Eur. J.*, 2016, **22**, 14434; (c) S. Schindler and S. M. Huber, *Top. Curr. Chem.*, 2014, **359**, 167.
- 5 (a) R. Tepper and U. S. Schubert, *Angew. Chem., Int. Ed.*, 2018, **57**, 6004; (b) A. Brown and P. D. Beer, *Chem. Commun.*, 2016, **52**, 8645.
- 6 (a) F. Heinen, E. Engelage, A. Dreger, R. Weiss and S. M. Huber, *Angew. Chem., Int. Ed.*, 2018, **57**, 3830; (b) A. Dreger, E. Engelage, B. Mallick, P. D. Beer and S. M. Huber, *Chem. Commun.*, 2018, **54**, 4013; (c) S. H. Jungbauer and S. M. Huber, *J. Am. Chem. Soc.*, 2015, **137**, 12110; (d) F. Kniep, S. H. Jungbauer, Q. Zhang, S. M. Walter, S. Schindler, I. Schnapperelle, E. Herdtweck and S. M. Huber, *Angew. Chem., Int. Ed.*, 2013, **52**, 7028; (e) F. Kniep, L. Rout, S. M. Walter, H. K. V. Bensch, S. H. Jungbauer, E. Herdtweck and S. M. Huber, *Chem. Commun.*, 2012, **48**, 9299.
- 7 (a) A. M. S. Riel, M. J. Jessop, D. A. Decato, C. J. Massena, V. R. Nascimento and O. B. Berryman, *Acta Crystallogr., Sect. B: Struct. Sci., Cryst. Eng. Mater.*, 2017, **73**, 203; (b) G. Ciancaleoni, A. Macchioni, L. Rocchigiani and C. Zuccaccia, *RSC Adv.*, 2016, **6**, 80604; (c) R. Puttreddy, O. Jurčák, S. Bhowmik, T. Mäkelä and K. Rissanen, *Chem. Commun.*, 2016, **52**, 2338; (d) O. Dumele, D. Wu, N. Trapp, N. Goroff and F. Diederich, *Org. Lett.*, 2014, **16**, 4722; (e) S. H. Jungbauer, D. Bulfield, F. Kniep, C. W. Lehmann, E. Herdtweck and S. M. Huber, *J. Am. Chem. Soc.*, 2014, **136**, 16740; (f) C. C. Robertson, R. N. Perutz, L. Brammer and C. A. Hunter, *Chem. Sci.*, 2014, **5**, 4179; (g) B. Hawthorne, H. Fan-Hagenstein, E. Wood, J. Smith and T. Hanks, *Int. J. Spectrosc.*, 2013, **2013**, 1; (h) C. Laurence, J. Graton, M. Berthelot and M. J. El Ghomari, *Chem.–Eur. J.*, 2011, **17**, 10431; (i) M. G. Sarwar, B. Dragisic, L. J. Salsberg, C. Gouliaras and M. S. Taylor, *J. Am. Chem. Soc.*, 2010, **132**, 1646; (j) R. Cabot and C. A. Hunter, *Chem. Commun.*, 2009, 2005; (k) P. Metrangolo, W. Panzeri, F. Recupero and G. Resnati, *J. Fluorine Chem.*, 2002, **114**, 27.
- 8 X. X. Zhang, J. S. Bradshaw and R. M. Izatt, *Chem. Rev.*, 1997, **97**, 3313.
- 9 (a) G. Bergamaschi, L. Lascialfari, A. Pizzi, M. I. M. Espinoza, N. Demitri, A. Milani, A. Gori and P. Metrangolo, *Chem. Commun.*, 2018, **54**, 10718; (b) R. Haraguchi, S. Hoshino, M. Sakai, S. Tanazawa, Y. Morita, T. Komatsu and S. Fukuzawa, *Chem. Commun.*, 2018, **54**, 10320; (c) J.-P. Gliese, S. H. Jungbauer and S. M. Huber, *Chem. Commun.*, 2017, **53**, 12052; (d) D. von der Heiden, E. Detmar, R. Kuchta and M. Breugst, *Synlett*, 2017, **28**, 1307.
- 10 (a) J. M. Pérez, P. Crosbie, S. Lal and S. Díez-González, *ChemCatChem*, 2016, **8**, 2222; (b) J. García-Álvarez, J. Díez and J. Gimeno, *Green Chem.*, 2010, **12**, 2127; (c) J. E. Hein, J. C. Tripp, L. B. Krasnova, K. B. Sharpless and V. V. Fokin, *Angew. Chem., Int. Ed.*, 2009, **48**, 8018; (d) B. H. M. Kuipers, G. C. T. Dijkmans, S. Groothuys, P. J. L. M. Quaedflieg, R. H. Blaauw, F. L. van Delft and F. P. J. T. Rutjes, *Synlett*, 2005, 3059.
- 11 M. Kaasik, S. Kaabel, K. Kriis, I. Järving and T. Kanger, *Synthesis*, 2019, DOI: 10.1055/s-0037-1610864.
- 12 M. Kaasik, S. Kaabel, K. Kriis, I. Järving, R. Aav, K. Rissanen and T. Kanger, *Chem.–Eur. J.*, 2017, **23**, 7337.
- 13 (a) J. Y. C. Lim, I. Marques, V. Félix and P. D. Beer, *Chem. Commun.*, 2018, **54**, 10851; (b) R. Tepper, B. Schulze, M. Jäger, C. Friebe, D. H. Scharf, H. Görls and U. S. Schubert, *J. Org. Chem.*, 2015, **80**, 3139.
- 14 M. Kaasik, A. Metsala, S. Kaabel, K. Kriis, I. Järving and T. Kanger, *J. Org. Chem.*, 2019, **84**, 4294–4303.
- 15 Freely available at <http://www.supramolecular.org> (accessed February 22, 2019).
- 16 (a) I. Krossing and I. Raabe, *Angew. Chem., Int. Ed.*, 2004, **43**, 2066; (b) S. H. Strauss, *Chem. Rev.*, 1993, **93**, 927.
- 17 (a) B. Nepal and S. Scheiner, *Chem.–Eur. J.*, 2015, **21**, 13330; (b) B. Nepal and S. Scheiner, *J. Phys. Chem. A*, 2015, **119**, 13064.
- 18 L. Maugeri, J. Asencio-Hernández, T. Lébl, D. B. Cordes, A. M. Z. Slawin, M. Delsuc and D. Philp, *Chem. Sci.*, 2016, **7**, 6422.
- 19 T. Yanai, D. Tew and N. Handy, *Chem. Phys. Lett.*, 2004, **393**, 51.
- 20 F. Weigend and R. Ahlrichs, *Phys. Chem. Chem. Phys.*, 2005, **7**, 3297.
- 21 T. Okino, Y. Hoashi and Y. Takemoto, *J. Am. Chem. Soc.*, 2003, **125**, 12672.
- 22 (a) A. Borisso, J. Y. C. Lim, A. Brown, K. E. Christensen, A. L. Thompson, M. D. Smith and P. D. Beer, *Chem. Commun.*, 2017, **53**, 2483; (b) J. Y. C. Lim, I. Marques, L. Ferreira, V. Félix and P. D. Beer, *Chem. Commun.*, 2016, **52**, 5527.



## Appendix 3

### Publication III

Kaasik, M.; Kaabel, S.; Kriis, K.; Järving, I.; Kanger, T. Synthesis of Chiral Triazole-Based Halogen Bond Donors. *Synthesis* **2019**, *51*, 2128–2135.

Reproduced by permission of Georg Thieme Verlag KG Stuttgart • New York.



# Synthesis of Chiral Triazole-Based Halogen Bond Donors

Mikk Kaasik<sup>1</sup>

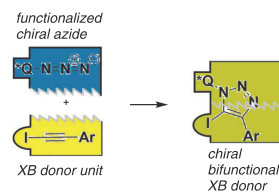
Sandra Kaabel

Kadri Kriis

Ivar Järving

Tõnis Kanger\*<sup>1</sup>

Department of Chemistry and Biotechnology,  
School of Science, Tallinn University of Technology,  
Akadeemia tee 15, 12618 Tallinn, Estonia  
tonis.kanger@taltech.ee



Received: 28.12.2018

Accepted after revision: 02.02.2019

Published online: 12.03.2019

DOI: 10.1055/s-0037-1610864; Art ID: ss-2018-t0869-op

**Abstract** The number of applications that use halogen bonding in the fields of self-assembly, supramolecular aggregation, and catalysis is growing. However, the accessibility of chiral halotriazoles shows that there is still a lot more to explore. The simple click-chemistry is applied for the straightforward synthesis of enantiomerically pure mono- and bidentate as well as multifunctional iodotriazole-based XB donors. The methodology is characterized by a wide variability due to easy access of chiral azides.

**Key words** click chemistry, nitrogen heterocycles, halogen bonds, hydrogen bonds, chiral compounds

Non-covalent interactions are of importance in biology and chemistry.<sup>1</sup> In chemistry, self-assembly, supramolecular aggregation, and often catalysis are based on these interactions. The past ten years have seen remarkable advances in the use of halogen bonding in these fields.<sup>2</sup> A halogen bond (XB) is similarly to a hydrogen bond (HB) a non-covalent interaction of an electrophilic atom with some Lewis base.<sup>3</sup> The strength of the XB depends on the structures of both the acceptor and the donor. The donor ability is connected with the polarizability of the halogen atom and changes in the order I > Br > Cl > F.<sup>4</sup> Electron-withdrawing groups connected with the halogen can further polarize the halogen atom and therefore increase its donor ability.<sup>5</sup>

Over the years the choice of XB donor scaffolds has considerably expanded. The first XB donors to be described were dihalogens and interhalogens (Figure 1).<sup>6</sup> However, organic scaffolds offer wider opportunities to modify the XB donor ability of the halogen atom. For example, the XB donor ability increases with an increase in the s-character on the carbon atom when comparing haloalkanes, haloarenes, and haloalkynes.<sup>4,7</sup> N-Haloimides have also been used as

strong XB donors, due to the strongly polarizing effect of the carbonyl groups.<sup>8</sup> Nitrogen-containing cycles (pyridines, imidazoles, and triazoles)<sup>9</sup> are especially valuable as the quaternization of the nitrogen atom makes it possible to increase the electronegativity of the core.<sup>5a,10</sup>

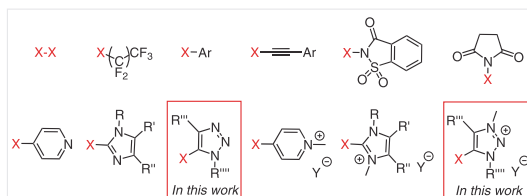


**Figure 1** Typical examples of halogen bond donor scaffolds. Most commonly the donor atom X in the XB donor is either iodine or bromine

Triazole-based XB donors are readily accessible via a copper-catalyzed click reaction between haloalkyne and organic azide.<sup>11</sup> Alternatively, terminal alkynes can also be used, in which case halogenation is carried out in situ.<sup>12</sup> The halotriazoles have been used in ion-pair recognition,<sup>13</sup> as anion receptors,<sup>10b,14</sup> in organocatalysis,<sup>15</sup> and in polymer chemistry.<sup>16</sup> Iodotriazoles as XB donors were first introduced by Beer.<sup>17</sup> In spite of a wide variety of available chiral azides, the application of chiral triazole-based XB donors is quite limited. The pioneering work in this field was published by Huber et al. in 2012.<sup>15a</sup> We have recently shown enantiodiscrimination via XBs using chiral iodotriazoles.<sup>18</sup> Beer et al. have used chiral triazole-based rotaxanes.<sup>19</sup> BINOL-based receptors have been designed for the enantioselective recognition of anions.<sup>14b,20</sup> Interestingly, a stereogenic unit was also used as a bridge between two XB donor units. In addition, a macrocyclic pseudopeptide containing

three triazole cores was used as a halide receptor by Kubik et al.<sup>14c</sup> Selected examples of chiral XB donors are depicted in Figure 2.

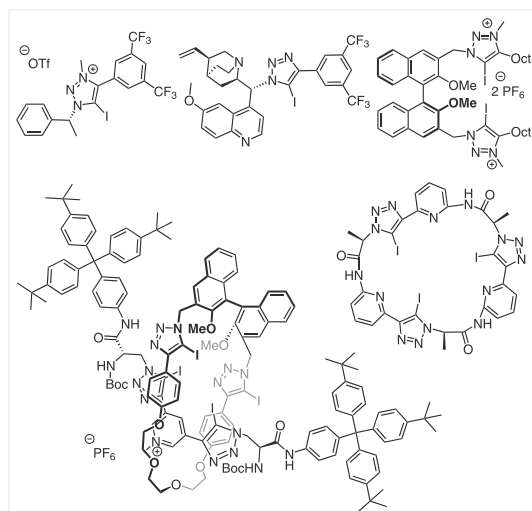


**Figure 2** Examples of chiral iodotriazole-based XB donors

To broaden the scope of available chiral XB donors, we describe herein the synthesis of enantiomerically pure triazole derivatives. The synthesis of mono- and bidentate as well as multifunctional donors containing both XB and hydrogen bond donor moieties will be discussed.

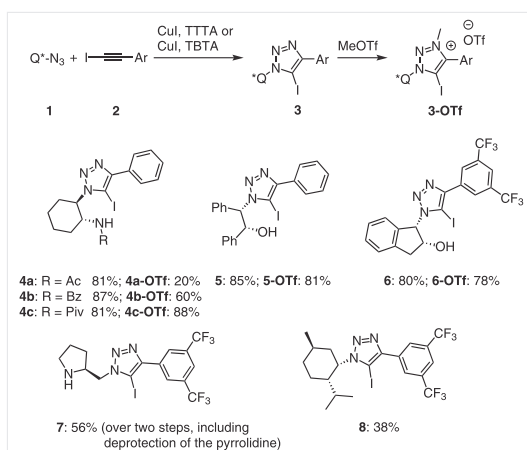
To start with, enantiomerically pure monodentate XB donors were synthesized from monoalkynes (iodoethynyl)benzene or 1-(iodoethynyl)-3,5-bis(trifluoromethyl)benzene (Scheme 1). Chiral amines or alcohols were used to obtain azides for a click reaction. Amines were directly converted into azides by reaction with imidazole-1-sulfonyl azide hydrochloride with the retention of the stereocenter. Alcohols were converted into corresponding mesylates and nucleophilic substitution resulted in azides with the inversion of the stereocenter (for details, see Supporting Information).

First, (1*R*,2*R*)-1,2-diaminocyclohexane was used as a chiral starting compound. Monoprotection of the diamine using phthalic anhydride, followed by acylation, then deprotection and azidation using imidazole-1-sulfonyl azide hydrochloride afforded azides with acyl-, benzoyl- or pivaloyl-protected amino groups.<sup>21,22</sup> A click reaction in the presence of CuI and tris[(1-*tert*-butyl-1*H*-1,2,3-triazolyl)methyl]amine (TTTA)<sup>11b</sup> led to triazoles **4a–c** in good yields (81–87%). The following quaternization with methyl trifluoromethanesulfonate (MeOTf) afforded XB donors **4a-OTf** to **4c-OTf** with an amide-based HB donor group.

The second group of XB donors contained a hydroxyl group as the HB donor unit (compounds **5** and **6**). *cis*-(1*S*,2*R*)-1-Amino-2-indanol and (1*S*,2*R*)-2-amino-1,2-diphenylethan-1-ol were transformed into the corresponding azides, which were then used to get XB donors **5** and **6** (85% and 80%, respectively) and corresponding triazolium salts (**5-OTf**, **6-OTf**).

For the synthesis of donors **7** and **8**, the second approach, converting the hydroxyl group into an azido group, was used. The synthesis of compound **7** started from Boc-protected (*S*)-prolinol. It was mesylated and treated with sodium azide to give the azide. After the formation of the triazole, the Boc-protecting group was removed affording the target containing a basic amino group in 56% yield (yield for two steps). A similar strategy was used to convert (–)-menthol into XB donor **8** with a bulky substituent. Unfortunately the click reaction worked reasonably well only with tris[(1-benzyl-1*H*-1,2,3-triazol-4-yl)methyl]amine (TBTA) and gave the product in a lower yield (38%; for details, see Supporting Information).

The iodotriazoles **8** and **4b-OTf** were analyzed and characterized by single-crystal X-ray crystallography (Figure 3). In the case of triazole **8**, an XB formed between the iodine atom of one donor and the nitrogen atom in the triazole core of another molecule of **8**. The distance of 2.947 Å corresponds to a reduction of the sum of the van der Waals radii by 16%. In the case of **4b-OTf** the carbonyl oxygen acted as an XB acceptor and the distance of 2.724 Å corresponds to a reduction of the sum of the van der Waals radii by 22%. Notably, in contrast to the triazolium salts previously studied,<sup>18</sup> which formed XBs to the counter anions, the carbonyl group of **4b-OTf** outcompeted the trifluoromethanesulfonate anion as an XB acceptor.



**Scheme 1** Synthesis of monodentate XB donors

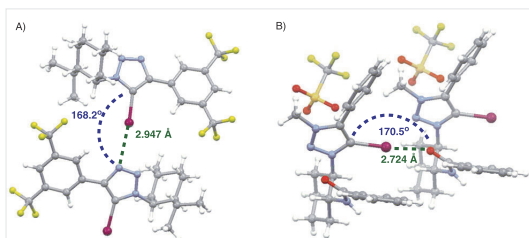
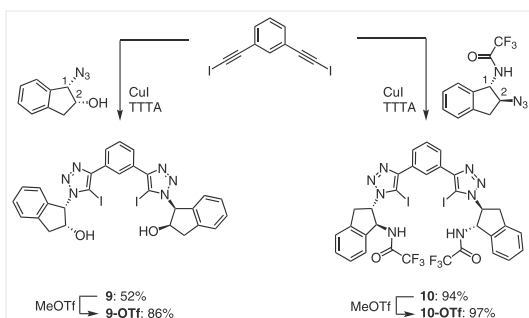


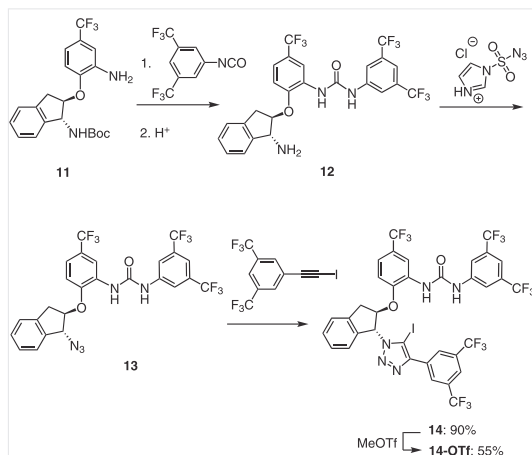
**Figure 3** Ball and stick representations of **8** (A) and **4b-OTf** (B) showing the angle and distances of the XB between the molecules (see Supporting Information for details)

Next, bidentate  $C_2$ -symmetric XB donors **9** and **10** were synthesized starting from *cis*-(1*S*,2*R*)-1-amino-2-indanol and *meta*-bis(iodoethynyl)benzene (Scheme 2). Compound **9** was obtained by azidating the free amino group, followed by a click reaction. On the other hand, the selective *N*-trifluoroacetylation of *cis*-aminoindanol allowed the transformation of the unprotected hydroxyl group into azide by the previously described mesylation/substitution method with inversion of the configuration. This synthon for the click reaction differed from the synthon obtained by direct azidation in the relative configuration of the substituents on the indane ring. Also, the azido group and the respective bond with the triazole ring changed from the first to the second position on the indane ring. The click reaction proceeded smoothly affording triazole **10** in an excellent yield. Compounds **9** and **10** were again converted into corresponding triazolium salts in high yields. The obtained XB donors possessed different HB moieties and formed chiral pockets for acceptors with different geometries.



**Scheme 2** Synthesis of bidentate XB donors

The synthetic potential of chiral azides and a click reaction was further harnessed to access triazole and urea-containing polyfunctional donor **14** (Scheme 3).



**Scheme 3** Synthesis of urea-containing XB donor **14-OTf**

Aminoindanol derivative **11** was used as a chiral linker to connect urea and triazole moieties.<sup>23</sup> The reaction of 3,5-bis(trifluoromethyl)phenyl isocyanate with the aromatic amine **11** afforded after acidic deprotection urea **12** in 92% yield. The following azidation with imidazole-1-sulfonyl azide hydrochloride and a click reaction resulted in the formation of triazole **14**.

In conclusion, we have shown a straightforward approach to enantiomerically pure XB donors. A click reaction provides a direct entry to the target compounds. Monodentate, bidentate, and polyfunctional XB donors can be obtained in high yields. Further studies on the applications of these compounds are ongoing.

NMR spectra were measured on a Bruker Avance III 400 MHz instrument. The spectra are reported in parts per million ( $\delta$ ) referenced to the residual solvent signal [ $CDCl_3$   $\delta$  = 7.26,  $CD_3OD$   $\delta$  = 3.31,  $DMSO-d_6$   $\delta$  = 2.50, acetone- $d_6$   $\delta$  = 2.05 (for  $^1H$  NMR);  $CDCl_3$   $\delta$  = 77.16,  $CD_3OD$   $\delta$  = 49.00,  $DMSO-d_6$   $\delta$  = 39.52, acetone- $d_6$   $\delta$  = 29.84 (for  $^{13}C$  NMR)]. High-resolution mass spectra were recorded on an Agilent Technologies 6540 UHD Accurate-Mass Q-TOF LC/MS spectrometer by using AJ-ESI ionization. Single crystal X-ray diffraction data was collected at 123K on Rigaku Compact HomeLab diffractometer, equipped with a Saturn 944 HG CCD detector and Oxford Cryostream cooling system using monochromatic Cu-K $\alpha$  radiation (1.54178Å) from a MicroMax<sup>TM</sup>-003 sealed tube microfocus X-ray source. Optical rotations were obtained using an Anton Paar GWB Polarimeter MCP 500. IR absorption frequencies in wavenumbers are listed, with the relative strength in parentheses (*w* = weak, *m* = medium, *s* = strong, *br* = broad). Pre-coated silica gel 60 F<sub>254</sub> plates from Merck were used for TLC, whereas for column chromatography, silica gel Kieselgel 40–63  $\mu m$  was used. The measured melting points are uncorrected. Purchased chemicals and solvents were used as received.  $CH_2Cl_2$  was distilled over  $P_2O_5$  and



MeOH was dried by distillation over Na metal. Petroleum ether (PE) has a boiling point of 40–60 °C. The reactions were performed without additional moisture elimination, unless stated otherwise.

#### Click Reaction; General Procedure

CuI (0.004 g, 0.021 mmol) and TTTA (0.010 mg, 0.023 mmol) were dissolved in freshly distilled THF (2.3 mL, 0.2 M) under argon atmosphere and stirred at r.t. for 30 min. The (iodoethyl)benzene or 1-(iodoethyl)-3,5-bis(trifluoromethyl)benzene (0.45 mmol) and azide (0.45 mmol) were added and the reaction mixture was stirred at r.t. overnight. The mixture was concentrated,  $\text{NH}_4\text{OH}$  (10 mL, 10% w/w) was added and the aqueous phase was extracted with  $\text{CH}_2\text{Cl}_2$  ( $3 \times 10$  mL). The combined organic phases were dried (anhyd  $\text{Na}_2\text{SO}_4$ ), concentrated, and purified by column chromatography on silica gel (starting from 10% EtOAc in PE) to provide the triazole.

#### Conversion of Triazoles into Triazolium Salts; General Procedure

The respective triazole (0.19 mmol) was dissolved in  $\text{CH}_2\text{Cl}_2$  (4 mL, 0.05 M) under argon atmosphere. MeOTf (0.033 mL, 0.29 mmol) was added dropwise and the reaction mixture was stirred at r.t. for 3 days.  $\text{Et}_2\text{O}$  was added to the mixture and the precipitate formed was filtered to provide the trifluoromethanesulfonic salt.

#### N-[(1*R*,2*R*)-2-(5-Iodo-4-phenyl-1*H*-1,2,3-triazol-1-yl)cyclohexyl]acetamide (4a)

Colorless solid; yield: 0.145 g (0.353 mmol, 81%); mp >187 °C (dec.);  $[\alpha]_{\text{D}}^{20}$  –11.9 (c 0.43,  $\text{CHCl}_3$ ).

IR (KBr): 3278 (s), 3073 (w), 2928 (s), 2857 (m), 1655 (s), 1552 (s), 1447 (m), 1375 (w), 1318 (w), 1228 (w), 1173 (w), 1065 (w), 985 (m), 807 (w), 768 (m), 697  $\text{cm}^{-1}$  (s).

$^1\text{H}$  NMR (400 MHz,  $\text{CDCl}_3$ ):  $\delta$  = 7.95–7.89 (m, 2 H), 7.48–7.43 (m, 2 H), 7.43–7.36 (m, 1 H), 5.57 (d,  $J$  = 8.2 Hz, 1 H), 4.77 (td,  $J$  = 10.8, 4.9 Hz, 1 H), 4.47–4.20 (m, 1 H), 2.30–2.08 (m, 3 H), 2.02–1.79 (m, 3 H), 1.76 (s, 3 H), 1.62–1.40 (m, 2 H).

$^{13}\text{C}$  NMR (101 MHz,  $\text{CDCl}_3$ ):  $\delta$  = 169.6, 149.0 (based on HMBC), 130.4, 128.7, 128.6, 127.9, 63.5 (based on HSQC), 53.8 (based on HSQC), 32.7, 31.9, 25.0, 24.9, 23.7. The iodine bonded C-atom was not detected because of low intensity of the signal.

HRMS (ESI):  $m/z$   $[\text{M} + \text{H}]^+$  calcd for  $\text{C}_{16}\text{H}_{20}\text{IN}_4\text{O}$ : 411.0676; found: 411.0674.

#### 1-[(1*R*,2*R*)-2-Acetamidocyclohexyl]-5-iodo-3-methyl-4-phenyl-1*H*-1,2,3-triazol-3-ium Trifluoromethanesulfonate (4a-OTf)

The product was crystallized twice; colorless solid; yield: 0.040 g (0.070 mmol, 20%); mp 192–194 °C;  $[\alpha]_{\text{D}}^{20}$  +40.7 (c 0.18, MeOH).

IR (KBr): 3311 (m), 2933 (m), 2862 (w), 1651 (s), 1554 (m), 1449 (w), 1372 (w), 1285 (s), 1253 (s), 1224 (w), 1163 (m), 1030 (s), 768 (w), 707 (w), 637  $\text{cm}^{-1}$  (s).

$^1\text{H}$  NMR (400 MHz,  $\text{CD}_3\text{OD}$ ):  $\delta$  = 7.81–7.48 (m, 5 H), 4.75–4.60 (m, 1 H), 4.23 (s, 3 H), 4.16 (s, 1 H), 2.44–2.27 (m, 2 H), 2.12–1.89 (m, 3 H), 1.84 (s, 3 H), 1.77–1.47 (m, 3 H).

$^{13}\text{C}$  NMR (101 MHz,  $\text{CD}_3\text{OD}$ ):  $\delta$  = 172.8, 147.8, 133.2, 131.3, 130.8, 124.3, 121.8 (q,  $J$  = 318.6 Hz), 92.3, 70.2, 55.2, 39.7, 32.2, 31.7, 25.4, 25.3, 22.8.

HRMS (ESI):  $m/z$   $[\text{M} - \text{CF}_3\text{O}_2\text{S}]^+$  calcd for  $\text{C}_{17}\text{H}_{23}\text{IN}_4\text{O}$ : 425.0833; found: 425.0829;  $m/z$   $[\text{OTf}]^-$  calcd for  $\text{CF}_3\text{O}_2\text{S}$ : 148.9526; found: 148.9529.

#### N-[(1*R*,2*R*)-2-(5-Iodo-4-phenyl-1*H*-1,2,3-triazol-1-yl)cyclohexyl]benzamide (4b)

Eluent for chromatography: starting from 5% of EtOAc in  $\text{CH}_2\text{Cl}_2$ ; colorless solid; yield: 0.335 g (0.709 mmol, 87%); mp 193–196 °C;  $[\alpha]_{\text{D}}^{20}$  –28.6 (c 0.30,  $\text{CHCl}_3$ ).

IR (KBr): 3318 (m), 3063 (w), 2940 (m), 2856 (m), 1638 (s), 1579 (w), 1543 (s), 1493 (m), 1447 (w), 1322 (s), 1286 (w), 1236 (w), 1170 (w), 983 (m), 803 (w), 769 (m), 695  $\text{cm}^{-1}$  (s).

$^1\text{H}$  NMR (400 MHz,  $\text{CDCl}_3$ ):  $\delta$  = 7.85–7.79 (m, 2 H), 7.57–7.50 (m, 2 H), 7.47–7.27 (m, 6 H), 6.13 (d,  $J$  = 8.0 Hz, 1 H), 4.97 (td,  $J$  = 10.8, 4.8 Hz, 1 H), 4.66–4.43 (m, 1 H), 2.37–2.16 (m, 3 H), 2.10–1.87 (m, 3 H), 1.62–1.47 (m, 2 H).

$^{13}\text{C}$  NMR (101 MHz,  $\text{CDCl}_3$ ):  $\delta$  = 167.3, 149.1 (based on HMBC), 134.6, 131.6, 130.4, 128.6, 128.6, 128.6, 127.9, 126.9, 63.2 (based on HSQC), 54.3 (based on HSQC), 32.8, 31.9, 25.1, 25.0. The iodine bonded C-atom was not detected because of low intensity of the signal.

HRMS (ESI):  $m/z$   $[\text{M} + \text{H}]^+$  calcd for  $\text{C}_{21}\text{H}_{22}\text{IN}_4\text{O}$ : 473.0833; found: 473.0828.

#### 1-[(1*R*,2*R*)-2-Benzamidocyclohexyl]-5-iodo-3-methyl-4-phenyl-1*H*-1,2,3-triazol-3-ium Trifluoromethanesulfonate (4b-OTf)

The product precipitated from the reaction mixture and was recrystallized from hot  $\text{CH}_2\text{Cl}_2$ ; colorless solid; yield: 0.187 g (0.294 mmol, 60%); mp >230 °C (dec.);  $[\alpha]_{\text{D}}^{20}$  –5.0 (c 0.21, MeOH).

IR (KBr): 3304 (m), 2938 (w), 2860 (w), 1641 (s), 1580 (w), 1535 (m), 1488 (w), 1455 (w), 1323 (m), 1283 (s), 1257 (s), 1225 (w), 1155 (m), 1031 (s), 771 (w), 697 (m), 638  $\text{cm}^{-1}$  (s).

$^1\text{H}$  NMR (400 MHz,  $\text{CD}_3\text{OD}$ ):  $\delta$  = 7.81–7.75 (m, 2 H), 7.70–7.53 (m, 4 H), 7.50–7.37 (m, 4 H), 4.84–4.78 (m, 1 H), 4.46 (ddd,  $J$  = 11.8, 10.1, 4.4 Hz, 1 H), 4.27 (s, 3 H), 3.35 (s, 1 H), 2.53–2.36 (m, 2 H), 2.21–1.85 (m, 4 H), 1.75–1.54 (m, 2 H).

$^{13}\text{C}$  NMR (101 MHz,  $\text{CD}_3\text{OD}$ ):  $\delta$  = 169.6, 147.8, 134.6, 133.2, 133.2, 131.2, 130.7, 129.6, 128.5, 124.2, 92.6, 70.3, 55.7, 39.8, 32.1, 31.9, 25.6, 25.4.

HRMS (ESI):  $m/z$   $[\text{M} - \text{CF}_3\text{O}_2\text{S}]^+$  calcd for  $\text{C}_{22}\text{H}_{25}\text{IN}_4\text{O}$ : 487.0989; found: 487.0985;  $m/z$   $[\text{OTf}]^-$  calcd for  $\text{CF}_3\text{O}_2\text{S}$ : 148.9526; found: 148.9529.

#### N-[(1*R*,2*R*)-2-(5-Iodo-4-phenyl-1*H*-1,2,3-triazol-1-yl)cyclohexyl]pivalamide (4c)

Reaction conducted in 0.3 M solution of THF; colorless solid; yield: 0.108 g (0.239 mmol, 81%); mp 206–210 °C;  $[\alpha]_{\text{D}}^{20}$  +3.8 (c 0.87,  $\text{CHCl}_3$ ).

IR (KBr): 3406 (m), 2932 (s), 2865 (w), 1650 (s), 1513 (s), 1477 (m), 1448 (m), 1317 (w), 1230 (m), 1193 (m), 1169 (w), 985 (m), 957 (w), 769 (m), 696  $\text{cm}^{-1}$  (m).

$^1\text{H}$  NMR (400 MHz,  $\text{CDCl}_3$ ):  $\delta$  = 7.92–7.79 (m, 2 H), 7.49–7.42 (m, 2 H), 7.42–7.36 (m, 1 H), 5.53 (d,  $J$  = 7.9 Hz, 1 H), 4.89 (dd,  $J$  = 16.2, 10.7 Hz, 1 H), 4.46–4.18 (m, 1 H), 2.30–2.04 (m, 3 H), 2.02–1.79 (m, 3 H), 1.59–1.42 (m, 2 H), 0.94 (s, 9 H).

$^{13}\text{C}$  NMR (101 MHz,  $\text{CDCl}_3$ ):  $\delta$  = 178.1, 149.1 (based on HMBC), 130.5, 128.6 (o- and m-C overlapped, based on HSQC), 127.9, 62.8 (based on HSQC), 53.9 (based on HSQC), 38.8, 32.8, 32.0, 27.5, 25.2, 25.1. The iodine bonded C-atom was not detected because of low intensity of the signal.

HRMS (ESI):  $m/z$   $[\text{M} + \text{H}]^+$  calcd for  $\text{C}_{19}\text{H}_{26}\text{IN}_4\text{O}$ : 453.1146; found: 453.1138.



**5-Iodo-3-methyl-4-phenyl-1-[(1*R*,2*R*)-2-pivalamidocyclohexyl]-1*H*-1,2,3-triazol-3-ium Trifluoromethanesulfonate (4c-OTf)**

Colorless solid; yield: 0.143 g (0.232 mmol, 88%); mp 218–219 °C;  $[\alpha]_D^{20} +54.3$  (c 0.20, MeOH).

IR (KBr): 3354 (m), 2937 (m), 2865 (w), 1623 (s), 1529 (s), 1485 (m), 1455 (m), 1367 (w), 1319 (w), 1284 (s), 1223 (m), 1149 (s), 1093 (w), 1032 (s), 826 (w), 766 (w), 697 (m), 637 cm<sup>-1</sup> (s).

<sup>1</sup>H NMR (400 MHz, CDCl<sub>3</sub>):  $\delta$  = 7.70–7.41 (m, 5 H), 6.55 (d,  $J$  = 8.0 Hz, 1 H), 5.08–4.87 (m, 1 H), 4.23 (s, 3 H), 4.15–4.03 (m, 1 H), 2.53–2.39 (m, 1 H), 2.25 (q,  $J$  = 12.5 Hz, 1 H), 2.11–1.75 (m, 4 H), 1.65–1.36 (m, 2 H), 1.07 (s, 9 H).

<sup>13</sup>C NMR (101 MHz, CDCl<sub>3</sub>):  $\delta$  = 179.3, 146.1, 132.2, 130.1, 129.9, 122.6, 89.1, 68.7, 54.7, 39.5, 38.8, 31.3, 31.1, 27.7, 24.7, 24.3.

HRMS (ESI):  $m/z$  [M – CF<sub>3</sub>O<sub>3</sub>S]<sup>+</sup> calcd for C<sub>20</sub>H<sub>29</sub>N<sub>4</sub>O: 467.1302; found: 467.1302;  $m/z$  [OTf]<sup>-</sup> calcd for CF<sub>3</sub>O<sub>3</sub>S: 148.9526; found: 148.9529.

**(1*R*,2*S*)-2-(5-Iodo-4-phenyl-1*H*-1,2,3-triazol-1-yl)-1,2-diphenylethan-1-ol (5)**

Reaction conducted in 0.3 M solution of THF; colorless solid; yield: 0.183 g (0.392 mmol, 85%); mp >164 °C (dec.);  $[\alpha]_D^{20} +63.1$  (c 0.25, CHCl<sub>3</sub>).

IR (KBr): 3227 (br m), 2924 (m), 1604 (w), 1494 (w), 1474 (w), 1454 (m), 1322 (w), 1239 (w), 1158 (w), 1048 (s), 985 (w), 828 (m), 761 (m), 748 (s), 718 (w), 697 cm<sup>-1</sup> (s).

<sup>1</sup>H NMR (400 MHz, CDCl<sub>3</sub>):  $\delta$  = 7.89–7.82 (m, 2 H), 7.47–7.22 (m, 13 H), 5.90 (dd,  $J$  = 5.5, 2.5 Hz, 1 H), 5.68 (d,  $J$  = 5.5 Hz, 1 H), 3.70 (d,  $J$  = 2.5 Hz, 1 H).

<sup>13</sup>C NMR (101 MHz, CDCl<sub>3</sub>):  $\delta$  = 149.4, 139.2, 133.9, 130.0, 129.2, 129.0, 128.8, 128.7, 128.5, 128.4, 128.4, 127.7, 126.9, 78.4, 75.6, 71.4.

HRMS (ESI):  $m/z$  [M + H]<sup>+</sup> calcd for C<sub>22</sub>H<sub>19</sub>N<sub>3</sub>O: 468.0567; found: 468.0562.

**1-[(1*S*,2*R*)-2-Hydroxy-1,2-diphenylethyl]-5-iodo-3-methyl-4-phenyl-1*H*-1,2,3-triazol-3-ium Trifluoromethanesulfonate (5-OTf)**

Colorless solid; yield: 0.099 g (0.157 mmol, 81%); mp 188–189 °C;  $[\alpha]_D^{20} -54.8$  (c 0.16, MeOH).

IR (KBr): 3386 (br w), 1487 (w), 1456 (w), 1251 (s), 1165 (m), 1030 (s), 756 (w), 703 (m), 639 cm<sup>-1</sup> (m).

<sup>1</sup>H NMR (400 MHz, CD<sub>3</sub>OD):  $\delta$  = 7.81–7.74 (m, 2 H), 7.70–7.58 (m, 3 H), 7.55–7.45 (m, 3 H), 7.45–7.31 (m, 7 H), 6.09 (d,  $J$  = 8.6 Hz, 1 H), 5.73 (d,  $J$  = 8.5 Hz, 1 H), 4.24 (s, 3 H).

<sup>13</sup>C NMR (101 MHz, CD<sub>3</sub>OD):  $\delta$  = 148.0, 141.1, 134.5, 133.3, 131.1, 131.0, 130.7, 130.7, 130.1, 130.0, 129.8, 128.0, 123.8, 93.1, 76.2, 75.5, 39.8.

HRMS (ESI):  $m/z$  [M – CF<sub>3</sub>O<sub>3</sub>S]<sup>+</sup> calcd for C<sub>23</sub>H<sub>21</sub>N<sub>3</sub>O: 482.0724; found: 482.0723;  $m/z$  [OTf]<sup>-</sup> calcd for CF<sub>3</sub>O<sub>3</sub>S: 148.9526; found: 148.9533.

**(1*S*,2*R*)-1-(4-[3,5-Bis(trifluoromethyl)phenyl]-5-iodo-1*H*-1,2,3-triazol-1-yl)-2,3-dihydro-1*H*-inden-2-ol (6)**

Et<sub>3</sub>N (2 equiv) was used instead of TTTA; eluent for chromatography: starting from 20% of EtOAc in PE; off-white solid; yield: 0.188 g (0.349 mmol, 80%); mp 114–116 °C;  $[\alpha]_D^{20} +109.3$  (c 1.45, CHCl<sub>3</sub>).

IR (KBr): 3396 (br m), 1621 (w), 1374 (w), 1307 (m), 1279 (s), 1127 (s), 897 (m), 847 (w), 809 (w), 746 (m), 699 (m), 683 cm<sup>-1</sup> (m).

<sup>1</sup>H NMR (400 MHz, CDCl<sub>3</sub>):  $\delta$  = 8.42 (br s, 2 H), 7.89 (br s, 1 H), 7.46–7.21 (m, 4 H), 6.10 (d,  $J$  = 6.4 Hz, 1 H), 4.99 (dq,  $J$  = 10.0, 6.7 Hz, 1 H), 3.40 (d,  $J$  = 6.8 Hz, 2 H), 2.93 (d,  $J$  = 10.1 Hz, 1 H).

<sup>13</sup>C NMR (101 MHz, CDCl<sub>3</sub>):  $\delta$  = 146.5, 141.3, 136.9, 132.1, 132.0 (q,  $J$  = 33.6 Hz), 130.1, 127.6, 127.4–127.2 (m), 125.7, 124.5, 123.1 (q,  $J$  = 272.9 Hz), 122.4–122.0 (m), 79.1, 73.8, 67.3, 40.1.

HRMS (ESI):  $m/z$  [M + H]<sup>+</sup> calcd for C<sub>19</sub>H<sub>13</sub>F<sub>6</sub>N<sub>3</sub>O: 540.0002; found: 540.0002.

**4-[3,5-Bis(trifluoromethyl)phenyl]-1-[(1*S*,2*R*)-2-hydroxy-2,3-dihydro-1*H*-inden-1-yl]-5-iodo-3-methyl-1*H*-1,2,3-triazol-3-ium Trifluoromethanesulfonate (6-OTf)**

White solid; yield: 0.091 g (0.129 mmol, 78%); mp 176–179 °C;  $[\alpha]_D^{25} -22.0$  (c 1.10, CHCl<sub>3</sub>).

IR (KBr): 3421 (m), 1623 (w), 1371 (m), 1283 (s), 1139 (s), 1030 (s), 911 (m), 848 (w), 757 (m), 704 (m), 680 (m), 640 cm<sup>-1</sup> (s).

<sup>1</sup>H NMR (400 MHz, CD<sub>3</sub>OD):  $\delta$  = 8.40 (br s, 1 H), 8.36 (br s, 2 H), 7.53–7.32 (m, 4 H), 6.51 (d,  $J$  = 6.3 Hz, 1 H), 5.09 (q,  $J$  = 6.7 Hz, 1 H), 4.19 (s, 3 H), 3.41 (dd,  $J$  = 16.1, 7.0 Hz, 1 H), 3.14 (dd,  $J$  = 16.2, 6.9 Hz, 1 H).

<sup>13</sup>C NMR (101 MHz, CD<sub>3</sub>OD):  $\delta$  = 145.5, 144.0, 136.0, 134.3 (q,  $J$  = 33.6 Hz), 132.8–132.5 (m), 132.0, 128.9, 127.8, 127.2, 127.1–126.9 (m), 126.6, 124.2 (q,  $J$  = 272.5 Hz), 94.4 (based on HMBC), 73.7, 73.2, 40.0, 39.9.

HRMS (ESI):  $m/z$  [M – CF<sub>3</sub>O<sub>3</sub>S]<sup>+</sup> calcd for C<sub>20</sub>H<sub>15</sub>F<sub>6</sub>N<sub>3</sub>O: 554.0159; found: 554.0159.

**(*S*)-4-[3,5-Bis(trifluoromethyl)phenyl]-5-iodo-1-(pyrrolidin-2-ylmethyl)-1*H*-1,2,3-triazole (7)**

Triazole **7** was synthesized by the general procedure for the click reaction [yield of Boc-protected **7**: 0.149 g (0.252 mmol, 88%)] followed by removal of the Boc-protecting group.

To a solution of *tert*-butyl (*S*)-2-[4-(3,5-bis(trifluoromethyl)phenyl)-5-iodo-1*H*-1,2,3-triazol-1-yl)methyl]pyrrolidine-1-carboxylate (0.126 g, 0.213 mmol) in CH<sub>2</sub>Cl<sub>2</sub> (1 mL) was added TFA (0.400 mL, 5.22 mmol) at 0 °C and the reaction mixture was stirred at r.t. for 3 h. The mixture was concentrated, triturated with Et<sub>2</sub>O, and filtered to provide the salt of **7**, which was treated with sat. aq NaHCO<sub>3</sub> (2 mL). After stirring for 15 min, the aqueous phase was extracted with CH<sub>2</sub>Cl<sub>2</sub> (7 × 3 mL), dried (Na<sub>2</sub>SO<sub>4</sub>), and concentrated. Removal of solvent under reduced pressure afforded triazole **7** as an off-white solid; yield: 0.068 g (0.139 mmol, 65%); mp 103–104 °C;  $[\alpha]_D^{20} +11.1$  (c 0.68, MeOH).

IR (KBr): 2926 (m), 1620 (w), 1373 (w), 1316 (m), 1285 (s), 1183 (m), 1128 (s), 896 (m), 821 (w), 698 (w), 683 cm<sup>-1</sup> (w).

<sup>1</sup>H NMR (400 MHz, CDCl<sub>3</sub>):  $\delta$  = 8.48 (br s, 2 H), 7.90 (br s, 1 H), 4.41 (qd,  $J$  = 13.7, 6.7 Hz, 2 H), 3.82 (ddd,  $J$  = 13.5, 7.4, 5.9 Hz, 1 H), 3.10–2.93 (m, 2 H), 2.03–1.74 (m, 4 H), 1.67–1.57 (m, 1 H).

<sup>13</sup>C NMR (101 MHz, CDCl<sub>3</sub>):  $\delta$  = 146.7, 132.5, 132.0 (q,  $J$  = 33.5 Hz), 127.4–127.2 (m), 123.2 (q,  $J$  = 272.7 Hz), 122.2–121.8 (m), 78.6, 57.7, 55.6, 46.5, 29.3, 25.3.

HRMS (ESI):  $m/z$  [M + H]<sup>+</sup> calcd for C<sub>15</sub>H<sub>14</sub>F<sub>6</sub>N<sub>4</sub>: 491.0162; found: 491.0157.

**4-[3,5-Bis(trifluoromethyl)phenyl]-5-iodo-1-[(1*S*,2*S*,5*R*)-2-isopropyl-5-methylcyclohexyl]-1*H*-1,2,3-triazole (8)**

TBTA was used instead of TTTA; eluent for chromatography: starting from 5% CH<sub>2</sub>Cl<sub>2</sub> in PE; colorless solid; yield: 0.048 g (0.088 mmol, 38%); mp 132–134 °C;  $[\alpha]_D^{20} +5.9$  (c 0.04, CHCl<sub>3</sub>).

IR (KBr): 2964 (m), 2845 (w), 1622 (w), 1462 (w), 1371 (m), 1309 (m), 1280 (s), 1243 (w), 1183 (s), 1139 (s), 898 (m), 846 (w), 809 (w), 711 (w), 700 (m), 682 cm<sup>-1</sup> (m).

<sup>1</sup>H NMR (400 MHz, CDCl<sub>3</sub>): δ = 8.50 (br s, 2 H), 7.89 (br s, 1 H), 5.07–4.93 (m, 1 H), 2.38 (qd, *J* = 13.2, 4.0 Hz, 1 H), 2.02–1.93 (m, 1 H), 1.93–1.76 (m, 3 H), 1.55–1.45 (m, 2 H), 1.44–1.35 (m, 1 H), 1.05 (qd, *J* = 13.2, 4.2 Hz, 1 H), 0.88 (d, *J* = 6.5 Hz, 3 H), 0.85 (d, *J* = 6.4 Hz, 3 H), 0.78 (d, *J* = 6.5 Hz, 3 H).

<sup>13</sup>C NMR (101 MHz, CDCl<sub>3</sub>): δ = 145.8, 132.8, 132.0 (q, *J* = 33.5 Hz), 127.7–127.4 (m), 123.4 (d, *J* = 274.7 Hz), 122.2–121.9 (m), 79.0, 59.6, 47.2, 40.6, 35.0, 29.0, 25.32, 25.28, 22.1, 21.5, 21.0.

HRMS (ESI): *m/z* [M + H]<sup>+</sup> calcd for C<sub>20</sub>H<sub>23</sub>F<sub>6</sub>N<sub>3</sub>: 546.0835; found: 546.0841.

**(1*S*,1'*S*,2*R*,2'*R*)-1,1'-[1,3-Phenylenebis(5-iodo-1*H*-1,2,3-triazole-4,1-diyl)]bis(2,3-dihydro-1*H*-inden-2-ol) (9)**

CuI (0.10 equiv) and TTTA (0.10 equiv) were used; eluent for chromatography: starting from 20% of EtOAc in PE; off-white solid; yield: 0.240 g (0.33 mmol, 52%); mp 198–203 °C; [α]<sub>D</sub><sup>20</sup> +23.4 (c 0.36, MeOH).

IR (KBr): 3406 (br s), 2918 (w), 1610 (w), 1461 (m), 1344 (m), 1241 (m), 1215 (w), 1169 (w), 1100 (s), 985 (m), 887 (w), 796 (m), 744 (s), 718 (w), 685 cm<sup>-1</sup> (m).

<sup>1</sup>H NMR (400 MHz, DMSO-*d*<sub>6</sub>): δ = 8.61–8.56 (m, 1 H), 7.98 (dt, *J* = 7.8, 1.9 Hz, 2 H), 7.66 (t, *J* = 7.8 Hz, 1 H), 7.45–7.20 (m, 8 H), 6.09 (d, *J* = 6.5 Hz, 2 H), 5.42 (d, *J* = 5.9 Hz, 2 H), 4.83 (tt, *J* = 6.5, 6.7 Hz, 2 H), 3.23 (dd, *J* = 15.6, 6.9 Hz, 2 H), 3.10 (dd, *J* = 15.7, 6.9 Hz, 2 H).

<sup>13</sup>C NMR (101 MHz, DMSO-*d*<sub>6</sub>): δ = 147.1, 142.2, 138.1, 131.1, 129.1, 129.0, 126.9, 126.6, 125.9, 125.3, 125.0, 83.0, 71.9, 66.8, 66.7.

HRMS (ESI): *m/z* [M + H]<sup>+</sup> calcd for C<sub>28</sub>H<sub>23</sub>I<sub>2</sub>N<sub>6</sub>O<sub>2</sub>: 728.9966; found: 728.9974.

**4,4'-(1,3-Phenylene)bis(1-[(1*S*,2*R*)-2-hydroxy-2,3-dihydro-1*H*-inden-1-yl]-5-iodo-3-methyl-1*H*-1,2,3-triazol-3-ium) Trifluoromethanesulfonate (9-OTf)**

White solid; yield: 0.164 g (0.155 mmol, 86%); mp 147–150 °C; [α]<sub>D</sub><sup>25</sup> –8.7 (c 0.70, MeOH).

IR (KBr): 3423 (br s), 1624 (w), 1556 (w), 1479 (w), 1254 (s), 1166 (s), 1100 (m), 1029 (s), 891 (w), 815 (w), 756 (m), 696 (w), 639 cm<sup>-1</sup> (s).

<sup>1</sup>H NMR (400 MHz, CD<sub>3</sub>OD): δ = 8.09–7.98 (m, 4 H), 7.53–7.40 (m, 6 H), 7.40–7.31 (m, 2 H), 6.51 (d, *J* = 6.5 Hz, 2 H), 5.09 (q, *J* = 6.8 Hz, 2 H), 4.24 (s, 6 H), 3.40 (dd, *J* = 16.1, 7.0 Hz, 2 H), 3.14 (dd, *J* = 16.1, 6.9 Hz, 2 H).

<sup>13</sup>C NMR (101 MHz, CD<sub>3</sub>OD): δ = 146.6, 144.0, 136.1, 135.1, 133.5, 132.3, 131.9, 128.8, 127.8, 126.5, 126.1, 93.9 (based on HMBC), 73.7, 73.0, 40.1, 39.9.

HRMS (ESI): *m/z* [M – 2 CF<sub>3</sub>O<sub>3</sub>S – CH<sub>3</sub>]<sup>+</sup> calcd for C<sub>29</sub>H<sub>25</sub>I<sub>2</sub>N<sub>6</sub>O<sub>2</sub>: 743.0123; found: 743.0124.

***N,N'*-{[(1*S*,1'*S*,2*S*,2'*S*)-1,3-Phenylenebis(5-iodo-1*H*-1,2,3-triazole-4,1-diyl)]bis(2,3-dihydro-1*H*-indene-2,1-diyl)]bis(2,2,2-trifluoroacetamide) (10)**

CuI (0.10 equiv) and TTTA (0.10 equiv) were used. 0.1 M solution. The product was purified mostly by crystallization. The crude product was dissolved in EtOAc (0.2 mL), then CH<sub>2</sub>Cl<sub>2</sub> (2 mL) was added and the fine precipitate formed was filtered to provide bistriazole **10** as off-white crystals [yield: 0.141 g (0.154 mmol, 67%)]. The mother liquor was concentrated and purified by column chromatography on silica gel (starting from 20% of acetone in PE) to provide an additional amount of **10** as a white solid; yield: 0.057 g (0.062 mmol, 27%); total yield: 94%; mp 172–174 °C; [α]<sub>D</sub><sup>25</sup> +31.9 (c 0.60, acetone).

IR (KBr): 3428 (br m), 3073 (w), 1713 (s), 1548 (m), 1462 (w), 1208 (s), 1166 (s), 983 (w), 929 (w), 791 (w), 750 (m), 717 cm<sup>-1</sup> (w).

<sup>1</sup>H NMR (400 MHz, acetone-*d*<sub>6</sub>): δ = 9.20 (d, *J* = 8.5 Hz, 2 H), 8.71 (t, *J* = 1.8 Hz, 1 H), 8.08 (dd, *J* = 7.8, 1.8 Hz, 2 H), 7.68 (t, *J* = 7.8 Hz, 1 H), 7.46–7.26 (m, 8 H), 6.19 (t, *J* = 7.9 Hz, 2 H), 5.76 (td, *J* = 8.5, 7.3 Hz, 2 H), 3.81 (dd, *J* = 16.1, 8.6 Hz, 2 H), 3.70 (dd, *J* = 16.0, 8.3 Hz, 2 H).

<sup>13</sup>C NMR (101 MHz, acetone-*d*<sub>6</sub>): δ = 157.91 (q, *J* = 37.0 Hz), 149.8, 139.8, 139.3, 132.1, 129.9, 129.8, 128.7, 128.2, 126.9, 125.8, 124.6, 116.9 (q, *J* = 287.9 Hz), 80.2, 67.0, 61.7, 37.9.

HRMS (ESI): *m/z* [M + H]<sup>+</sup> calcd for C<sub>32</sub>H<sub>23</sub>F<sub>6</sub>N<sub>6</sub>O<sub>2</sub>: 918.9932; found: 918.9925.

**4,4'-(1,3-Phenylene)bis(5-iodo-3-methyl-1-[(1*S*,2*S*)-1-(2,2,2-trifluoroacetamido)-2,3-dihydro-1*H*-inden-2-yl]-1*H*-1,2,3-triazol-3-ium) Trifluoromethanesulfonate (10-OTf)**

Colorless solid; yield: 0.135 g (0.108 mmol, 97%); mp >213 °C (dec.); [α]<sub>D</sub><sup>20</sup> +21.0 (c 0.70, acetone).

IR (KBr): 3456 (br m), 1720 (s), 1555 (m), 1482 (w), 1251 (s), 1166 (s), 1031 (s), 757 (w), 639 (m), 518 cm<sup>-1</sup> (w).

<sup>1</sup>H NMR (400 MHz, acetone-*d*<sub>6</sub>): δ = 9.40 (d, *J* = 7.8 Hz, 2 H), 8.36–8.00 (m, 4 H), 7.56–7.22 (m, 8 H), 6.09 (dt, *J* = 8.8, 6.6 Hz, 2 H), 6.1–5.9 (m, 2 H), 4.44 (s, 6 H), 4.04 (dd, *J* = 16.7, 8.5 Hz, 2 H), 3.78 (dd, *J* = 16.7, 6.8 Hz, 2 H).

<sup>13</sup>C NMR (101 MHz, acetone-*d*<sub>6</sub>): δ = 158.46 (q, *J* = 37.3 Hz), 147.0, 139.4, 138.2, 134.9, 133.3, 132.0, 130.4, 129.0, 125.9, 125.6, 124.8, 116.78 (q, *J* = 287.7 Hz), 92.8, 70.4, 62.6, 40.5, 38.0.

HRMS (ESI): *m/z* [M – 2 CF<sub>3</sub>O<sub>3</sub>S]<sup>2+</sup> calcd for C<sub>34</sub>H<sub>28</sub>F<sub>6</sub>N<sub>6</sub>O<sub>2</sub>: 474.0159; found: 474.0165; *m/z* [OTf]<sup>+</sup> calcd for CF<sub>3</sub>O<sub>3</sub>S: 148.9526; found: 148.9542.

**1-(2-[(1*R*,2*R*)-1-Azido-2,3-dihydro-1*H*-inden-2-yl]oxy)-5-(trifluoromethyl)phenyl)-3-[3,5-bis(trifluoromethyl)phenyl]urea (13)**

The urea **12** was prepared following the literature procedure.<sup>22</sup> Ammonia **12** (0.408 g, 0.725 mmol) was dissolved in a suspension of K<sub>2</sub>CO<sub>3</sub> (0.151 g, 1.088 mmol) and CuSO<sub>4</sub>·5H<sub>2</sub>O (0.002 mg, 0.007 mmol) in MeOH (10 mL). Imidazole-1-sulfonyl azide hydrochloride (0.182 g, 0.868 mmol) was added and the mixture stirred overnight at r.t. The solvent was removed under reduced pressure, then the solid was dissolved in H<sub>2</sub>O (5 mL), acidified with aq HCl (10 mL, 1 M), and extracted with CH<sub>2</sub>Cl<sub>2</sub> (5 × 10 mL). The combined organic layers were dried (MgSO<sub>4</sub>), filtered, and concentrated. The crude product was purified by column chromatography on silica gel (starting from 5% of EtOAc in PE) to provide the azide **13**, after removal of solvent under reduced pressure, as an off-white solid; yield: 0.297 g (0.504 mmol, 70%); mp >205 °C (dec.); [α]<sub>D</sub><sup>20</sup> –87.0 (c 0.98, MeOH).

IR (KBr): 3346 (m), 2103 (m), 1659 (m), 1556 (m), 1490 (m), 1447 (m), 1386 (m), 1339 (m), 1279 (s), 1181 (s), 1135 (s), 920 (w), 885 (w), 682 cm<sup>-1</sup> (w).

<sup>1</sup>H NMR (400 MHz, DMSO-*d*<sub>6</sub>): δ = 10.05 (s, 1 H), 8.52 (s, 1 H), 8.41 (s, 1 H), 8.06 (s, 2 H), 7.66 (s, 1 H), 7.49 (d, *J* = 7.1 Hz, 1 H), 7.46–7.32 (m, 5 H), 5.34 (s, 1 H), 5.31 (dd, *J* = 7.1, 3.8 Hz, 1 H), 3.69 (dd, *J* = 17.0, 7.0 Hz, 1 H), 3.11 (dd, *J* = 16.9, 3.7 Hz, 1 H).

<sup>13</sup>C NMR (101 MHz, DMSO-*d*<sub>6</sub>): δ = 152.1, 148.3, 141.2, 140.0, 137.1, 130.8 (q, *J* = 32.8 Hz), 129.6, 129.0, 127.5, 125.4, 124.8, 124.3 (q, *J* = 271.2 Hz), 123.2 (q, *J* = 272.8 Hz), 121.8 (q, *J* = 31.9 Hz), 119.8–119.7 (m), 117.9–117.7 (m), 115.4–115.2 (m), 114.8–114.7 (m), 113.0, 83.9, 69.2, 36.6.

HRMS (ESI): *m/z* [M – N<sub>2</sub> + H]<sup>+</sup> calcd for C<sub>25</sub>H<sub>17</sub>F<sub>9</sub>N<sub>3</sub>O<sub>2</sub>: 562.1172; found: 562.1185.

### 1-[3,5-Bis(trifluoromethyl)phenyl]-3-([2-((1*R*,2*R*)-1-[4-[3,5-bis(trifluoromethyl)phenyl]-5-iodo-1*H*-1,2,3-triazol-1-yl]-2,3-dihydro-1*H*-inden-2-yl)oxy]-5-(trifluoromethyl)phenyl)urea (**14**)

Triazole **14** was synthesized by the general procedure for the click reaction; eluent for chromatography: starting from 15% EtOAc in PE; off-white solid; yield: 0.171 g (0.179 mmol, 90%); mp 197–199 °C;  $[\alpha]_D^{20}$  –69.0 (c 0.43, CHCl<sub>3</sub>).

IR (KBr): 3369 (w), 1671 (w), 1617 (w), 1547 (m), 1477 (w), 1445 (w), 1386 (m), 1338 (m), 1280 (s), 1133 (s), 899 (w), 702 (w), 683 cm<sup>-1</sup> (w).

<sup>1</sup>H NMR (400 MHz, DMSO-*d*<sub>6</sub>): δ = 9.98 (s, 1 H), 8.65–8.59 (m, 1 H), 8.54–8.50 (m, 1 H), 8.45 (s, 2 H), 8.25–8.15 (m, 1 H), 8.08 (s, 2 H), 7.71–7.62 (m, 1 H), 7.52–7.48 (m, 1 H), 7.45 (dd, *J* = 7.5 Hz, 1 H), 7.37–7.27 (m, 1 H), 7.26–7.17 (m, 1 H), 7.17–7.08 (m, 2 H), 6.55 (d, *J* = 5.0 Hz, 1 H), 6.09–5.98 (m, 1 H), 3.95 (dd, *J* = 16.1, 7.3 Hz, 1 H), 3.43 (dd, *J* = 16.4, 5.3 Hz, 1 H).

<sup>13</sup>C NMR (101 MHz, DMSO-*d*<sub>6</sub>): δ = 151.5, 147.5, 145.5, 140.7, 139.3, 136.7, 132.3, 130.3 (q, *J* = 32.8 Hz), 130.2 (q, *J* = 33.0 Hz), 129.3, 129.1, 127.3, 126.8–126.5 (m), 124.9, 123.7, 122.7 (q, *J* = 272.7 Hz), 122.6 (q, *J* = 273.3 Hz), 121.7, 121.5–121.4 (m), 121.8 (q, *J* = 31.9 Hz), 120.2 (q, *J* = 270.0 Hz), 118.9, 117.5–117.2 (m), 115.0–114.6 (m), 114.3–114.1 (m), 113.8–113.7 (m), 84.0, 70.0, 36.3. The iodine bonded C-atom was not detected because of low intensity of the signal.

HRMS (ESI): *m/z* [M + H]<sup>+</sup> calcd for C<sub>35</sub>H<sub>20</sub>F<sub>15</sub>IN<sub>5</sub>O<sub>2</sub>: 954.0417; found: 954.0406.

### 4-[3,5-Bis(trifluoromethyl)phenyl]-1-[(1*R*,2*R*)-2-(2-[3-[3,5-bis(trifluoromethyl)phenyl]ureido)-4-(trifluoromethyl)phenoxy]-2,3-dihydro-1*H*-inden-1-yl]-5-iodo-3-methyl-1*H*-1,2,3-triazol-3-ium Trifluoromethanesulfonate (**14-OTf**)

Colorless solid; yield: 0.068 g (0.061 mmol, 55%); mp 144–146 °C;  $[\alpha]_D^{20}$  –88.1 (c 0.82, MeOH).

IR (KBr): 3372 (w), 1550 (m), 1445 (w), 1387 (m), 1282 (s), 1135 (s), 1030 (m), 704 (w), 682 (w), 639 cm<sup>-1</sup> (w).

<sup>1</sup>H NMR (400 MHz, CD<sub>3</sub>OD): δ = 8.60 (d, *J* = 1.8 Hz, 1 H), 8.41 (s, 1 H), 8.37 (s, 2 H), 8.08 (s, 2 H), 7.61–7.50 (m, 4 H), 7.48–7.36 (m, 2 H), 7.30 (d, *J* = 8.6 Hz, 1 H), 6.90 (d, *J* = 2.7 Hz, 1 H), 5.92 (dt, *J* = 6.3, 2.9 Hz, 1 H), 4.24 (s, 3 H), 4.03 (dd, *J* = 17.3, 6.7 Hz, 1 H), 3.44 (dd, *J* = 17.3, 3.1 Hz, 1 H).

<sup>13</sup>C NMR (101 MHz, CD<sub>3</sub>OD): δ = 154.0, 149.2, 146.4, 143.8, 142.7, 135.9, 134.3 (q, *J* = 34.4 Hz), 133.3 (q, *J* = 33.1 Hz), 132.7–132.5 (m), 132.2, 130.8, 129.3, 127.3, 127.2–126.9 (m), 126.89, 126.9, 125.7 (q, *J* = 273.6 Hz), 124.7 (q, *J* = 271.8 Hz), 124.2 (q, *J* = 272.5 Hz), 121.8 (q, *J* = 318.5 Hz), 121.4–121.1 (m), 119.4–119.0 (m), 118.0–117.8 (m), 116.4–116.1 (m), 114.1, 94.0, 84.7, 76.5, 40.1, 38.7.

HRMS (ESI): *m/z* [M – CF<sub>3</sub>O<sub>3</sub>S]<sup>+</sup> calcd for C<sub>36</sub>H<sub>22</sub>F<sub>15</sub>IN<sub>5</sub>O<sub>2</sub>: 968.0573; found: 968.0575.

## Funding Information

The authors thank the Estonian Ministry of Education and Research (Grant Nos. IUT 19-32, IUT 19-9, and PUT1468), the Centre of Excellence in Molecular Cell Engineering, and the Archimedes Foundation (2014-2020.4.01.15-0013) for financial support.

## Acknowledgment

We thank Raminton Gnanagurunathan, Benjamin Schröder, Maria Volokhova, Rudolf Ristkoc, and Trine Kasemägi for their help in the synthesis of the triazoles, and Dr. Aleksander-Mati Müürisepp for IR and MS spectra.

## Supporting Information

Supporting information for this article is available online at <https://doi.org/10.1055/s-0037-1610864>.

## References

- (1) Mahadevi, A. S.; Sastry, G. N. *Chem. Rev.* **2016**, *116*, 2775.
- (2) For recent reviews, see: (a) Politzer, P.; Murray, J. S. *ChemPhysChem* **2013**, *14*, 278. (b) Beale, T. M.; Chudzinski, M. G.; Sarwar, M. G.; Taylor, M. S. *Chem. Soc. Rev.* **2013**, *42*, 1667. (c) Gilday, L. C.; Robinson, S. W.; Barendt, T. A.; Langton, M. J.; Mullaney, B. R.; Beer, P. D. *Chem. Rev.* **2015**, *115*, 7118. (d) Bulfield, D.; Huber, S. M. *Chem. Eur. J.* **2016**, *22*, 14434. (e) Cavallo, G.; Metrangolo, P.; Milani, R.; Pilati, T.; Priimagi, A.; Resnati, G.; Terraneo, G. *Chem. Rev.* **2016**, *116*, 2478. (f) Mendez, L.; Henriquez, G.; Sirimulla, S.; Narayan, M. *Molecules* **2017**, *22*, 1397. (g) Kolář, M. H.; Tabarrini, O. J. *Med. Chem.* **2017**, *60*, 8681. (h) Tepper, R.; Schubert, U. S. *Angew. Chem. Int. Ed.* **2018**, *57*, 6004.
- (3) Desiraju, G. R.; Ho, P. S.; Kloos, L.; Legon, A. C.; Marquardt, R.; Metrangolo, P.; Politzer, P.; Resnati, G.; Rissanen, K. *Pure Appl. Chem.* **2013**, *85*, 1711.
- (4) Clark, T.; Hennemann, M.; Murray, J. S.; Politzer, P. *J. Mol. Model.* **2007**, *13*, 291.
- (5) (a) Nepal, B.; Scheiner, S. *Chem. Eur. J.* **2015**, *21*, 13330. (b) Nepal, B.; Scheiner, S. *J. Phys. Chem. A* **2015**, *119*, 13064.
- (6) (a) Hassel, O.; Hvosløf, J. *Acta Chem. Scand.* **1954**, *8*, 873. (b) Zingaro, R.; Hedges, R. J. *Chem. Commun.* **1961**, 65, 1132.
- (7) (a) Cabot, R.; Hunter, C. A. *Chem. Commun.* **2009**, 2005. (b) Sarwar, M. G.; Dragisic, B.; Salsberg, L. J.; Gouliaras, C.; Taylor, M. S. *J. Am. Chem. Soc.* **2010**, *132*, 1646. (c) Dumele, O.; Wu, D.; Trapp, N.; Goroff, N.; Diederich, F. *Org. Lett.* **2014**, *16*, 4722.
- (8) (a) Raatikainen, K.; Rissanen, K. *Chem. Sci.* **2012**, *3*, 1235. (b) Puttreddy, R.; Jurček, O.; Bhowmik, S.; Mäkelä, T.; Rissanen, K. *Chem. Commun.* **2016**, 52, 2338.
- (9) (a) Xu, K.; Ho, D. M.; Pascal, R. A. *J. Org. Chem.* **1995**, *60*, 7186. (b) Maugeri, L.; Asencio-Hernandez, J.; Lebl, T.; Cordes, D. B.; Slawin, A.; Delsuc, M.-A.; Philp, D. *Chem. Sci.* **2016**, *7*, 6422. (c) Sabater, P.; Zapata, F.; López, B.; Fernández, I.; Caballero, A.; Molina, P. *Dalton Trans.* **2018**, 47, 15941.
- (10) (a) Cametti, M.; Raatikainen, K.; Metrangolo, P.; Pilati, T.; Terraneo, G.; Resnati, G. *Org. Biomol. Chem.* **2012**, *10*, 1329. (b) Tepper, R.; Schulze, B.; Jäger, M.; Friebe, C.; Scharf, D. H.; Görls, H.; Schubert, U. S. *J. Org. Chem.* **2015**, *80*, 3139. (c) Riel, A. M. S.; Decato, D. A.; Sun, J.; Massena, C. J.; Jessop, M. J.; Berryman, O. B. *Chem. Sci.* **2018**, *9*, 5828.
- (11) (a) Kuijpers, B. H. M.; Dijkmans, G. C. T.; Groothuys, S.; Quaedflieg, P. J. L. M.; Blaauw, R. H.; van Delft, F. L.; Rutjes, F. P. J. T. *Synlett* **2005**, 3059. (b) Hein, J. E.; Tripp, J. C.; Krasnova, L. B.; Sharpless, K. B.; Fokin, V. V. *Angew. Chem. Int. Ed.* **2009**, *48*, 8018. (c) García-Álvarez, J.; Díez, J.; Gimeno, J. *Green Chem.* **2010**, *12*, 2127. (d) Pérez, J. M.; Crosbie, P.; Lal, S.; Díez-González, S. *ChemCatChem* **2016**, *8*, 2222.

- (12) (a) Barsoum, D.; Brassard, C. J.; Deeb, J. H. A.; Okashah, N.; Sreenath, K.; Simmons, J. T.; Zhu, L. *Synthesis* **2013**, *45*, 2372. (b) Li, L.; Hao, G.; Zhu, A.; Liu, S.; Zhang, G. *Tetrahedron Lett.* **2013**, *54*, 6057. (c) Barsoum, D. N.; Okashah, N.; Zhang, X.; Zhu, L. *J. Org. Chem.* **2015**, *80*, 9542. (d) Li, L.; Xing, X.; Zhang, C.; Zhu, A.; Fan, X.; Chen, G.; Zhang, G. *Tetrahedron Lett.* **2018**, *59*, 3563.
- (13) (a) Tepper, R.; Schulze, B.; Bellstedt, P.; Heidler, J.; Görls, H.; Jägerab, M.; Schubert, U. S. *Chem. Commun.* **2017**, *53*, 2260. (b) Zhou, L.; Lu, Y.; Xu, Z.; Peng, C.; Liu, H. *Struct. Chem.* **2018**, *29*, 533.
- (14) (a) Mercurio, J. M.; Knighton, R. C.; Cookson, J.; Beer, P. D. *Chem. Eur. J.* **2014**, *20*, 11740. (b) Borissov, A.; Lim, J. Y. C.; Brown, A.; Christensen, K. E.; Thompson, A. L.; Smith, M. D.; Beer, P. D. *Chem. Commun.* **2017**, *53*, 2483. (c) Mungalpara, D.; Stegmüller, S.; Kubik, S. *Chem. Commun.* **2017**, *53*, 5095.
- (15) (a) Kniep, F.; Rout, L.; Walter, S. M.; Bensch, H. K. V.; Jungbauer, S. H.; Herdtweck, E.; Huber, S. M. *Chem. Commun.* **2012**, *48*, 9299. (b) Jungbauer, S. H.; Huber, S. M. *J. Am. Chem. Soc.* **2015**, *137*, 12110. (c) von der Heiden, D.; Detmar, E.; Kuchta, R.; Breugst, M. *Synlett* **2017**, *28*, 1307. (d) Haraguchi, R.; Hoshino, S.; Sakai, M.; Tanazawa, S.; Morita, Y.; Komatsu, T.; Fukuzawa, S. *Chem. Commun.* **2018**, *54*, 10320. (e) Dreger, A.; Engelage, E.; Mallick, B.; Beer, P. D.; Huber, S. M. *Chem. Commun.* **2018**, *5*, 4013.
- (16) Tepper, R.; Bode, S.; Geitner, R.; Jäger, M.; Görls, H.; Vitz, J.; Dietzek, B.; Schmitt, M.; Popp, J.; Hager, M. D.; Schubert, U. S. *Angew. Chem. Int. Ed.* **2017**, *56*, 4047.
- (17) (a) Kilah, N. L.; Wise, M. D.; Serpell, C. J.; Thompson, A. L.; White, N. G.; Christensen, K. E.; Beer, P. D. *J. Am. Chem. Soc.* **2010**, *132*, 11893. (b) Kilah, N. L.; Wise, M. D.; Beer, P. D. *Cryst. Growth Des.* **2011**, *11*, 4565.
- (18) Kaasik, M.; Kaabel, S.; Kriis, K.; Järving, J.; Aav, R.; Rissanen, K.; Kanger, T. *Chem. Eur. J.* **2017**, *23*, 7337.
- (19) Lim, J. Y. C.; Marques, I.; Félix, V.; Beer, P. D. *J. Am. Chem. Soc.* **2017**, *139*, 12228.
- (20) (a) Lim, J. Y. C.; Marques, I.; Ferreira, L.; Félix, V.; Beer, P. D. *Chem. Commun.* **2016**, *52*, 5527. (b) González, L.; Zapata, F.; Caballero, A.; Molina, P.; de Arellano, V.; Alkorta, I.; Elguero, J. *Chem. Eur. J.* **2016**, *22*, 7533. (c) Lim, J. Y. C.; Marques, I.; Félix, V.; Beer, P. D. *Chem. Commun.* **2018**, *54*, 10851.
- (21) Kaik, M.; Gawroński, J. *Tetrahedron: Asymmetry* **2003**, *14*, 1559.
- (22) Goddard-Borger, E. D.; Stick, R. V. *Org. Lett.* **2007**, *9*, 3797.
- (23) Probst, N.; Madarsz, A.; Valkonen, A.; Papai, I.; Rissanen, K.; Neuvonen, A.; Pihko, P. M. *Angew. Chem. Int. Ed.* **2012**, *51*, 8495.

## Appendix 4

### Publication IV

Kaasik, M.; Metsala, A.; Kaabel, S.; Kriis, K.; Järving, I.; Kanger, T. Halo-1,2,3-triazolium Salts as Halogen Bond Donors for the Activation of Imines in Dihydropyridinone Synthesis. *J. Org. Chem.* **2019**, *84*, 4294–4303.

Reproduced by permission of the American Chemical Society.



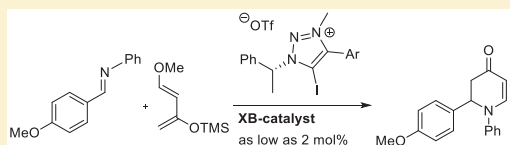
# Halo-1,2,3-triazolium Salts as Halogen Bond Donors for the Activation of Imines in Dihydropyridinone Synthesis

Mikk Kaasik, Andrus Metsala, Sandra Kaabel, Kadri Kriis, Ivar Järving, and Tõnis Kanger\*<sup>✉</sup>

Department of Chemistry and Biotechnology, Tallinn University of Technology, Tallinn 12618, Estonia

## Supporting Information

**ABSTRACT:** In the past decade halogen bond (XB) catalysis has gained considerable attention. Halo-triazoles are known XB donors, yet few examples detail their use as catalysts. As a continuation of our previous work the catalytic properties of substituted enantiomerically pure halo-triazolium salts were explored in the reaction between an imine and Danishefsky's diene leading to the formation of dihydropyridinone. The catalytic activity of the XB donors was highly dependent on the choice of the halogen atom and on the counterion. Also, it was found that impurities in the diene affected the rate of the reaction.

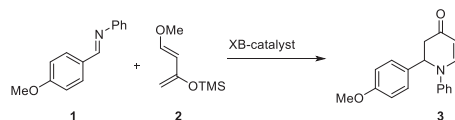


## INTRODUCTION

Halogen bonding is the process in which a Lewis acidic halogen atom interacts with a Lewis base.<sup>1</sup> It has been applied mainly in supramolecular chemistry and its use in solution is also growing.<sup>2–4</sup> Halogen bonds (XBs) are similar to hydrogen bonds (HBs), which have been extensively used in catalysis.<sup>5</sup> Alternatively, some properties of XBs can be considered more advantageous than HBs in catalysis, namely the high directionality of XBs and the use of soft donor atoms.<sup>6,7</sup> In 2008, Bolm et al. showed the potential of XBs in organocatalysis.<sup>8</sup> Since then there have been several reports describing the use of XBs to catalyze Diels–Alder,<sup>9</sup> Michael addition,<sup>10</sup> halogen abstraction<sup>11</sup> and other miscellaneous reactions.<sup>12</sup> In addition, computational studies have explored the catalytic potential of XB donors.<sup>13</sup> Nevertheless, the field is only starting to expand and even more importantly no examples of asymmetric catalysis based solely on XB activation have been reported. There are some examples of enantioselective reactions in which simultaneous different interactions, including XBs, are involved to achieve asymmetric induction.<sup>14</sup> Surprisingly, there are a limited number of examples utilizing halo-1,2,3-triazoles and their salts as catalysts, although these compounds are known XB donors,<sup>9a,11b,e,15</sup> even more so, considering the ease of triazole synthesis via a copper-catalyzed click reaction between alkyne and azide.<sup>16</sup> Easy access to a wide variety of chiral azides and the opportunities to modify the triazole ring make these compounds very attractive potential catalysts. The catalytic activity of the triazoles can be increased via quaternization, making the core of the triazole more electronegative and increasing the magnitude of the  $\sigma$  hole on the halogen atom.<sup>15c,17</sup> We have previously shown that chiral halogen substituted triazolium salts form complexes with imines and thioureas, and are additionally capable of enantiodiscrimination in solution.<sup>18</sup> To evaluate the catalytic potential of the triazolium salts, we used them in an aza-Diels–

Alder<sup>19</sup> reaction between imine **1** and Danishefsky's diene **2** (Scheme 1).

## Scheme 1. Model Reaction under Study



In this work, we demonstrate the high catalytic activity of the triazolium salts and describe how the catalytic activity is affected by the structure of the XB donor. In addition, an alternative mechanistic pathway for product formation is proposed and the importance of diene quality is described.

## RESULTS AND DISCUSSION

First, the set of synthesized XB donors was expanded compared to the one described in our previous publication<sup>18</sup> using the same general synthetic scheme (Figure 1).<sup>20</sup>

The reaction of azide **4** derived from (*R*)- $\alpha$ -methyl benzyl amine and differently substituted aromatic 1-iodoalkynes **5** in the presence of copper(I)iodide and tris(1-*tert*-butyl-1*H*-1,2,3-triazolyl)methylamine (TTTA) afforded 5-iodo-1,2,3-triazole derivatives **6**, which were converted into triazolium salts **7** or tetrafluoroborate salts **8**. In addition, tetrakis-3,5-bis-(trifluoromethyl)phenylborate (BARF) salt **9a** was also synthesized. Bromotriazole **10** was obtained starting from the corresponding bromoalkyne,<sup>21</sup> chloro derivative **11** via halogen exchange from **6a**<sup>22</sup> and hydrogen analogue **12** from the terminal alkyne (see Experimental Section for details). The

Received: January 25, 2019

Published: March 11, 2019



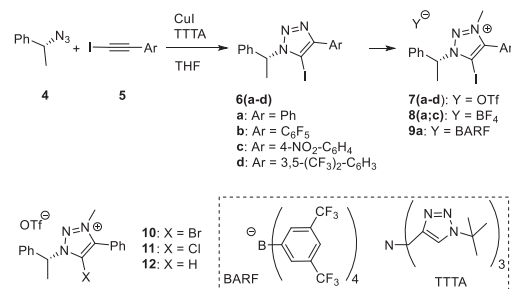


Figure 1. Triazolium salts used in the study.

substitution pattern of the phenyl ring involves various electronegative groups (**6b–d**).

The electrostatic potential surfaces (ESP) of the triazoles and corresponding cationic structures (Table 1) were modeled to find structural factors that most influenced the  $\sigma$  hole. The DFT calculations were carried out with the Gaussian09 program<sup>23</sup> using the CAM-B3LYP<sup>24</sup> and M062X<sup>25</sup> functional with the DEF2TZVP<sup>26</sup> basis set. ESP values were calculated with the help of the Multiwfn program<sup>27</sup> and visualization was made with the MOLEKEL<sup>28</sup> program. Charge has the most influence on the magnitude of the  $\sigma$  hole and similarly to previous results a positive charge of the triazole core increased the size of the  $\sigma$  hole on the halogen atom (Table 1, comparing entries 1–6 to entries 7–12).<sup>15c,17</sup> Next, the polarizability of the halogen atom had a smaller influence on the size of the  $\sigma$  hole (Table 1, comparing entries 4–6 or entries 10–12). The aromatic substituent of the triazole ring had a more subtle influence on the  $\sigma$  hole and can thus be used for the fine-tuning of the properties of the catalyst (Table 1, entries 1–4).

Calculations show, in addition to the previously obtained affinity constant of  $K_a(\text{CDCl}_3) = 8$ ,<sup>18</sup> that halogen bonding between imine **1** and iodo-triazolium salt **7d** is plausible. Interestingly, in the minimum energy structure of **7d** the triflate counterion is not halogen bonded to the iodine atom

(Figure 2A). On the basis of solid state data we assumed that a XB to the counterion would be favored.<sup>18</sup> This conformer is

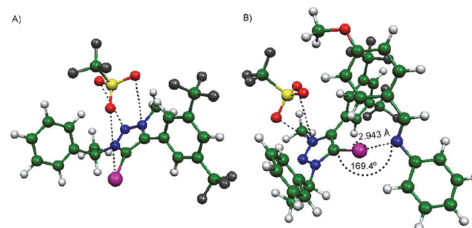


Figure 2. A) The most stable conformer of the XB donor **7d**; and B) the most stable conformer of **7d** + **1** adduct.

stable, but higher in energy (For further details, see Supporting Information, SI, Figure S2 and Table S1). When imine **1** is added to the **7d** system a stable adduct is formed containing an almost linear XB with an angle of 169.4° and a bond length of 2.943 Å (Figure 2B). These data reveal that the activation of imine **1** by triazolium salt **7d** using a XB is plausible.

On the basis of previous results by Minakata et al., the azadiels–Alder reaction between imine **1** and Danishefsky's diene **2** was chosen as a model reaction (Scheme 1).<sup>9b</sup> Since neutral triazoles **6** showed no catalytic activity in this reaction, they were omitted from the later part of the study. Proceeding to catalytic experiments, we also had to take into account the solubility of the donors in dichloromethane. Compounds **7d** and **8a** were not used as catalysts because of their poor solubility. On the basis of the previous, triflate **7a** was chosen as the reference catalyst in the study. A pentafluorophenyl group and a 4-nitrophenyl group have an influence on the  $\sigma$  hole comparable to that of a 3,5-bis(trifluoromethyl)phenyl group (Table 1, entries 1–3). Fortunately, the corresponding salts **7b** and **7c** were soluble in dichloromethane and could thus be used to probe the influence of the aromatic substituent on the reaction. Also, salts **8c**, **9a**, **10**, **11**, and **12** were included in the

Table 1. Most Positive Electrostatic Potential Value  $V_{S,\text{max}}$  (a.u.) (Mapped on Electron Density Isosurface of 0.001 a.u.) on the Halogen Atom X in the XB Donor Structure<sup>a</sup>

Entry	Ar	X	$V_{S,\text{max}}$	Entry	Ar	X	$V_{S,\text{max}}$
1	4-NO <sub>2</sub> C <sub>6</sub> H <sub>4</sub>	I	0.1644	7	4-NO <sub>2</sub> C <sub>6</sub> H <sub>4</sub>	I	0.0597
2	3,5-(CF <sub>3</sub> ) <sub>2</sub> C <sub>6</sub> H <sub>3</sub>	I	0.1642	8	3,5-(CF <sub>3</sub> ) <sub>2</sub> C <sub>6</sub> H <sub>3</sub>	I	0.0589
3	C <sub>6</sub> F <sub>5</sub>	I	0.1646	9	C <sub>6</sub> F <sub>5</sub>	I	0.0570
4	Ph	I	0.1565	10	Ph	I	0.0479
5	Ph	Br	0.1443	11	Ph	Br	0.0370
6	Ph	Cl	0.1350	12	Ph	Cl	0.0287

<sup>a</sup>The ESP values were modeled only for the cationic part of the XB donors **7a–d**, **10**, and **11** to avoid the anion having an influence on the  $V_{S,\text{max}}$  value on X and to evaluate the effect of the halogen atom, aromatic substituent and positive charge on the  $V_{S,\text{max}}$  value.



study to evaluate the influence of the counterion and halogen atom.

The reaction in the presence of triazolium salt **7a** gave promising results showing high conversion of imine **1** in a reasonable time. Although the triazolium salts were enantiomerically pure we observed no stereoselectivity in any of the following reactions. To get a better understanding of the reaction, we decided to run it in  $\text{CD}_2\text{Cl}_2$  with 20 mol % of the catalyst and follow it by  $^1\text{H}$  NMR, using *p*-xylene as an internal standard to determine the conversion. This change helped to reveal an unexpected lag period that preceded a rapid period of conversion of imine **1** to product **3** (Figure 3, purple line).

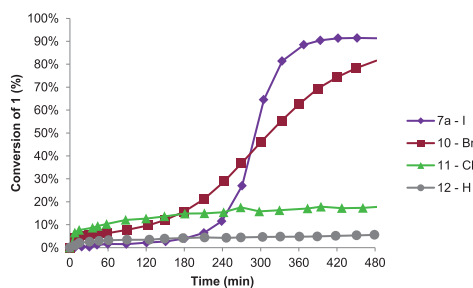


**Figure 3.** Dependence of the conversion of the model reaction on the halogen/hydrogen atom on the triazole ring of the catalyst.

Control experiments supported the idea that the reaction proceeded by XB activation. The hydrogen analogue **12** was markedly less active than **7a** (Figure 3, comparing purple and gray lines). After a few days only a moderate level of conversion was achieved. Also, no reaction took place if TBA-Cl was added to the reaction mixture with catalyst **7a**.<sup>29</sup> Bases have been successfully used to exclude the possibility of Brønsted acid catalysis.<sup>9b,11f</sup> Unfortunately, the product was not formed if  $\text{K}_2\text{CO}_3$ ,  $\text{Et}_3\text{N}$ , or Hünig's base was added to the reaction mixture. However, in all instances we observed the decomposition of **7a** into **12**. This indicates toward an unwanted interaction between the base and the XB catalyst. Therefore, the reactions in the presence of an added base were inconclusive and the possibility of hidden Brønsted acid catalysis could not be ruled out. Bromotriazole derivative **10** (Figure 3, magenta line) exhibited a similar reaction profile to **7a** with a gentler slope. The conversion of imine remained below 20% in the presence of chloro derivative **11** (Figure 3, green line) during the first 8 h. This is in agreement with our computations and previous results that have reported on the dependence of the XB donor ability on halogen atom polarizability.<sup>11c,30</sup> Elemental halogens might form in solution and act as the true catalysts. To rule this out, the reaction with bromotriazolium salt **10** was run in the presence of cyclohexene, which should quench free  $\text{Br}_2$  and  $\text{HBr}$ .<sup>10b,11d</sup> Fortunately, we observed no change in reaction profile compared to the reaction with only **10** (For further details see SI Figure S4). In our opinion these results show that the catalytic activity comes from the halogen, and the rest of the structure is relatively inactive.

The rate of the reaction was highly dependent on the quality and on the batch of the diene **2** used. The delay present in the reaction with **7a** was different in the case of various batches of diene (Figure 4, comparing the purple line to the others).

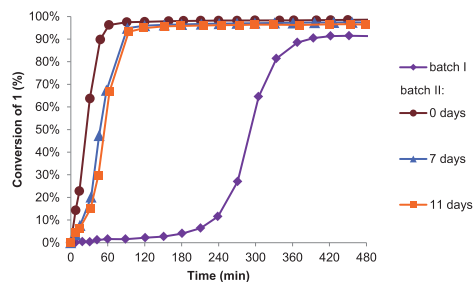


**Figure 4.** Influence of different batches of Danishefsky's diene **2** and time after opening on the model reaction with catalyst **7a**.

Also, the reaction was slower when the diene was used sometime after its first use (Figure 4, comparing the brown, orange, and blue lines). Therefore, all comparable studies were carried out with the same batch of diene in a minimal time frame. Although these findings significantly complicate the interpretation of data, we feel confident that general observations can still be made. The lag period, although shorter, was still present when different batches of diene were used with the catalyst **7a**. It was assumed that self-aggregation of the catalyst may also reduce its effective concentration in solution. We have observed the dependence of the chemical shift values of the catalyst on its concentration (For further details, see SI Figure S5). Therefore, the delay may have been caused by the kinetics of deaggregation to achieve sufficient concentration of the catalyst to activate imine **1**. Initially we assumed that product formation could increase the speed of deaggregation. To determine the influence of other reaction components on the catalyst, we incubated imine **1**, diene **2**, and product **3** in separate experiments with the catalyst for 30 min before adding the second reactant (For further details, see SI Figure S6).<sup>31</sup> Only in the case of incubation with the diene **2** was the reaction slower than the reference reaction and hence compounds **1** and **3** do not accelerate the reaction through facilitating deaggregation and exclude the possibility of autocatalysis.<sup>32</sup> Alternatively, diene **2** or its decomposition products might inhibit the catalyst. It is known that trimethylsilyl trifluoromethanesulfonate (TMSOTf) can catalyze Mannich<sup>33</sup> reaction and Diels–Alder reaction.<sup>34</sup> However, we did not detect the formation of TMSOTf by HRMS during the course of the reaction. Also, if TMSOTf is the actual catalyst, then we should not observe any dependency of the reaction on the choice of halogen atom.

Next, the influence of the counterion on the catalytic activity was investigated (Figure 5). Surprisingly, compound **8c** containing the tetrafluoroborate counterion was completely inactive (Figure 5, red line). The BARF counterion containing compound **9a** (Figure 5, green line) exhibited no delay at the start of the reaction. However, the reaction did not go to completion within 8 h. Both of these counterions are considered to be less coordinating than the triflate counterion and therefore compounds **8c** and **9a** should give a stronger XB with the imine.<sup>35</sup> Hence, these compounds should be more active than the triflate salt **7a**. Unusual and unpredictable influence of the counterion on the catalytic activity of the XB donors has also been described in earlier papers.<sup>11c,36,37</sup> The inactivity of **8c** can partly be explained by its lower stability in the reaction mixture compared to the others salts (For further

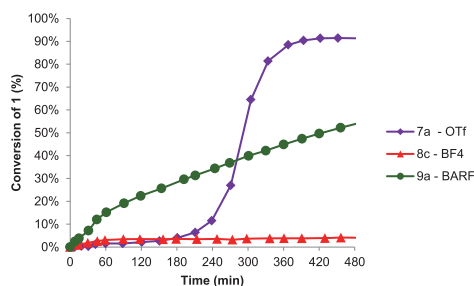


**Figure 5.** Dependence of the conversion of the model reaction on the counterion of the catalyst.

details, see SI Figure S8). However, the absence of product formation again implies that the decomposition products were not catalytically active.

The influence of the aromatic substitution pattern of triflate salts 7a–c on the reaction was investigated (Figure 6).

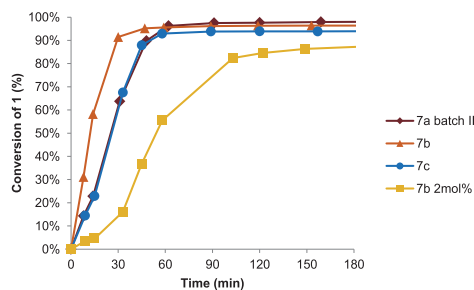


**Figure 6.** Influence of the aromatic substituent of the catalyst on the conversion of the model reaction.

Pentafluorophenyl derivative **7b** was a very efficient catalyst. The reaction was complete in almost 30 min (Figure 6, orange line). The lag period could not be observed but also not excluded on such a short time-scale with the better XB donor **7b** compared to donor **7a**. When we lowered the catalyst loading of **7b** from 20 to 2 mol % (Figure 6, yellow line), the lag period was again detected, and the reaction profile was similar to that of the reaction with catalyst **7a**. The reaction was almost complete within 2 h, indicating high efficiency of the catalyst. *p*-Nitrophenyl derivative **7c** was as active as catalyst **7a**.<sup>38</sup>

Finally, a more thorough study of NMR spectra revealed the formation of some new peaks that were converted into peaks corresponding to the product **3** during the course of the reaction (Figure 7). On the basis of HRMS and NMR analysis, this compound could correspond to the Mannich intermediate **14** (Scheme 2A).<sup>39</sup> It is assumed that the iodotriazolium salt **7** activates imine **1** toward a nucleophilic attack of silyl enol ether. Preliminary results by Minakata et al. also showed the feasibility of using a XB donor to catalyze the Mannich reaction.<sup>9b</sup> The intermediate **16** is formed by cyclization via an aza-Michael reaction followed by demethoxylation. The target compound **3** is obtained after desilylation. The initially expected 4 + 2 cycloaddition pathway could also be at work in parallel (Scheme 2B).<sup>40</sup>

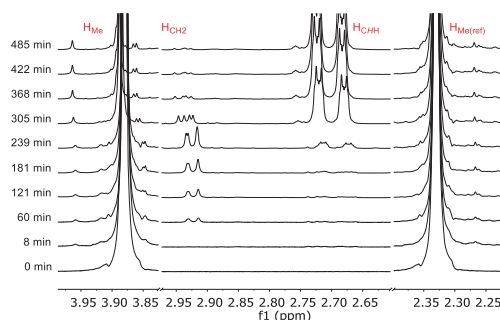
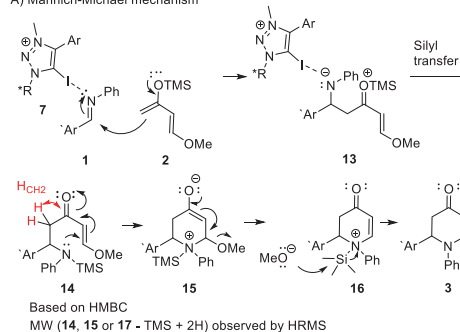


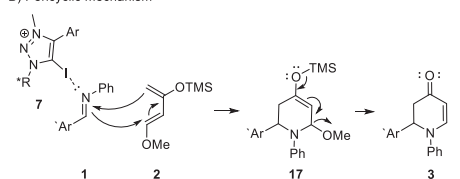
**Figure 7.** Outtake of  $^1\text{H}$  NMR spectra ( $\text{CD}_2\text{Cl}_2$ , 297 K, 400 MHz) from the reaction catalyzed by **7a** showing the methyl protons  $\text{H}_{\text{Me}}$  of **1**, the methylene protons  $\text{H}_{\text{CH}_2}$  of **14**, one of the methylene protons  $\text{H}_{\text{CHH}}$  of **3**, and the methyl protons  $\text{H}_{\text{Me(ref)}}$  of *p*-xylene.

## Scheme 2. A) Mannich/Michael Path to Product **3**; and B) 4 + 2 Cycloaddition Path to Product **3**

### A) Mannich-Michael mechanism



### B) Pericyclic mechanism



## CONCLUSIONS

Halo-1,2,3-triazole-based XB donors were successfully used as catalysts to obtain dihydropyridinone **3**, although no enantioenriched products were formed. By modifying the structure of triazolium salts, we were able to tune the catalytic properties of the XB donors to varying degrees. By introducing a pentafluorophenyl substituent, the catalyst loading could be lowered from 20 to 2 mol % without significant loss in activity. Both the choice of halogen atom and the counterion had a significant impact on the catalytic activity of the XB donors. Yet again, the counterion affected catalytic activity in an inexplicable way and therefore counterion effects in XB catalysis should receive closer examination. From a catalyst design perspective, we are now interested in using different azides in the click reaction to move toward stereoselective XB catalysis. As the product might form through a tandem

Mannich–Michael pathway, the catalytic potential of these compounds in the Mannich reaction could be of interest.

## EXPERIMENTAL SECTION

All commercially available reagents were used without further purification. MeOH was dried by distillation over sodium metal. All air or moisture sensitive reactions were carried out under argon atmosphere using oven-dried glassware. The reactions were monitored by thin layer chromatography (TLC) with silica gel-coated aluminum plates (Merck 60 F254) and visualized with KMnO<sub>4</sub>, anisaldehyde, vaniline, or ninhydrine stain. Yields refer to chromatographically purified or crystallized products. <sup>1</sup>H NMR spectra were recorded on a Bruker Avance III instrument at 400 MHz and are reported in parts per million (δ) referenced to the residual solvent signal (CDCl<sub>3</sub> δ = 7.26, CD<sub>3</sub>OD δ = 3.31 ppm, [D<sub>6</sub>]DMSO δ = 2.50 ppm). Data for <sup>1</sup>H NMR spectra are as follows: chemical shift δ (ppm), multiplicity (s = singlet, bs = broad singlet, d = doublet, t = triplet, q = quartet, dd = doublet of doublets, m = multiplet), coupling constant J Hz, and relative integration. <sup>13</sup>C{<sup>1</sup>H} NMR spectra were recorded at 101 MHz and are reported in parts per million (δ) referenced to the residual solvent signal (CDCl<sub>3</sub> δ = 77.16, CD<sub>3</sub>OD δ = 49.00 ppm, [D<sub>6</sub>]DMSO δ = 39.52 ppm). HRMS spectra were recorded with an Agilent Technologies 6540 UHD Accurate-Mass Q-TOF LC/MS spectrometer by using AJ-ESI ionization. Optical rotations were obtained with an Anton Paar GWB Polarimeter MCP500. IR spectra were recorded on a Bruker Tensor 27 FT-IR spectrophotometer. IR absorption frequencies in wavenumbers are listed, with the relative strength in parentheses (w = weak, m = medium, s = strong). (Iodoethyl)benzene,<sup>20</sup> 4,<sup>41</sup> 6a,<sup>18</sup> 6d,<sup>18</sup> 7a,<sup>18</sup> and 7d<sup>18</sup> are known and were prepared following the literature procedure. A CEM Discover microwave reactor was used for the microwave assisted synthesis of (R)-5-chloro-4-phenyl-1-(1-phenylethyl)-1H-1,2,3-triazole. The reaction vessel was sealed with a Teflon cap and the reaction temperature was monitored by a noncontact infrared sensor.

**(R)-5-Iodo-4-(perfluorophenyl)-1-(1-phenylethyl)-1H-1,2,3-triazole (6b).** 1-Ethynyl-2,3,4,5,6-pentafluorobenzene: Bromopentafluorobenzene (3.0 mL, 24.1 mmol), PdCl<sub>2</sub>(PPh<sub>3</sub>)<sub>2</sub> (0.342 g, 0.49 mmol), and CuI (0.187 g, 0.46 mmol) were dissolved in THF (60 mL). Hünig's base (16.0 mL, 89.9 mmol) was added, followed by ethynyltrimethylsilane (6.8 mL, 49.1 mmol), and the mixture was stirred for 24 h at 72 °C. The suspension was poured onto a pad of diatomaceous earth, washed with THF, and the filtrate was concentrated under vacuum. Purification by flash column chromatography on silica gel (100% petroleum ether) afforded the Sonogashira coupling product and the Glaser coupling product as a mixture. The mixture was concentrated under vacuum and dissolved in MeOH (100 mL) and KOH (50%, 0.078 mL) was added. The reaction was stirred for 1 h, then quenched with H<sub>2</sub>O (30 mL), and acidified with HCl (7 mL, 1M). The combined organic phase was dried over MgSO<sub>4</sub> and purification by distillation (130 °C, 1 atm) gave 1-ethynyl-2,3,4,5,6-pentafluorobenzene as an orange oil (0.74 g, 16% yield, solvent impurities were not completely removed). <sup>1</sup>H NMR (400 MHz, CDCl<sub>3</sub>) δ 3.62–3.61 (m, 1H), 1,2,3,4,5-pentafluoro-6-(iodoethyl)benzene: 1-ethynyl-2,3,4,5,6-pentafluorobenzene (0.30 g, 1.56 mmol), dissolved in THF (4 mL), was treated with CuI (0.029 g, 0.15 mmol) and 4-iodomorpholine hydroiodide (0.59 g, 2.0 mmol), and the reaction mixture was stirred for 3.5 h at rt. The suspension was poured onto a pad of neutral alumina, the solid phase was washed with THF and CH<sub>2</sub>Cl<sub>2</sub>, and the filtrate was concentrated under vacuum. The combined organic fractions were pooled and washed with a solution of Na<sub>2</sub>S<sub>2</sub>O<sub>3</sub> (100 mL, 5% w/w) and a solution of saturated NaCl (50 mL). The organic phase was dried over Na<sub>2</sub>SO<sub>4</sub>, concentrated, and purified by column chromatography on silica gel (100% petroleum ether) to provide 1,2,3,4,5-pentafluoro-6-(iodoethyl)benzene as an orange oil (0.35 g, 70% yield). <sup>13</sup>C{<sup>1</sup>H} NMR (101 MHz, CDCl<sub>3</sub>) δ 150.1–147.0 (m), 139.2–136.1 (m), 143.5–140.4 (m), 100.5–99.9 (m), 77.7 (q, J = 3.6 Hz), and 21.7 (q, J = 3.9 Hz). **6b:** CuI (0.006 g, 0.032 mmol) and TTTA (0.015 g,

0.035 mmol) were dissolved in freshly distilled THF (3.5 mL) under argon atmosphere and stirred at rt for 30 min. Then (R)-(1-azidoethyl)benzene (0.097 mL, 0.680 mmol) and 1,2,3,4,5-pentafluoro-6-(iodoethyl)benzene (0.215 g, 0.676 mmol) were added, and the reaction mixture was stirred at rt for 23 h. The reaction mixture was concentrated, NH<sub>4</sub>OH (20 mL, 10% w/w) was added, and the aqueous phase was extracted with CH<sub>2</sub>Cl<sub>2</sub> (2 × 25 mL). The combined organic phase was passed through a phase separator, concentrated, and purified by column chromatography on silica gel (from 10% of EtOAc in petroleum ether) to provide triazole **6b** as colorless crystals (0.271 g, 86% yield). mp 157–160 °C; α<sub>D</sub><sup>20</sup> 32.0 (c 0.21, CHCl<sub>3</sub>); <sup>1</sup>H NMR (400 MHz, CDCl<sub>3</sub>) δ 7.43–7.28 (m, 5H), 5.79 (q, J = 7.1 Hz, 1H), 2.14 (d, J = 7.1 Hz, 3H). <sup>13</sup>C{<sup>1</sup>H} NMR (101 MHz, CDCl<sub>3</sub>) δ 139.7, 129.2, 128.6, 126.7, 82.7, 62.3, 22.4. IR (KBr) ν = 1659 (w), 1554 (m), 1495 (s), 1413 (w), 1393 (w), 1238 (m), 1165 (m), 1126 (m), 1046 (m), 987 (s), 917 (w), 841 (s), 765 (m), 698 (s) cm<sup>-1</sup>. HRMS (ESI/Q-TOF) m/z: [M + H]<sup>+</sup> Calcd for C<sub>16</sub>H<sub>9</sub>F<sub>5</sub>IN<sub>3</sub>; 465.9834; found: 465.9831.

**(R)-5-Iodo-4-(4-nitrophenyl)-1-(1-phenylethyl)-1H-1,2,3-triazole (6c).** 1-(Iodoethyl)-4-nitrobenzene: Iodoform (4.10 g, 10.42 mmol), triphenylphosphine (2.87 g, 10.94 mmol), and tBuOK (1.11 g, 9.93 mmol) were added to THF (20 mL) under argon atmosphere. The suspension was stirred at rt for 5 min and turned brown. 4-nitrobenzaldehyde (0.75 g, 4.96 mmol) was added. After 30 min, the brown suspension was cooled to -78 °C and tBuOK (2.80 g, 24.95 mmol) was added. After an additional 30 min, the reaction was quenched with brine (90 mL) at -78 °C. After warming to rt, the two layers were separated and the aqueous phase was extracted with diethyl ether (3 × 90 mL). The combined organic phase was passed through a phase separator, concentrated, and purified by column chromatography on silica gel (starting from 0% of EtOAc in petroleum ether) to provide the product as a yellow solid (1.17 g, 86% yield). <sup>1</sup>H NMR (400 MHz, CDCl<sub>3</sub>) δ 8.24–8.15 (m, 2H), 7.62–7.54 (m, 2H). <sup>13</sup>C{<sup>1</sup>H} NMR (101 MHz, CDCl<sub>3</sub>) δ 147.5, 133.3, 130.1, 123.7, 92.5, 14.3. **6c:** CuI (0.006 g, 0.032 mmol) and TTTA (0.015 g, 0.035 mmol) were dissolved in freshly distilled THF (3.5 mL) under argon atmosphere and stirred at rt for 30 min. Then 1-(iodoethyl)-4-nitrobenzene (0.186 g, 0.681 mmol) and (R)-(1-azidoethyl)benzene (0.097 mL, 0.680 mmol) were added, and the reaction mixture was stirred at rt for 5 h. The reaction mixture was concentrated, NH<sub>4</sub>OH (20 mL, 10% w/w) was added, and the aqueous phase was extracted with CH<sub>2</sub>Cl<sub>2</sub> (2 × 25 mL). The combined organic phase was dried over Na<sub>2</sub>SO<sub>4</sub>, filtered, concentrated, and purified by column chromatography on silica gel (from 10% of EtOAc in petroleum ether) to provide triazole **6c** as yellow crystals (0.253 g, 88% yield). mp 153 °C dec in the presence of visible light; α<sub>D</sub><sup>20</sup> 25.9 (c 0.16, CHCl<sub>3</sub>); <sup>1</sup>H NMR (400 MHz, CDCl<sub>3</sub>) δ 8.34–8.28 (m, 2H), 8.23–8.14 (m, 2H), 7.41–7.29 (m, 5H), 5.82 (q, J = 7.1 Hz, 1H), 2.14 (d, J = 7.1 Hz, 3H). <sup>13</sup>C{<sup>1</sup>H} NMR (101 MHz, CDCl<sub>3</sub>) δ 147.7, 147.6, 139.8, 136.8, 129.1, 128.6, 128.1, 126.7, 124.0, 78.3, 62.0, 22.5. IR (KBr) ν = 2992 (w), 2937 (w), 1602 (s), 1521 (s), 1458 (m), 1382 (m), 1346 (s), 1288 (m), 1245 (w), 1110 (m), 989 (m), 977 (m), 855 (s), 712 (s), 604 (w), 540 (w) cm<sup>-1</sup>. HRMS (ESI/Q-TOF) m/z: [M + H]<sup>+</sup> Calcd for C<sub>16</sub>H<sub>13</sub>IN<sub>3</sub>O<sub>2</sub>; 421.0156; found: 421.0151.

**(R)-5-Bromo-4-phenyl-1-(1-phenylethyl)-1H-1,2,3-triazole.** (Bromoethyl)benzene: To ethynylbenzene (0.75 mL, 6.85 mmol), dissolved in acetone (70 mL), were added NBS (1.35 g, 7.59 mmol) and AgNO<sub>3</sub> (0.119 g, 0.70 mmol). The resulting mixture was stirred at rt for 3.5 h. The suspension was filtered, and the filtrate was concentrated under reduced pressure. Then, the resulting crude mixture was added to water (50 mL) and extracted with Et<sub>2</sub>O (3 × 50 mL). The combined organic phase was dried over K<sub>2</sub>CO<sub>3</sub>, concentrated, and purified by column chromatography on silica gel (100% petroleum ether) to provide (bromoethyl)benzene as a yellow oil (1.13 g, 91% yield). <sup>1</sup>H NMR (400 MHz, CDCl<sub>3</sub>) δ 7.54–7.42 (m, 2H), 7.42–7.28 (m, 3H). <sup>13</sup>C{<sup>1</sup>H} NMR (101 MHz, CDCl<sub>3</sub>) δ 132.1, 128.8, 128.5, 122.8, 80.2, 49.9. The triazole: Cu(OAc)<sub>2</sub> (0.024 g, 0.132 mmol), CuBr (0.019 g, 0.132 mmol), and TTTA (0.058 g, 0.135 mmol) were dissolved in freshly distilled THF



(6.0 mL) under argon atmosphere and stirred at rt for 30 min. (bromoethyl)benzene (0.239 g, 1.32 mmol) and (R)-(1-azidoethyl)benzene (0.194 g, 1.32 mmol) were added, and the reaction mixture was stirred at 60 °C for 2 weeks. The reaction mixture was concentrated, NH<sub>4</sub>OH (28 mL, 18% w/w) was added, and the aqueous phase was extracted with CH<sub>2</sub>Cl<sub>2</sub> (3 × 30 mL). The combined organic phase was dried over anhydrous Na<sub>2</sub>SO<sub>4</sub>, concentrated, and purified by column chromatography on silica gel (from 10% of EtOAc in petroleum ether) to provide the Br-triazole as colorless crystals (0.176 g, 41% yield).  $\alpha_D^{20}$  27.0 (c 0.18, CHCl<sub>3</sub>); <sup>1</sup>H NMR (400 MHz, CDCl<sub>3</sub>)  $\delta$  8.00–7.95 (m, 2H), 7.48–7.41 (m, 2H), 7.41–7.28 (m, 6H), 5.78 (q, *J* = 7.1 Hz, 1H), 2.11 (d, *J* = 7.2 Hz, 3H). <sup>13</sup>C{<sup>1</sup>H} NMR (101 MHz, CDCl<sub>3</sub>)  $\delta$  144.8, 140.0, 129.8, 129.0, 128.7, 128.6, 128.4, 127.0, 126.6, 108.1, 60.0, 22.0. IR (KBr)  $\nu$  = 3031 (w), 2988 (m), 2943 (w), 1607 (w), 1494 (m), 1477 (m), 1447 (m), 1374 (m), 1306 (w), 1280 (m), 1232 (s), 1049 (m), 989 (m), 975 (m), 771 (s), 733 (s), 698 (s), 536 (m) cm<sup>-1</sup>. HRMS (ESI/Q-TOF) *m/z*: [M + H]<sup>+</sup> Calcd for C<sub>16</sub>H<sub>14</sub>BrN<sub>3</sub> 328.0444; found: 328.0439 (<sup>79</sup>Br). The assignment is supported by an X-ray crystallographic structure.

**(R)-5-Chloro-3-methyl-4-(1-phenylethyl)-1H-1,2,3-triazole. 6a** (0.186 g, 0.496 mmol) was suspended in MeCN (1.5 mL) and EtOAc (0.5 mL) in a microwave vial, water (1.0 mL), and KCl (0.110 g, 1.47 mmol) were added to the mixture, and the vial was sealed with a Teflon cap. The suspension of the reaction mixture was heated until most of the triazole **6a** was dissolved. The vial was placed into a microwave reactor and heated at 150 °C for 30 min. The reaction mixture was cooled, diluted with water, and the aqueous phase was extracted with EtOAc (2 × 10 mL) and with DCM (3 × 10 mL). The combined organic phase was dried over anhydrous MgSO<sub>4</sub>, concentrated and purified with column chromatography on silica gel (starting from 5% of EtOAc in petroleum ether) to provide the Cl-triazole as pale yellow crystals (0.115 g, 81% yield). mp 115–116 °C;  $\alpha_D^{20}$  22.6 (c 0.37, CHCl<sub>3</sub>); <sup>1</sup>H NMR (400 MHz, CDCl<sub>3</sub>)  $\delta$  8.00–7.94 (m, 2H), 7.49–7.41 (m, 2H), 7.40–7.28 (m, 6H), 5.75 (q, *J* = 7.1 Hz, 1H), 2.11 (d, *J* = 7.1 Hz, 3H). <sup>13</sup>C{<sup>1</sup>H} NMR (101 MHz, CDCl<sub>3</sub>)  $\delta$  142.1, 139.7, 129.5, 129.1, 128.8, 128.6, 128.5, 126.6, 126.5, 121.6, 59.1, 21.6. HRMS (ESI/Q-TOF) *m/z*: [M + H]<sup>+</sup> Calcd for C<sub>16</sub>H<sub>14</sub>ClN<sub>3</sub> 284.0949; found: 284.0954.

**(R)-4-Phenyl-1-(1-phenylethyl)-1H-1,2,3-triazole.** CuI (0.010 g, 0.053 mmol) and TTTA (0.021 g, 0.049 mmol) were dissolved in freshly distilled THF (3.5 mL) under argon atmosphere and stirred at rt for 30 min. Phenylacetylene (0.231 g, 1.013 mmol) and (R)-(1-azidoethyl)benzene (0.150 g, 1.019 mmol) dissolved in THF (2.0 mL) were added, and the reaction mixture was stirred at rt for 21 h. The reaction mixture was concentrated, NH<sub>4</sub>OH (20 mL, 10% w/w) was added, and the aqueous phase was extracted with CH<sub>2</sub>Cl<sub>2</sub> (4 × 20 mL). The combined organic phase was dried over anhydrous Na<sub>2</sub>SO<sub>4</sub>, concentrated, and purified by column chromatography on silica gel (starting from 0% of EtOAc in petroleum ether) to provide the H-triazole as colorless crystals (0.320 g, 84% yield). mp 115–116 °C;  $\alpha_D^{20}$  -48.9 (c 0.20, CHCl<sub>3</sub>); <sup>1</sup>H NMR (400 MHz, CDCl<sub>3</sub>)  $\delta$  7.85–7.75 (m, 2H), 7.64 (s, 1H), 7.47–7.28 (m, 8H), 5.87 (q, *J* = 7.1 Hz, 1H), 2.03 (d, *J* = 7.1 Hz, 3H). <sup>13</sup>C{<sup>1</sup>H} NMR (101 MHz, CDCl<sub>3</sub>)  $\delta$  147.9, 140.0, 130.8, 129.2, 128.9, 128.7, 128.2, 126.7, 125.8, 118.5, 60.4, 21.5. IR (KBr)  $\nu$  = 3121 (m), 3091 (w), 2985 (m), 1606 (w), 1496 (m), 1481 (m), 1463 (m), 1449 (m), 1356 (m), 1232 (m), 1219 (m), 1153 (m), 1075 (s), 1026 (m), 992 (m), 916 (w), 818 (m), 764 (s), 714 (s), 692 (s), 521 (m) cm<sup>-1</sup>. HRMS (ESI/Q-TOF) *m/z*: [M + H]<sup>+</sup> Calcd for C<sub>16</sub>H<sub>15</sub>N<sub>3</sub> 250.1339; found: 250.1336.

**(R)-5-Iodo-3-methyl-4-(perfluorophenyl)-1-(1-phenylethyl)-1H-1,2,3-triazol-3-ium Trifluoromethanesulfonate (7b).** Triazole **6b** (0.200 g, 0.230 mmol) was dissolved in CH<sub>2</sub>Cl<sub>2</sub> (9.0 mL) under argon atmosphere. Methyl triflate (0.073 mL, 0.645 mmol) was added dropwise, and the reaction mixture was stirred at rt for 21 h. After removal of the solvents under reduced pressure the solid was dissolved in CH<sub>2</sub>Cl<sub>2</sub> (6.0 mL) and Et<sub>2</sub>O (10.0 mL) was added to the solution and after 10 min a fine precipitate formed which was filtered to provide triflic salt **7b** as colorless crystals (0.231 g, 85% yield). mp 134–137 °C;  $\alpha_D^{20}$  12.6 (c 0.21, CHCl<sub>3</sub>); <sup>1</sup>H NMR (400 MHz,

CDCl<sub>3</sub>)  $\delta$  7.49–7.37 (m, 5H), 6.10 (q, *J* = 6.9 Hz, 1H), 4.39 (s, 3H), 2.18 (d, *J* = 7.0 Hz, 3H). <sup>13</sup>C{<sup>1</sup>H} NMR (101 MHz, CDCl<sub>3</sub>)  $\delta$  136.2, 130.0, 129.8, 127.2, 120.6 (q, *J* = 320.4 Hz), 77.5, 67.5, 40.6, 21.7. IR (KBr)  $\nu$  = 3034 (w), 1661 (m), 1505 (s), 1450 (m), 1246 (s), 1161 (s), 1078 (m), 1030 (s), 994 (s), 867 (m), 754 (m), 699 (m), 638 (s), 574 (w), 518 (m) cm<sup>-1</sup>. HRMS (ESI/Q-TOF) *m/z*: [M - CF<sub>3</sub>O<sub>3</sub>S]<sup>+</sup> Calcd for C<sub>17</sub>H<sub>17</sub>F<sub>3</sub>IN<sub>3</sub> 479.9991; found: 479.9998; [OTf]<sup>-</sup> Calcd for CF<sub>3</sub>O<sub>3</sub>S 148.9526; found 148.9550.

**(R)-5-Iodo-3-methyl-4-(4-nitrophenyl)-1-(1-phenylethyl)-1H-1,2,3-triazol-3-ium Trifluoromethanesulfonate (7c).** Triazole **6c** (0.102 g, 0.243 mmol) was dissolved in CH<sub>2</sub>Cl<sub>2</sub> (5.0 mL) under argon atmosphere. Methyl triflate (0.041 mL, 0.363 mmol) was added dropwise, and the reaction mixture was stirred at rt for 23 h. The reaction mixture was concentrated and dissolved in CH<sub>2</sub>Cl<sub>2</sub> (1.5 mL). Et<sub>2</sub>O (10.0 mL) was added to the reaction mixture, and a precipitate formed after 20 min, which was filtered to provide triflic salt **7c** as colorless crystals (0.123 g, 87% yield). mp 84–87 °C;  $\alpha_D^{20}$  34.8 (c 0.25, MeOH); <sup>1</sup>H NMR (400 MHz, CDCl<sub>3</sub>)  $\delta$  8.48–8.36 (m, 2H), 8.01–7.89 (m, 2H), 7.51–7.37 (m, 5H), 6.02 (q, *J* = 6.9 Hz, 1H), 4.32 (s, 3H), 2.19 (d, *J* = 7.0 Hz, 3H). <sup>13</sup>C{<sup>1</sup>H} NMR (101 MHz, CDCl<sub>3</sub>)  $\delta$  149.8, 145.4, 136.4, 132.1, 129.7, 129.6, 128.4, 127.1, 124.6, 120.5 (q, *J* = 320.0 Hz), 88.7, 67.0, 39.9, 21.6. IR (KBr)  $\nu$  = 3107 (w), 1605 (m), 1527 (s), 1488 (w), 1454 (w), 1349 (s), 1277 (s), 1158 (s), 1030 (s), 856 (m), 757 (w), 704 (m), 638 (s), 600 (w), 574 (w) cm<sup>-1</sup>. HRMS (ESI/Q-TOF) *m/z*: [M - CF<sub>3</sub>O<sub>3</sub>S]<sup>+</sup> Calcd for C<sub>17</sub>H<sub>16</sub>IN<sub>3</sub>O<sub>2</sub> 435.0312; found 435.0327; [OTf]<sup>-</sup> Calcd for CF<sub>3</sub>O<sub>3</sub>S 148.9526; found 148.9549. The assignment is supported by an X-ray crystallographic structure.

**(R)-5-Iodo-3-methyl-4-phenyl-1-(1-phenylethyl)-1H-1,2,3-triazol-3-ium Tetrafluoroborate (8a).** Triazole **6a** (0.124 g, 0.330 mmol) was dissolved in CH<sub>2</sub>Cl<sub>2</sub> (6.5 mL) under argon atmosphere. Trimethyloxonium tetrafluoroborate (0.061 mg, 0.412 mmol) was added, and the reaction mixture was stirred at rt for 24 h. The reaction was quenched by adding MeOH (10.0 mL) and stirred for 1 h. After removal of the solvents under reduced pressure, the crude product was dissolved in MeOH (10.0 mL) and Et<sub>2</sub>O (5.0 mL) was added to the solution and a fine precipitate formed which was filtered. The crystallization was repeated a second time using MeOH (5.0 mL) and Et<sub>2</sub>O (25.0 mL) to provide tetrafluoroborate salt **8a** as colorless crystals (in total: 0.140 g, 89% yield). mp 193–195 °C;  $\alpha_D^{20}$  36.0 (c 0.16 in MeOH); <sup>1</sup>H NMR (400 MHz, CD<sub>3</sub>OD)  $\delta$  7.77–7.57 (m, 5H), 7.55–7.37 (m, 5H), 6.23 (q, *J* = 6.9 Hz, 1H), 4.27 (s, 3H), 2.12 (d, *J* = 6.9 Hz, 3H). <sup>13</sup>C{<sup>1</sup>H} NMR (101 MHz, CD<sub>3</sub>OD)  $\delta$  148.6, 138.8, 133.1, 131.4, 130.7, 130.4, 130.3, 128.2, 124.3, 91.3, 67.4, 39.8, 22.0. HRMS (ESI/Q-TOF) *m/z*: [M - BF<sub>4</sub>]<sup>+</sup> Calcd for C<sub>17</sub>H<sub>17</sub>IN<sub>3</sub> 390.0462; found 390.0455; [BF<sub>4</sub>]<sup>-</sup> Calcd for BF<sub>4</sub>: 86.0071; found 86.0072 (<sup>10</sup>B), 87.0037 (<sup>11</sup>B). The assignment is supported by an X-ray crystallographic structure.

**(R)-5-Iodo-3-methyl-4-(4-nitrophenyl)-1-(1-phenylethyl)-1H-1,2,3-triazol-3-ium Tetrafluoroborate (8c).** Triazole **6c** (0.112 g, 0.267 mmol) was dissolved in CH<sub>2</sub>Cl<sub>2</sub> (5.5 mL) under argon atmosphere. Trimethyloxonium tetrafluoroborate (0.055 mg, 0.372 mmol) was added, and the reaction mixture was stirred at rt for 3 days. The reaction was quenched by adding MeOH (5.5 mL) and stirred for 40 min. After removal of the solvents under reduced pressure the solid was dissolved in CH<sub>2</sub>Cl<sub>2</sub> (2.0 mL) and Et<sub>2</sub>O (5.0 mL) was added to the solution and a precipitate formed after 20 min, which was filtered to provide tetrafluoroborate salt **8c** as pale yellow crystals (0.132 g, 95% yield). mp 98–101 °C;  $\alpha_D^{20}$  39.4 (c 0.19, MeOH); <sup>1</sup>H NMR (400 MHz, CD<sub>3</sub>OD)  $\delta$  8.56–8.45 (m, 2H), 8.01–7.88 (m, 2H), 7.56–7.36 (m, 5H), 6.25 (q, *J* = 6.9 Hz, 1H), 4.32 (s, 3H), 2.13 (d, *J* = 6.9 Hz, 3H). <sup>13</sup>C{<sup>1</sup>H} NMR (101 MHz, CD<sub>3</sub>OD)  $\delta$  151.3, 146.9, 138.7, 133.2, 130.38, 130.37, 130.3, 128.2, 125.5, 92.1, 67.6, 40.0, 22.0. IR (KBr)  $\nu$  = 1605 (w), 1526 (s), 1487 (w), 1453 (w), 1348 (s), 1287 (w), 1061 (s), 855 (m), 763 (w), 704 (m), 600 (w) cm<sup>-1</sup>. HRMS (ESI/Q-TOF) *m/z*: [M - BF<sub>4</sub>]<sup>+</sup> Calcd for C<sub>17</sub>H<sub>16</sub>IN<sub>3</sub>O<sub>2</sub> 435.0312; found 435.0315; [BF<sub>4</sub>]<sup>-</sup> Calcd for BF<sub>4</sub> 86.0071; found: 86.0089 (<sup>10</sup>B), 87.0054 (<sup>11</sup>B). The assignment is supported by an X-ray crystallographic structure.

**(R)-5-Iodo-3-methyl-4-phenyl-1-(1-phenylethyl)-1H-1,2,3-triazol-3-ium Tetrakis(3,5-bis(trifluoromethyl)phenylborate) (9a).** Sodium tetrakis(3,5-bis(trifluoromethyl)phenylborate): A three-neck round-bottom flask fitted with a reflux condenser was evacuated, flame-dried and filled with argon prior to use. Magnesium (1.11 g, 45.7 mmol), NaBF<sub>4</sub> (0.71 g, 6.4 mmol), and Et<sub>2</sub>O (150 mL) were added to the flask. To start the reaction dibromoethane (0.49 mL, 5.7 mmol) was added, and the flask was heated for 5 min followed by the dropwise addition of 3,5-bis(trifluoromethyl)bromobenzene (5.0 mL, 35.9 mmol) dissolved in Et<sub>2</sub>O (40 mL) over 70 min. The solution was then stirred overnight at rt. As all of the magnesium had not reacted the reaction was refluxed for an additional 24 h. Then the reaction mixture was quenched by the addition of Na<sub>2</sub>CO<sub>3</sub> (16.2 g, 153 mmol) dissolved in H<sub>2</sub>O (200 mL) and stirred for 1 h and filtered. The aqueous phase was extracted three times with Et<sub>2</sub>O (50 mL), the combined organic phase was dried over Na<sub>2</sub>SO<sub>4</sub>. The solvent was removed and the remaining crude product was dissolved in toluene (50 mL) and concentrated to remove remaining traces of water, this was repeated three more times. The product was dried under reduced pressure with heating (100 °C) for 10 h to yield a brown solid. This solid was washed with CH<sub>2</sub>Cl<sub>2</sub> and toluene, dried under reduced pressure with heating (100 °C) in the presence of P<sub>2</sub>O<sub>5</sub> for 2 days to yield the NaBARF as a pale gray solid (2.70 g, 47% yield). <sup>1</sup>H NMR (400 MHz, [D<sub>6</sub>]DMSO) δ 7.64 (s, 4H), 7.61 (s, 8H). <sup>13</sup>C{<sup>1</sup>H} NMR (101 MHz, [D<sub>6</sub>]DMSO) δ 161.0 (q, J = 49.9 Hz), 134.9, 129.1–127.9 (m), 124.0 (q, J = 272.2 Hz), 118.0–117.1 (m). Tetramethylammonium tetrakis(3,5-bis(trifluoromethyl)-phenylborate: NaBARF (1.76 g, 1.99 mmol) was suspended in CH<sub>2</sub>Cl<sub>2</sub> (100 mL) and tetramethylammonium iodide (0.60 g, 2.98 mmol) was added, and the reaction mixture was stirred at rt for 3 days open to air (moisture helps to increase the solubility of NaBARF). Then the mixture was filtered and the filtrate concentrated under reduced pressure. The obtained solid was suspended in Et<sub>2</sub>O and then filtered (to remove excess Me<sub>3</sub>NI). The filtrate was concentrated under reduced pressure and the resulting solid was recrystallized from CH<sub>2</sub>Cl<sub>2</sub> at 0 °C for three times to yield the tetramethylammonium BARF salt as a colorless powder (in total: 1.49 g, 80% yield). <sup>1</sup>H NMR (400 MHz, [D<sub>6</sub>]DMSO) δ 7.66 (s, 4H), 7.64–7.57 (m, 8H), 3.10 (s, 12H). <sup>13</sup>C{<sup>1</sup>H} NMR (101 MHz, [D<sub>6</sub>]DMSO) δ 161.0 (q, J = 49.9 Hz), 134.0 (s), 129.1–127.9 (m), 124.0 (q, J = 272.4 Hz), 117.9–117.27 (m), 54.7–54.0 (m). **9a:** Triazolium **7a** (0.153 g, 0.284 mmol) was dissolved in a mixture of CH<sub>2</sub>Cl<sub>2</sub> (17.4 mL) and MeOH (5.8 mL), tetramethylammonium BARF (0.293 g, 0.313 mmol) was added, and the reaction mixture was stirred at rt for 22 h. After removal of the solvents under reduced pressure, the precipitate was suspended in Et<sub>2</sub>O (11.5 mL) and stirred for 45 min at 0 °C. The precipitate was removed by filtration, and the filtrate was concentrated. The obtained solid was suspended in CHCl<sub>3</sub> (11.5 mL) and stirred for 30 min at 0 °C. The precipitate was removed by filtration, and the filtrate was concentrated under reduced pressure to provide BARF salt **9a** as colorless crystals (0.342 g, 96% yield). mp 173–174 °C; α<sub>D</sub><sup>20</sup> 12.5 (c 0.37, CHCl<sub>3</sub>); <sup>1</sup>H NMR (400 MHz, CDCl<sub>3</sub>) δ 7.67–7.56 (m, 9H), 7.53–7.47 (m, 2H), 7.43 (s, 4H), 7.39–7.30 (m, 3H), 7.30–7.25 (m, 2H), 7.24–7.19 (m, 2H), 5.87 (q, J = 7.0 Hz, 1H), 4.04 (s, 3H), 1.99 (d, J = 7.0 Hz, 3H). <sup>13</sup>C{<sup>1</sup>H} NMR (101 MHz, CDCl<sub>3</sub>) δ 161.8 (q, J = 49.9 Hz), 147.9, 135.1–134.8 (m), 135.0, 133.5, 130.7, 130.5, 130.0, 129.7–128.5 (m), 129.3, 127.0, 124.63 (q, J = 272.6 Hz), 120.6, 117.8–117.5 (m), 86.4, 67.7, 39.5, 21.3. IR (KBr) ν = 1610 (m), 1355 (s), 1277 (s), 1131 (s), 888 (m), 839 (m), 763 (w), 745 (m), 715 (m), 697 (m), 683 (m), 670 (m) cm<sup>-1</sup>. HRMS (ESI/Q-TOF) *m/z*: [M – C<sub>32</sub>H<sub>12</sub>BF<sub>24</sub>]<sup>+</sup> Calcd for C<sub>17</sub>H<sub>17</sub>IN<sub>3</sub> 390.0462; found 390.0460; [BARF]<sup>-</sup>: Calcd for C<sub>32</sub>H<sub>12</sub>BF<sub>24</sub> 862.0691; found 862.0696 (<sup>10</sup>B).

**(R)-5-Bromo-3-methyl-4-phenyl-1-(1-phenylethyl)-1H-1,2,3-triazol-3-ium Trifluoromethanesulfonate (10).** The Br-triazole (0.096 g, 0.29 mmol) was dissolved in CH<sub>2</sub>Cl<sub>2</sub> (6.0 mL) under argon atmosphere. Methyl triflate (0.050 mL, 0.439 mmol) was added dropwise, and the reaction mixture was stirred at rt for 22 h. After removal of the solvents under reduced pressure the product was purified by column chromatography on silica gel (from 5% of MeOH

in CH<sub>2</sub>Cl<sub>2</sub>) to provide triflic salt **10** as a colorless oil (0.049 g, 34% yield). α<sub>D</sub><sup>20</sup> –1.6 (c 0.18, CHCl<sub>3</sub>); <sup>1</sup>H NMR (400 MHz, CDCl<sub>3</sub>) δ 7.70–7.55 (m, 5H), 7.49–7.37 (m, 5H), 6.06 (q, J = 7.0 Hz, 1H), 4.31 (s, 3H), 2.19 (d, J = 7.0 Hz, 3H). <sup>13</sup>C{<sup>1</sup>H} NMR (101 MHz, CDCl<sub>3</sub>) δ 143.2, 136.6, 132.4, 130.2, 129.8, 129.8, 129.7, 127.1, 122.4, 120.8 (q, J = 320.4 Hz), 116.5, 65.4, 39.9, 21.3. IR (film) ν = 3063 (w), 1566 (w), 1493 (m), 1455 (m), 1266 (s), 1225 (m), 1154 (s), 1031 (s), 795 (w), 760 (m), 702 (s), 638 (s), 573 (w) cm<sup>-1</sup>. HRMS (ESI/Q-TOF) *m/z*: [M – CF<sub>3</sub>O<sub>3</sub>S]<sup>+</sup> Calcd for C<sub>17</sub>H<sub>17</sub>BrN<sub>3</sub> 342.0600; found 342.0601 (<sup>79</sup>Br); [OTf]<sup>-</sup> Calcd for CF<sub>3</sub>O<sub>3</sub>S 148.9526; found 148.9525.

**(R)-5-Chloro-3-methyl-4-phenyl-1-(1-phenylethyl)-1H-1,2,3-triazol-3-ium Trifluoromethanesulfonate (11).** Triazole **11** (0.1005 g, 0.354 mmol) was dissolved in CH<sub>2</sub>Cl<sub>2</sub> (6.0 mL) under argon atmosphere. Methyl triflate (0.060 mL, 0.531 mmol) was added dropwise, and the reaction mixture was stirred at rt for 23 h. After removal of the solvents under reduced pressure, the product was mixed overnight in MeOH (1 mL) in the presence of activated charcoal (0.025 g) to remove some of the colored impurities. In addition, **11** was purified by column chromatography on silica gel (from 5% of MeOH in CH<sub>2</sub>Cl<sub>2</sub>) to provide triflic salt **11** as a colorless oil (0.132 g, 83% yield). α<sub>D</sub><sup>20</sup> –15.5 (c 0.27, CHCl<sub>3</sub>); <sup>1</sup>H NMR (400 MHz, CDCl<sub>3</sub>) δ 7.63–7.49 (m, 5H), 7.43–7.28 (m, 5H), 6.00 (q, J = 7.0 Hz, 1H), 4.24 (s, 3H), 2.14 (d, J = 7.0 Hz, 3H). <sup>13</sup>C{<sup>1</sup>H} NMR (101 MHz, CDCl<sub>3</sub>) δ 140.5, 136.4, 132.5, 130.1, 129.9, 129.8, 129.7, 129.2, 127.0, 120.7, 64.4, 40.0, 20.9. IR (film) ν = 1494 (w), 1455 (w), 1266 (s), 1225 (m), 1155 (s), 1032 (s), 761 (m), 701 (m), 638 (s), 574 (w) cm<sup>-1</sup>. HRMS (ESI/Q-TOF) *m/z*: [M – CF<sub>3</sub>O<sub>3</sub>S]<sup>+</sup> Calcd for C<sub>17</sub>H<sub>17</sub>ClN<sub>3</sub> 298.1106; found 298.1110; [OTf]<sup>-</sup> Calcd for CF<sub>3</sub>O<sub>3</sub>S 148.9526; found 148.9544.

**(R)-3-Methyl-4-phenyl-1-(1-phenylethyl)-1H-1,2,3-triazol-3-ium Trifluoromethanesulfonate (12).** (R)-4-Phenyl-1-(1-phenylethyl)-1H-1,2,3-triazole (0.050 g, 0.201 mmol) was dissolved in CH<sub>2</sub>Cl<sub>2</sub> (4.0 mL) under argon atmosphere. Methyl triflate (0.045 mL, 0.401 mmol) was added dropwise, and the reaction mixture was stirred at rt for 21 h. After removal of the solvents under reduced pressure the product was purified by column chromatography on silica gel (from 3% of MeOH in CH<sub>2</sub>Cl<sub>2</sub>) to provide triflic salt **12** as a colorless oil (0.074 g, 89% yield). α<sub>D</sub><sup>20</sup> –27.6 (c 0.09, CHCl<sub>3</sub>); <sup>1</sup>H NMR (400 MHz, CDCl<sub>3</sub>) δ 8.54 (s, 1H), 7.63–7.50 (m, 7H), 7.48–7.38 (m, 3H), 6.17 (q, J = 7.1 Hz, 1H), 4.26 (s, 3H), 2.11 (d, J = 7.0 Hz, 3H). <sup>13</sup>C{<sup>1</sup>H} NMR (101 MHz, CDCl<sub>3</sub>) δ 143.6, 136.7, 132.1, 130.0, 129.8, 129.7, 129.6, 128.0, 127.7, 122.0, 120.9 (q, J = 320.3 Hz), 65.4, 38.8, 20.3. HRMS (ESI/Q-TOF) *m/z*: [M – CF<sub>3</sub>O<sub>3</sub>S]<sup>+</sup> Calcd for C<sub>17</sub>H<sub>18</sub>N<sub>3</sub> 264.1495; found 264.1502; [OTf]<sup>-</sup> Calcd for CF<sub>3</sub>O<sub>3</sub>S: 148.9526; found 148.9551.

**General Procedure for the Reactions with <sup>1</sup>H NMR Monitoring between 1 and 2.** All of the crystallized XB donors were additionally purified by column chromatography (from 5% of MeOH in CH<sub>2</sub>Cl<sub>2</sub>) before their use in the catalytic experiments. Danishefskýs diene of purity 96% was purchased from Alfa Aesar and used as received. (E)-1-(4-Methoxyphenyl)-N-phenylmethanimine **1**: MgSO<sub>4</sub> (6.8 g, 56.4 mmol) was suspended in CH<sub>2</sub>Cl<sub>2</sub> (13 mL), then *p*-anysaldehyde (1.8 mL, 13.8 mmol) and aniline (1.2 mL, 13.1 mmol) were added. The reaction mixture was stirred at rt for 24 h and filtered. After removal of the solvent under reduced pressure, the crude product was purified by crystallization from a mixture of CH<sub>2</sub>Cl<sub>2</sub> and Et<sub>2</sub>O to yield imine **1** as colorless crystals (1.94 g, 70% yield). <sup>1</sup>H NMR (400 MHz, CDCl<sub>3</sub>) δ 8.40 (s, 1H), 7.93–7.79 (m, 2H), 7.40 (dd, J = 8.7, 6.9 Hz, 2H), 7.22 (td, J = 7.6, 7.2, 1.5 Hz, 3H), 7.04–6.93 (m, 2H), 3.87 (s, 3H). <sup>13</sup>C{<sup>1</sup>H} NMR (101 MHz, CDCl<sub>3</sub>) δ 162.3, 159.8, 152.5, 130.6, 129.4, 129.2, 125.7, 121.0, 114.3, 55.5.

The XB donor (0.052 mmol, 0.2 equiv) was dissolved in a stock solution of CD<sub>2</sub>Cl<sub>2</sub> (0.650 mL) containing imine **1** (0.4 M, 1.0 equiv) and *p*-xylene (0.2 M, 0.5 equiv). Then 0.600 mL of the solution was transferred to a NMR tube and the <sup>1</sup>H spectrum was measured. Then Danishefskýs diene **2** (0.063 mL, 1.3 equiv) was added, and the <sup>1</sup>H spectra were measured at approximately 8, 15, and 30 min intervals for at least the first 8 h of the reaction. In certain cases the product **3** was isolated by purification with column chromatography on silica gel

(from 20% of EtOAc in petroleum ether) to provide **3** as a yellow oil with yields usually 10% lower than the corresponding conversion.

Parameters specific to the experiment:  $T = 297$  K, relaxation delay = 36 s, number of scans = 8. Data processing was performed using MestreNova. The spectra were phased, baseline-corrected and zero-filled (to spectrum size 128 K). Then line fitting function (deconvolution) was used to more accurately integrate the peaks corresponding to the protons of the methoxy group of imine **1** and methyl group of *p*-xylene.

2-(4-Methoxyphenyl)-1-phenyl-2,3-dihydropyridin-4(1H)-one (**3**):  $^1\text{H}$  NMR (400 MHz,  $\text{CDCl}_3$ )  $\delta$  7.64 (dd,  $J = 7.8, 1.2$  Hz, 1H), 7.35–7.27 (m, 2H), 7.21–7.15 (m, 2H), 7.15–7.07 (m, 1H), 7.07–7.00 (m, 2H), 6.90–6.81 (m, 2H), 5.32–5.26 (m, 1H), 5.24 (dd,  $J = 6.9, 3.2$  Hz, 1H), 3.76 (s, 3H), 3.26 (dd,  $J = 16.3, 7.0$  Hz, 1H), 2.75 (ddd,  $J = 16.3, 3.3, 1.2$  Hz, 1H).  $^{13}\text{C}\{^1\text{H}\}$  NMR (101 MHz,  $\text{CDCl}_3$ )  $\delta$  190.5, 159.2, 148.3, 144.8, 129.9, 129.6, 127.5, 124.5, 118.8, 114.4, 102.9, 61.4, 55.4, 43.7.

## ■ ASSOCIATED CONTENT

### Supporting Information

The Supporting Information is available free of charge on the ACS Publications website at DOI: 10.1021/acs.joc.9b00248.

Copies of  $^1\text{H}$  and  $^{13}\text{C}\{^1\text{H}\}$  spectra, spectra and chromatograms used for the mechanistic study, computational details, and crystallographic details (DOCX)

Crystallographic details (CIF)

Crystallographic details (CIF)

Crystallographic details (CIF)

Crystallographic details (CIF)

## ■ AUTHOR INFORMATION

### Corresponding Author

\*E-mail: tonis.kanger@taltech.ee.

### ORCID

Tõnis Kanger: 0000-0001-5339-9682

### Notes

The authors declare no competing financial interest.

## ■ ACKNOWLEDGMENTS

The authors thank the Estonian Ministry of Education and Research (Grant Nos. IUT 19-32, IUT 19-9, PUT692, and PUT1468) and the Centre of Excellence in Molecular Cell Engineering 2014-2020.4.01.15-0013 for financial support. This work has been partially supported by ASTRA “TUT Institutional Development Programme for 2016–2022 Graduate School of Functional Materials and Technologies” (2014-2020.4.01.16-0032). We thank Dr. Marina Kudrjašova for the  $^{19}\text{F}$  NMR measurements, Dr. Riina Aav for advice on the NMR experiments, Dr. Aleksander-Mati Müürisepp for IR, and Ms. Jevgenija Martõnova for the X-ray measurements.

## ■ REFERENCES

- Desiraju, G. R.; Ho, P. S.; Kloo, L.; Legon, A. C.; Marquardt, R.; Metrangolo, P.; Politzer, P.; Resnati, G.; Rissanen, K. Definition of the halogen bond (IUPAC Recommendations 2013). *Pure Appl. Chem.* **2013**, *85*, 1711–1713.
- For general reviews, see: (a) Montaña, Á. M. The  $\sigma$  and  $\pi$  Holes. The Halogen and Tetrel Bondings: Their Nature, Importance and Chemical, Biological and Medicinal Implications. *ChemistrySelect* **2017**, *2*, 9094–9112. (b) Cavallo, G.; Metrangolo, P.; Milani, R.; Pilati, T.; Priimagi, A.; Resnati, G.; Terraneo, G. The Halogen Bond. *Chem. Rev.* **2016**, *116*, 2478–2601. (c) Wang, H.; Wang, W.; Jin, W. J.  $\sigma$ -Hole Bond vs  $\pi$ -Hole Bond: A Comparison Based on Halogen

Bond. *Chem. Rev.* **2016**, *116*, 5072–5104. (d) Gilday, L. C.; Robinson, S. W.; Barendt, T. A.; Langton, M. J.; Mullaney, B. R.; Beer, P. D. Halogen Bonding in Supramolecular Chemistry. *Chem. Rev.* **2015**, *115*, 7118–7195.

(3) For reviews focusing on the use of XBs in crystal engineering, see: (a) Christopherson, J.-C.; Topić, F.; Barrett, C. J.; Frisčić, T. Halogen-Bonded Cocrystals as Optical Materials: Next-Generation Control over Light–Matter Interactions. *Cryst. Growth Des.* **2018**, *18*, 1245–1259. (b) Li, B.; Zang, S.-Q.; Wang, L.-Y.; Mak, T. C. W. Halogen bonding: A powerful, emerging tool for constructing high-dimensional metal-containing supramolecular networks. *Coord. Chem. Rev.* **2016**, *308*, 1–21. (c) Berger, G.; Soubhye, J.; Meyer, F. Halogen bonding in polymer science: from crystal engineering to functional supramolecular polymers and materials. *Polym. Chem.* **2015**, *6*, 3559–3580. (d) Mukherjee, A.; Tothadi, S.; Desiraju, G. R. Halogen Bonds in Crystal Engineering: Like Hydrogen Bonds yet Different. *Acc. Chem. Res.* **2014**, *47*, 2514–2524.

(4) For reviews focusing on the use of XBs in solution, see: (a) Tepper, R.; Schubert, U. S. Halogen Bonding in Solution: Anion Recognition, Templated Self-Assembly, and Organocatalysis. *Angew. Chem., Int. Ed.* **2018**, *57*, 6004–6016. (b) Brown, A.; Beer, P. D. Halogen bonding anion recognition. *Chem. Commun.* **2016**, *52*, 8645–8658. (c) Jentzsch, A. V. Applications of halogen bonding in solution. *Pure Appl. Chem.* **2015**, *87*, 15–41. (d) Carlsson, A.-C. C.; Veiga, A. X.; Erdélyi, M. Halogen Bonding in Solution. *Top. Curr. Chem.* **2014**, *359*, 49–76. (e) Beale, T. M.; Chudzinski, M. G.; Sarwar, M. G.; Taylor, M. S. Halogen bonding in solution: thermodynamics and applications. *Chem. Soc. Rev.* **2013**, *42*, 1667–1680.

(5) For reviews, see: (a) Nishikawa, Y. Recent topics in dual hydrogen bonding catalysis. *Tetrahedron Lett.* **2018**, *59*, 216–223. (b) Zhao, B.-L.; Li, J.-H.; Du, D.-M. Squaramide-Catalyzed Asymmetric Reactions. *Chem. Rev.* **2017**, *17*, 994–1018. (c) Fang, X.; Wang, C.-J. Recent advances in asymmetric organocatalysis mediated by bifunctional amine–thioureas bearing multiple hydrogen-bonding donors. *Chem. Commun.* **2015**, *51*, 1185–1197. (d) Chauhan, P.; Mahajan, S.; Kaya, U.; Hack, D.; Enders, D. Bifunctional Amine-Squaramides: Powerful Hydrogen-Bonding Organocatalysts for Asymmetric Domino/Cascade Reactions. *Adv. Synth. Catal.* **2015**, *357*, 253–281. (e) Albrecht, L.; Jiang, H.; Jørgensen, K. A. Hydrogen-Bonding in Aminocatalysis: From Proline and Beyond. *Chem. - Eur. J.* **2014**, *20*, 358–368.

(6) (a) Rissanen, K. Halogen bonded supramolecular complexes and networks. *CrystEngComm* **2008**, *10*, 1107–1113. (b) Lommerse, J. P. M.; Stone, A. J.; Taylor, R.; Allen, F. H. The Nature and Geometry of Intermolecular Interactions between Halogens and Oxygen or Nitrogen. *J. Am. Chem. Soc.* **1996**, *118*, 3108–3116.

(7) (a) Riel, A. M. S.; Jessop, M. J.; Decato, D. A.; Massena, C. J.; Nascimento, V. R.; Berryman, O. B. Experimental investigation of halogen-bond hard–soft acid–base complementarity. *Acta Crystallogr., Sect. B: Struct. Sci., Cryst. Eng. Mater.* **2017**, *73*, 203–209. (b) Robertson, C. C.; Perutz, R. N.; Brammer, L.; Hunter, C. A. A solvent-resistant halogen bond. *Chem. Sci.* **2014**, *5*, 4179–4183.

(8) Bruckmann, H. A.; Pena, M. A.; Bolm, C. Organocatalysis through Halogen-Bond Activation. *Synlett* **2008**, 900–902.

(9) (a) Haraguchi, R.; Hoshino, S.; Sakai, M.; Tanazawa, S.; Morita, Y.; Komatsu, T.; Fukuzawa, S. Bulky iodotriazolium tetrafluoroborates as highly active halogen-bonding-donor catalysts. *Chem. Commun.* **2018**, *54*, 10320–10323. (b) Takeda, Y.; Hisakuni, D.; Lin, C.-H.; Minakata, S. 2-Halogenoimidazolium Salt Catalyzed Aza-Diels–Alder Reaction through Halogen-Bond Formation. *Org. Lett.* **2015**, *17*, 318–321. (c) Jungbauer, S. H.; Walter, S. M.; Schindler, S.; Rout, L.; Kniep, F.; Huber, S. M. Activation of a carbonyl compound by halogen bonding. *Chem. Commun.* **2014**, *50*, 6281–6284.

(10) (a) von der Heiden, D.; Detmar, E.; Kuchta, R.; Breugst, M. Activation of Michael Acceptors by Halogen-Bond Donors. *Synlett* **2018**, *29*, 1307–1313. (b) Gliese, J.-P.; Jungbauer, S. H.; Huber, S. M. A halogen-bonding-catalyzed Michael addition reaction. *Chem. Commun.* **2017**, *53*, 12052–12055.



- (11) (a) Benz, S.; Poblador-Bahamonde, A. I.; Low-Ders, N.; Matile, S. Catalysis with Pnictogen, Chalcogen, and Halogen Bonds. *Angew. Chem., Int. Ed.* **2018**, *57*, 5408–5412. (b) Dreger, A.; Engelage, E.; Mallick, B.; Beer, P. D.; Huber, S. M. The role of charge in 1,2,3-triazol(ium)-based halogen bonding activators. *Chem. Commun.* **2018**, *54*, 4013–4016. (c) Jungbauer, S. H.; Huber, S. M. Cationic Multidentate Halogen-Bond Donors in Halide Abstraction Organocatalysis: Catalyst Optimization by Preorganization. *J. Am. Chem. Soc.* **2015**, *137*, 12110–12120. (d) Kniep, F.; Walter, S. M.; Herdtweck, E.; Huber, S. M. 4,4'-Azobis(halopyridinium) Derivatives: Strong Multidentate Halogen-Bond Donors with a Redox-Active Core. *Chem. - Eur. J.* **2012**, *18*, 1306–1310. (e) Kniep, F.; Rout, L.; Walter, S. M.; Bensch, H. K. V.; Jungbauer, S. H.; Herdtweck, E.; Huber, S. M. 5-Iodo-1,2,3-triazolium-based multidentate halogen-bond donors as activating reagents. *Chem. Commun.* **2012**, *48*, 9299–9301. (f) Walter, S. M.; Kniep, F.; Herdtweck, E.; Huber, S. M. Halogen-Bond-Induced Activation of a Carbon–Heteroatom Bond. *Angew. Chem., Int. Ed.* **2011**, *50*, 7187–7191.
- (12) For reviews, see: (a) Breugst, M.; von der Heiden, D. Mechanisms in Iodine Catalysis. *Chem.—Eur. J.* **2018**, *24*, 9187–9199. (b) Bulfield, D.; Huber, S. M. Halogen Bonding in Organic Synthesis and Organocatalysis. *Chem. - Eur. J.* **2016**, *22*, 14434–14450. (c) Schindler, S.; Huber, S. M. Halogen Bonds in Organic Synthesis and Organocatalysis. *Top. Curr. Chem.* **2014**, *359*, 167–203. (13) (a) von der Heiden, D.; Bozkus, S.; Klusmann, M.; Breugst, M. Reaction Mechanism of Iodine-Catalyzed Michael Additions. *J. Org. Chem.* **2017**, *82*, 4037–4043. (b) Kee, C. W.; Wong, M. W. In Silico Design of Halogen-Bonding-Based Organocatalyst for Diels–Alder Reaction, Claisen Rearrangement, and Cope-Type Hydroamination. *J. Org. Chem.* **2016**, *81*, 7459–7470. (c) Nzioku, V. de P. N.; Scheiner, S. Catalysis of the Aza-Diels–Alder Reaction by Hydrogen and Halogen Bonds. *J. Org. Chem.* **2016**, *81*, 2589–2597. (d) Breugst, M.; Detmar, E.; von der Heiden, D. Origin of the Catalytic Effects of Molecular Iodine: A Computational Analysis. *ACS Catal.* **2016**, *6*, 3203–3212.
- (14) (a) Kuwano, S.; Suzuki, T.; Hosaka, Y.; Arai, T. A chiral organic base catalyst with halogen-bonding-donor functionality: asymmetric Mannich reactions of malononitrile with N-Boc aldimines and ketimines. *Chem. Commun.* **2018**, *54*, 3847–3850. (b) Arai, T.; Suzuki, T.; Inoue, T.; Kuwano, S. Chiral Bis(imidazolidine)-iodobenzene (I-Bidine) Organocatalyst for Thiochromane Synthesis Using an Asymmetric Michael/Henry Reaction. *Synlett* **2016**, *28*, 122–127. (c) Lindsay, V. N. G.; Charette, A. B. Design and Synthesis of Chiral Heteroleptic Rhodium(II) Carboxylate Catalysts: Experimental Investigation of Halogen Bond Rigidity Effects in Asymmetric Cyclopropanation. *ACS Catal.* **2012**, *2*, 1221–1225.
- (15) (a) Robinson, S. W.; Beer, P. D. Halogen bonding rotaxanes for nitrate recognition in aqueous media. *Org. Biomol. Chem.* **2017**, *15*, 153–159. (b) Lim, J. Y. C.; Marques, L.; Ferreira, L.; Félix, V.; Beer, P. D. Enhancing the enantioselective recognition and sensing of chiral anions by halogen bonding. *Chem. Commun.* **2016**, *52*, 5527–5530. (c) Tepper, R.; Schulze, B.; Jäger, M.; Friebe, C.; Scharf, D. H.; Görls, H.; Schubert, U. S. Anion Receptors Based on Halogen Bonding with Halo-1,2,3-triazoliums. *J. Org. Chem.* **2015**, *80*, 3139–3150.
- (16) For recent reviews, see: (a) Jalani, H. B.; Karagöz, A. C.; Tsoogova, S. B. *Synthesis* **2016**, *49*, 29–41. (b) Schulze, B.; Schubert, U. S. *Chem. Soc. Rev.* **2014**, *43*, 2522–2571.
- (17) Nepal, B.; Scheiner, S. Competitive Halide Binding by Halogen Versus Hydrogen Bonding: Bis-triazole Pyridinium. *Chem. - Eur. J.* **2015**, *21*, 13330–13335.
- (18) Kaasik, M.; Kaabel, S.; Kriis, K.; Järving, I.; Aav, R.; Rissanen, K.; Kanger, T. Synthesis and Characterisation of Chiral Triazole-Based Halogen-Bond Donors: Halogen Bonds in the Solid State and in Solution. *Chem. - Eur. J.* **2017**, *23*, 7337–7344.
- (19) For reviews on asymmetric aza-Diels–Alder reactions, see: (a) Eschenbrenner-Lux, V.; Kumar, K.; Waldmann, H. The Asymmetric Hetero-Diels–Alder Reaction in the Syntheses of Biologically Relevant Compounds. *Angew. Chem., Int. Ed.* **2014**, *53*, 11146–11157. (b) Masson, G.; Lalli, C.; Benhoud, M.; Dagouset, G. Catalytic enantioselective [4 + 2]-cycloaddition: a strategy to access aza-hexacycles. *Chem. Soc. Rev.* **2013**, *42*, 902–923.
- (20) Hein, J. E.; Tripp, J. C.; Krasnova, L. B.; Sharpless, K. B.; Fokin, V. V. Copper(I)-Catalyzed Cycloaddition of Organic Azides and Iodoalkynes. *Angew. Chem., Int. Ed.* **2009**, *48*, 8018–8021.
- (21) Kuijpers, B. H. M.; Dijkmans, G. C. T.; Groothuys, S.; Quaedflieg, P. J. L. M.; Blaauw, R. H.; van Delft, F. L.; Rutjes, F. P. J. T. Copper(I)-Mediated Synthesis of Trisubstituted 1,2,3-Triazoles. *Synlett* **2005**, 3059–3062.
- (22) Worrell, B. T.; Hein, J. E.; Fokin, V. V. Halogen Exchange (Halex) Reaction of 5-Iodo-1,2,3-triazoles: Synthesis and Applications of 5-Fluorotriazoles. *Angew. Chem., Int. Ed.* **2012**, *51*, 11791–11794.
- (23) Frisch, M. J.; Trucks, G. W.; Schlegel, H. B.; Scuseria, G. E.; Robb, M. A.; Cheeseman, J. R.; Scalmani, G.; Barone, V.; Mennucci, B.; Petersson, G. A.; Nakatsuji, H.; Caricato, M.; Li, X.; Hratchian, H. P.; Izmaylov, A. F.; Bloino, J.; Zheng, G.; Sonnenberg, J. L.; Hada, M.; Ehara, M.; Toyota, K.; Fukuda, R.; Hasegawa, J.; Ishida, M.; Nakajima, T.; Honda, Y.; Kitao, O.; Nakai, H.; Vreven, T.; Montgomery, J. A., Jr.; Peralta, J. E.; Ogliaro, F.; Bearpark, M.; Heyd, J. J.; Brothers, E.; Kudin, K. N.; Staroverov, V. N.; Kobayashi, R.; Normand, J.; Raghavachari, K.; Rendell, A.; Burant, J. C.; Iyengar, S. S.; Tomasi, J.; Cossi, M.; Rega, N.; Millam, J. M.; Klene, M.; Knox, J. E.; Cross, J. B.; Bakken, V.; Adamo, C.; Jaramillo, J.; Gomperts, R.; Stratmann, R. E.; Yazyev, O.; Austin, A. J.; Cammi, R.; Pomelli, C.; Ochterski, J. W.; Martin, R. L.; Morokuma, K.; Zakrzewski, V. G.; Voth, G. A.; Salvador, P.; Dannenberg, J. J.; Dapprich, S.; Daniels, A. D.; Farkas, Ö.; Foresman, J. B.; Ortiz, J. V.; Cioslowski, J.; Fox, D. J. *Gaussian 09*, Revision D.01; Gaussian, Inc.: Wallingford CT, 2009.
- (24) Yanai, T.; Tew, D.; Handy, N. A new hybrid exchange–correlation functional using the Coulomb-attenuating method. *Chem. Phys. Lett.* **2004**, *393*, 51–57.
- (25) Zhao, Y.; Truhlar, D. G. The M06 suite of density functionals for main group thermochemistry, thermochemical kinetics, non-covalent interactions, excited states, and transition elements: two new functionals and systematic testing of four M06-class functionals and 12 other functionals. *Theor. Chem. Acc.* **2008**, *120*, 215–241.
- (26) Weigend, F.; Ahlrichs, R. Balanced basis sets of split valence, triple zeta valence and quadruple zeta valence quality for H to Rn: Design and assessment of accuracy. *Phys. Chem. Chem. Phys.* **2005**, *7*, 3297–3305.
- (27) Lu, T.; Chen, F. Multiwfn: A multifunctional wavefunction analyzer. *J. Comput. Chem.* **2012**, *33*, 580–592.
- (28) Varetto, U. *Molekul*, 54.
- (29) The **7a** + TBACl complex precipitates at 0.4 M concentration, if the reaction were run under ten times more dilute conditions, then the complex was still in solution, however no reaction took place.
- (30) Surprisingly, Minakata et al. observed a reverse trend between halogen atom polarizability and catalytic activity in ref **9b**.
- (31) This was in addition to the 20 min delay in adding the diene **2** after solubilizing the catalyst present in the other reactions.
- (32) Zhang, X.; Hao, X.; Liu, L.; Pham, A.-T.; López-Andarias, J.; Frontera, A.; Sakai, N.; Matile, S. Primary Anion– $\pi$  Catalysis and Autocatalysis. *J. Am. Chem. Soc.* **2018**, *140*, 17867–17871.
- (33) Pilli, R. A.; Russowsky, D. Secondary Mannich bases via trimethylsilyl trifluoromethanesulphonate promoted addition of silyl enol ethers to Schiff bases. *J. Chem. Soc., Chem. Commun.* **1987**, 1053–1054.
- (34) Kawęcki, R. Aza Diels–Alder reactions of sulfonimines with the Rawal diene. *Tetrahedron: Asymmetry* **2006**, *17*, 1420–1423.
- (35) For reviews, see: (a) Krossing, I.; Raabe, I. Noncoordinating Anions—Fact or Fiction? A Survey of Likely Candidates. *Angew. Chem., Int. Ed.* **2004**, *43*, 2066–2090. (b) Strauss, S. H. The Search for Larger and More Weakly Coordinating Anions. *Chem. Rev.* **1993**, *93*, 927–942.
- (36) Saito, M.; Tsuji, N.; Kobayashi, Y.; Takemoto, Y. Direct Dehydroxylative Coupling Reaction of Alcohols with Organosilanes through Si–X Bond Activation by Halogen Bonding. *Org. Lett.* **2015**, *17*, 3000–3003.

(37) Surprisingly, in ref 9a tetrafluoroborate containing triazolium salts were used to catalyse aza-Diels–Alder reaction. The authors claim that steric bulk of the substituents on the triazolium ring significantly influence the catalytic activity of the salts. In the work, the less sterically crowded catalysts (that are more comparable to our compounds 8) gave lower yields than those that were more crowded.

(38) We were able to recover 80% of the catalyst after the reaction, see SI Figure S45B.

(39) Compounds with  $m/z$  ratios corresponding to intermediates 13/14/15/17 and 16 were detected by HRMS in the reaction mixture. By HMBC we infer that a methylene group is nearby to a carbonyl group in the intermediate, which cannot be possible in the case of intermediate 16. We speculate that the TMS substituent is located on the nitrogen atom in 14 based on the observation that 14 is quite persistent in the reaction medium in the case of hydrogen containing triazole salt 12. All attempts at isolating the intermediate were unsuccessful. For further details see SI.

(40) Girling, P. R.; Kiyoi, T.; Whiting, A. Mannich–Michael versus formal aza-Diels–Alder approaches to piperidine derivatives. *Org. Biomol. Chem.* **2011**, *9*, 3105–3121.

(41) de Oliveira Freitas, L. B.; Eisenberger, P.; Crudden, C. M. Mesoionic Carbene–Boranes. *Organometallics* **2013**, *32*, 6635–6638.



## Author`s other publications and conference presentations

### Other publications

1. Kaasik, M.; Noole, A.; Reitel, K.; Järving, I.; Kanger, T. Organocatalytic Conjugate Addition of Cyclopropylacetaldehyde Derivatives to Nitro Olefins: en Route to  $\beta$ - and  $\gamma$ -Amino Acids. *Eur. J. Org. Chem.*, **2015**, 2015, 1745–1753

### Conference presentations

1. Kaasik, M. Triazole-based XB donors and their application in catalysis. *Frontiers in Organic Synthesis*, **2019**, Tallinn, Estonia. (Oral)
2. Kaasik, M.; Kaabel, S.; Metsala, A.; Peterson, A.; Kriis, K. Järving, I.; Aav, R.; Rissanen, K.; Adamson, J.; Kanger, T. Triazole-based XB donors in solution and applications in catalysis. *International Symposium on Synthesis and Catalysis 2019 (ISySyCat2019)*, **2019**, Evora, Portugal. (Oral and Poster)
3. Kaasik, M.; Kaabel, S.; Metsala, A.; Peterson, A.; Kriis, K. Järving, I.; Aav, R.; Rissanen, K.; Adamson, J.; Kanger, T. Triazole-based XB donors and their application in catalysis. *Münster Symposium on Cooperative Effects in Chemistry 2019 (MSCEC 2019)*, **2018**, Münster, Germany. (Poster)
4. Kaasik, M.; Kriis, K.; Kanger, T. Halotriazolium Salts as Organocatalysts in Aza-Diels-Alder Reaction. *XXII International Conference on Organic Synthesis (22-ICOS)*, **2018**, Florence, Italy. (Poster)
5. Kaasik, M.; Kriis, K.; Kanger, T. Synthesis of Halotriazolium Salts and Their Use in the Aza-Diels-Alder Reaction. *Balticum Organicum Syntheticum 2018 (BOS 2018)*, **2018**, Tallinn, Estonia. (Poster)
6. Kaasik, M.; Kriis, K.; Kanger, T. Synthesis of Halotriazolium Salts and Their Use in the Aza-Diels-Alder Reaction. *3rd International Symposium on Halogen Bonding (ISXB3)*, **2018**, Greenville, USA. (Poster)
7. Kaasik, M.; Kaabel, S.; Kriis, K.; Järving, I.; Aav, R.; Rissanen, K.; Kanger, T. Synthesis and Characterisation of Chiral Triazole-Based Halogen Bond Donors: Halogen Bonds in the Solid State and in Solution. *European Symposium on Organic Chemistry 2017 (ESOC 2017)*, **2017**, Cologne, Germany. (Poster)
8. Kaasik, M.; Kriis, K.; Kaabel, S.; Kanger, T. Synthesis of triazole-based halogen-bond donors. *Ischia Advanced School of Organic Chemistry (IASOC 2016)*, **2016**, Ischia, Italy. (Poster)
9. Kaasik, M.; Kriis, K.; Kaabel, S.; Kanger, T. Synthesis of triazole-based halogen-bond donors. *Balticum Organicum Syntheticum 2016 (BOS 2016)*, **2016**, Riga, Latvia. (Poster)
10. Kaasik, M.; Reitel, K.; Noole, A.; Lopp, M.; Kanger, T. Asymmetric organocatalytic synthesis of cyclopropane containing  $\beta$ -amino acid precursors. *Balticum Organicum Syntheticum 2014 (BOS 2014)*, **2014**, Vilnius, Lithuania. (Poster)

# Curriculum vitae

## Personal data

Name: Mikk Kaasik  
Date of birth: 25.10.1989  
Place of birth: Tallinn, Estonia  
Citizenship: Estonian

## Contact data

E-mail: Mikk.Kaasik@taltech.ee

## Education

2015 – ... Tallinn University of Technology, Chemistry and Biotechnology, Ph.D.  
2013 – 2015 Tallinn University of Technology, Applied Chemistry and Biotechnology, M.Sc. (*cum laude*)  
2009 – 2012 Tallinn University of Technology, Applied Chemistry and Biotechnology, B.Sc. (*cum laude*)  
2006 – 2009 Kuristiku Gymnasium of Tallinn (silver medal)

## International research experience

2018 – 2019 University of Cologne (Germany), Department of Chemistry, visiting Ph.D. student in the group of Dr. Martin Breugst

## International studies

2014 – 2015 KTH Royal Institute of Technology (Sweden), exchange studies.

## Language competence

Estonian (native), English (fluent), German (beginner)

## Professional employment

2015 – ... Tallinn University of Technology, Department of Chemistry and Biotechnology, early stage researcher

## Professional associations

2017 – ... The Estonian Chemical Society, member

## Honours and awards

2018 – 2019 Dora Plus Ph.D. student mobility (T1.2) Scholarship (The Archimedes Foundation, Estonia)  
2018 Kristjan Jaak Scholarship (The Archimedes Foundation, Estonia)  
2018 Poster prize at the 3rd International Symposium on Halogen Bonding (USA)  
2014 Cambrex Tallinn Master Study Scholarship (The TalTech Development Fund, Estonia)

## Supervised theses

2019 Trine Kasemägi, B.Sc.  
*Synthesis of two chiral bifunctional catalysts from (1R,2R)-diaminocyclohexane* (Tallinn University of Technology, Department of Chemistry and Biotechnology)

## Teaching experience

Spring 2017 Stereochemistry, exercise tutorials (graduate course)  
2016 – 2017 Organic chemistry I and II, exercise tutorials (undergraduate course).

# Elulookirjeldus

## Isikuandmed

Nimi: Mikk Kaasik  
Sünniaeg: 25.10.1989  
Sünnikoht: Tallinn, Eesti  
Kodakondsus: eesti

## Kontaktandmed

E-post: Mikk.Kaasik@taltech.ee

## Hariduskäik

2015 – ... Tallinna Tehnikaülikool, Keemia ja biotehnoloogia, Ph.D.  
2013 – 2015 Tallinna Tehnikaülikool, Rakenduskeemia ja biotehnoloogia, M.Sc.  
(*cum laude*)  
2009 – 2012 Tallinna Tehnikaülikool, Rakenduskeemia ja biotehnoloogia, B.Sc.  
(*cum laude*)  
2006 – 2009 Tallinna Kuristiku Gümnaasium (hõbemedal)

## Rahvusvaheline teadustöö

2018 – 2019 Kölni Ülikool (Saksamaa), Keemia instituut, külalisdoktorant Dr.  
Martin Breugst uurimisgrupis

## Rahvusvaheline õppetöö

2014 – 2015 Kuninglik Tehnoloogiainstituut (KTH) (Rootsi), vahetusüliõpilane

## Keelteoskus

eesti (emakeel), inglise (kõrgtase), saksa (algtase)

## Teenistuskäik

2015 – ... Tallinna Tehnikaülikool, Keemia ja biotehnoloogia instituut,  
nooremteadur

## Kuuluvus erialaühingutesse

2017 – ... Eesti keemiaselts, liige

## Teaduspreemiad ja tunnustused

2018 – 2019 Doktorantide õpirände stipendium (T1.2) (SA Archimedes, Eesti)  
2018 Kristjan Jaagu stipendium (SA Archimedes, Eesti)  
2018 Posterauhind konverentsil ISXB3 (USA)  
2014 AS Cambrex Tallinn stipendium (TalTech Arengufond, Eesti)

## Juhendatud väitekirjad

2019 Trine Kasemägi, B.Sc.  
*Kahe kiraalse bifunktsionaalse katalüsaatori süntees*  
(*1R,2R*)-diaminotsükloheksaanamiinist (Tallinna Tehnikaülikool,  
Keemia ja biotehnoloogia instituut)

## Õpetamiskogemus

Kevad 2017 Stereokeemia, harjutustunnid (magistriõpe)  
2016 – 2017 Orgaaniline keemia I ja II, harjutustunnid (bakalaureuseõpe)